Role of Semaphorin 3A in osteosarcoma

Daniëlle de Ridder

A thesis submitted in fulfilment of the requirements for the degree of
Doctor of Philosophy

The University of Sheffield
Faculty of Medicine, Dentistry & Health
Department of Oncology and Metabolism

July 2018

To my family

Declaration

I hereby declare that this thesis has been composed by me and the work described within, except where specifically acknowledged, is my own and that it has not been accepted in any previous application for a degree. Parts of this thesis have been published in Scientific Reports as of May 2018 (de Ridder et al., 2018). The information obtained from sources other than this study is acknowledged in the text included in the references. Images that were used from other sources than my own have been processed through copyright clearance and included in the references.

Daniëlle de Ridder

Acknowledgements

In the first place, I would like to thank and express my gratitude to my primary supervisor Dr Aymen Idris for giving me the opportunity to do my MSc project and a little while later to return as a PhD candidate on the Sema3A project. I am grateful for all the opportunities you offered including those on other projects allowing me to gain a variety of skills I would not have otherwise. Thank you for your enthusiasm and passion for science in general.

I would also like to express my thanks to my co-supervisor Prof Dominique Heymann for the lively discussions, his vast knowledge on bone sarcomas and the valuable input in this project. Thank you to Dr Nathalie Renema for her invaluable help with the *in vivo* studies and Séverine Battaglia for the training on the microCT scanner at the INSERM UMR957 University of Nantes, France. Thank you especially to the Bone Cancer Research Trust for awarding me the PhD studentship.

I would like to thank my colleagues of the Department of Oncology and Metabolism in the University of Sheffield for their support. A special thanks to Dr Silvia Marino for being a great friend and mentor in the laboratory, soon to be Dr Ryan Bishop for being an amazing colleague and friend throughout our PhD studies and soon to be Dr Abdullah Al Jeffrey for his support and help during the process and I would to extend my thanks to the other colleagues and previous students of the Idris group. Thank you to all my friends for your continuous support and friendship and especially Alyssa Varhol for making the first year of my PhD a year to remember.

Last but not least thank you to my family I would not be who I am and where I am without you. Zonder de steun, het begrip, aanmoediging en vertrouwen had ik me nooit aan een PhD gewaagd en had ik het de laatste 3 jaren niet gered. In het speciaal Joost, dank voor alle steun, vertrouwen, dat je altijd voor me klaar stond en dat je me hebt laten zien dat er meer is in het leven dan alleen werk.

Publications

Papers

de Ridder D, Marino S, Bishop RT, Renema N, Chenu C, Heymann D, Idris AI. Bidirectional regulation of bone formation by exogenous and osteosarcoma-derived Sema3A. *Sci Rep. 2018 May 2;8(1):6877.*

Peramuhendige P, Marino S, Bishop RT, **de Ridder D**, Khogeer A, Baldini I, Capulli M, Rucci N, Idris AI. TRAF2 in osteotropic breast cancer cells enhances skeletal tumour growth and promotes osteolysis. *Sci Rep. 2018* Jan 8;8(1):39.

Ryan T. Bishop, Silvia Marino, **Daniëlle de Ridder,** Richard J Allen, Diane V. Lefley, Ning Wang, Penelope D. Ottewell and Aymen I. Idris. Regulation of breast cancer osteolytic metastasis by the IKKε/TBK1 axis *Oncogene. 2018 (Submitted)*

Ryan T. Bishop, Silvia Marino, **Daniëlle de Ridder,** D. Giovana Carrasco G. Richard J Allen, , Ning Wang, Aymen I. Idris. Targeting of TRAF6/NFκB reduces breast cancer metastasis, skeletal tumour burden and osteolysis. *(In preparation)*

Silvia Marino, **Daniëlle de Ridder,** Ryan T. Bishop, Marco Ponzetti, Nathalie Renema, Dominique Heymann, Nadia Rucci, and Aymen I. Idris. Regulation of cancer associated bone disease by MAGL. *(In preparation)*

Daniëlle de Ridder and Aymen I Idris. NFκB and primary bone cancer. *(review in preparation)*

Book chapter

Silvia Marino, Ryan T. Bishop, **Daniëlle de Ridder**, Jesus Delgado-Calle and Michaela R Reagan. 2D and 3D in vitro co-culture for cancer and bone cell interaction studies. *Methods Mol Biol. 2018 (In press)*

Abstracts

Daniëlle de Ridder, Silvia Marino, Nathalie Renema, Chantal Chenu, Dominique Heymann, Aymen Idris. Bidirectional regulation of osteosarcoma associated bone formation by exogenous and tumour-derived Sema3A. *Calcif Tissue Int (2017)* 100:S15–S16 OB2.1

Oral presentations and Awards

Daniëlle de Ridder, Silvia Marino, Nathalie Renema, Chantal Chenu , Dominique Heymann , Aymen Idris. Bidirectional regulation of osteosarcoma associated bone formation by exogenous and tumour-derived Sema3A.
Presented at **European Calcified Tissue Society, Salzburg, Austria** May 2017
Received: **ECTS Travel Award.**

Daniëlle de Ridder, Silvia Marino, Nathalie Renema, Chantal Chenu , Dominique Heymann , Aymen Idris. Bidirectional regulation of osteosarcoma associated bone formation by exogenous and tumour-derived Sema3A.
Presented at **Medical School Annual Research meeting, Sheffield** June 2017

Daniëlle de Ridder, Silvia Marino, Nathalie Renema, Chantal Chenu , Dominique Heymann , Aymen Idris. Bidirectional regulation of osteosarcoma associated bone formation by Sema3A.
Presented at **1st Sheffield Workshop of Translational Research in Bone Sarcoma, Sheffield** June 2017

Lay presentations

Daniëlle de Ridder, Silvia Marino, Nathalie Renema, Chantal Chenu , Dominique Heymann , Aymen Idris. The role of Sema3A in osteosarcoma.
Presented at **BCRT lab open day visit , Sheffield** July 2016

Daniëlle de Ridder, Silvia Marino, Nathalie Renema, Chantal Chenu , Dominique Heymann , Aymen Idris. The role of Sema3A in osteosarcoma.
Presented at **BCRT lab open day visit , Sheffield** July 2017

Daniëlle de Ridder, Silvia Marino, Nathalie Renema, Chantal Chenu , Dominique Heymann , Aymen Idris. Bidirectional regulation of osteosarcoma associated bone formation by Sema3A.
Presented at **Bone cancer conference (BCRT), Birmingham** July 2017

Table of Contents

Abbreviations

ALP	Alkaline Phosphatase
AKT	Protein Kinase B
ANOVA	Analysis of variance
ATP	Adenosine triphosphate
αMEM	Alpha-Minimum Essential Medium
BCA	Bicinchoninic acid
BMP	Bone morphogenic protein
BSA	Bovine serum albumin
BV	Bone volume
BV/TV	Bone volume/Total volume
c-Fms	Colony-stimulating factor-1 receptor
CBF-α1	Core-binding factor subunit alpha-1
CD14	Cluster of differentiation 14
Cdk5	Cyclin dependent kinase 5
CKI	Casein kinase-1
CRMP2	Collapsin response mediating protein-2
CTX	C-terminal telopeptide of type 1 collagen
CXCL5	CXC Motif Chemokine Ligand 5
DAP12	TYRO protein tyrosine kinase binding protein
dH_2O	Distilled water
DKK1	Dickkopf-related protein 1
DMEM	Dulbecco's Modified Eagle's Medium
DMSO	Dimethyl sulfoxide
DTT	DL-Dithiothreitol
EDTA	Ethylenediaminetetraacetic acid
ERK	Extracellular signal-regulated kinases
FAK	Focal adhesion kinase
FARP2	FERM, RhoGEF And Pleckstrin Domain Protein 2
FCS	Fetal calf serum
FFPC	Furin-like pro-protein convertases
FLT3 ligand	Fms-related tyrosine kinase 3 ligand
GAPDH	Glyceraldehyde 3-phosphate dehydrogenase
GSK3β	Glycogen synthase kinase 3 beta
H&E	Haemotoxylin and Eosin

HGF	Hepatocyte growth factor
Ig	Immunoglobulin
IGF-1	Insulin growth factor 1
IκB	Inhibitor of kappa B
IL17A	Interleukin 17A
ITAM	Immunoreceptor tyrosine-based activation motif
ITAM	Immunoreceptor tyrosine-based activation motif
kDa	kilodalton
LDH	Lactate dehydrogenase
LIMK1	LIM kinase 1
MAPK	Mitogen activated protein kinases
M-CSF	Macrophage colony stimulating factor
MicroCT	Micro computed tomography
MIF	Macrophage migration inhibitory factor
MRI	Magnetic resonance imaging
MSC	Mesenchymal stem cells
NFκB	Nuclear factor kappa-light-chain-enhancer of activated B cells
NGF	Nerve growth factor
Nrp1	Neuropilin-1
Nrp2	Neuropilin-2
Ob.N	Osteoblast number
Ob.S	Osteoblast surface
Oc.N	Osteoclast number
Oc.S	Osteoclast surface
OPG	Osteoprotegerin
P65	Transcription factor p65 (RELA)
PBS	Phosphate-buffered saline
PBST	Phosphate-buffered saline and tween
PBMC	Peripheral blood mononuclear cells
PET	Positron emission tomography
PINP	Procollagen type 1 N propeptide
PI3K	Phosphatidylinositol-4,5-bisphosphate 3-kinase
pNPP	p-nitrophenyl phosphate
PPARγ	Peroxisome proliferator-activated receptor-γ
PSI	Plexin-semaphorin-integrin
PTH	Parathyroid hormone

PTX3	Pentraxin-related protein 3
PVDF	Polyvinylidene difluoride
RA	Rheumatoid arthritis
RANK	Receptor activator of nuclear factor κB
RANKL	Receptor activator of nuclear factor κB ligand
REQC	ATP-dependent DNA helicase
Runx2	Runt-related transcription factor
Sema	Semaphorin
Sema3A	Semaphorin 3A
Sema3B	Semaphorin 3B
Sema3C	Semaphorin 3C
Sema3D	Semaphorin 3D
Sema3E	Semaphorin 3E
Sema3F	Semaphorin 3F
Sema3G	Semaphorin 3G
Sox	Sex determining region Y-related high-mobility group box
TBST	Tris-Buffered Saline and Tween
Tb.N	Trabecular Number
Tb.Pf	Trabecular pattern factor
Tb.Sp	Trabecular Seperation
Tb.Th	Trabecular thickness
TGF-β	Transforming growth factor-β
TRAcP	Tartrate-resistant Acid Phosphatase (TRAcP)
TREM2	Triggering receptor expressed on myeloid cells 2
TSP1	Thrombospondin-1
VEGF	Vascular endothelial growth factor
VEGFR	Vascular endothelial growth factor receptor
Wnt	Wingless and Int-1

List of Figures

List of Tables

Abstract

Osteosarcoma is the most prevalent malignant primary bone tumour and mainly affects children and adolescents. Since the introduction of chemotherapy the survival rate for osteosarcoma patients has not improved, implicating the need for new therapeutic targets. Semaphorin 3A (Sema3A), a secreted member of the Semaphorin family, is essential for bone metabolism and plays an important role in the regulation of tumorigenesis and metastasis, but its function in osteosarcoma remains unknown. The aim of this thesis was to study the effects of human recombinant Sema3A and Sema3A overexpression on tumour growth, metastasis, osteosarcoma-associated bone damage and ectopic bone formation in preclinical models of human osteosarcoma.

Exposure to recombinant Sema3A enhanced alkaline phosphatase activity in a panel of osteosarcoma cell lines and inhibited their migration without affecting cell viability *in vitro*. Administration of exogenous Sema3A in mice increased bone volume in the healthy and osteosarcoma-bearing legs these effects were accompanied with a trend towards more osteoblasts and less osteoclasts. Sema3A overexpression reduced viability, migration and invasion of KHOS cells *in vitro* however, both overexpression and administration of recombinant Sema3A had no effect on tumour growth. Surprisingly, overexpression of Sema3A reduced ectopic bone formation. Continuous exposure of osteoblasts to conditioned medium from Sema3A overexpressing cells inhibited mineralization and Wnt/β-catenin signalling without affecting osteoblast viability. This effect may be partially explained by the upregulated expression of DKK1 in Sema3A overexpressing KHOS cells.

In conclusion, these studies suggest that Sema3A acts as a tumour inhibitor on osteosarcoma *in vitro*. Administration of recombinant Sema3A partially protected the bone from osteosarcoma-associated osteolysis. In contrast, Sema3A overexpression reduced osteosarcoma-associated ectopic bone formation in mice. Thus, Sema3A is of potential therapeutic efficacy in osteosarcoma-associated bone damage. However, inhibition of bone formation associated with continuous exposure to Sema3A may limit its long-term use as therapeutic agent in osteolytic bone diseases.

Graphical abstract

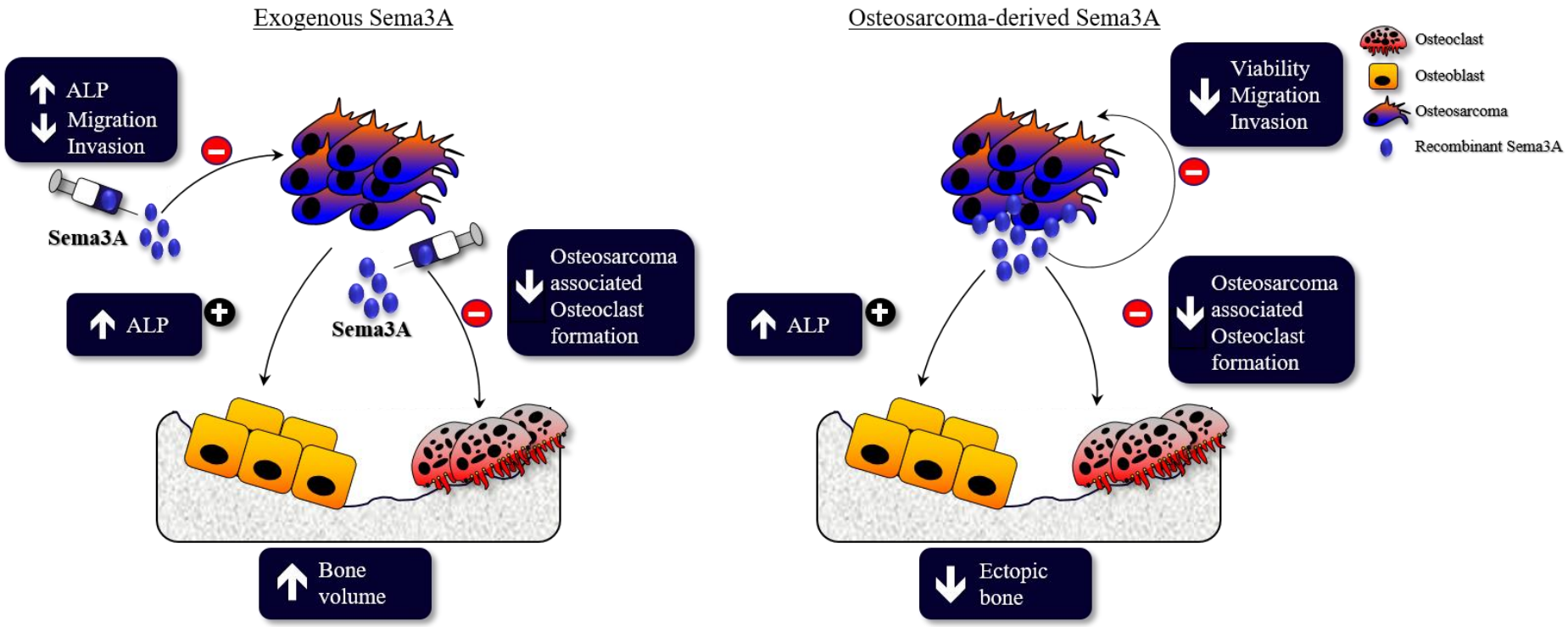

Schematic representation of the role of Sema3A in osteosarcoma-bone cell interactions.

Exogenous Sema3A increased osteoblast and osteosarcoma alkaline phosphatase activity, reduced migration *in vitro* and enhanced bone volume in mice. Osteosarcoma-derived Sema3A reduced migration invasion and osteosarcoma cell viability *in vitro* and reduced ectopic bone formation. For a detailed description see results chapter 3-7.

CHAPTER ONE

General Introduction

1 Introduction

1.1 Bone

Bone is a highly dynamic tissue that together with cartilage and the joints comprises the skeleton. Bone has several functions, including providing the support and protection of organs (J.Favus, 2006, Lerner, 2006). Furthermore, bone acts as mineral storage for calcium and phosphorus thereby serving a metabolic function for the maintenance of mineral homeostasis in the serum (Hadjidakis and Androulakis, 2006).

Bones are categorized in roughly two main categories, depending on their shape and mechanism of development. Flat bones such as the skull, mandible and sternum are formed by intramembranous ossification. The long bones such as the femur are formed by a combination of intramembranous ossification and endochondral ossification. The long bones have a cylindrical shape and are composed of a hollow shaft, the diaphysis which contains the bone marrow, the two metaphysis containing the growth plate and the two epiphysis which are the rounded ends of the long bone. The diaphysis is primarily composed of dense cortical bones whereas the metaphysis and epiphysis are mostly composed of an intricate trabecular network (Clarke, 2008, J.Favus, 2006).

Bone is comprised of two structural components; the cortical and cancellous bone. The skeleton consists of 20% cancellous (trabecular bone) and 80% cortical bone. Cortical bone is the dense outer layer of bone that functions mainly as protection, offers strength to the skeleton and has a low bone turnover rate. Cortical bone is organized in osteons (haversian system) that contain a central canal that accommodates the blood and nerve vessels surrounded by concentric lamellae Figure 1.1 (J.Favus, 2006, Clarke, 2008). The framework of trabecular bone provides mechanical strength to the bone. The trabecular component is highly metabolically active with a high bone turnover rate acting as a mineral reservoir. Trabecular bone structure is similar to cortical bone structure in that trabecular bone also contains osteons but the lamellae run parallel to each other instead of in concentric orientation (J.Favus, 2006, Hadjidakis and Androulakis, 2006).

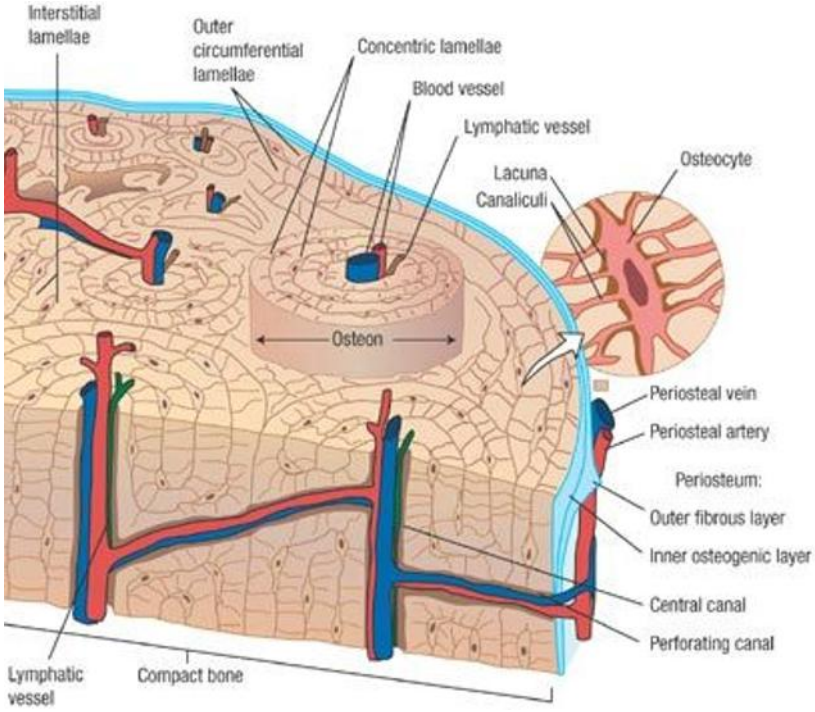

Figure 1.1. Structure of bone
The general structure of bone showing the osteons containing the blood and lymphatic vessels surrounded by concentric lamellae. Adapted from (Taylor et al., 2007) see appendix section 10.6.

Bone consists of both organic and inorganic components comprising 20-40% and 50-70% of the bone respectively. Collagen I fibres represent approximately 90% of the organic matrix of bone. The remainder of the organic compartment consists of proteoglycans and other non-collagenous proteins such as osteopontin, osteocalcin and osteonectin. The inorganic component of the bone mainly consists of hydroxyapatite [Ca3(PO4)2]3Ca(OH)2 crystals, other inorganic components are magnesium, sodium and bicarbonate (J.Favus, 2006, Clarke, 2008).

1.2 Bone cells

The main cellular components of bone are osteoblasts, osteoclasts, lining cells and osteocytes. These cells play an important role in bone remodelling. Other cell types that are not directly involved in bone remodelling but are essential for the formation of the long bones are the chondrocytes. All surfaces of bone tissues are covered with a single cell layer of bone lining cells (Lerner, 2006). The osteoblasts are responsible for bone formation where osteoclasts are responsible for bone resorption (J.Favus, 2006).

1.2.1 **Osteoblasts**

Osteoblasts are specialized mononucleated cuboidal cells responsible for bone formation. They are located in the bone marrow stroma and at the periosteal surfaces. (J.Favus, 2006). Osteoblasts derive from mesenchymal stem cells (MSCs). The commitment of MSCs towards the different bone related lineages is controlled by a number of growth factors and transcription factors including but not limited to, sex determining region Y-related high-mobility group box (Sox), peroxisome proliferator-activated receptor-γ (PPARγ) and runt-related transcription factor 2 (Runx2) (Figure 1.2). Sox9 is important for MSC differentiation towards the chondrocyte lineage whereas PPARγ is important for MSC to adipocyte differentiation (Katagiri and Takahashi, 2002, Ducy, 2000) (Akiyama et al., 2002).

Runx2, also known as core-binding factor subunit alpha-1 (CBF-α-1), is the major transcription factor responsible for commitment of MSCs towards the osteoblastic lineage and is a regulator of bone formation (Ducy, 2000). Bone morphogenic proteins (BMP) belong to the transforming growth factor-β (TGF-β) superfamily and play a role in osteoblast differentiation through upregulation of Runx2 (Katagiri and Takahashi, 2002). Runx2 remains important for the upregulation of osteocalcin expression in mature osteoblasts (Ducy, 2000). An additional transcription factor of importance in osteoblast differentiation and bone formation is osterix which exerts its action by acting downstream of Runx2 (Nakashima et al., 2002).

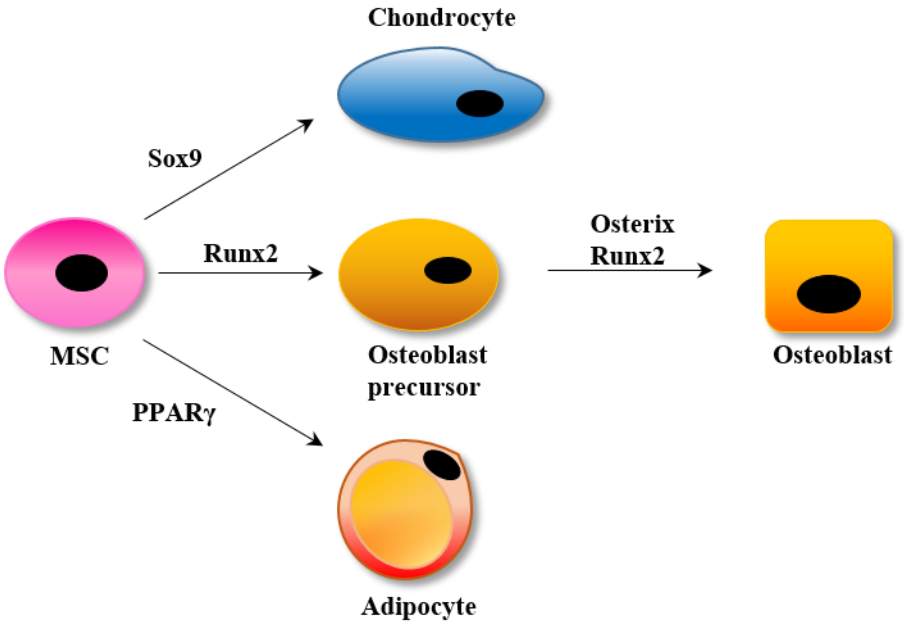

Figure 1.2. Schematic of mesenchymal stem cell differentiation by transcription factors. Mesenchymal stem cells differentiate into chondrocytes, osteoblast precursors or adipocytes under the influence of several transcription factors such as Sox9, Runx2 and PPARγ. Abbreviations: MSC, mesenchymal stem cell, Sox, sex determining region Y-related high-mobility group box, Runx2, runt-related transcription factor 2, PPARγ, peroxisome proliferator-activated receptor-γ.

Another pathway that plays an important role in osteoblast differentiation is the canonical Wnt pathway. Wnt proteins are secreted proteins that signal through receptor complexes consisting of transmembrane G-protein coupled receptors of the frizzled family and of the Lrp family (Karner and Long, 2017). When the Wnt pathway is inactive, β-catenin is phosphorylated by casein kinase-1 (CKI) and GSK3-β leading to its degradation by a destruction complex (Reya and Clevers, 2005). Wnt mediated β-catenin signalling inhibits adipogenesis and promotes osteoblast differentiation (Cawthorn et al., 2012, Day et al., 2005).

Mature osteoblasts are characterized by the expression of several bone related extracellular matrix proteins such as, but not limited to type I collagen, osteocalcin, and osteopontin, osteoblasts also exhibit high enzyme activity of alkaline phosphatase (ALP) (Katagiri and Takahashi, 2002, J.Favus, 2006). In addition to osteoid matrix proteins, osteoblasts produce a variety of growth factors including, insulin-like growth factors (IGF), BMPs and TGF-β (Hadjidakis and Androulakis, 2006). Osteoblasts have two main functions. The first is to synthesize and deposit osteoid matrix, the unmineralised bone matrix, and mineralization. The second is to support osteoclastogenesis, by stimulating osteoclast differentiation and supporting mature

osteoclast survival (Katagiri and Takahashi, 2002). Osteoblasts produce regulators of osteoclast differentiation, survival, function and activation, namely macrophage colony stimulating factor (M-CSF), receptor activator of nuclear factor kappa-B ligand (RANKL) and osteoprotegerin (OPG), the soluble decoy receptor for RANKL. RANKL is produced in response to a wide arrange of signalling proteins including Vitamin D and parathyroid hormone (PTH) (Troen, 2003). Osteoblasts perform a unique function in bone, however they are not terminally differentiated. The majority of osteoblasts at remodelling sites die by apoptosis. The remaining fraction of osteoblasts change into bone lining cells and a small part of osteoblasts become entombed in the bone matrix and differentiate into osteocytes (Noble, 2008, Manolagas, 2000).

1.2.2 **Osteoclasts**

Osteoclasts are multinucleated cells originating from haematopoietic stem cells and are responsible for bone resorption. They form by the fusion of mononuclear progenitors derived from the monocyte lineage. The two main essential molecules for osteoclast formation, survival and activation are M-CSF and RANKL. (Teitelbaum, 2000). Secreted M-CSF by osteoblasts binds to the colony-stimulating factor-1 receptor (c-Fms) receptor on osteoclast precursors and induces the expression of receptor activator nuclear factor kappa-B (RANK). M-CSF is essential for the survival of mature osteoclasts and their precursors (Ross, 2006).

RANKL expressed by osteoblasts binds to RANK on mononuclear osteoclast precursors and commits the cell to the osteoclast lineage, thereby inducing their fusion into multinucleated osteoclasts (Teitelbaum, 2000). OPG is a soluble decoy for RANKL and by binding to RANKL inhibits osteoclastogenesis, therefore the rate of OPG/RANKL in the bone microenvironment determines the osteoclast formation (Troen, 2003). During osteoclast differentiation, the osteoclast progenitor cells express osteoclast markers such as tartrate resistant acid phosphatase (TRAcP), calcitonin receptor and RANK (Katagiri and Takahashi, 2002).

1.2.3 **Osteocytes**

Osteocytes are terminally differentiated cells from the osteoblast lineage that form when mature osteoblasts become entrapped in the bone matrix (Noble, 2008).

Osteocytes are the most abundant cell in bone and are mainly defined by their morphology and location in bone. Osteocytes express osteocalcin, osteonectin and osteopontin but lack the high alkaline phosphatase activity found in osteoblasts (Klein-Nulend et al., 2003). Osteocytes maintain contact with neighbouring cells through large network via the dendritic processes that lie in the lacunae and canaliculi of the mineralized bone (Noble, 2008).

The precise roles and functions of osteocytes remain unclear but there are several indications that they play an important role in bone remodelling and mechano-sensing (Noble, 2008, Uda et al., 2017). Osteocytes sense mechanical stimuli which are then transcribed into biological signals. The main pathways induced by mechanical stimuli are calcium, ATP, nitrogen oxide, prostaglandin and wnt pathways, some of these pathways affect osteoblasts and osteoclasts (Uda et al., 2017). Osteocytes produce Sclerostin, a wnt signalling pathway antagonist that inhibits bone formation. Osteocytes have also been shown to produce RANKL and M-CSF further strengthening that they play a role in osteoclastogenesis (Noble, 2008).

1.2.4 **Chondrocytes**

Chondrocytes are derived from the mesenchymal stem cell lineage (Figure 1.2). Chondrocytes play essential roles during osteogenesis. Furthermore, they are pivotal for joint mobility(Karsenty and Wagner, 2002). Chondrogenesis is the first step in the formation of the skeleton. MSCs first differentiate in chondrocytes that express aggrecan and type II collagen (Karsenty and Wagner, 2002). The main transcription factor that is essential for chondrocyte differentiation and endochondral bone formation is Sox9. Sox9 expression is also required for two other members of the sox family that play an important role in chondrogenesis, Sox5 and Sox6 (Akiyama et al., 2002). Sox9 and Runx2 are essential transcriptional regulators for articular chondrocytes and articular cartilage formation (Goldring, 2012). Once chondroblasts have formed the cartilage layer, they further differentiate into hypertrophic chondrocytes under the influence of Runx2. Eventually the terminal layer of hypertrophic chondrocytes will be invaded by blood vessels and the growth plate will gradually be replaced by calcified extracellular matrix and the chondrocytes embedded in the bone will die through apoptosis (Karsenty and Wagner, 2002, Komori, 2018).

1.3 Bone remodelling

Bone remodelling is a highly dynamic, tightly regulated process that is essential for mineral homeostasis, repair of microfractures and maintenance of bone mass. Bone undergoes constant remodelling throughout life and about 10% of bone is remodelled and renewed every year (Kenkre and Bassett, 2018). The bone remodelling process is divided into three distinct phases, bone resorption, reversal phase and bone formation.

1.3.1 **Bone resorption**

Old bone is replaced by newly formed bone to adapt to mechanical loading, micro-fractures and strain. In response to mechanical loading and micro-damage, osteoclast precursors migrate to the site that requires resorption (Hadjidakis and Androulakis, 2006). Osteoblasts produce RANKL and M-CSF and induce maturation of the osteoclast precursors into multinucleated cells that bind to the surface of bone matrix through integrins (Lerner, 2006, Hadjidakis and Androulakis, 2006, Teitelbaum, 2000). Once attached to bone, osteoclasts polarise their membranes to allow formation of the actin ring that tightly isolates a region between the active osteoclast and bone surface known as the sealing zone (Teitelbaum, 2000).

Protons are then released by mature osteoclasts to acidify the site of resorption and dissolve the hydroxyapatite crystals [Ca3(PO4)2]3Ca(OH)2, to Ca^{2+}, HPO_4^{2-} and H_2O (Bar-Shavit, 2007). This process exposes the organic component of bone which is then degraded by proteases, cathepsin K and Matrix metallopeptidase 9 (MMP9). Osteoclasts remove the products of bone resorption, both organic and inorganic, by endocytosis and secrete them in the extracellular space (Troen, 2003, Teitelbaum, 2000). In healthy humans, the resorption phase lasts 10 to 14 days (Lerner, 2006, Hadjidakis and Androulakis, 2006).

The phase between bone resorption and bone formation is the reversal phase. This phase is characterized by apoptosis of osteoclasts and subsequently, osteoblast precursors migrate to the site (Lerner, 2006, Hadjidakis and Androulakis, 2006).

1.3.2 **Bone formation**

The next phase of the remodelling cycle is the bone formation phase. Bone formation starts with the recruitment of osteoblast precursors followed by the formation of new bone by osteoblasts. At the resorbed site, osteoblasts precursors proliferate, differentiate and mature in preparation of the bone formation phase (Neve et al., 2011). The migration and activation of osteoblast precursors is thought to be mediated by the presence of several growth factors that are released during the bone resorption phase including insulin growth factor-I (IGF-I) and transforming growth factor-β (TGF-β) (Mundy et al., 1982, Lerner, 2006).

Mature osteoblasts produce type I collagen, and non-collagen proteins osteocalcin, osteonectin, osteopontin, bone sialoprotein and proteoglycans to form osteoid (Katagiri and Takahashi, 2002, J.Favus, 2006). The osteoblasts also secrete ALP that in turn induces matrix maturation and mineralization. In addition, osteoblasts release matrix vesicles within the collagen scaffold containing calcium, phosphate and various proteins that induce formation of hydroxyapatite crystals. This process converts the osteoid into mineralised bone (Katagiri and Takahashi, 2002, J.Favus, 2006).

1.4 Abnormal bone remodelling

The balance of bone remodelling is dependent on tight coupling of bone resorption by osteoclasts and bone formation by osteoblasts. Imbalances in the bone remodelling process are the primary cause of bone diseases such as Paget's disease of bone, osteoporosis and rheumatoid arthritis (Galson and Roodman, 2014, Rodan and Martin, 2000, Smolen et al., 2018). Furthermore, benign and malignant underlying diseases such as primary bone tumours and secondary cancer to bone that also results in abnormal bone remodelling.

Paget's disease of bone is one of the most common bone disorders. Paget's is characterized by an initial increase in osteoclast number and osteoclast size leading to enhanced bone resorption followed by abundant and aberrant bone formation (Galson and Roodman, 2014). Due to this rapid turnover the bone is mechanically weak and disorganized (Ralston et al., 2008). The disease is most often diagnosed in patients over 50 years of age and several genetic abnormalities have been linked to the disease (Singer, 2015). Paget's disease of bone is one of the risk factors for adult onset osteosarcoma (Geller and Gorlick, 2010).

Osteoporosis is a systemic osteolytic bone disease and is characterized by a reduction in bone mass and a deteroriation of the microarchitecture of the bone, thereby increasing the susceptibility for bone fractures (Rodan and Martin, 2000, Meunier et al., 1999). The main causes of osteoporosis are oestrogen deficiency (postmenopausal osteoporosis) and as a complication of glucocorticoid therapy (Eastell et al., 1998, Meunier et al., 1999).

Rheumatoid arthritis is a chronic inflammatory autoimmune disease that is characterized by destruction of the cartilage and bone in the joints. (Smolen et al., 2018, Sweeney and Firestein, 2004). Synoviocytes and cellular invasion by immune cells into the cartilage are the main processes that lead to the cartilage destruction seen in the joints. The bone erosion that accompanies cartilage destruction is due to excessive bone resorption caused by osteoclasts. RANKL expressed by synoviocytes and T cells attracted to the inflammatory site induces the maturation and activation of osteoclasts that lead to the bone erosion (Smolen et al., 2018, Sweeney and Firestein, 2004, Rodan and Martin, 2000).

1.5 Primary bone tumours

Primary bone tumours are rare, they originate from the different types of bone cells and are classified based on the type of matrix production and on the cell type of origin. Some benign and malignant bone tumours have childhood and adolescent onsets (Fletcher, 2013). The early onset of these tumours may be attributed to the higher bone turnover seen in children and adolescents in comparison to adults (Teti, 2011).

1.5.1 **Benign primary bone tumours**

Benign bone tumours form a variety of different tumours that can develop in any site of the skeleton. Like malignant primary bone tumours, benign bone tumours are divided into categories based on their cell type of origin. The main categories are cartilage forming cells, bone forming cells and connective tissue. In general, there are 8 different types of benign primary bone tumours. Of these 8 osteochondroma, giant cell tumour of bone and osteoblastoma are the most prevalent (Table 1.1). Even though benign bone tumours rarely progress to a malignant state, depending on the location of the tumour they may compress healthy tissues and compromise their function. Furthermore, their presence may still lead to discomfort and pathological fractures which necessitates the need for treatment. (Hakim et al., 2015).

Benign bone tumours are diagnosed with conventional radiology and biopsies. Treatments for benign bone tumours depend on several factors including the risk of recurrence and local tissue invasion. Benign bone tumours often follow the same treatment regime as malignant bone tumour treatments consisting of surgery, drugs and radiotherapy (Hakim et al., 2015, Fritzsche et al., 2017).

1.5.2 **Malignant primary bone tumours**

Malignant bone tumours are uncommon but despite their rarity, they are among the most frequent groups of cancer in children and adolescents worldwide with an incidence of 10 to 26 cases per million each year (Stiller, 2007). The treatment regime of malignant bone tumours consists of a combination of surgery, chemotherapy and radiotherapy and depends on several factors including, the type of tumour, the stage of disease and tumour location (ESMO, 2014).

Malignant bone tumours are divided in distinct categories that are based on the cell of origin and the type of matrix produced by the tumour. Approximately 75% of all malignant bone tumours are osteosarcoma, Ewing's sarcoma or chondrosarcoma in the United Kingdom with osteosarcoma being the most prevalent of these three malignant entities (Whelan et al., 2012) (Table 1.1).

Table 1.1 Most common benign and malignant bone tumours.

Matrix/cell type	Benign	Incidence (%)[1]	Malignant	Incidence (%)[1]
Bone	Osteoblastoma Osteoma Osteoid osteoma	14% 12% 12%	Osteosarcoma	52%
Cartilage	Osteochondroma Chondroma	30% 2.6%	Chondrosarcoma	6%
Connective tissue	Aneurysmal bone cyst Fibrous dysplasia	~9% 5-7%	Adamantinoma	0.1-0.5%
Osteoclast like	Giant cell tumour of bone	20%	Malignant Giant cell tumour of bone	<5%
Uncertain differentiation	-	-	Ewing's sarcoma	34%

[1]Incidences are percentages of all benign or all malignant bone tumours (Hakim et al., 2015, Stiller et al., 2006, Jain et al., 2008).

The introduction of chemotherapy significantly improved the survival of malignant bone cancer patients. During the last decades there have not been any significant changes in the survival rates of patients suffering from any of the most common malignant bone tumours (Whelan et al., 2012). This stagnation in survival rates illustrates the need for new therapeutic targets to treat bone cancer.

1.6 Osteosarcoma

Osteosarcoma is the most prevalent malignant primary bone tumour with a peak incidence during adolescence and another peak of incidence between the age of 60-80 years (Meyers and Gorlick, 1997). The onset of osteosarcoma at the age of 60-80 is often attributed to radiotherapy or underlying metabolic bone diseases. Paget's disease of bone is seen in approximately 33-50% of adult osteosarcoma cases, therefore adult osteosarcoma is often classified as secondary osteosarcoma (Geller and Gorlick, 2010). In the UK, the bone sarcoma crude incidence rate is 0.8 per 100.000 with osteosarcoma being the most common occurring bone sarcoma (CancerresearchUK, 2018). In the US, the incidence rate of osteosarcoma is 0.4 per 100.000 (Society, 2018).

Osteosarcoma preferentially arises in actively growing bones and occurs more frequently in males with a male: female ratio of approximately 1:1.4 (Bielack et al., 2009, Alfranca et al., 2015). In females the peak incidence of osteosarcoma lies at an earlier age than males, 10-14 and 15-19 years of age respectively, this discrepancy is most likely due to the earlier onset of the growth spurt in females (Stiller, 2007).

1.6.1 **Pathophysiology**

Osteosarcoma is characterized by severe chromosomal instability (Alfranca et al., 2015). The chromosomal instability leads to an extreme variability in tumours between patients and is one of the underlying challenges in finding a treatment that would benefit the majority of osteosarcoma patients. The oncogenic events leading to osteosarcoma development and metastasis are still poorly understood. Currently there are two main hypotheses to the cell type of origin. Mesenchymal stem cells (MSCs) have been hypothesized to be the cell type of origin for several bone sarcomas, including osteosarcoma (Mohseny et al., 2009, Xiao et al., 2013). Deregulation of several known pathways implicated in cancer such as p53-, retinoblastoma-, PI3K-AKT- and MAPK pathways are thought to be involved in the development of bone sarcomas (Xiao et al., 2013).

However, there is also evidence that supports the hypothesis that osteosarcoma arises from a more differentiated osteoblastic cell population, MSC derived osteogenic precursors (Mutsaers and Walkley, 2014). Mice expressing the c-*fos* transgene

develop spontaneous osteosarcoma which was suggested to be caused by the disruption of normal growth control and phenotype of osteoblastic cells by Fos (Grigoriadis et al., 1993). Conditional deletion of *p53* in a mouse model resulted in bone sarcoma development with the most common tumour being osteosarcoma (Lin et al., 2009). Inactivation of *p53* specifically in osteoblast precursors was shown to be sufficient for osteosarcoma formation (Berman et al., 2008). Altogether, these studies suggest that the most plausible cell type of origin of osteosarcoma are either undifferentiated MSCs or a more differentiated form of MSC derived osteogenic precursors.

1.6.2 **Clinical presentation**

The most common symptoms that patients present with are swelling and pain in the affected bone. The pain is often severe to an extent that the pain interrupts their sleep (Bielack et al., 2002, Isakoff et al., 2015). In younger patients, pain is often attributed to growing pains thereby delaying the time of diagnosis and possibly prognosis (Geller and Gorlick, 2010). At the time of diagnosis, some patients have pathological fractures and about 10-20% of patients present with macroscopic metastases mainly found in the lungs (Bielack et al., 2002, Luetke et al., 2014). The most common sites of osteosarcoma tumours are the femur, the tibia and the humerus. Only about 10% of osteosarcoma develops in the axial skeleton which are more prevalent in older patients (Luetke et al., 2014).

Osteosarcoma is diagnosed using conventional radiological imaging methods such as X-ray, magnetic resonance imaging (MRI), computed tomography (CT) and positron emission tomography (PET) followed up with a biopsy (Geller and Gorlick, 2010). In most cases serum markers are of no additional value in the diagnosis of osteosarcoma except for alkaline phosphatase (ALP) and lactate dehydrogenase (LDH) which are elevated in 40% and 30% of osteosarcoma cases respectively. Osteosarcoma often presents as a mixed osteoblastic and osteolytic lesion. Cortical destruction and ectopic bone formation in a typical sunburst pattern are common accompanying features of osteosarcoma (Geller and Gorlick, 2010).

Biopsies are essential to determine the type of osteosarcoma. Osteosarcomas are defined by the production of osteoid and several histological types of osteosarcoma are differentiated depending on their localization, high or low grade and histological

manifestation including conventional, telangiectatic and small cell osteosarcoma (Luetke et al., 2014, Klein and Siegal, 2006). The conventional type of osteosarcoma is a high-grade malignancy and comprises approximately 80-90% of osteosarcomas. The conventional type is subdivided based on the predominant features of the cell and of the extracellular matrix within the tumour. The most frequent subtypes are osteoblastic, chondroblastic and fibroblastic osteosarcoma. This subdivision of osteosarcoma has no impact on survival and treatment strategies for the three different histological types is comparable (Klein and Siegal, 2006, Bielack et al., 2009).

1.6.3 **Genetic risk factors**

There are some genetic predispositions that account for a small number of osteosarcoma cases. Among these genetic conditions are hereditary retinoblastoma, Li Fraumeni syndrome, and several syndromes that are caused by autosomal recessive mutations in the genes encoding the RECQ helicases including Werner syndrome, Rothmund-Thomson syndrome, Baller-Gerold syndrome, Rapadilino syndrome and Bloom syndrome (Wang, 2005, Gianferante et al., 2017).

Hereditary retinoblastoma, caused by an autosomal dominant germline mutation, gives rise to malignant tumours of the retina in early childhood due to mutations in the retinoblastoma gene and increases the risk of second primary tumours including osteosarcoma (Eng et al., 1993, Lohmann, 2010). In contrast, Li Fraumeni syndrome, results from mutations in *Tp53* which increases the chance on a wide range of primary tumours of which the most common are breast carcinomas, soft tissue sarcomas and osteosarcomas (Bougeard et al., 2015). Rothmund-Thomson syndrome, Baller-Gerold syndrome and Rapadilino syndrome have mutations in the RECQL4 gene whereas Werner syndrome and Bloom syndrome arise from mutations in the RECQL2 and RECQL3 helicases respectively (Wang et al., 2001, Gianferante et al., 2017). Each of these syndromes results in a higher than expected incidence of osteosarcoma but the risk of osteosarcoma development differs between the different syndromes (Gianferante et al., 2017).

1.6.4 **Treatment**

Treatment of osteosarcoma is based on tumour type, site and presence of metastasis at the time of diagnosis (Carrle and Bielack, 2006). In general there are three major therapeutic options: surgery, chemotherapy and palliative radiotherapy (Ando et al., 2013). Since osteosarcomas are relatively radio-resistant, radiotherapy is predominantly used in patients with surgically inaccessible osteosarcoma in axial sites as palliative treatment. Currently the standard for curative treatment is a combination of chemotherapy and limb-salvage surgery with the aim to maximally preserve the limb with as much function as possible (Bielack et al., 2009, Luetke et al., 2014).

Bisphosphonates, like zoledronic acid, inhibit bone resorption and have been shown to significantly reduce pain in cancer-induced bone disease (Zhu et al., 2013) potentially making these agents ideal candidates for osteosarcoma patients. Despite several studies reporting positive effects of zoledronic acid on osteosarcoma tumour growth, angiogenesis and osteosarcoma associated bone damage (Labrinidis et al., 2010, Ohba et al., 2014, Heymann et al., 2005) a trial that investigated the effects of zoledronic acid in combination with standard chemotherapy was terminated for futility. This resulted in a negative recommendation for zoledronic acid for the treatment of osteosarcoma (Piperno-Neumann et al., 2016).

Despite many other clinical trials investigating novel treatments in the form of small molecule inhibitors and immunomodulators (Heymann et al., 2016, Brown et al., 2018), the standard systemic treatment of osteosarcoma remains chemotherapy (Bielack et al., 2016). The standard chemotherapy regimens for osteosarcoma include combinations of ifosfamide, etoposide doxorubicin, methotrexate and cisplatin with the latter three often forming the basis of chemotherapeutic therapy. Combinations of these chemotherapeutic agents were found to be the most efficacious in osteosarcoma patients in both preoperative and postoperative setting (Luetke et al., 2014, ESMO, 2014, Botter et al., 2014).

1.6.5 **Prognosis**

Osteosarcoma may develop in any bone. Osteosarcoma tumours often originate in the metaphysis of the long bones, with the distal femur and the proximal tibia being the most frequent sites (Bielack et al., 2002). These sites are known to have a relatively favorable prognosis. The proximal tibia is associated with a 5-year survival rate of 77.5% which is slightly more favorable than the distal femur with a 5-year survival rate of 66%. In contrast, osteosarcomas with a proximal and axial location, e.g. spinal and pelvic osteosarcoma, have a considerably worse prognosis due to their inaccessibility for surgical removal (Ozaki et al., 2002, Ozaki et al., 2003, Bielack et al., 2002).

Osteosarcomas are known to have an aggressive clinical course, characterized by local bone, muscle and soft tissue destruction. Furthermore, osteosarcoma is characterized by a high propensity for distant metastasis to the lungs (Mutsaers and Walkley, 2014). About 30-40% of patients will develop a relapse (Kempf-Bielack et al., 2005), with the lungs as the main site of relapse (90%); although metastases also occur in bone (8-10%) and rarely in other sites (Bacci et al., 2006b). Interestingly, patients with metastasis to bone have a considerably worse prognosis in comparison to patients with lung metastasis (Bacci et al., 2006a, Aung et al., 2003).

The 5-year survival of metastatic osteosarcoma patients has not improved since the 1970s and remains around 25-30%. In contrast, the 5-year survival of primary osteosarcoma patients significantly increased with the introduction of chemotherapy in the 1970s to about 60%. There has been no further significant improvement in survival rates over the last thirty years (Allison et al., 2012), illustrating the need to investigate and develop novel therapies.

1.7 The Semaphorin class 3

Semaphorins are a large highly conserved family of secreted and membrane associated signalling proteins that are divided in 8 classess. All classess of semaphorins contain a class-specific C terminus and a conserved extracellular ~500 amino-acid semaphorin (sema) domain (Figure 1.3) (1999, Sakurai et al., 2012). The semaphorin family was initially identified through their role in axonal growth cone guidance and nerve development. (Luo et al., 1993, Kolodkin et al., 1993) Of the 8 different classess of semaphorins, semaphorin class 3-7 are expressed in vertebrates and only the class 3 semaphorins are secreted (Table 1.2) (1999).

Table 1.2 The Semaphorin family

Class	Members	Organism	Category
Sema V	A-B	Virus	Secreted
Sema 1	a-b	Invertebrate	Transmembrane
Sema 2	a	Invertebrate	Secreted
Sema 3	A-G	Vertebrate	Secreted
Sema 4	A-G	Vertebrate	Transmembrane
Sema 5	A-B	Vertebrate	Transmembrane
Sema 6	A-C	Vertebrate	Transmembrane
Sema 7	A	Vertebrate	Membrane-anchored

All class 3 semaphorins contain a Sema domain, plexin-semaphorin-integrin (PSI) domain, immunoglobulin (Ig) domain and a basic domain as their main structure and are involved in various physiological and pathophysiological processes (Yazdani and Terman, 2006, Worzfeld and Offermanns, 2014). All class-3 semaphorins are synthesized as pro-proteins and contain pro-protein convertase recognition sites, cleavage at these sites by Furin-like pro-protein convertases (FFPC) leads to peptide products of approximately 60kDA (Adams et al., 1997, Varshavsky et al., 2008).

Plexins are the primary receptors for semaphorins, they also contain a sema domain and are divided in four categories (A-D) (Tamagnone et al., 1999). In addition to plexins, class 3 semaphorins require neuropilin-1 (Nrp1) or neuropilin-2 (Nrp2) as co-receptors to initiate plexin signalling (Kruger et al., 2005). Semaphorin 3E is an exception to this rule and is able to bind and initiate signalling via plexin-D1

independent of neuropilins (Gu et al., 2005). Semaphorin 3A requires Nrp1 to transduce its signal via type A plexins (Takahashi et al., 1999). All of the secreted semaphorin class 3 proteins play an important role during embryonic development (Yazdani and Terman, 2006). Unlike the other class 3 semaphorins only Sema3C knockout results in embryonic lethallity due to impaired development of the aortic arch that is most likely caused by abnormal migration of the cardiac crest cells in Sema3C deficient mice (Feiner et al., 2001).

Only 3 members of the class 3 semaphorins are implicated in bone, Sema3A, which will be discussed later in this thesis, Sema3B and Sema3E. Sema3B is expressed by osteoblasts and overexpression of osteoblastic Sema3B *in vivo,* results in osteopenia by increased osteoclastogenesis without affecting osteoblasts (Sutton et al., 2008). Sema3E was found to be expressed by both proliferating and mineralizing osteoblasts and recombinant Sema3E reduced osteoblast migration and formation of osteoclasts *in vitro* (Hughes et al., 2012). Each semaphorin protein exerts different effects on tumour growth and metastatic spread and these effects even differ between different tumour types (Maione et al., 2012, Tamagnone, 2012). Unlike the other semaphorin 3 proteins, research carried out to this date indicates Sema3F to be a tumour suppressor across all investigated tumour types (Table 1.3).

Table 1.3 The Semaphorin class 3

Semaphorin	Receptors	Embryonic development	Bone		Cancer	References
			Expression	Function		
Sema3A	Plexin-A1 Plexin-A2 Plexin-A3 Plexin-A4 Neuropilin 1 Neuropilin 2	Axon branching in the cerebellum Dorsal muscle innervation Cardiac nerve patterning Vascular patterning of the kidney and cerebral microvessel density	Osteoblast Chondrocyte	↑Osteoblast ↓Osteoclast ↑Bone formation ↓Bone resorption	Tumour suppressive/promoting effects - Increased glioblastoma dispersal - Increased motility of pancreatic cancer - Increased progression in liver cancer - Reduced invasiveness of prostate cancer - Reduced breast tumour growth - Reduced melanoma tumour growth - Reduced oral tumour growth - Inhibitor of angiogenesis	(Kolodkin et al., 1997, Chen et al., 1997, Nasarre et al., 2009, Takahashi et al., 1999, Rohm et al., 2000a, Tamagnone et al., 1999, Schwarz et al., 2008, Hayashi et al., 2012, Cioni et al., 2013, Masuda et al., 2013, Messersmith et al., 1995, Behar et al., 1996, Ieda et al., 2007, Reidy et al., 2009, Hou et al., 2015, Li et al., 2015a, Lee et al., 2017, Muller et al., 2007, Bagci et al., 2009, Hu et al., 2016, Casazza et al., 2011, Mishra et al., 2015b, Chakraborty et al., 2012, Huang et al., 2017, Xu, 2014)
Sema3B	Plexin-A2 Plexin-A4 Neuropilin 1 Neuropilin 2	Positioning of the anterior commissure in the brain	Osteoblast Osteoclast	↑Osteoclast	Tumour suppressive/promoting effects - Inhibits ovarian tumour growth - Reduced expression lead to esophageal lymph node metastasis - Inhibited breast tumour growth - Inhibited lung tumour growth - Increased metastasis in breast and lung cancer	(van der Weyden et al., 2005, Varshavsky et al., 2008, Sharma et al., 2012, Sabag et al., 2014, Falk et al., 2005, Sutton et al., 2008, Joseph et al., 2010, Castro-Rivera et al., 2004, Castro-Rivera et al., 2008, Tse et al., 2002, Tang et al., 2016, Rolny et al., 2008).

Sema3C	Plexin-A2 Neuropilin 1 Neuropilin 2	Aortic arch development	-	Tumour promoting effects - Reduced expression inhibited gastric tumour growth - Reduced expression inhibited breast cancer cell migration - Increased expression lead to shorter overall survival in glioma	(Feiner et al., 2001, Chen et al., 1997, Takahashi et al., 1998, Brown et al., 2001, Miyato et al., 2012, Zhu et al., 2017, Vaitkiene et al., 2015)
Sema3D	Neuropilin 1	Development of the heart, pulmonary vein connections and patterning and thymus	-	Tumour suppressive/promoting effects - Reduced glioblastoma tumour growth - Correlated with improved survival in colorectal cancer patients - Reduced expression inhibited prostate cancer metastasis	(Feiner et al., 1997, Wolman et al., 2004, Degenhardt et al., 2013, Takahashi et al., 2008, Sabag et al., 2012, Wang et al., 2017b, Foley et al., 2015)
Sema3E	Plexin-D1	Intersomitic vascular development, striatum synapse formation and vascular patterning	Osteoblasts ↓Osteoclast ↓Osteoblast migration	Tumour suppressive/promoting effects - Correlated with metastasis in colorectal and breast cancer tumours - Correlated with melanoma progression - Poor overall survival in pancreatic patients - Expression reduced gastric cancer tumour burden - Reduced expression inhibited gastric cancer growth - Reduced expression inhibited metastasis in breast cancer - Overexpression inhibited tumour	(Gu et al., 2005, Ding et al., 2011, Hughes et al., 2012, Casazza et al., 2010, Luchino et al., 2013, Casazza et al., 2012, Yong et al., 2016, Chen et al., 2015, Maejima et al., 2016)

				growth in colon, melanoma and lung cancer	
Sema3F	Plexin-A1 Plexin-A2 Plexin-A3 Plexin-A4 Neuropilin 1 Neuropilin 2	Development of cranial nerves and limbic system tracts	-	Tumour suppressive effects - Inhibited ovarian tumour formation - Inhibited tumour angiogenesis - Inhibited growth and metastasis in colorectal carcinoma - Inhibited gastro-intestinal neuroendocrine tumours and metastasis - Anti-lymphangiogencic factor	(Takahashi and Strittmatter, 2001, Waimey et al., 2008, Chen et al., 1997, Renzi et al., 1999, Nasarre et al., 2003, Sahay et al., 2003, Matsuda et al., 2010, Xiang et al., 2002, Kessler et al., 2004, Futamura et al., 2007, Wu et al., 2011, Bollard et al., 2015, Doci et al., 2015).
Sema3G	Neuropilin 2	No abnormalities or morphological defects described	-	- Inhibited motility of glioblastoma	(Taniguchi et al., 2005, Zhou et al., 2012).

1.7.1 **Plexins**

Plexins are large membrane proteins that are organized in four classess (A-D). Plexins contain a highly conserved intracellular domain, an extracellular domain that shares homology with scatter factor receptors as well as a semaphorin binding domain (Tamagnone et al., 1999). The intracellular region of plexins contains two segments that are separated by an insertion region, that when these two segments are folded together they exhibit an intrinsic GTPase activating protein (GAP) activity (Figure 1.3) (Rohm et al., 2000b, Tong et al., 2009, Sakurai et al., 2012). The cytoplasmic region of the plexins have been reported to bind to over 20 proteins to transduce signalling and depending on the plexin class displays different substrate specificity (Pascoe et al., 2015).

The semaphorin-plexin system is important for a wide variety of adult physiological functions predominantly in angiogenesis, the immune system and nervous system (Pasterkamp, 2012, Kumanogoh and Kikutani, 2013, Neufeld et al., 2012). Besides physiological processes, the semaphorin-plexin system has also been implicated in immune disorders and tumour growth and metastasis (Takamatsu and Kumanogoh, 2012, Tamagnone, 2012). While semaphorin receptor gene mutations in cancer tend to be rare (Tamagnone, 2012), overexpression of Plexin-B1 was found in the majority of primary prostate cancer samples and more important 89% of prostate cancer bone metastases showed mutations in Plexin-B1 (Wong et al., 2007). In contrast, in breast cancer, low expression of Plexin-B1 was associated with poor survival (Malik et al., 2015).

1.7.2 **Neuropilin**

Neuropilins are transmembrane cell surface receptors of approximately 130-140kDa. The neuropilin family in vertebrates consists of only 2 members; Nrp1 and Nrp2 that share the same overall domain structure of a large extracellular domain, a short transmembrane domain and a short intracellular domain (Parker et al., 2012, Geretti et al., 2008). The extracellular domains of the neuropilins are divided into three domains A-C, each domain containing binding properties for different ligands (Figure 1.3) (Geretti et al., 2008, Sakurai et al., 2012). Neuropilins are receptors for the vascular endothelial growth factor (VEGF) family and the class-3 semaphorins (Kolodkin et al., 1997, Chen et al., 1997, Soker et al., 1998, Karpanen et al., 2006).

Due to their importance in semaphorin class-3 and VEGF signalling, neuropilins are involved in a wide variety of physiological and pathological processes. Mice deficient in Nrp1 die *in utero* most likely due to cardiovascular defects and abnormalities seen in the projection of spinal and cranial nerves, limb innervation and abnormal hindbrain vascular sprouting (Kitsukawa et al., 1997, Gerhardt et al., 2004). Furthermore, the vessel formation of the yolk sac was also impaired which may contribute to the *in utero* death of Nrp1 deficient mice (Kawasaki et al., 1999, Jones et al., 2008). As expected, Nrp1 deficient embryos have severe defects in the branchial arteries, heart outflow tracts and exhibit disrupted blood flow (Kawasaki et al., 1999, Jones et al., 2008). Mice expressing a Nrp1 variant that lacks the Semaphorin binding site but express an intact VEGF binding site display predominantly nervous system defects without obvious vascular abnormalities. This indicates that the vascular defects are probably attributed to impaired Nrp1-VEGF signalling (Gu et al., 2003, Piper et al., 2009). This hypothesis is further strengthened by the vascular defects seen in mice with specific deletions of Nrp1 in the endothelial cells (Gu et al., 2003, Mukouyama et al., 2005).

In contrast to Nrp1 deficient mice, Nrp2 deficient mice are viable into adulthood even though there is an increased mortality rate. However, Nrp2 deficient mice display a range of nervous system defects including impaired cranial and spinal nerve projection and several brain defects (Giger et al., 2000). Nrp2 deficient mice show impaired motor function and object memory that are most likely the result of the hippocampal brain defects (Shiflett et al., 2015). Although no large vascular abnormalities or collecting lymph duct defects have been associated with Nrp2 deficiency, mice lacking Nrp2 have a reduced number of lymphatic vessels and in some cases absence of small lymphatic vessels (Yuan et al., 2002).

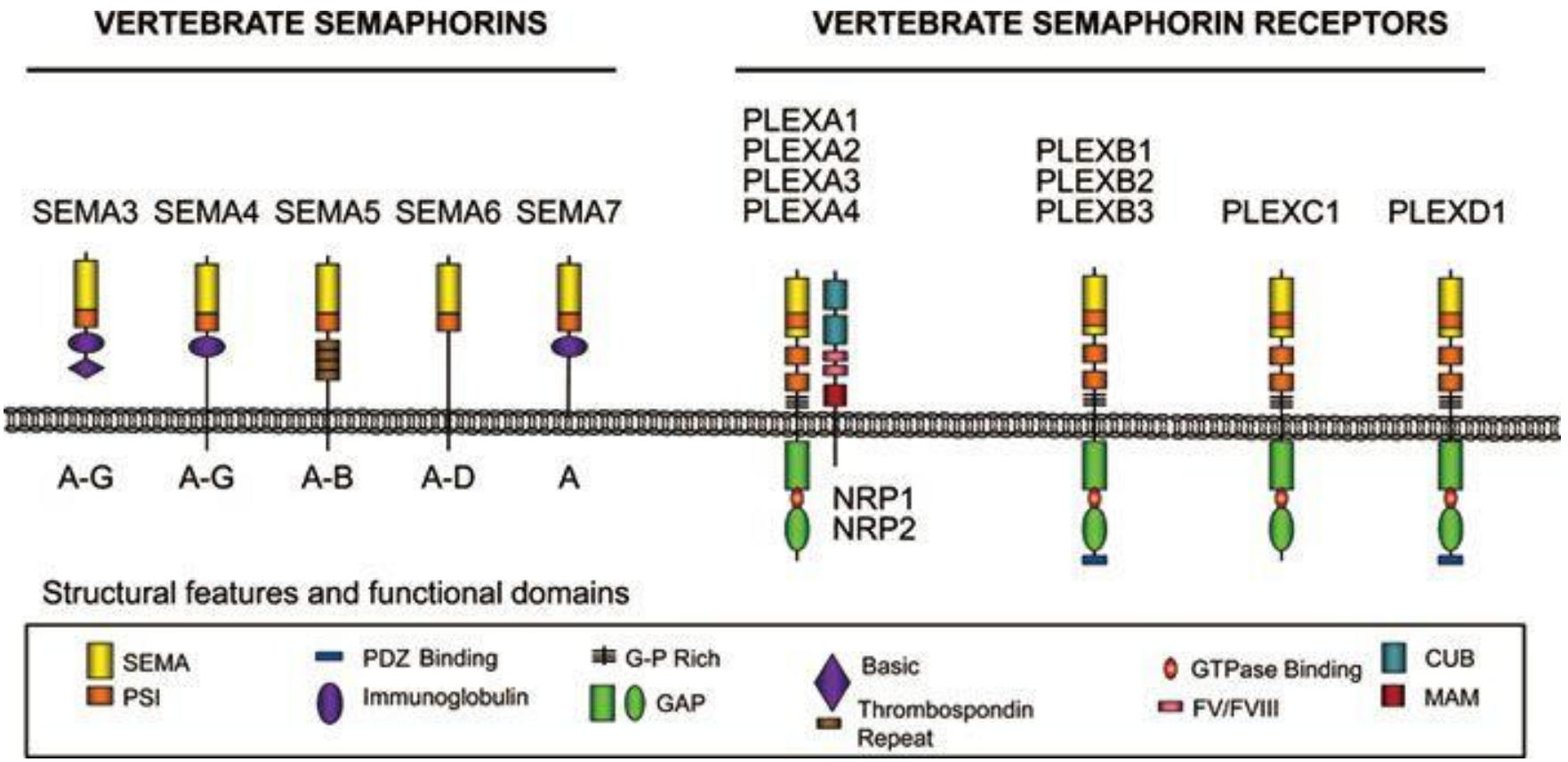

Figure 1.3 Structure of semaphorins and semaphorin receptors.
Semaphorins class 3-7, plexin A-D and Nrp 1 and Nrp2 are expressed in vertebrates. All semaphorins and plexins contain a Sema and PSI domain. The semaphorins contain class specific functional domains such as immunoglobulin domains. Neuropilins have intrinsic GAP activity and are required to transducer semaphorin signals via the plexins. Image is adapted from (Sakurai et al., 2012) see appendix section 10.6.

1.8 Semaphorin 3A

Semaphorin 3A (Sema3A), a member of the class 3 semaphorins, is synthesized as a precursor protein (~125kDa) (Adams et al., 1997). The precursor protein is then proteolytically processed into two active proteins of 95kDa and 65kDa that are both secreted (Adams et al., 1997, Klostermann et al., 1998, Catalano et al., 2006). The 65kDa isoform of Sema3A elicits reduced repulsive activity in comparison to the 95kDa isoform, the proposed mechanism for this difference is the absence of the COOH-terminal which is required for association of Sema3A homodimers (Klostermann et al., 1998).

1.8.1 **Semaphorin 3A receptors**

Sema3A binds to Nrp1 with high affinity and lower affinity to Nrp2 (Kolodkin et al., 1997, Chen et al., 1997). Nrp1 is essential for Sema3A signalling as demonstrated by absence of chemorepulsive activity in the presence of Nrp1 blocking antibodies (Chedotal et al., 1998). While Sema3A was shown to bind to Nrp2 with low affinity, one study found that blocking Nrp2 signalling was sufficient to remove the effect of Sema3A on a glioma cell line *in vitro* (Nasarre et al., 2009). This study suggest that Sema3A signals via Nrp2 in a cell type specific manner, which may explain the limited number of studies reporting functional Sema3A/Nrp2 signalling.

Sema3A signals via the class A plexins together with Nrp1. Nrp1 forms a receptor complex together with plexin-A1 allowing for Sema3A signalling as illustrated by the absence of Sema3As chemorepellent activity when a truncated Plexin-A1 was present (Takahashi et al., 1999, Rohm et al., 2000a, Tamagnone et al., 1999). A similar lack of effect to Sema3A was observed in sensory ganglia when a dominant-negative form of plexin-A2 was introduced (Rohm et al., 2000a). While plexin-A1 and plexin-A2 are important for Sema3A signalling, plexin-A3 and plexin-A4 were also shown to transduce Sema3A signals as plexin-A3 or plexin-A4 knockout mice showed aberrant facial axon branching (Schwarz et al., 2008).

1.8.2 **Semaphorin 3A signalling**

1.8.2.1 Axons

The downstream signalling of Sema3A causes actin reorganization in neurons, how this process is regulated remains to be elucidated. FERM, RhoGEF and Pleckstrin Domain Protein 2 (FARP2) proved to be essential in Sema3A-mediated axonal repulsion. FARP2 binds to plexin-A1 with mediation of Nrp1 and upon Sema3A stimulation, FARP2 activates Rac which is required for Sema3A-induced growth cone collapse (Toyofuku et al., 2005). Sema3A was found to induce dephosphorylation and activation of the actin degrading enzyme cofilin via the regulator LIM kinase-1 (LIMK1) (Aizawa et al., 2001). There is evidence to suggest that this process is regulated by Sema3A induced Rac-1 activation.

In neurons, Sema3A also activates other intracellular pathways via tyrosine kinases that regulate microtubule dynamics and reorganization of actin. Sema3A induces tyrosine and serine phosphorylation of focal adhesion kinase (FAK) which is essential for dendritic growth in both newborn and adult neurons and is likely to be dependent at least in part on cyclin dependent kinase 5 (Cdk5) (Ng et al., 2013). Cdk5 activation by Sema3A also leads to phosphorylation of collapsin response mediating protein 2 (CRMP2). The phorphorylation of CRMP2 by Cdk5 conveys a structural change allowing Sema3A activated GSK3β to phosphorylate CRMP2, dual-phosphorylated CRMP2 in turn regulates microtubule organization (Eickholt et al., 2002, Uchida et al., 2005, Neufeld and Kessler, 2008).

Although the exact molecular mechanisms are still unclear, in endothelial and neuronal cells, Sema3A has been implicated to induce apoptosis via inhibition of downstream signalling of extracellular signal-regulated kinases (ERK) 1 and ERK 2 and activation of caspase 3 (Neufeld and Kessler, 2008). Sema3A signalling was also implicated in apoptosis of chondrocytes in osteoarthritis via inhibition of the phosphatidylinositol-4,5-bisphosphate 3-kinase(PI3K)/ AKT serine/threonine kinase (AKT) (Sun et al., 2018). These studies suggest the involvement of PI3K/AKT and ERK signalling pathways in the regulation of apoptosis by Sema3A.

Vascular endothelial growth factor (VEGF) is essential for blood vessel formation and plays an important role in physiological and pathological processes (Yancopoulos et al., 2000). The main receptors for VEGF are vascular endothelial growth factor receptor (VEGFR)-1, VEGFR-2 and VERGFR-3 and Nrp1 and Nrp2 function as co-receptors (Yancopoulos et al., 2000, Coultas et al., 2005).

Nrp1 binds to some of the members of the class-3 semaphorins, including Sema3A, with the extracellular A and B binding domains and also binds to members of the VEGF family with the B domain. The interaction of both ligands with the B domain suggests overlapping binding sites that could result in functional competition (Geretti et al., 2008). Both Sema3A and VEGF binding to Nrp1 has also been shown to induce internalization of the Nrp1 thereby reducing available Nrp1 for further ligand binding by either VEGF or a Sema3 protein (Narazaki and Tosato, 2006).

Sema3A and VEGF have been shown to compete for Nrp1 binding leading to competition of effects on endothelial cell motility, chemorepulsive activity on dorsal root ganglions and migratory and apoptotic effects in a neuroectodermal progenitor cell line (Miao et al., 1999, Bagnard et al., 2001). The Sema3A/VEGF balance is essential for correct development of the facial nerves where the relationship between these proteins work in corporation, Sema3A is essential for the axon guidance whereas VEGF is required for the somata positioning within the neural tube (Schwarz et al., 2004)

1.8.2.2 Osteoblasts

The molecular mechanisms of Sema3A are not fully understood. Sema3A deficiency resulted in a suppressed wnt3a induced β-catenin accumulation and an inhibited wnt3a induced activation of Rac but not RhoA in calvarial cells (Hayashi et al., 2012). The canonical Wnt pathway is known to promote osteoblast differentiation and inhibit adipocyte differentiation (Krishnan et al., 2006). Sema3A induced Rac activation was suggested to be regulated by FARP2 (Toyofuku et al., 2005). In support of this, introduction of a dominant negative form of FARP2 inhibited osteoblast differentiation of calvarial cells even in the presence of Sema3A, indicating that Sema3A stimulates the canonical Wnt pathway through the FARP2 induced Rac activation during osteoblast differentiation (Figure 1.4) (Hayashi et al., 2012).

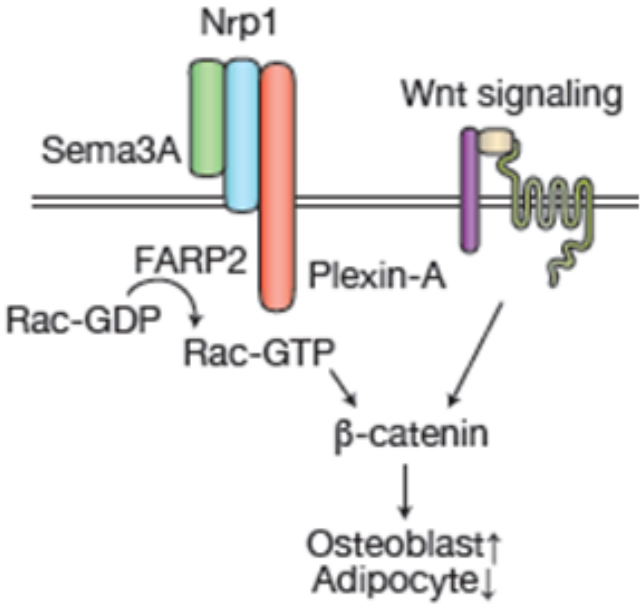

Figure 1.4. Mechanism of Sema3A in promoting osteoblast differentiation.
Upon binding to Nrp1 and Plexin-A, Sema3A initiates FARP2 induced Rac activation thereby stimulating the canonical Wnt induced β-catenin accumulation during osteoblast differentiation. Adapted from (Hayashi et al., 2012) see appendix section 10.6.

1.8.2.3 Osteoclasts

Interestingly while Sema3A stimulates the canonical Wnt pathway through FARP2 in osteoblasts (Hayashi et al., 2012), FARP2 was found to be essential for osteoclast podosome rearrangements and osteoclast resorbtion (Takegahara et al., 2010). Takegahara and colleagues showed that FARP2 osteoclast deficiency reduced osteoclast formation and resorption pits (Takegahara et al., 2010). Sema3A inhibits osteoclastogenesis by sequestering plexin-A1 for the plexinA1-Nrp1-Sema3A complex, however; after RANKL stimulation the expression of Nrp1 is downregulated, thereby releasing plexin-A1 from the plexinA1-Nrp1-Sema3A complex to form the plexinA1-TREM2-DAP12 complex to mediate osteoclast differentiation (Figure 1.5) (Hayashi et al., 2012). In osteoclasts plexin-A1 promotes osteoclastogenesis by the association of plexin-A1 with TREM2-DAP12 in response to ligands such as Sema6D thereby activating the immunoreceptor tyrosine-based activation motif (ITAM) signal (Takegahara et al., 2006). However, plexinA1 was found to be constitutively associated with Nrp1 (Takahashi and Strittmatter, 2001).

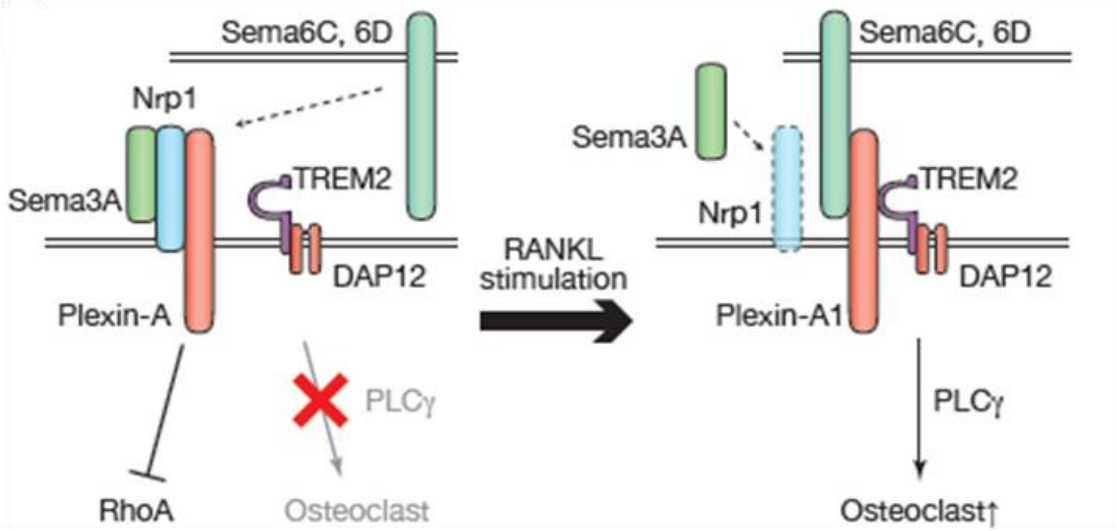

Figure 1.5. Mechanism of inhibition of osteoclastogenesis by Sema3A.
Sema3A sequesters plexinA1 and Nrp1 thereby preventing the formation of the plexinA1-TREM2-DAP12 required for osteoclastogenesis. Upon RANKL stimulation, Nrp1 expression is downregulated, leading to release of plexinA1. Adapted from (Hayashi et al., 2012) see appendix section 10.6.

1.8.3 **Semaphorin 3A in embryonic development**

Initially Sema3A was characterized for its function as a chemorepellent for axons during neuronal development, however; Sema3A is also widely expressed in other organs such as the heart and bones and shown to be essential for their development (Messersmith et al., 1995, Behar et al., 1996). Sema3A knockout mice are viable but only a small percentage of mice reach adulthood (Behar et al., 1996). Sema3A deficient mice exhibit many developmental abnormalities in the nervous system such as reduced terminal axon branching in the cerebellum and impaired dorsal muscle innervation (Cioni et al., 2013, Masuda et al., 2013). Furthermore, Sema3A knockout mice have abnormal trajectory of spinal and cranial nerves during early development that are corrected during further embryonic development (White and Behar, 2000, Taniguchi et al., 1997). However Sema3A deficient mice have abnormal adult olfactory bulb spatial arrangement of nerves and neonatal mice displayed reduced branching of cortical dendrites (Taniguchi et al., 2003, Fenstermaker et al., 2004), suggesting that not all nerve abnormalities caused by Sema3A deficiency are corrected during late embryonic development.

Sema3A deficiency leads to hypertrophy of the right atrium and ventricle of the heart which might be due to the abnormal cardiac sympathetic nerve patterning (Behar et al., 1996, Ieda et al., 2007). Abnormalities were also seen in the vascular patterning of the kidney and the cerebral microvessel density and vascular permeability (Reidy et al., 2009, Hou et al., 2015). As Sema3A is a competitor for VEGF, the underlying mechanism for the vascular abnormalities observed in Sema3A deficient mice could be due to an imbalance in VEGF versus Sema3A signalling rather than the absolute expression of both proteins.

1.8.4 **Semaphorin 3A in bone metabolism**

Behar and colleagues reported that Semaphorin III (Sema3A) was vital for normal development of nerves and heart using a Sema3A knock out mouse model. In addition to abnormal neuron migration and axon guidance, a Sema3A deficit lead to abnormalities in bone development (Behar et al., 1996). In the skeleton, Sema3A, plexinA1, plexinA2 and Nrp1 were found to be expressed by osteoblasts and osteoclasts, however, Sema3A expression was absent in osteoclasts. In addition, chondrocytes were also shown to express Sema3A, Nrp1 and both plexin A1 and plexin A2 during differentiation. Sema3A and Nrp1 were shown to be coexpressed during all stages of endochondral ossification by chondrocytes and osteoblasts (Gomez et al., 2005).

Hayashi and colleagues reported a severe low bone mass phenotype in Sema3A deficient mice. A similar phenotype was observed in $Nrp1^{sema-}$ knock-in mice, in which the Nrp1 lacks the Semaphorin binding domain. These mice displayed a severe low bone mass in both trabecular and cortical bones. Osteoblastic bone formation was decreased and accompanied by an increase in osteoclast number and resorption (Hayashi et al., 2012). Implicating that the bone abnormalities are in fact caused by absent Sema3A signaling rather than an imbalance in VEGF/Sema3A. Interestingly like the $Nrp1^{sema-}$ knock-in mice, Nrp2 deficient mice show a low bone mass phenotype characterized by reduction in trabecular bone volume and an increase in bone resorption accompanied by a reduction in osteoblast numbers (Verlinden et al., 2013). However, it is unclear whether the effect seen in Nrp2 deficient mice is linked to VEGF or Semaphorin signaling.

Sema3A administration decreased bone loss in ovariectomized mice by inhibition of bone resorption and promotion of bone formation. These results indicate a possible therapeutic application due to the osteoprotective role of Sema3A by binding to Nrp1 and as a result, stimulating bone formation and differentiation of osteoblasts and suppress bone resorption by inhibition of osteoclastogenesis (Figure 1.6) (Hayashi et al., 2012). In further support of this, a more recent study showed that local injection of Sema3A promoted fracture healing and callus remodeling in a rat model of osteoporosis (Li et al., 2015a).

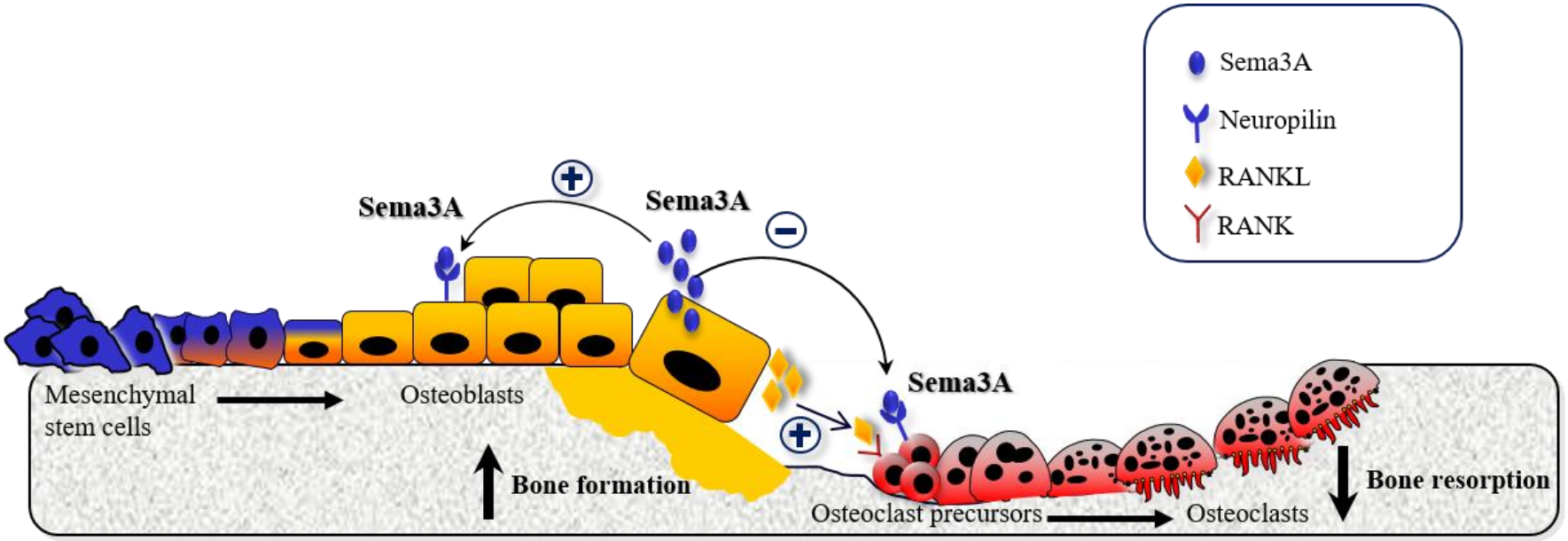

Figure 1.6. Sema3A-mediated regulation of bone remodeling.
Sema3A is produced by osteoblasts. Sema3A inhibits RANKL induced osteoclast formation and also directs osteoblast lineage cells towards osteoblast differentiation.

Fukuda and colleagues confirmed the anti-osteoclast and pro-osteoblast effect of Sema3A, however, they suggested that the absence of Sema3A expression in osteoblasts is not the sole and primary cause of bone abnormalities in Sema3A deficient mice. Mice with osteoblast specific Sema3A deficiency showed normal bone formation and bone mass. In contrast, a Sema3A deficiency specifically in neurons caused significant reductions in bone mass in both male and female mice (Fukuda et al., 2013). Altogether these studies imply an important role of Sema3A in osteoblast differentiation and bone formation and may present a novel therapeutic agent in skeletal bone remodeling disorders (Xu, 2014).

1.8.5 **Semaphorin 3A and pain**

Sema3A reduces part of nerve growth factor (NGF) induced pain responses, but was found to be unable to fully prevent progression of neuropathic pain in a rat model (Tang et al., 2004). Tanelian and colleagues observed that expression of Sema3A in rabbit corneal epithelial cells caused repulsion of A-delta and C fiber trigeminal sensory afferents in normal corneas and inhibited entry of nerve sprouts in the wounded cornea (Tanelian et al., 1997).

Hayashi and colleagues showed that administration of Sema3A intrathecally after peripheral nerve injury in rats prevented the development of neuropathic pain-related behaviour such as mechanical and heat hypersensitivities (Hayashi et al., 2011). However, Sema3A had no effect on sprouting of myelinated nerve terminals suggesting that the inhibition of neuropathic pain of Sema3A may be due to a more complicated mechanism than just morphological changes of nerve terminals. In contrast to these observations, Maeda and colleagues showed that Sema3A knockdown in lung cancer cells significantly attenuated the decline in weight bearing of the hind leg (Maeda et al., 2016). However, this result might be predominantly due to a reduction in tumour burden rather than a direct effect on pain responses.

1.8.6 **Semaphorin 3A in cancer**

Sema3A has been shown to affect tumour cell behavior in various cancers. Expression of Sema3A promoted glioblastoma multiforme spread via Nrp1 in an autocrine manner and treatment with Sema3A antibodies inhibited glioblastoma growth in a patient derived xenograft model (Lee et al., 2017). Furthermore, Sema3A enhanced cancer progression in hepatocellular carcinoma and increased invasiveness and scattering of pancreatic tumour cells (Muller et al., 2007, Bagci et al., 2009, Hu et al., 2016). Expression of Sema3A in patient samples was also correlated with a poor prognosis in pancreatic cancer and liver cancer patients (Muller et al., 2007, Hu et al., 2016).

In contrast, decreased Sema3A expression was correlated with poor prognosis in non-small cell lung cancer patients and overexpression of Sema3A reduced the invasiveness of prostate cancer cells (Herman and Meadows, 2007, Zhou et al., 2014). Inhibition of Nrp1 expression, a reduced Sema3A expression or a plexin-A1 dominant negative mutant, enhanced breast cancer cell migration. These results indicate an autocrine pathway involving Sema3A, plexin-A1 and Nrp1 that disrupts the chemotaxis of breast carcinoma cells (Bachelder et al., 2003). Furthermore, overexpression of Sema3A in breast cancer cells significantly reduced breast cancer cell motility and suppressed breast tumour growth *in vivo* (Pan and Bachelder, 2010, Mishra et al., 2015b).

Overexpression of Sema3A in 4T1, 66cl4 mammary carcinoma and MDA-MB-435 melanoma cells did not affect proliferation or survival *in vitro*, however; *in vivo* tumour growth was significantly inhibited due to inhibition of tumour angiogenesis (Casazza et al., 2011). Reductions in tumour growth were also reported in melanoma tumours and oral cancer tumours after Sema3A overexpression (Chakraborty et al., 2012, Huang et al., 2017). These contrasting observations in different tumour types might be explained due to differences in receptor expression and signalling pathways involved in different cell types. Bones are a common site of metastasis for both breast and prostate cancer. Sema3A expression was shown to be involved in the pro-osteoblastic activity of C4-2 prostate cancer cells (Liu et al., 2015). A similar effect was observed in the MCF-7 breast cancer cells where knock down of Sema3A significantly decreased osteoblastic differentiation (Shen et al., 2015).

The balance between Sema3A and VEGF expression has also been implicated in cancer. A high VEGF/Sema3A ratio was correlated with higher recurrence rate in meningioma and Catalano and colleagues have shown that VEGF increased Sema3A expression in mesothelial cells but this negative regulatory pathway was absent in malignant mesothelial cells (Catalano et al., 2004, Barresi and Tuccari, 2010).

1.8.7 **Neuropilin receptors in osteosarcoma**

The role of Sema3A in osteosarcoma remains unknown. However, there are indications of the involvement of neuropilins in osteosarcoma. RANKL, a key regulator in bone metabolism, affects RANK positive human osteosarcoma cell line Saos-2 by upregulation of genes affected by RANKL, including upregulation of Sema3A, and downregulation of genes implicated in protein metabolism, nucleic acid metabolism, intracellular transport and cytoskeleton organization (Mori et al., 2006). Nrp1 was found to be overexpressed in osteosarcoma tissue when compared to non-cancerous bone tissues and was reported to be an independent factor for predicting prognosis (Zhu et al., 2014).

Nrp2 was overexpressed in several osteosarcoma cell lines in comparison to normal osteoblasts. Furthermore, Nrp2 knockdown inhibited *in vivo* tumour growth, due to inhibited vessel formation (Ji et al., 2015). Nrp2 expressing osteosarcoma tumours showed increased vascularity and showed a poorer prognosis (Handa et al., 2000). Another study by Boro and colleagues showed that patients with Nrp2 but not Nrp1 positive osteosarcoma have a significantly shorter overall survival (Boro et al., 2015). However, it is unclear whether these observations are predominantly due to Sema3A signalling. As discussed previously in section 1.7.2 and section 1.8.2.1, both Nrp1 and Nrp2 are also involved in vascular endothelial growth factor (VEGF) signalling and angiogenesis (Guo and Vander Kooi, 2015). Altogether, the overexpression of Nrp1 and Nrp2 could contribute to tumour progression by enhanced vascularity of the tumour rather than Sema3A signalling.

1.9 Aims of this study

Sema3A enhances osteoblast differentiation and increases bone formation. Several studies have implicated Sema3A in tumour motility and growth. Moreover, the Sema3A receptors have been implicated in osteosarcoma but the effects of recombinant and tumour-derived Sema3A on osteosarcoma remains unknown.

We hypothesize that overexpression of Sema3A in osteosarcoma cells and treatment with human recombinant (exogenous) Sema3A inhibits osteosarcoma cell growth, metastasis and ability to cause osteolysis and ectopic bone formation in mice.

The specific aims of the work reported in this thesis are:

- To investigate whether treatment with exogenous Sema3A or overexpression of Sema3A (osteosarcoma-derived) in osteosarcoma cells affects:
    - The viability, migration and invasion, alkaline phosphatase activity and ability to influence osteoclastogenesis of osteosarcoma cells in a panel of osteosarcoma cell lines *in vitro*.
    - Osteosarcoma tumour growth, metastasis, bone damage and ectopic bone formation *in vivo*.
    - Osteosarcoma-associated osteolysis and osteoclast formation.
    - Osteosarcoma-associated ectopic bone formation and osteoblast activity and differentiation.
- To investigate the effects of Sema3A on cell signalling pathways and cytokine production by examining the effects of:
    - Osteosarcoma-derived Sema3A on osteoblast Wnt/β-catenin signalling.
    - Overexpression of Sema3A on osteosarcoma cytokine production.

CHAPTER TWO

Materials and Methods

2 Material and methods

2.1 Cell culture medium

Mouse MC3T3-E1 clone 4 and RAW 264.7 cell lines (table 2.1) were purchased from (ATCC, Manassas, VA, USA). Tissue culture medium (DMEM and alpha-MEM) was obtained from Gibco, Thermofisher (Leicestershire, UK). Human osteosarcoma cells (section 2.4.1 and table 2.1) were cultured in DMEM Glutamax (Gibco, UK) supplemented with 10% fetal calf serum (FCS), 100U/ml penicillin and 100 μg/ml streptomycin (standard DMEM). Mouse cell lines MC3T3-E1, RAW 264.7, mouse bone-marrow (BM), murine calvarial osteoblasts and murine osteoclasts were cultured in αMEM Glutamax supplemented with 10% fetal calf serum (FCS), 100U/ml penicillin and 100 μg/ml streptomycin (standard αMEM).

2.1.1 **Cell culture conditions**

Cell culture was performed in laminar flow cabinets which were sprayed with 70% IMS. All solutions were warmed to 37ºC before use. Pre-sterilized or autoclaved plastic ware supplied by various manufacturers was used. Cultures were maintained under standard conditions of 5% CO2: 95% air at 37 ºC in a humidified atmosphere, unless stated otherwise. Phase-contrast microscopy was used to observe cells throughout the culture period.

Table 2.1 Cell lines utilized in this thesis

Cell line	Species	Cell type
MC3T3-E1	Mouse	Preosteoblast
RAW 264.7	Mouse	Macrophage
MG-63	Human	Osteosarcoma, male origin
Saos-2	Human	Osteosarcoma, female origin
MNNG/HOS	Human	Osteosarcoma, female origin
KHOS	Human	Osteosarcoma, female origin

2.2 Bone marrow and monocyte cultures

Bone marrow cells were isolated, cultured and TRAcP stained as previously described by (Marino et al., 2014).

2.2.1 **Isolation of bone marrow cells**

Bone marrow cells were isolated from the tibia and femur of 8-12 week old C57BL/6 female mice sacrificed by cervical dislocation according to Schedule 1 of the Animals (Scientific Procedures) Act (University of Edinburgh, United Kingdom) as previously described by (Marino et al., 2014). Due to previous collaboration of Dr Idris with the University of Edinburgh during the first year of my research, pups for osteoblasts and osteoclasts were sacrificed in Edinburgh by the animal house staff and calvaria and legs were transported to Sheffield for further research each time Dr Silvia Marino or Dr Aymen Idris visited the Edinburgh facilities. Sterilized equipment was used and bone marrow cell isolation was performed in a laminar flow hood. Freshly isolated hind legs were placed in a Petri dish. Soft tissue was removed with a scalpel and the ends of the bone were cut in order to expose the bone marrow. The long bones were transferred to a petri dish containing standard αMEM and the bone marrow cells were extracted using a 5 ml syringe with a 25 gauge (G) needle containing standard αMEM to flush the bone marrow. A single cell suspension was obtained by passing the bone marrow cells through needles of decreasing size (19G - 25G). The cell suspension was collected in a 15 ml tube and centrifuged at 1200rpm for 3 minutes. The pellet was resuspended in standard αMEM and plated in 96 well plates supplemented with 25ng/ml M-CSF and 100ng/ml RANKL. Cultures were kept under standard condition. Protocols adapted from (Edinburgh thesis S. Marino).

2.2.2 **RANKL and M-CSF generated osteoclasts in coculture with osteosarcoma cells**

The bone marrow cultures that were plated in 96 well plates (see previous section) were left to adhere for 24 hours. After 24 hours, 50 µl medium was added with consisting of standard αMEM supplemented with 100ng/ml RANKL and 25ng/ml M-CSF and the cultures were treated with the desired compounds to assess the effect of Sema3A on osteoclast formation in the presence of osteosarcoma cells or osteosarcoma cell conditioned medium (100 osteosarcoma cells or conditioned

medium (20%) in presence of 300 ng/ml Sema3A or vehicle) for 48 hours. After 48 hours 33% of the medium was removed and replaced by fresh medium supplemented 100ng/ml RANKL and 25ng/ml M-CSF, in case of cultures treated with Sema3A, 300 ng/ml Sema3A was added and in case of cultures with conditioned medium, conditioned medium (20%) was added. After 6-7 days of culture, cells were rinsed with phosphate-buffered saline (PBS) and fixed with 4% paraformaldehyde. Osteoclasts were identified using TRAcP staining (section 2.2.5) and counted to assess the effect of Sema3A on osteoclast formation in the presence of osteosarcoma cells or conditioned medium derived from osteosarcoma cells.

2.2.3 **RAW 264.7 differentiation into osteoclasts in the presence of osteosarcoma or osteoblast cells**

The RAW264.7 cell line was used in these experiment for its potential to differentiate and fuse into osteoclasts. To assess the effect of Sema3A on osteoclast formation in the presence of MC3T3-E1 or osteosarcoma MG-63 cells, RAW 264.7 cells were plated at 400 cells/well in 96 well plates. After 24 hours in standard DMEM, medium was removed and MC3T3-E1 (500cells/well) or MG-63 (500cells/well) were added to the wells supplemented with 50 ng/ml RANKL and vehicle (PBS) or Sema3A 300 ng/ml. Every 48 hours, 50% of the medium was replaced with standard DMEM supplemented with 50 ng/ml RANKL and vehicle (PBS) or Sema3A 300 ng/ml. After 5 days cells were rinsed with PBS and fixed with 4% paraformaldehyde. Osteoclasts were identified using TRAcP staining (section 2.2.5) and counted to assess the effect of Sema3A on osteoclast formation in the presence of MC3T3-E1 preosteoblasts or MG-63 osteosarcoma cells.

2.2.4 **Culture fixation**

At the time of termination of osteoclast cultures, the culture medium was removed and the cells were rinsed with PBS and fixed with 4% (v/v) paraformaldehyde (150µl per 96 well). Paraformaldehyde was removed and cells were washed with PBS before addition of 200 µl of 70% (v/v) ethanol and stored at 4°C.

2.2.5 **Tartrate-resistant Acid Phosphatase (TRAcP) staining**

Multinucleated osteoclasts were identified using Tartrate-resistant Acid Phosphatase (TRAcP) staining as previously described (Marino et al., 2014). The TRAcP staining solution was freshly prepared (Appendix 10.5). Briefly, cells were fixed with 4%

paraformaldehyde for 10 minutes and washed with PBS before 100 µl of TRAcP staining solution was added to each well, plates were then incubated at 37˚C for 30-60 minutes. TRAcP staining solution was removed and cells were rinsed twice with sterile PBS and stored in 200 µl in 70% (v/v) ethanol at 4 °C. TRAcP positive cells (TRAcP+) with 3 or more nuclei were considered to be osteoclasts and manually counted using 10 x and 20 x lenses on a Leica Light microscope.

2.3 Osteoblast cultures

The following paragraphs on osteoblasts, describe osteoblast isolation and characterization as previously described by (Logan et al., 2013).

2.3.1 **Isolation of primary osteoblasts**

Primary calvarial osteoblasts were obtained by repeated collagenase digestion from the calvarial bones of 2 day-old C57BL/6J mice sacrificed by decapitation according to Schedule 1 of the Animals (Scientific Procedures) Act (University of Edinburgh, United Kingdom see section 2.2.1) as previously described by (Logan et al., 2013). Briefly, calvaria were washed in PBS. Calvaria were then incubated in 3 ml of collagenase type 1 (1 mg/ml) in PBS and incubated for 10 minutes at 37 ºC in a shaking water bath. After the first digestion, supernatant was discarded and the calvaria were incubated in 4 ml collagenase in PBS for 30 minutes in a shaking water bath. The supernatant was collected (fraction 1) and the calvaria were washed twice with 2 ml PBS which was added to the collected supernatant (fraction 1) and topped up with standard αMEM. The remaining tissue was incubated in PBS supplemented with 5mM EDTA and incubated for 10 minutes at 37 ºC. The supernatant was collected (fraction 2) and tissues were washed twice with 2 ml PBS which was added to the collected supernatant (fraction 2) and topped up with standard αMEM. The remaining tissues were incubated in 4 ml of collagenase type 1 (1 mg/ml) in PBS for 30 minutes in order to obtain the fraction 3. The three cell suspensions were pooled and centrifuged at 1200 rpm for 3 minutes. The supernatant was removed and the cell pellet was resuspended in standard αMEM and cultured in 75cm^2 flasks under standard conditions at a density of 3 calvaria per flask. After 24 hours the medium was changed to remove non-adherent cells and the media was changed every 48 hours thereafter until confluence was reached. Protocols adapted from (Edinburgh thesis S. Marino).

2.3.2 **Passage of primary osteoblasts**

When confluence was reached, the osteoblasts were rinsed with PBS and detached by incubation with 2 ml of trypsin for 3 minutes at 37^{o}C. Trypsin was deactivated by adding 8 ml of standard αMEM. The cell suspension was centrifuged at 1200 rpm for 3 minutes. The supernatant was discarded and the pellet was resuspended, used for experiments and the left over was cultured in 75cm^2 flasks. Cultures were kept under standard conditions.

2.3.3 **Osteoblast viability**

Primary osteoblasts were plated in 96-well plates at 7 x 10^3 cells/well in 150 µl of standard αMEM. MC3T3-E1 were seeded at 5 x 10^3 cells/well 100 µl of standard αMEM. After 24 hours primary osteoblasts and MC3T3-E1 were treated with conditioned medium (20%), vehicle or Sema3A 300 ng/ml and left for 48 and 72 hours before cell viability was analysed by the Alamar Blue assay.

2.3.4 **Alamar Blue assay**

Alamar Blue assay was used to measure the viability of bone and cancer cells. Alamar Blue assay utilises a nontoxic dye containing resazurin that is non-fluorescent and blue in colour when in an oxidized state. The dye is taken up by metabolically active cells and reduced to resorufin that is fluorescent and red in colour. The degree of change in colour/fluorescence is proportional to the number of viable metabolically active cells. Briefly, 10% (v/v) Alamar Blue reagent was added to each well at the end of the culture period. The plate was incubated for 3 hours in standard culture conditions and fluorescence was measured (excitation, 530 nm, emission 590 nm) using a SpectraMax® M5 microplate reader (Logan et al., 2013). AlamarBlue was also added to wells containing standard medium without cells or treatments to obtain background fluorescence.

2.3.5 **Alkaline phosphatase assay**

Osteoblast differentiation was observed using the Alkaline Phosphatase assay (ALP) as previously described by (Logan et al., 2013). The assay is based on the conversion of p-nitrophenol phosphate (colourless) (pNpp) into p-nitrophenol (yellow) by the alkaline phosphatase enzyme, highly expressed by osteoblasts.

Primary osteoblasts were isolated as described in section 2.3.1. Primary calvarial osteoblasts and the MC3T3-E1 were seeded into 96-well plates at 7 x 10^3 cells and 5 x 10^3 cells per well respectively in standard αMEM. KHOS, MNNG/HOS, Saos-2 and MG-63 osteosarcoma cells were seeded into 96-well plates at 4 x 10^3 cells per well in standard DMEM. After 24 hours cells were treated with vehicle (PBS) or exogenous Sema3A (300 ng/ml) in serum free medium with the exception of primary osteoblasts that were cultured in standard α-MEM. After a 48 hour incubation with the treatment the viability of the cells was assessed using Alamar Blue.

After viability assessment the cell monolayer was washed with PBS and incubated with 150 µl of ALP lysis buffer for 20 minutes. Cells were observed under a light microscope to ensure they were completely lysed. Test samples (50µl/well) were pipetted in a fresh 96 well plate. An equal amount of substrate solution was added and the absorbance was measured using the SpectraMax® M5 microplate reader at wavelength of 414 nm at 37°C, every 5 minutes for 30 minutes. ALP activity was determined from the slope of the linear part of the standard kinetic curve and was expressed as fold stimulation over the vehicle control. Alkaline ALP activity was normalised to cell viability as determined by the Alamar Blue assay section 2.3.4.

2.3.6 **Mineralization of Saos-2**

Saos-2 cells were plated in 24 well plates at 75 x 10^3cells/well in standard DMEM. Once the cells reached confluence, Saos-2 were treated with conditioned medium 20% (v/v) in osteogenic medium containing (50µg/ml Ascorbic Acid, 10nM Dexamethasone and 2mM β-Glycerophosphate, 1% FCS) every 48 hours for 9 days. In the intermittent exposure mineralization experiments, Saos-2 cells were exposed to conditioned medium 20% v/v in osteogenic medium as described above for 6 hours out of the 48 hour cycle. The other 42 hours cells were cultured in 1% FCS osteogenic DMEM. After 9 days, cells were lysed in 500 µl of ALP lysis buffer for 20 minutes. Or fixed in 1ml 70% ethanol for at least 24 hours before Alizarin Red staining.

2.3.7 **Alizarin Red stain**

Alizarin Red S is used to stain calcium deposits in tissue and cell culture. Staining of osteoblasts and osteoblast like cells was previously described by (Logan et al., 2013).

The 70% ethanol was removed from the well and the cell layer was washed 4 times with 3 ml distilled H_2O (dH_2O). After removal of the dH_2O 1ml of 40mM Alizarin red at pH 4.2 was added to the well and incubated for 20 minutes at room temperature. The Alizarin red solution was removed and the cell layer was washed 4 times with 2 ml distilled H_2O (dH_2O) for 5 minutes. Excess water was removed and plates were left to dry at room temperature. Area of mineralization was quantified using ImageJ analysis after the plates were scanned using Epson perfection 4990 photo scanner. Mineralization was also quantified using destaining of the Alizarin red as described in the following section.

2.3.8 **Destain of Alizarin red**

After the plates were dried overnight, 1 ml/well of 10% (w/v) cetylpyridinum chloride in 10mM sodium phosphate (pH 7.0) was added to the Alizarin red stained wells. Plates were incubated on a rocking table at room temperature for 2 hours and the absorbance of the extracted stain using a SpectraMax® M5 microplate reader at wavelength of 562 nm was measured at 30 minute intervals.

2.4 Cancer cells

2.4.1 **Cancer cell lines**

Human KHOS, MNNG/HOS, Saos-2 and MG-63 osteosarcoma cell lines (table 2.1) were purchased from (ATCC, Manassas, VA, USA). KHOS, MNNG/HOS, Saos-2 and MG-63 osteosarcoma cells were cultured in DMEM + Glutamax (Gibco, UK) supplemented with 10% FCS, 100U/ml penicillin and 100 μg/ml streptomycin (standard DMEM). Cancer cells were cultured in 25 cm^2 flasks and passaged every 48-72 hours at a ratio of 1:5-1:10. Culture medium was removed, the cells washed in PBS and detached by treatment with trypsin. Standard medium was added to inactivate the trypsin and cells were transferred to a fresh sterile 15 ml and centrifuged at 1200 rpm for 3 minutes. The supernatant was discarded and cells were resuspended in 1 ml standard medium before a percentage of the suspension was placed into a new flask 25 cm^2 flask containing 5 ml standard medium.

2.4.2 **Conditioned medium preparation**

In case of studies requiring conditioned medium, human KHOS osteosarcoma control or KHOS Sema3A overexpressing cells were plated in 6 well plates and cultured in standard medium until 80% confluence was reached. Standard medium was removed from the cells and replaced with serum free medium. After 16 hours, the conditioned medium was removed and filtered through a 0.45 μm filter.

2.4.3 **Cancer cell line drug treatments**

Sema3A treatment was achieved using commercially available human recombinant Sema3A protein (R&D) reconstituted in PBS according to manufacterer's instructions. The concentration of Sema3A used was determined based on previous studies on osteoclasts and breast cancer cell lines in our laboratory (de Ridder MSc thesis unpublished data) and on concentrations of Sema3A previously described by Hayashi and colleagues (Hayashi et al., 2012). Human KHOS osteosarcoma cells were seeded at density of 1000 cells/well, MNNG/HOS cells were seeded at a density of 2000 cells/well and Saos-2 and MG-63 were seeded at 3000 cells/well in 96 well plates. After 24 hours under standard culture conditions, the media was replaced with serum free DMEM with Sema3A (300 ng/ml) or vehicle control. After 24 and 48 hours, cell viability was assessed by Alamar Blue assay 2.3.4.

2.5 Lentiviral transduction

2.5.1 **Kill curve and antibiotic selection**

Cells were plated at 5000 cells/well in 96 well plate. Puromycin (Gibco) was prepared in standard DMEM at concentrations from 0 to 10µg/ml. Hygromycin (Invitrogen) was prepared in standard DMEM at concentrations from 0 to 800 µg/ml. Blasticidin (Invitrogen) was prepared in standard DMEM at concentrations from 0 to 20 µg/ml. Growth medium was refreshed with medium containing dilutions of puromycin, hygromycin or blasticidin and incubated at 37°C for 48 hours. The AlamarBlue assay was used to measure cell viability and percentage of cell survival was calculated. The minimum antibiotic concentration that killed 100% of the cells was determined to be 1 µg/ml for puromycin, 500 µg/ml for hygromycin and 5 µg/ml for blasticidin and were subsequently used to select for successfully transfected cells.

2.5.2 **Lentiviral transduction**

Lentiviral activation particles (Santa Cruz), control (sc-437282) and Sema3A lentiviral activation particles (sc-400716-LAC) were used to transduce human KHOS osteosarcoma cells according to manufacturer's protocol. Lentiviral activation particles encode a synergistic activation mediator (SAM) complex that is designed to activate the transcription to upregegulate endogenous gene expression. The SAM complex binds to a site-specific region, guided by a target specific guide RNA, upstream of the transcriptional start site and recruits transcription factors for highly efficient gene activation. The Lentiviral activation particles contain three activation plasmids essential for the gene upregulation. Deactivated Cas9 (dCas9) nuclease (D10A and N863A) is fused to the transactivation domain VP64 and blasticidin resistance genes this construction allows the complex to bind to the DNA without cleaving the DNA. Particle 2 is a MS2-p65-HSF1 fusion protein containing a hygromycin resistance gene required for increasing the efficiency of transcription activation. The last particle contains a target-specific 20 nt. guide RNA (guide RNA for Sema3A) and a Puromycin resistance gene (Figure 2.1). In case of the Sema3A lentiviral activation particles, the complex enhances endogenous Sema3A expression by activating the transcription. In case of the mock control, the third plasmid contains a non-specific guide RNA.

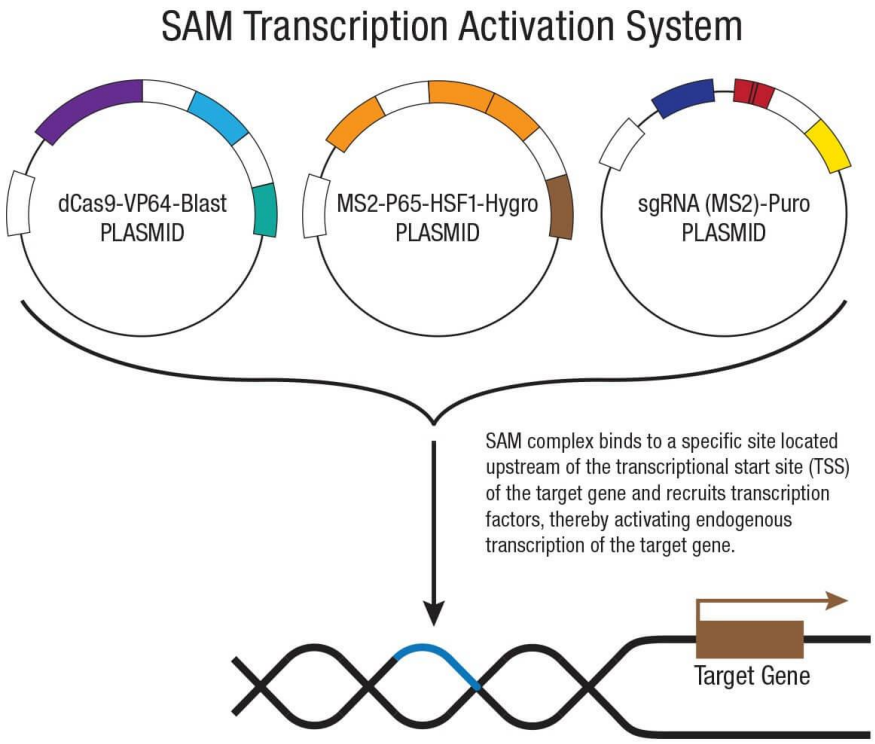

Figure 2.1. Schematic representation of the SAM activation system.
The Lentiviral activation particles contain three activation plasmids as part of the SAM transcription activation system essential for the gene upregulation. Particle 1 is a deactivated Cas9 (dCas9) nuclease (D10A and N863A) fused to the transactivation domain VP64 and blasticidin resistance genes. Particle 2 is a MS2-p65-HSF1 fusion protein containing hygromycin resistance genes and is required for increasing the efficiency of transcription activation. The last particle contains a target-specific 20 nt, and a puromycin resistance. Image provided by Santa Cruz (SantaCruz) .

Briefly cells were plated in 6 well plates at $0.1x10^6$ per well and left to adhere overnight. Medium was replaced with standard medium supplemented with 5 µg/ml Polybrene and cells were infected with 40 µl vehicle, control viral particles or Sema3A activation particles. After 24 hours of incubation the medium was replaced with standard medium for 24 hours. Medium was then replaced by antibiotic selection media containing three antibiotics (as described in section 2.5.1). Antibiotic selection media was replaced every 48 hours until control non-infected cells were killed.

2.6 Western blot

The following sections are describing the assessment of protein expression by western blot as previously described in (Idris, 2012).

2.6.1 **Cell lysates**

Cells were plated in 6-well plates at 1-3 x 10^5 cells/well in standard medium until 80% confluence was reached. Before harvesting the cell lysates, cells were incubated in standard or serum free medium for 16 hours. In case of short term protein signalling, cells were exposed to the desired condition (vehicle, Sema3A or conditioned medium) in serum free medium for 15 minutes before cell lysis. Medium was removed and the monolayer was washed with cold PBS and gently scraped in 50-90 µl of RIPA lysis buffer (appendix 10.5) with 2% (v/v) protease inhibitor cocktail and 0.4% (v/v) phosphatase inhibitor cocktail and left on ice to incubate for 5 minutes. The lysate was transferred to an eppendorf tube and centrifuged at 14000g for 10 minutes at 4^{o}C. The supernatant was collected and stored at -20^{o}C.

2.6.2 **Cytoplasmic and nuclear fractionation**

Cells were plated as stated in the previous section. Cells were incubated in serum free medium for 16 hours and exposed to vehicle or Sema3A (300 ng/ml) in fresh serum free medium for 45 minutes. Cells were washed with cold PBS and lysed with 100 µl of cytosolic buffer (appendix 10.5) with 2% (v/v) protease inhibitor cocktail and 0.4% (v/v) phosphatase inhibitor cocktail. Cells were incubated 1-5 minutes until cytosolic lysis was observed using a Leica light microscope. The cells were gently scraped, collected into eppendorf tubes and incubated for 5 minutes on ice. The lysate was centrifuged at 8000g for 5 minutes at 4^{o}C and the supernatant was collected as the cytosolic fraction. To remove residual cytosolic protein, the pellet was resuspended in 100 µl cytosol buffer centrifuged at 8000g for 5 minutes at 4^{o}C, this step was performed twice. After removal of the supernatant, the remaining pellet was resuspended in RIPA lysis buffer (appendix 10.5) with 2% (v/v) protease inhibitor cocktail and 0.4% (v/v) phosphatase inhibitor cocktail, incubated on ice for 15 minutes and resuspended every 5 minutes. The samples were centrifuged at 16000g for 15 minutes at 4^{o}C and the supernatant was collected as the nuclear fraction.

2.6.3 **Conditioned medium for western blot**

Cells were cultured in a T25 until 80% confluent. Once confluence was reached, standard medium was replaced with serum free medium. Conditioned medium was collected after 16 hours of culture and concentrated using Pierce Protein Concentrators, 9K MWCO (Thermofisher) to a volume of 400µl according to manufacturers' instructions. Protein concentration was measured as described in the following section.

2.6.4 **Protein concentration**

Protein concentration was measured with the bicinchoninic acid (BCA) Pierce protein assay (Pierce, USA). The standard curve was generated with serial dilutions of bovine serum albumin (BSA) standards (0-2000 µg/µl). Standard BCA dilution standards (10 µl) and protein samples (1:5 diluted in dH_2O) were plated in duplicate in a 96-well plate. 200 µl of BCA solution (copper sulphate diluted in bicinchoninic acid at 1:50) was added to each well and incubated for 30 minutes at 37^oC. Absorbance was measured at 562 nm using a SpectraMax® M5 microplate reader and protein concentration in each sample was calculated from the BSA standard curve.

2.6.5 **Gel electrophoresis and transfer**

CriterionTM XT BioRad (12% Bis-Tris) pre-cast gels were placed in a vertical Bio-Rad electrophoresis tank filled with Tris-Glycine (1x) running buffer. Cell lysates (70-100 µg) were mixed with 5X sample loading protein buffer (appendix 10.5) and heated at 95°C for 5 minutes before loading into the gel wells. Kaleidoscope pre-stained standard and Magic Marker XP western standard were used to identify molecular weights. Gels were run at constant voltage of 150V for ~1.5 hours. The Bio-Rad Transblot turbo midi-size polyvinylidene difluoride (PVDF) membrane was activated in 100% methanol and equilibrated in transfer buffer for 5 minutes before the separated proteins on the CriterionTM XT Bio-Rad (12% Bis-Tris) gel were transferred to the PVDF membrane. The gel and PVDF membrane were sandwiched between two midi size transfer stacks pre-soaked in transfer buffer and placed in the Transblot turbo transfer system (Bio-Rad) for 7 minutes at 2.5A and 25V.

2.6.6 **Immunostaining and antibody detection**

The PVDF membrane was then incubated in 5% BSA in TBST solution (appendix 10.5) or 5% milk (w/v in TBST) to block non-specific antibody binding sites at room temperature on a rocker for 1 hour. The membrane was then washed in TBST 3 times for 10 minutes and incubated overnight at 4°C on a rocker with the desired primary antibody (at 1:1000 in 5% BSA in TBST) for a list of the primary antibodies used in this thesis see appendix 10.2. The next day the membrane was washed with TBST 3 times for 10 minutes and incubated with the anti-rabbit HRP-conjugated secondary antibody (at 1:10000 in 5% milk in TBST) on a rocker with a low speed for 1 hour at room temperature. After incubation with the secondary antibody the membrane was washed 6 times with TBST for 10 minutes each wash. Protein bands were visualised using Clarity^{TM} western ECL substrate (Bio-Rad) chemiluminescent detection system on a Chemidoc imaging system (BioRad). Quantification of the bands was performed with the use of Imagelab software from BioRad.

2.7 Cytokine array kit

Secreted cytokines of KHOS mock and KHOS Sema3A overexpressing cells were measured in the conditioned medium with the Proteome Profiler Human XL Cytokine Array Kit R&D systems. This cytokine array measures the levels of 102 human cytokines simultaneously and was used according to manufacturer's instructions. Cells were counted, plated and conditioned medium was prepared. All incubation steps were performed on a rocking platform shaker. Briefly, the membrane was blocked using the blocking buffer for 1 hour at room temperature before overnight incubation with the conditioned medium sample at 4^{o}C. The membrane was washed 3 times 10 minutes with washing buffer and then incubated with detection antibody cocktail for an hour. The membrane was then washed 3 times in washing buffer before the Streptavidin-HRP conjugate was added to the membrane and incubated for 30 minutes. The membrane was washed 3 times as described above and the membrane was visualised with the chemi reagent mix on a Chemidoc imaging system (BioRad). Quantification of the cytokine spots was performed with the Imagelab software from BioRad after 20 minutes of visualisation and expression was registered when intensity of spots reached a threshold of 50000 (Au). Expression of cytokines were indicated as different when expression was higher than 200% or below 75% of control expression.

2.8 PINP and CTX ELISA

Serum procollagen type 1 N propeptide (P1NP) and C-terminal telopeptide of type 1 collagen (CTX) were measured in the systemic Sema3A administration xenograft model (section 2.10.1) using the mouse/rat competitive enzyme immunoassay kits (IDS, Boldon, UK), according to the manufacturer's instructions. Briefly, standards, control and 1:10 samples were added to the wells of the antibody coated plate. PINP or CTX biotin were added and incubated on a microplate shaker at room temperature for 1 hour. Plates were then washed 3x with wash buffer and excess wash buffer was removed before enzyme conjugate was added to the wells and incubated for 30 minutes at room temperature. Plates were washed as previously described and TMB substrate was added to the wells and incubated for 30 minutes at room temperature. Stop solution was added to the wells and absorbance was measured at 450nm using a SpectraMax® M5 microplate reader. The above described experiment was performed in full by Ryan T. Bishop.

2.9 Cell motility

2.9.1 **Wound healing assay**

The wound healing assay was performed as previously described by (Logan et al., 2013). 2D directional migration of cells was assessed by the wound healing assay. Osteosarcoma cells KHOS, MNNG/HOS, MG-63 and Saos-2 were seeded in 24 well plates (0.15×10^6) and osteoblast MC3T3-E1-E1 at (0.1×10^6), were seeded in 24 well plates in standard DMEM and left to adhere overnight. The confluent monolayer was wounded using a p10 plastic pipette tip. The cells were washed 5 times with serum free medium to remove any cell debris and then treated with 1ml of standard medium containing vehicle or Sema3A 300 ng/ml. The plate was placed in a microscope humidity chamber maintained at 37°C and supplemented with 5% CO2. Migration was monitored for 24 hours with a Leica AF6000 Time Lapse imaging system. Sequential images were captured at 15 minute intervals. Percentage of wound closure was calculated using T scratch software (Geback et al., 2009).

2.9.2 **Random migration assay**

For random migration assays KHOS cells ($1x10^3$) were plated in 24 well plates in standard DMEM and left to adhere overnight. The medium was refreshed and the plate was placed in a microscope humidity chamber maintained at 37°C and supplemented with 5% CO2. Migration was monitored for 8 hours with a Leica AF6000 Time Lapse imaging system. Sequential images were captured at 15 minute intervals. Accumulated distance (total track length) and velocity were measured using the Chemotaxis and Migration tool in ImageJ. Cells that were in division, touched neighbouring cells, or left the image field during the experiment were excluded from data analysis, 30 cells were tracked per experiment. Cell viability was measured using Alamar Blue assay at the end of the migration assays.

2.9.3 **Transwell invasion assay**

Cancer cell invasion was measured using Corning™ transwell inserts coated with matrigel. Matrigel was thawed and diluted with serum free DMEM to 1.5mg/ml. The inserts were coated with 20 µl of Matrigel solution and left to set in the incubator at 37°C for 3 hours. KHOS cell suspensions were prepared ($2.5x10^4$ cells/ml) in serum free DMEM and 200 µl of cell suspension was pipetted onto the matrigel. Outer wells were filled with 500 µl standard DMEM. After 48 hour incubation under standard culture conditions, a cotton swab was inserted into the top to remove the medium and matrigel. The cells on the mesh were then fixed in 100% ethanol for 5 minutes followed by staining in eosin for 1 minute, haematoxylin for 5 minutes and were then rinsed with tap water and mounted onto glass slides.

2.10 Animal work

All experimental protocols were approved by the French ministry of Agriculture and were realized in accordance with the institutional guidelines of the regional ethical committee (CREEA Pays de la Loire, France) and under supervision of authorized investigators at the University of Nantes, France. The method of osteosarcoma induction has previously been described by Jaqcues and colleagues (Jacques et al., 2018).

2.10.1 **Systemic Sema3A administration xenograft model**

The effects of recombinant Sema3A treatment on osteosarcoma growth, metastasis and osteosarcoma associated bone damage were studied by intramuscular para-osseous (paratibial) injection. Four week-old female Rj: NMRI nude mice were purchased from Janvier Breedings (Le Genest Saint Isle, France) and allowed to acclimatize for a week after arrival. Mice were maintained under pathogen free conditions throughout the experiment. Mice were anesthetized by inhalation of an isoflurane/air mixture (2%, 1 L/min). Primitive osteosarcoma was induced by intramuscular paratibial injection of $1.0x10^6$ human KHOS osteosarcoma cells. Weight was measured before injection and monitored three times a week throughout the experiment. Tumour volume was measured three times weekly (length*width*depth*0.5). Mice were treated via intraperitoneal injection 2 days after tumour inoculation with vehicle (PBS) or 0.7 mg/kg recombinant Sema3A twice a week for the duration of the study. Mice were sacrificed when the tumour volume reached 10% of body weight or $2500mm^3$ for ethical reasons. All mice were sacrificed 21 days after tumour inoculation. Healthy and tumour bearing legs were harvested and fixed in formalin 4% for 72 hours for microCT analysis and immunohistochemistry analysis and lungs were collected for immunohistochemistry and metastases analysis and serum was collected for serum markers, see Figure 2.2. The above described experiment was performed in full by Dr Nathalie Renema in France.

2.10.2 **Tumour-derived Sema3A xenograft model**

The effects of Sema3A overexpression in KHOS osteosarcoma cells on primary tumour growth and bone histomorphometry were studied by intramuscular paratibial injection. Four week-old female Rj: NMRI nude mice were purchased from Janvier Breedings (Le Genest Saint Isle, France) and allowed to acclimatize for a week after arrival. Mice were maintained under pathogen free conditions throughout the experiment. Mice were anesthetized by inhalation of an isoflurane/air mixture (2%, 1 L/min). Primitive osteosarcoma was induced by intramuscular paratibial injection of $1.5x10^6$ human KHOS osteosarcoma cells or human KHOS Sema3A overexpressing osteosarcoma cells. During injection the bone was scratched to allow rapid bone invasion. Weight was measured before injection and monitored three times a week throughout the experiment. Tumour volume was measured three times weekly (length*width*depth*0.5). Mice were sacrificed when the tumour volume reached 10% of body weight or 2500 mm^3 for ethical reasons. All mice were sacrificed 16 days after injection. Healthy and tumour bearing legs were harvested for immunohistochemistry and microCT analysis and lungs were collected for immunohistochemistry and metastases analysis, see Figure 2.2. The above described experiment was performed in full by Dr. Nathalie Renema in France.

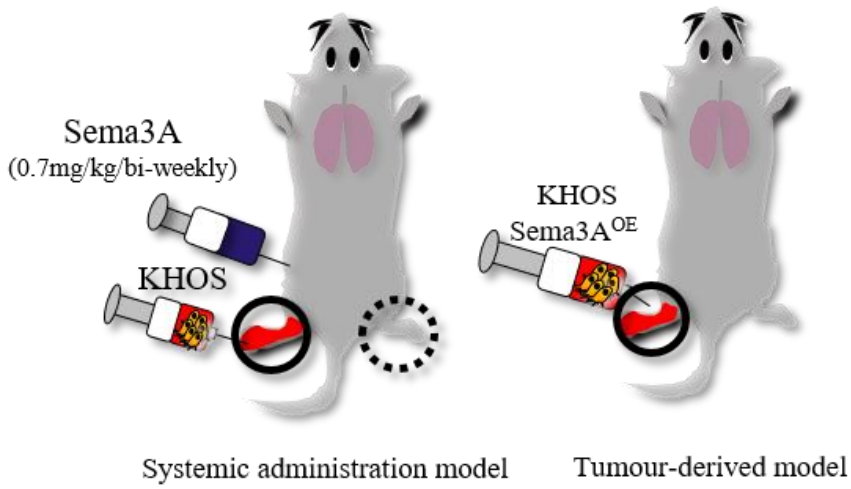

Figure 2.2. Schematic representation of the mouse models.
For the systemic treatment model in female Rj: NMRI nude mice (left), osteosarcoma was induced by paratibial injection of KHOS osteosarcoma cells and mice were given a biweekly IP injection with 0.7 mg/kg Sema3A or vehicle until the experiment was terminated, lungs and legs were collected for analysis. In the tumour-derived female Rj: NMRI nude mice model osteosarcoma was induced with KHOS mock or KHOS Sema3A overexpressing cells (right) and lungs and legs were collected for analysis. For a detailed description of the models see text.

2.11 Micro-Computed Tomography

Legs were scanned using a Skyscan 1076 (Brucker, Belgium) set at 48kV and 200mA at a resolution of 18µm for the animal experiment comparing the mock versus Sema3A overexpressing KHOS osteosarcoma cells and at a resolution of 9µm for the experiment investigating the difference between treatment with recombinant Sema3A (0.7 mg/kg) and vehicle. After obtaining the xray scans, the Skyscan NRecon program was used to reconstruct the images with a thresholding of 0.009 to 0.09 and a Beam hardening correction of 20%. Trabecular, cortical and ectopic bone formation were then analysed using the Skyscan CTAn program (Brucker, Belgium) (Campbell and Sophocleous, 2014).

2.11.1 **Trabecular analysis**

For the proximal tibia and the distal femur, the mineralised cartilage bridge was used as a reference point starting trabecular analysis 10 (18µm) and 20 (9µm) slices down from the point of reference for 100 slices total in the 18µm and a total of 200 slices in the 9µm resolution scans (equals 1.8 mm for both experiments) as described by (van 't Hof, 2012).

2.11.2 **Cortex**

Cortical analysis was performed for 100 slices total in the 18µm and a total of 200 slices in the 9µm resolution scans (equals 1.8 mm for both experiments) the last slice of the trabecular analysis was used as the reference slide for cortical analysis (110 and 220 slices from the mineralised cartilage bridge in 18µm and 9µm resolution respectively) (van 't Hof, 2012).

2.11.3 **Ectopic bone**

For ectopic bone analysis in the tibia and the fibula 2 points of reference where used. The first point of reference was the mineralised cartilage bridge in the tibia and the second point of reference was the merging of the fibula with the tibia. Tumour-bearing tibia and fibulae were analysed separately and compared to their contralateral tibia and fibula see figure 2.2 and figure 2.3 for a visualization of ectopic bone by microCT and histology respectively.

Figure 2.3. Visualization ectopic bone of the fibula by microCT.
On the left in panel **A.** the healthy fibula with the area of bone volume (blue) that was analysed. On the right in panel **B.** the total bone volume comprises of the regular bone (blue) and ectopic bone formation(red). that the total bone volume of the osteosarcoma-bearing fibula was divided by the total bone volume of the healthy fiblula to calculate percentage of osteosarcoma bone volume.

2.12 Histology

After legs were scanned, they were decalcified and embedded in paraffin. Lungs were embedded after the 72 hour fixation period using the following methods.

2.12.1 **Decalcification of legs**

Legs were decalcified prior to embedding. Decalcification was performed using a KOS microwave histoSTATION (milestone) in a solution of EDTA solution of EDTA 4.13% NaOH 0.2% PFA 4% PBS 1X pH 7.4. Duration of decalcification (1-3 months) depended on the sample and was assessed by X-ray during the process. When decalcification was complete legs were embedded. Decalcification was performed in full by Dr. Nathalie Renema in France.

2.12.2 **Embedding of tissues**

Tissue embedding was performed by Dr. Nathalie Renema in France. Lungs and legs were paraffin embedded with a tissue processor (microm Microtech). Samples were dehydrated with in stages of ethanol dilutions, clearing in buthanol and paraffin embedding as shown in Table 2.2.

Table 2.2 Stages and reagents of the microm microtech processor programme.

Stage	Reagent
1	80% Ethanol
2	95% Ethanol
3	95% Ethanol
4	95% Ethanol
5	100% Ethanol
6	100% Ethanol
7	100% Ethanol
8	Buthanol
9	Buthanol
10	Buthanol
11	Paraffin wax
12	Paraffin wax

2.12.3 **Cutting of tissues**

Tissues were cut on a Leica microtome (Leica microsystems, Germany) and sections of 4µm were mounted on microscope slides (Thermo Fisher, UK). For each histological analysis 3 separate depths per tissue sample were analysed.

2.12.4 **Haematoxylin and eosin staining**

Tissue slides were dewaxed, stained and rehydrated before coverslips were applied to tissue slides using DPX mounting fluid. Tissues were dehydrated as follows:

1. Dewax the sections in xylene twice in fresh solutions for 5 minutes each.
2. Incubate sections in 100% ethanol twice for 5 minutes each to remove xylene.
3. Incubate sections in 95% ethanol for 5 minutes.
4. Incubate sections in 70% ethanol for 5 minutes.
5. Rinse sections in tap water for 1 minute.

Sections of the tumour-bearing legs were stained with TRAcP and counter stained with haematoxylin as discussed in section 2.12.6. Lung tissues were stained with haematoxylin and eosin (H&E) after dehydration as follows:

6. Stain in Gill's haematoxylin solution for 90 seconds.
7. Incubate in tap water for 3 minutes.
8. Stain with 1% eosin in 1% (w/v) calcium carbonate solution for 5 minutes.
9. Incubate in tap water for 3 minutes

Tissues were then rehydrated as follows:

10. Incubate sections in 70% ethanol for 10 seconds.
11. Incubate sections in 95% ethanol for 10 seconds.
12. Incubate sections in 100% ethanol twice for 30 seconds each.
13. Incubate sections in xylene twice for 1 and 3 minutes respectively
14. Mount coverslips with DPX mounting fluid.

2.12.5 **Lung metastasis analysis**

Tumour nodule area of lung metastasis was analysed with a x4 objective using the Osteomeasure system (OsteoMetrics, Inc). Nodules were counted and quantified by measuring tumour area on lung sections stained with H&E. Three seperate depths per

lung were analysed for number of nodules and total tumour area, the average of these three depths was used as total lung tumour area for each mouse.

2.12.6 **TRAcP staining of bones**

Sections were dewaxed as described in section 2.12.4. TRAcP solutions (section 10.5) were made fresh before every staining. After dewaxing and dehydration sections were placed in warmed acetate-tartrate buffer for 5 minutes. Tissue slides were then incubated for 30 minutes in TRAcP solution A at 37°C. The solution was removed and tissue slides were incubated in solution B for 19 minutes. Tissue slides were then washed in tap water and counterstained with Gill's haematoxylin for 20 seconds, washed again in tap water and then dehydrated and mounted with DPX as described in the previous section.

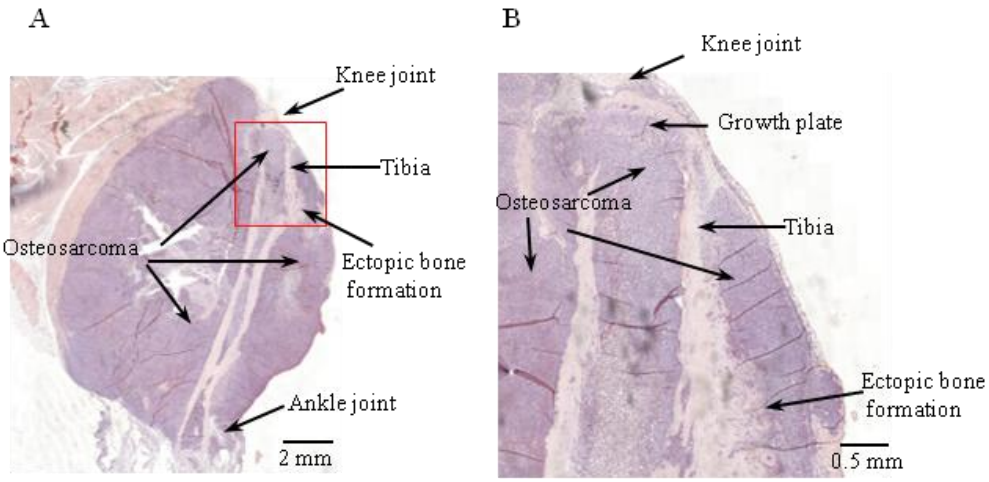

Figure 2.4. Visualization of an osteosarcoma-bearing mouse leg with the features indicated.
This figure depicts an osteosarcoma-bearing mouse leg with a visible tumour and tibia. **A.** Lower magnification image of the osteosarcoma-bearing leg with landmark features (ankle joint, knee joint and tibia) and osteosarcoma and ectopic bone formation indicated with arrows. The red square depicts the magnified image in **B.** Magnified image of an osteosarcoma-bearing mouse leg with a focus around the knee joint and proximal tibia showing landmark features (knee joint and tibia) and osteosarcoma and ectopic bone formation indicated with arrows.

2.12.7 **Histomorphometry**

Histomorphometry was performed with a x20 objective using the Osteomeasure histomorphometry system (OsteoMetrics, Inc) on TRAcP stained sections with a haematoxylin counterstain as described in section 2.12.6. Histomorphometry was performed as previously described by (Erben and Glosmann, 2012). Only TRAcP

positive multi-nucleated cells that were in contact with the bone were counted as osteoclasts and measured for osteoclast surface. Osteoblasts were identified by their morphology, surface was measured and osteoblasts were counted if they were in contact with the bone.

2.13 Statistical analysis

All statistical analysis was performed using GraphPad Prism version 7.0. Student's T test was performed to determine whether differences between two sets of results were significant. For statistical analysis in case of multiple groups, the analysis of variance (ANOVA) followed by Bonferroni post-hoc test was used. *In vivo* results were analysed with the unpaired nonparametric Kruskal-Wallis test p- value of 0.05 or below was considered statistically significant.

CHAPTER THREE

Effects of exogenous Sema3A on growth and metastatic behaviour of osteosarcoma cells *in vitro* and *in vivo*

3 CHAPTER THREE

3.1 Summary

Osteosarcoma is the most prevalent primary bone tumour mainly affecting children and young adults. Semaphorin 3A, a secreted member of the semaphorin family, is important for the early development of the skeletal system, bone homeostasis and fracture healing. Sema3A is produced by osteoblasts and is an important regulator of osteoblast-osteoclast coupling and bone metabolism. Furthermore, Sema3A is implicated in cancer and acts as a tumour promoter or tumour inhibitor depending on the cancer cell type. The role of Sema3A in osteosarcoma remains unknown. In this chapter, I studied the effects of exogenous Sema3A treatment on the viability, motility and alkaline phosphatase of osteoblasts and a panel of human osteosarcoma cells with a range of different metastatic abilities *in vitro*. Furthermore, I investigated the effect of exogenous Sema3A on tumour growth and lung metastasis in the xenograft KHOS mouse model.

Treatment with exogenous Sema3A significantly reduced the 2D directed migration of both the panel of osteosarcoma cell lines tested and osteoblast-like MC3T3-E1 *in vitro*. Sema3A enhanced osteoblast alkaline phosphatase activity in MC3T3-E1 and in the low metastatic osteosarcoma cell lines MG-63 and Saos-2 without affecting cell viability *in vitro*. *In vivo*, exogenous Sema3A had no effect on tumour growth and showed a trend towards less metastasis. Overall this chapter established that Sema3A increased alkaline phosphatase activity and inhibited migratory and osteolytic features of osteosarcoma cells.

3.2 Introduction

Gomez and colleagues reported that both osteoclasts and osteoblasts express the receptors for Sema3A (Gomez et al., 2005). Furthermore, osteoblasts but not osteoclasts were shown to produce Sema3A. In recent studies, Sema3A produced by the osteoblasts was shown to promote osteoblast differentiation leading to a reduction in bone resorption and enhanced bone formation (Hayashi et al., 2012, Fukuda et al., 2013). In cancer, several studies have shown that Sema3A affects the motility of various cancer cells, including glioblastoma, breast, prostate and pancreatic cancer. Depending on the type of cancer, Sema3A exerts tumour promoting or tumour inhibiting effects (Table 1.3) (Bachelder et al., 2003, Herman and Meadows, 2007, Mishra et al., 2015b, Muller et al., 2007, Bagci et al., 2009). Together these studies showed that Sema3A affects cancer cell migration and is essential for the development of bone and differentiation of osteoblasts, this led us to investigate the role of Sema3A in osteosarcoma

Osteosarcoma is a rare malignant primary bone tumour mainly affecting children and young adults (Meyers and Gorlick, 1997). Osteosarcoma derives from mesenchymal stem cells or a more differentiated mesenchymal osteoblast precursor lineage (Xiao et al., 2013, Mutsaers and Walkley, 2014). Osteosarcoma is an aggressive type of cancer characterized by skeletal tumour burden and a high propensity to metastasize to the lungs (Geller and Gorlick, 2010, Klein and Siegal, 2006, Mutsaers and Walkley, 2014). Very few studies have been conducted investigating the role of Sema3A and its receptors in osteosarcoma. Osteosarcoma cell lines express the Sema3A receptor Nrp1 (Yue et al., 2014). There is conflicting data suggesting that expression of the Sema3A receptor Nrp1 is an indicator for a poor prognosis (Zhu et al., 2014, Boro et al., 2015). However, the role of exogenous Sema3A in osteosarcoma remains to be elucidated.

This chapter describes the effects of exogenous Sema3A on viability, motility, alkaline phosphatase activity and osteosarcoma-associated osteoclast formation in a panel of osteosarcoma cell lines with a range of metastatic abilities.

3.3 Aim

The aim of this chapter was to investigate the role of human recombinant (exogenous) Sema3A in human osteosarcoma cancer cell behaviour *in vitro* and *in vivo*. This aim was achieved by (a) treating mouse MC3T3-E1 osteoblast-like cells and a panel of human osteosarcoma cells with a range of different metastatic abilities with exogenous Sema3A and assess their ability to grow, migrate and to express alkaline phosphatase activity and (b) administration of Sema3A in a xenograft mouse model of osteosarcoma and assess tumour growth and lung metastasis.

3.4 Results

3.4.1 **Exogenous Sema3A reduced osteosarcoma and osteoblast migration *in vitro***

Several studies have indicated that Sema3A affects cancer cell motility in a range of different cell types and depending on cell type Sema3A acts as a simulator or inhibitor of cancer cell motility (Bachelder et al., 2003, Herman and Meadows, 2007, Muller et al., 2007, Bagci et al., 2009). In addition, studies from our laboratories have shown that Sema3A inhibits the motility of breast cancer and osteotropic breast cancer cells (de Ridder MSc thesis unpublished data).

To investigate the effect of exogenous Sema3A on osteosarcoma tumour cell migration, a panel of osteosarcoma cells MG-63, Saos-2, MNNG/HOS and KHOS ranging from low to highly metastatic were exposed to exogenous Sema3A (300 ng/ml) or vehicle (PBS) after a scratch was applied to create a wound in the cell monolayer and 2D directed migration was monitored overnight and assessed by wound closure. As shown in Figure 3.1, Sema3A significantly reduced the migration of the low metastatic osteosarcoma cell lines MG-63 (29%, $p < 0.01$) and Saos-2 (50%, $p < 0.05$) after 8 hours. Exogenous Sema3A also significantly reduced directed migration of the highly metastatic cell lines MNNG/HOS (18%, $p < 0.01$) and KHOS (18%, $p < 0.01$) after 6 and 2 hours respectively.

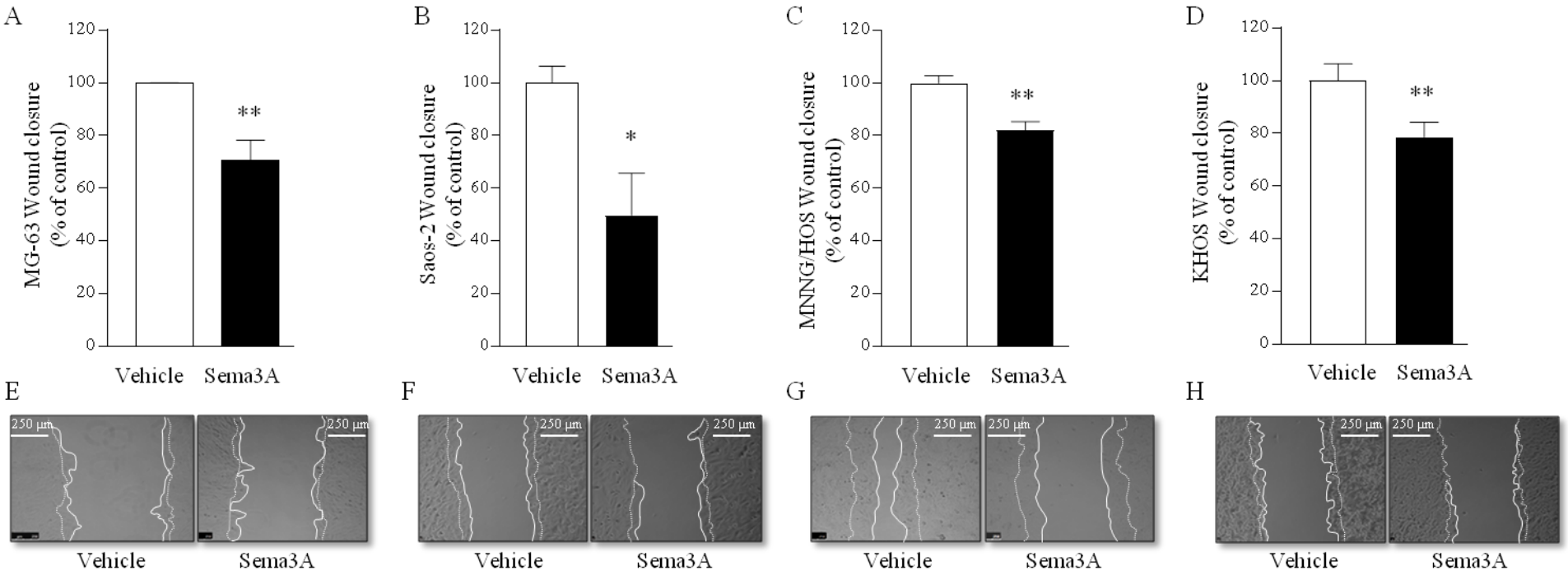

Figure 3.1. Exogenous Sema3A reduced osteosarcoma cell migration *in vitro*.
The figure describes the effect of Sema3A on osteosarcoma cell 2D directed migration by wound healing assay. Quantification of **A.** MG-63 **B.** Saos-2 **C.** MNNG/HOS **D** KHOS osteosarcoma cell 2D directed migration after exposure to vehicle (PBS) or Sema3A (300 ng/ml). **E.** Representative photomicrographs of MG-63 cultures exposed to vehicle (PBS) or Sema3A (300 ng/ml) of experiments described in panel A at 8 hours of treatment exposure and migration. **F.** Representative photomicrographs of Saos-2 cultures exposed to vehicle (PBS) or Sema3A (300 ng/ml) of experiments described in panel B at 8 hours. **G.** Representative photomicrographs of MNNG/HOS cultures exposed to vehicle (PBS) or Sema3A (300 ng/ml) of experiments described in panel C at 6 hours. **H.** Representative photomicrographs of KHOS cultures exposed to vehicle (PBS) or Sema3A (300 ng/ml) of experiments described in panel D at 2 hours. Solid thick white lines represent the cell front at the timepoint that was analysed and shown in panel **A-D**, thin white lines represent the cell front at 0 hours. White scalebar at the top corner of the images indicates 250 µm. Values in the graphs are mean ± SD and are obtained from 3 independent experiments * $p < 0.05$, ** $p < 0.01$.

The effect of exogenous Sema3A on osteoblast migration is motility. Therefore, I also investigated the effect of exogenous Sema3A on migration of the mouse osteoblast-like MC3T3-E1 cells *in vitro*. MC3T3-E1 cells were exposed to vehicle or Sema3A (300 ng/ml) and migration was measured by wound healing assay (section 2.9.1). As shown in Figure 3.2, Sema3A significantly reduced osteoblast migration by 21% ($p < 0.01$) after 8 hours.

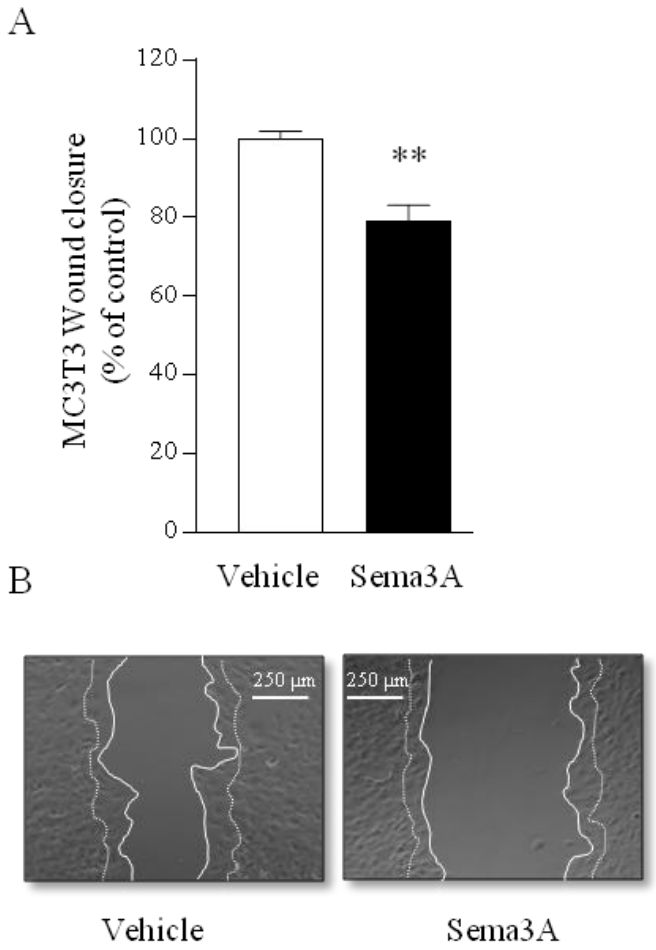

Figure 3.2. Exogenous Sema3A reduced osteoblast migration *in vitro*.
The figure describes the effect of Sema3A on MC3T3-E1 cell 2D directed migration by wound healing assay. **A**. Quantification of wound closure of MC3T3-E1 cells after exposure to vehicle (PBS) or Sema3A (300 ng/ml). **B.** Representative photomicrographs of MC3T3-E1 cultures exposed to vehicle (PBS) or Sema3A (300 ng/ml) of experiments described in panel A at 8 hours. Solid thick white lines represent the cell front at the timepoint that was analysed and shown in panel **A**, thin white lines represent the cell front at 0 hours. White scalebar at the top corner of the images indicates 250 µm. Values in the graphs are mean ± SD and are obtained from 3 independent experiments ** $p < 0.01$.

3.4.2 **Exogenous Sema3A enhanced alkaline phosphatase activity of osteosarcoma cell lines *in vitro***

Osteosarcoma cells are hypothesized to derive from an osteoblastic mesenchymal lineage (Xiao et al., 2013, Mutsaers and Walkley, 2014). Here, I investigated whether exogenous Sema3A affects alkaline phosphatase activity in the low metastatic and more osteoblastic osteosarcoma cell lines MG-63 and Saos-2 and the highly metastatic MNNG/HOS and KHOS osteosarcoma cells. As shown in Figure 3.3, Sema3A(300 ng/ml) significantly increased alkaline phosphatase activity in MG-63 and Saos-2 by 79% and 24% respectively ($p<0.01$ and $p<0.05$) after 48 hours. Interestingly, exogenous Sema3A had no effect on the alkaline phosphatase activity of MNNG/HOS cells. Alkaline phosphatase activity was not detected in the KHOS osteosarcoma cell line.

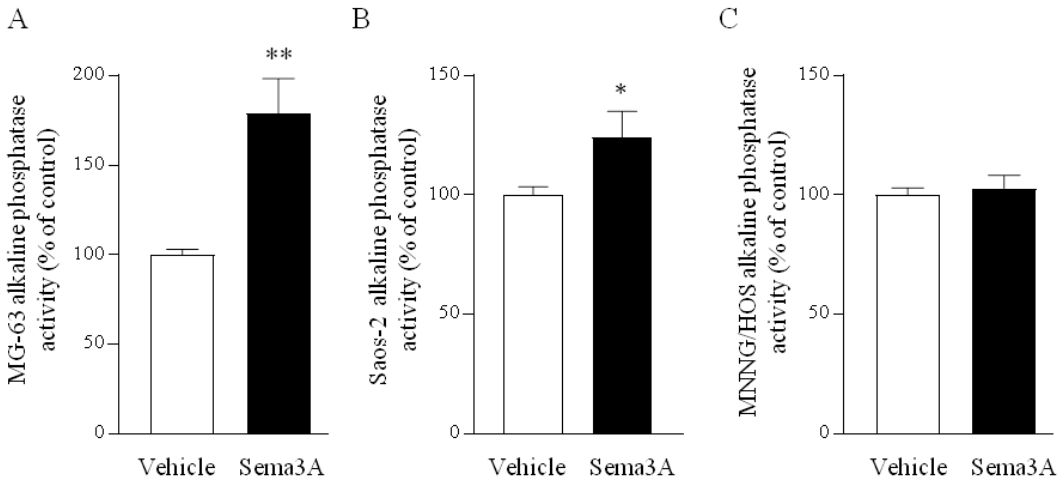

Figure 3.3. Exogenous Sema3A enhanced alkaline phosphatase activity in low metastatic osteosarcoma cell lines.
This experiment was performed to assess the effect of exogenous Sema3A on the alkaline phosphatase activity of several osteosarcoma cell lines. Quantification of alkaline phosphatase activity of **A.** MG-63, **B.** Saos-2, **C.** MNNG/HOS osteosarcoma cells after 48 hour exposure to vehicle (PBS) or Sema3A (300 ng/ml). Values in the graph are mean ± SD and are obtained from 3 independent experiments * $p < 0.05$, ** $p < 0.01$.

Hayashi and colleagues reported that Sema3A enhanced the differentiation of osteoblasts (Hayashi et al., 2012). To investigate and confirm whether exogenous Sema3A affects alkaline phosphatase activity in osteoblasts I measured the alkaline phosphatase activity of the mouse osteoblast-like MC3T3-E1 cell line after 48 hours. Treatment with exogenous Sema3A(300 ng/ml) significantly enhanced MC3T3-E1 alkaline phosphatase activity by 33% (Figure 3.4, $p < 0.001$)

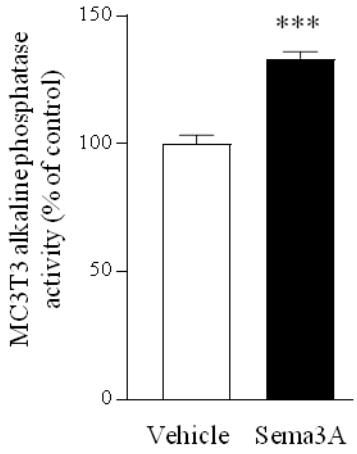

Figure 3.4. Exogenous Sema3A enhanced osteoblast alkaline phosphatase activity.
This figure describes the effect of exogenous Sema3A (300 ng/ml) on the osteoblastic alkaline phosphatase activity of MC3T3-E1 cells. Quantification of alkaline phosphatase activity of the mouse osteoblast precursor MC3T3-E1. Values in the graph are mean ± SD and are obtained from 3 independent experiments *** $p < 0.001$.

3.4.3 **Exogenous Sema3A had no effect on osteosarcoma or osteoblast cell viability *in vitro***

The effect of exogenous Sema3A on osteosarcoma tumour cell growth was investigated in a panel of human osteosarcoma cell lines (MG-63, Saos-2, MNNG/HOS and KHOS) with a range of different metastatic abilities. Osteosarcoma cells were exposed to vehicle or exogenous Sema3A and cell viability was measured by the Alamar blue assay (section 2.3.4). Sema3A(300 ng/ml) had no significant effect on osteosarcoma cell viability in any of the tested cell lines at a concentration that inhibited cell motility *in vitro* (Figure 3.5).

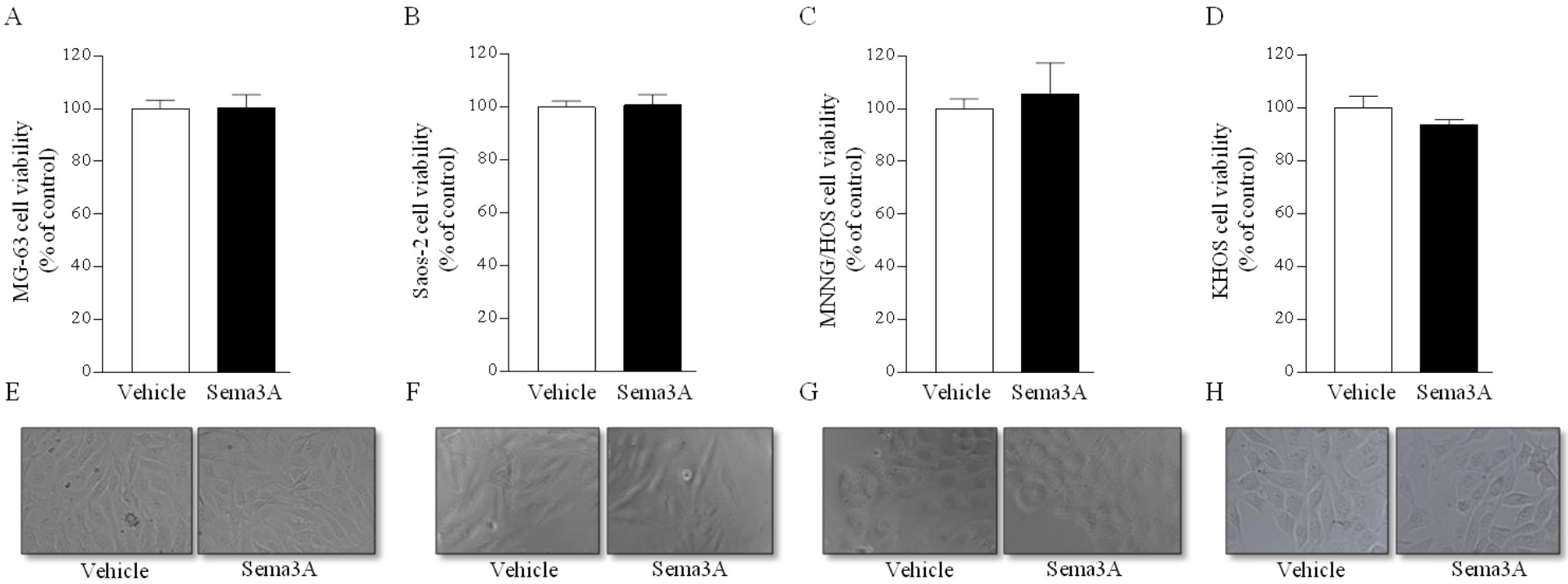

Figure 3.5. Exogenous Sema3A has no effect on osteosarcoma cell viability *in vitro*.
Cell viability was measured in response to exogenous Sema3A using the Alamar blue assay. Quantification of cell viability of **A.** MG-63 **B.** Saos-2 **C.** MNNG/HOS **D.** KHOS osteosarcoma cells after 48 hour exposure to vehicle (PBS) or Sema3A (300 ng/ml). **E.** Representative photomicrographs of MG-63 cultures exposed to vehicle (PBS) or Sema3A (300 ng/ml) of experiments described in panel A. **F.** Representative photomicrographs of Saos-2 cultures exposed to vehicle (PBS) or Sema3A (300 ng/ml) of experiments described in panel B. **G.** Representative photomicrographs of MNNG/HOS cultures exposed to vehicle (PBS) or Sema3A (300 ng/ml) of experiments described in panel C. **H.** Representative photomicrographs of KHOS cultures exposed to vehicle (PBS) or Sema3A (300 ng/ml) of experiments described in panel D. Values in the graphs are mean ± SD and are obtained from 3 independent experiments.

Next, I tested the effects of exogenous Sema3A on osteoblast cell viability, using the mouse osteoblast precursor cell line MC3T3-E1. MC3T3-E1 viability was not affected by treatment with exogenous Sema3A (300 ng/ml) after 48 hours as shown in Figure 3.6.

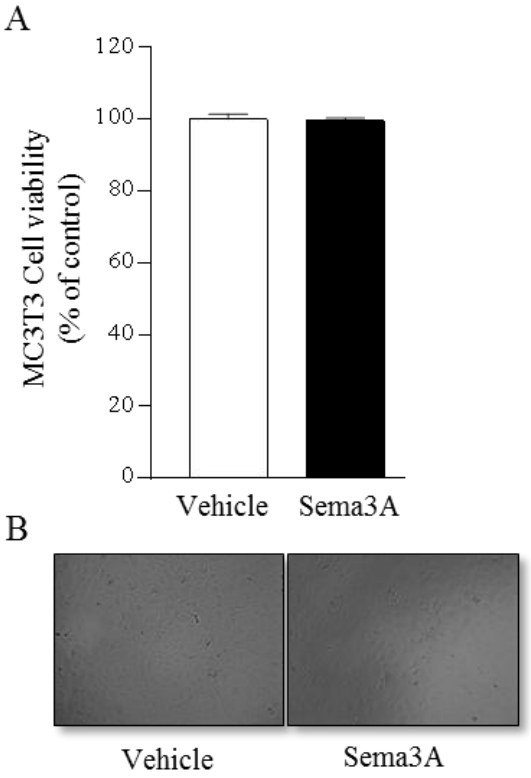

Figure 3.6. Treatment with Sema3A has no effect on osteoblast viability *in vitro*.
The effect of exogenous Sema3A on MC3T3-E1 viability was assessed using the Alamar blue assay. **A**. Quantification of MC3T3-E1 cell viability after exposure to vehicle (PBS) or Sema3A (300 ng/ml) for 48 hours. **B.** Representative photomicrographs of MC3T3-E1 cultures exposed to vehicle (PBS) or Sema3A (300 ng/ml) of experiments described in panel A. Values in the graphs are mean ± SD and are obtained from 3 independent experiments.

3.4.4 **Exogenous Semaphorin 3A had no effect on tumour growth *in vivo***

To investigate the effect of administration of exogenous Sema3A on osteosarcoma tumour growth, mice were paratibially injected with human KHOS osteosarcoma cells and two days after tumour initiation mice received the first injection of vehicle or 0.7 mg/kg Sema3A. Sema3A was administered biweekly. Tumour growth was monitored throughout the experiment and all mice were sacrificed after three weeks (section 2.10.1). As shown in Figure 3.7 exogenous Sema3A had no effect on osteosarcoma tumour growth *in vivo*.

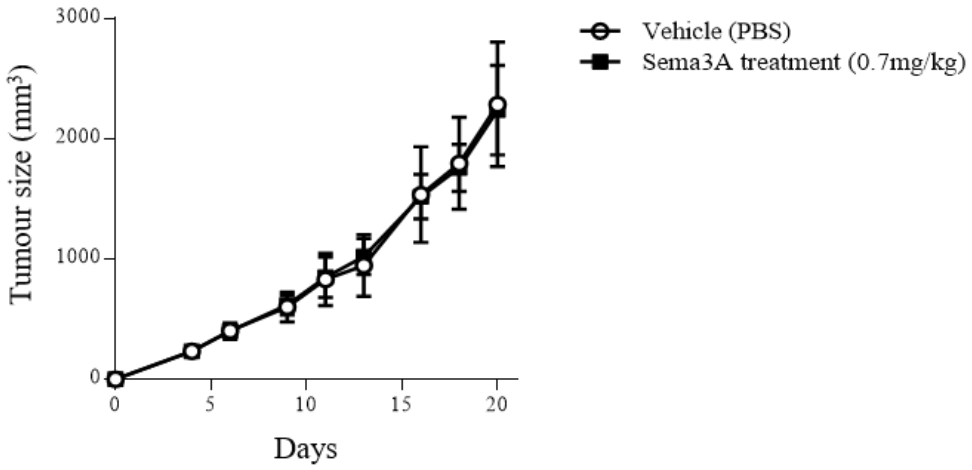

Figure 3.7. Treatment with recombinant Sema3A has no effect on osteosarcoma tumour growth. Osteosarcoma tumours were induced by paratibial injection of KHOS osteosarcoma cells in female Rj: NMRI nude mice. Mice were treated with IP injections biweekly of vehicle (PBS) or recombinant Sema3A (0.7 mg/kg) for the duration of the experiment (21 days) to assess the effect of recombinant Sema3A on osteosarcoma cell growth. Tumour growth was measured using callipers throughout the experiment. N = 7. Values are mean ± SD.

3.4.5 **Exogenous Semaphorin 3A showed a trend towards less lung metastasis**

Osteosarcoma is characterized by a high propensity to metastasize to the lungs (Mutsaers and Walkley, 2014). Here, I investigated the development of micro-metastases in the lungs of mice that received exogenous Sema3A or vehicle. Lungs were paraffin embedded, sectioned and stained with H&E. Metastatic nodules were counted and nodule size was analysed at three separate depths. Of the vehicle treated mice, 6 out of 7 lungs showed metastatic nodules versus 2 out of 7 of the mice that received exogenous Sema3A. Mice administrated with exogenous Semaphorin 3A also showed a trend towards fewer and smaller lung micro-metastasis nodules (Figure 3.8).

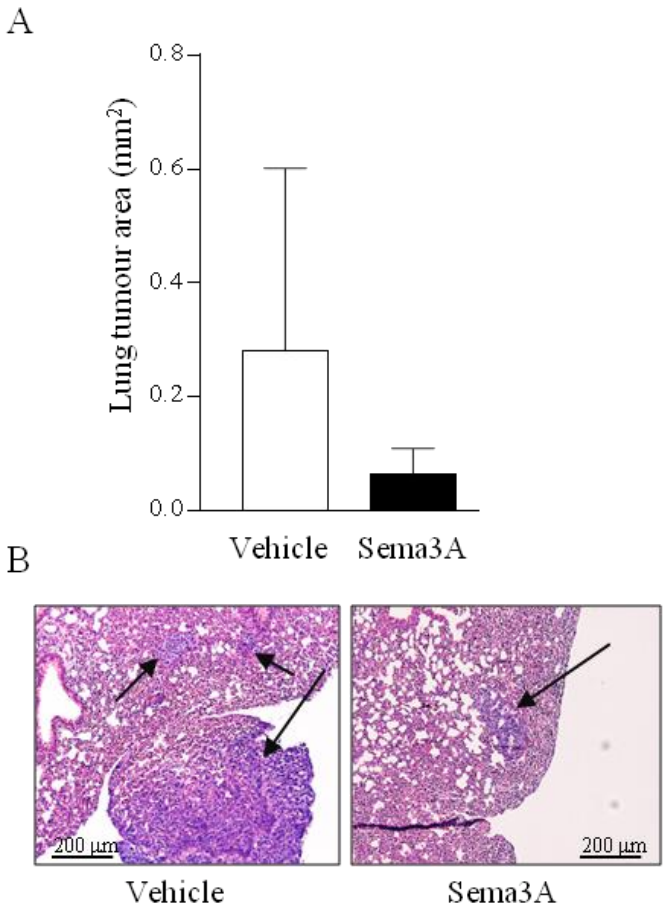

Figure 3.8. Sema3A treatment showed a trend towards reducing lung metastasis.
Osteosarcoma tumours were induced by paratibial injection of KHOS osteosarcoma cells in female Rj: NMRI nude mice. Mice were treated with IP injections biweekly of vehicle (PBS) or recombinant Sema3A (0.7 mg/kg) for the duration of the experiment (21 days) to assess the effect of recombinant Sema3A on lung metastasis. The lungs were sectioned and stained with H&E to assess the effect of recombinant Sema3A on the size and number of metastatic nodules in the lungs. Metastatic nodules were counted at three different depths per mouse and size of metastatic nodules was assessed using the Osteomeasure. **A.** Quantification of the size of micro-metastases in the lungs of mice treated with vehicle or recombinant Sema3A. **B**. Representative microphotographs (10X) of tumour nodules in lungs of mice treated with vehicle or recombinant Sema3A. Black arrows indicate nodules. Scalebar in the bottom corner of the images indicates 200 µm. Values in the graph are mean ± SD N=7.

3.5 Discussion

Sema3A plays a key role in bone development and bone remodelling by predominantly acting on osteoblasts (Hayashi et al., 2012, Fukuda et al., 2013, Teng et al., 2017). Previous studies have shown that osteosarcoma cells express and produce Sema3A in response to RANKL (Mori et al., 2007, Yue et al., 2014). However, the effects of Sema3A on osteosarcoma cell growth and metastatic behaviour *in vitro* and *in vivo* have not been investigated. The aim of this chapter was to investigate the effect of exogenous Sema3A on the osteoblastic and metastatic features of osteosarcoma cells.

Several studies have shown that Sema3A affects cell motility in physiological and pathophysiological conditions (Neufeld and Kessler, 2008). Sema3A signalling leads to neuronal growth cone collapse and was shown to inhibit the migration of neurons and endothelial cells (Dontchev and Letourneau, 2002, Neufeld and Kessler, 2008, Bagnard et al., 2001, Miao et al., 1999). My results show for the first time that Sema3A inhibits migration of osteoblasts. Furthermore, Sema3A inhibited migration in both low and highly metastatic osteosarcoma cell lines implying that Sema3A has tumour suppressive effects in osteosarcoma *in vitro*. These results resemble the effects of Sema3A seen on the motility of breast and prostate cancer cells *in vitro* (Bachelder et al., 2003, Mishra et al., 2015b, Herman and Meadows, 2007).

Exogenous Sema3A increased the alkaline phosphatase activity in the osteosarcoma cell lines with a lower metastatic ability and the osteoblast-like MC3T3-E1 cells without affecting cell viability. This chapter demonstrates that Sema3A, in agreement with previous data (Fukuda et al., 2013, Hayashi et al., 2012) enhances osteoblast differentiation as evidenced by an increase in alkaline phosphatase activity without affecting cell viability. Altogether, these observations suggest that the effect of Sema3A on osteosarcoma cell viability and alkaline phosphatase activity in low metastatic osteosarcoma cell lines is comparable with the effects of Sema3A on calvarial osteoblasts as reported by (Hayashi et al., 2012).

Several studies studied the effects of cancer-derived Sema3A by overexpression or knockdown of Sema3A in several types of cancer cell lines including breast, oral and melanoma cancer cell lines (Casazza et al., 2011, Chakraborty et al., 2012, Huang et al., 2017). To date there is one study that examined effects of systemic Semaphorin 3A treatment on cancer. Cassaza and colleagues reported that systemic delivery of Sema3A, by administration of a lentiviral vector to express Sema3A, reduced tumour growth *in vivo* (Casazza et al., 2011). The effect of exogenous Sema3A on osteosarcoma has not been investigated. Our aim was to investigate the effects of exogenous Sema3A on the metastatic behaviour of osteosarcoma *in vivo*. The aim was achieved by using administration of exogenous Sema3A in a xenograft osteosarcoma mouse model. Administration of exogenous Sema3A had no effect on osteosarcoma tumour growth. This was consistent with the lack of effect of exogenous Sema3A on osteosarcoma cell viability. In contrast, exogenous Sema3A showed a trend towards a reduction of size and number of metastatic nodules in the lungs. These observations are in agreement with the inhibition of osteosarcoma migration by exogenous Sema3A *in vitro*. One of the limitations of this model is the rapid spread and tumour growth which might explain the lack of effect of exogenous Sema3A on tumour growth and lung metastasis.

In summary, the results in this chapter demonstrate that exogenous Sema3A treatment significantly reduced osteoblast and osteosarcoma cell migration without affecting cell viability. Moreover, exogenous Sema3A significantly enhanced alkaline phosphatase activity in osteoblasts and in the lower metastatic osteosarcoma cell lines *In vivo*, exogenous Sema3A showed a trend towards fewer and smaller metastatic nodules in the lungs (see Figure 3.9).

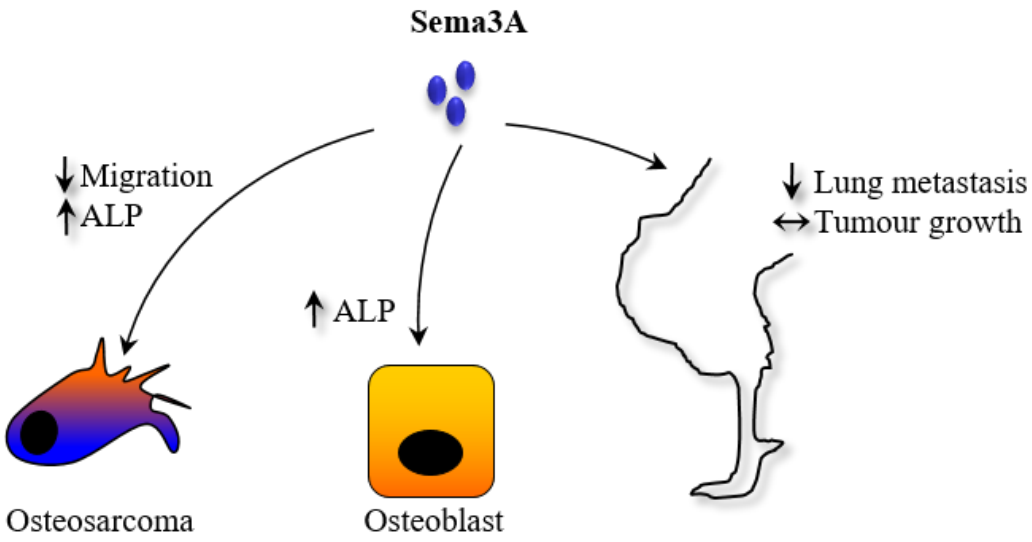

Figure 3.9. Schematic representation of the effects of treatment with exogenous Sema3A.
Sema3A treatment had no effect on osteoblast or osteosarcoma viability but enhanced alkaline phosphatase activity and reduced migration *in vitro* and showed a trend towards less lungs metastasis without affecting tumour growth *in vivo*.

CHAPTER FOUR

Effects of exogenous Sema3A on osteosarcoma induced osteolysis

4 CHAPTER FOUR

4.1 Summary

Recent studies have shown that administration of exogenous Sema3A reduces ovariectomy induced bone loss by stimulating osteoblast differentiation and inhibition of osteoclast formation. Sema3A administration also enhanced bone and enhanced fracture healing in rodents. While there are studies investigating the effect of Sema3A overexpression on cancer, to date the effect of Sema3A treatment on cancer-induced osteoclast activity and osteolysis is unknown. In this chapter, I investigated the effects of administration of exogenous Sema3A on bone damage in a xenograft mouse model of osteosarcoma.

In confirmation with previous studies, administration of exogenous Sema3A enhanced bone volume in the non-inoculated tibia and femur and enhanced femoral cortical bone volume. Treatment with exogenous Sema3A enhanced bone volume in the osteosarcoma-bearing leg, suggesting a reduction of osteosarcoma-induced osteolysis. This bone protective effect was accompanied by a trend towards reduced osteoclasts and increased osteoblast numbers. Interestingly, administration of Sema3A had no effect on osteosarcoma-associated ectopic bone formation. Altogether the results presented in this chapter confirmed that administration of Sema3A enhances bone volume in the absence of cancer and showed for the first time that Sema3A protects against osteosarcoma-induced osteolysis.

4.2 Introduction

In 1996, the importance of Sema3A in bone development was implicated for the first time (Behar et al., 1996). Later work by Gomez and colleagues showed that osteoblasts produce Sema3A and express the receptors for Sema3A (Gomez et al., 2005). Recently a deficiency in Sema3A or presence of an Nrp1 unable to bind Sema3A have been shown to lead to a severe low bone mass phenotype (Hayashi et al., 2012). Furthermore, administration of exogenous Sema3A has been shown to reduce ovariectomy induced bone loss in mice by inhibition of osteoclast formation while concurrently stimulating the differentiation of osteoblasts and regulating both bone formation and resorption (Hayashi et al., 2012). In support of these observations, administration of exogenous Sema3A also stimulated fracture healing in osteoporotic rats (Li et al., 2015a). These studies have shown that Sema3A plays an important role in bone remodelling.

Osteolytic bone damage and ectopic bone formation are common features in osteosarcoma (Geller and Gorlick, 2010). The role of Sema3A in these processes is unknown, but there are indications of the involvement of the semaphorin class-3 coreceptor. Zhu and colleagues showed that overexpression of the Sema3A receptor Nrp1, in osteosarcoma was shown to be a predicting factor of patient prognosis (Zhu et al., 2014). In contrast, another study reported that patients with Nrp2 positive osteosarcoma but not Nrp1 positivity have a significantly shorter overall survival (Boro et al., 2015). Altogether these findings indicate that the neuropilin Sema3A coreceptors play a role in osteosarcoma cell behaviour but whether Sema3A plays a role in osteosarcoma remains unknown.

I showed in chapter 3, Sema3A enhances osteoblast and osteosarcoma alkaline phosphatase activity but the effects of Sema3A on the ability to influence osteoclasts has not been investigated. These findings encouraged us to study the effect of administration of exogenous Sema3A on osteoclastogenesis, osteosarcoma-associated bone damage and ectopic bone formation.

4.3 Aim

The aim of this chapter was to investigate the effects of exogenous Sema3A on osteosarcoma-associated bone disease *in vivo*. The aim was achieved by investigating the effect of exogenous Sema3A on osteosarcoma-associated osteolysis and ectopic bone formation in a xenograft mouse model of osteosarcoma.

4.4 Results

4.4.1 **Exogenous Semaphorin 3A enhanced bone volume in the absence of cancer**

Previous studies have shown that Sema3A treatment enhanced bone volume in osteoporotic mice and enhanced fracture healing in rats (Hayashi et al., 2012, Li et al., 2015a). In view of these observations, I investigated the effects of exogenous Sema3A on bone in the absence and presence of osteosarcoma by microCT (section 2.10.1). Administration of exogenous Semaphorin 3A (0.7 mg/kg) significantly enhanced trabecular bone volume in the tibia as illustrated by enhanced bone volume/total volume (BV/TV, 38% $p<0.01$) and trabecular number (Tb.N, 38% $p<0.01$), reduced trabecular separation (Tb.Sp, 22% $p<0.05$) and enhanced connectivity assessed by trabecular pattern factor (Tb.Pf, 22% $p<0.01$) while there was no change in trabecular thickness (Tb,Th) as observed in Figure 4.1.

In accordance with the bone anabolic effect in the tibia, administration of exogenous Semaphorin 3A (0.7 mg/kg) significantly enhanced bone volume in the femur as illustrated by enhanced BV/TV (70%, $p<0.01$), Tb.Th (9%, $p<0.05$) and Tb.N (58%, $p<0.01$) and reduced Tb.Sp (27%, $p<0.05$), and connectivity assessed by Tb.Pf (32%, $p<0.01$) as observed in Figure 4.2.

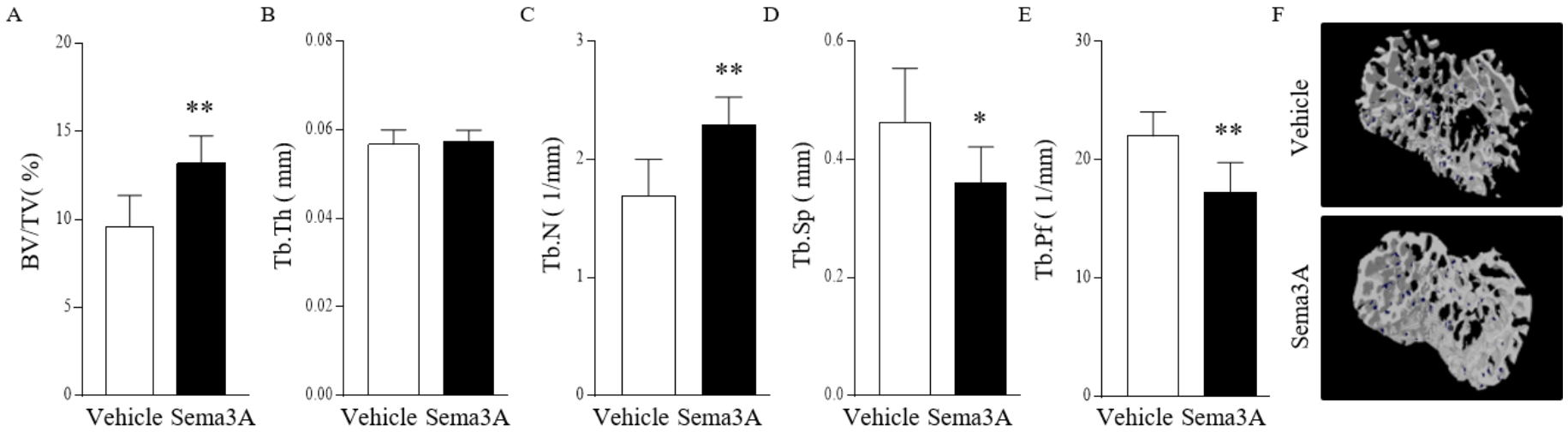

Figure 4.1. Sema3A treatment enhanced bone volume in the healthy tibia.
Osteosarcoma tumours were induced by paratibial injection of KHOS osteosarcoma cells in female Rj: NMRI nude mice. Mice were treated with IP injections biweekly of vehicle (PBS) or recombinant Sema3A (0.7 mg/kg) for the duration of the experiment (21 days) to assess the effect of recombinant Sema3A on bone health. The contralateral legs without osteosarcoma inoculation (healthy leg) were analysed using microCT to assess the effects of recombinant Sema3A on the trabecular compartment of the healthy tibia (Panel A-F). **A.** Quantification of Trabecular bone volume (BV/TV), **B.** Trabecular thickness (Tb.Th), **C.** Trabecular number (Tb.N), **D.** Trabecular separation (Tb.Sp) and **E.** Trabecular pattern factor (Tb.Pf) of the tibia in mice treated with vehicle(PBS) or recombinant Sema3A (0.7 mg/kg/2-weekly). **F.** 3D reconstruction images of tibia from the experiment described in panel A-E. Values in the graph are mean ± SD N=7. * $p < 0.05$, ** $p < 0.01$

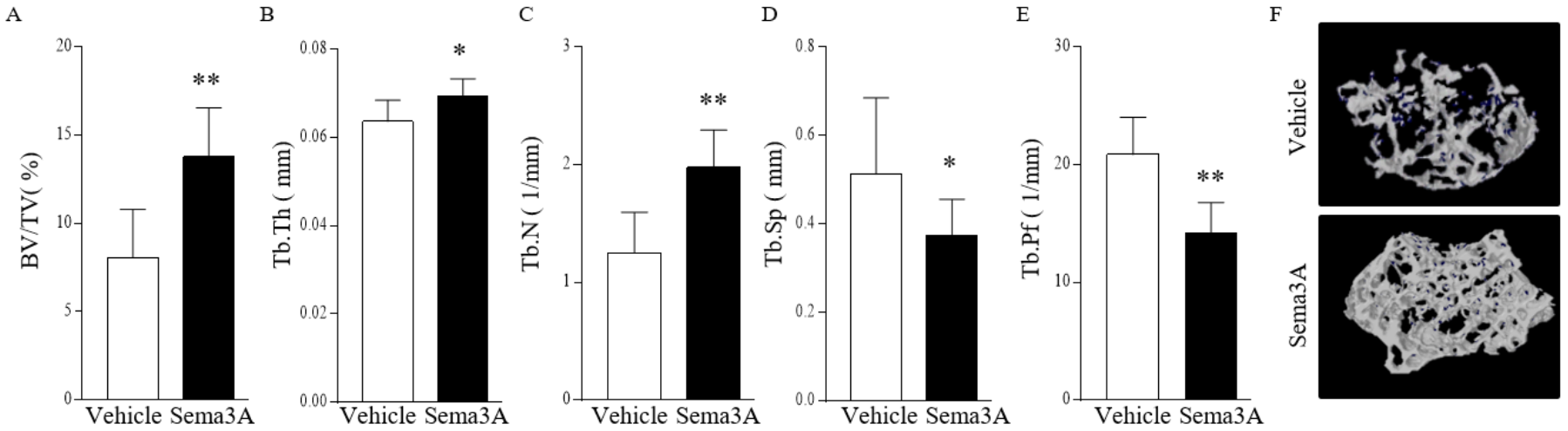

Figure 4.2. Treatment with Sema3A enhanced bone volume in the healthy femur.
Osteosarcoma tumours were induced by paratibial injection of KHOS osteosarcoma cells in female Rj: NMRI nude mice. Mice were treated with IP injections biweekly of vehicle (PBS) or recombinant Sema3A (0.7 mg/kg) for the duration of the experiment (21 days) to assess the effect of recombinant Sema3A on bone health. The contralateral legs without osteosarcoma inoculation (healthy leg) were analysed using microCT to assess the effects of recombinant Sema3A on the trabecular compartment of the healthy femur (Panel A-F).. **A.** Quantification of Trabecular bone volume (BV/TV), **B.** Trabecular thickness (Tb.Th), **C.** Trabecular number (Tb.N), **D.** Trabecular separation (Tb.Sp) and **E.** Trabecular pattern factor (Tb.Pf) of the femur in mice treated with vehicle (PBS) or recombinant Sema3A (0.7 mg/kg/2-weekly). **F.** Representative 3D reconstruction images of tibia from the experiment described in panel A-E. Values in the graph are mean ± SD N=7. * $p < 0.05$, ** $p < 0.01$

Furthermore, exogenous Semaphorin 3A (0.7 mg/kg) significantly enhanced cortical bone volume (BV) in the femur by 10% ($p<0.05$) but had no effect on the cortical bone volume of the tibia (Figure 4.3).

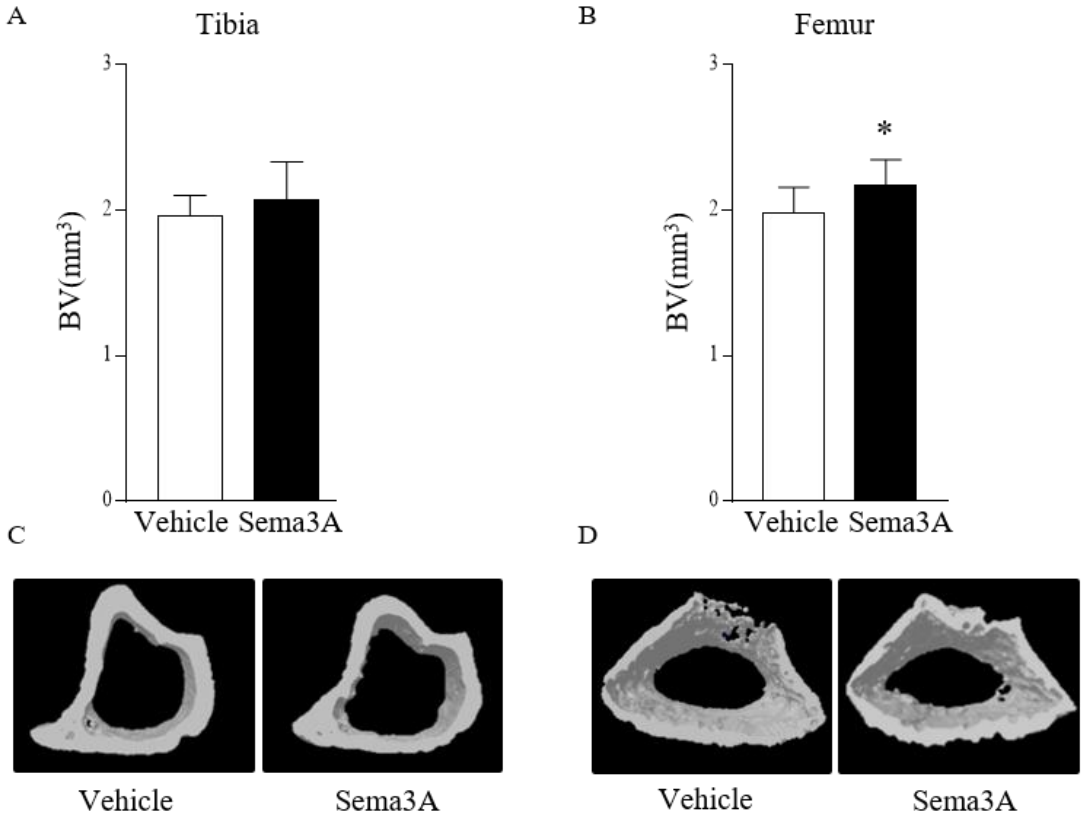

Figure 4.3. Sema3A treatment enhanced femoral cortical bone volume in the healthy leg. Osteosarcoma tumours were induced by paratibial injection of KHOS osteosarcoma cells in female Rj: NMRI nude mice. Mice were treated with IP injections biweekly of vehicle (PBS) or recombinant Sema3A (0.7 mg/kg) for the duration of the experiment (21 days) to assess the effect of recombinant Sema3A on bone health. The contralateral legs without osteosarcoma inoculation (healthy leg) were analysed using microCT to assess the effects of recombinant Sema3A on the trabecular compartment of the healthy femur. The cortex of the femur and tibia from the healthy leg of mice treated with vehicle or Sema3A were analysed using microCT to assess the effect of recombinant Sema3A on cortical bone volume. Quantification of cortical bone volume in the **A.** tibia and **B.** femur in mice treated with vehicle (PBS) or human recombinant Sema3A (0.7 mg/kg/2-weekly). **C.** 3D reconstruction images of tibia and **D.** femur from the experiment described in panel A-B. Values in the graph are mean ± SD N=7. * $p < 0.05$

4.4.2 **Exogenous Semaphorin 3A enhanced osteoblasts and reduced osteoclasts**

Mice treated with exogenous Sema3A exhibited enhanced bone volume with a corresponding reduction of osteoclast number and increased osteoblast surface (Hayashi et al., 2012). To study the effects of Sema3A on osteoblast and osteoclast number *in vivo*, I utilized the non-inoculated leg to assess the osteoblast and osteoclast parameters. Osteoblast and osteoclast histomorphometric analysis was performed on TRAcP stained slides of the tibia (section 2.12.7). As shown in Figure 4.4, exogenous Sema3A (0.7 mg/kg) significantly enhanced osteoblast number (50%, $p<0.01$) and osteoblast surface (51%, $p<0.01$) and reduced osteoclast number (51, $p<0.01$) and osteoclast surface (47%, $p<0.01$).

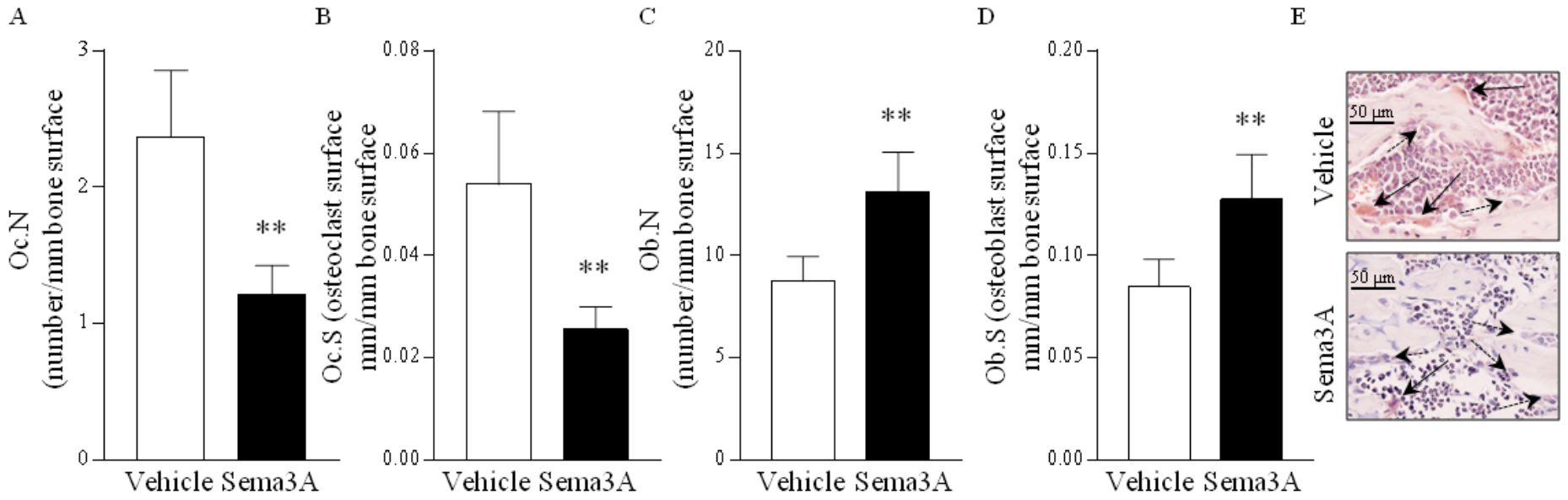

Figure 4.4. Sema3A enhanced osteoblasts and reduced osteoclast numbers in the tibia.
Osteosarcoma tumours were induced by paratibial injection of KHOS osteosarcoma cells in female Rj: NMRI nude mice. Mice were treated with IP injections biweekly of vehicle (PBS) or recombinant Sema3A (0.7 mg/kg) for the duration of the experiment (21 days) to assess the effect of recombinant Sema3A on bone health. Healthy tibia of mice treated with vehicle or recombinant Sema3A were cut and TRAcP stained to assess the cellular parameters in the trabeculae to assess the effect of recombinant Sema3A on osteoclast number and osteoclast surface and osteoblast number and osteoblast surface. Histomorphometric analysis of **A.** osteoclast number (Oc.N), **B.** osteoclast surface (OC.S), **C.** osteoblast number (Ob.N) **D.** osteoblast surface (Ob.S) of the tibia in mice treated with vehicle (PBS) or human recombinant Sema3A (0.7 mg/kg/2-weekly). **E.** Representative photomicrographs of TRAcP positive osteoclasts indicated with solid arrows and osteoblasts indicated with dotted arrows from the experiment described in panel A-E. Scalebar in the top left of the images indicates 50 µm. Values in the graph are mean ± SD N=5.

4.4.3 **Exogenous Semaphorin 3A enhanced bone volume in the presence of osteosarcoma**

Next, I analysed the skeletal parameters of the tumour-bearing legs and investigated the effect of exogenous Sema3A on osteosarcoma-associated bone damage in the trabecular and cortical compartment. Sema3A (0.7 mg/kg) enhanced trabecular bone volume 96% ($p<0.05$) of the tibia in the presence of osteosarcoma but had no significant effects on trabecular thickness, trabecular number, trabecular separation and trabecular pattern factor Figure 4.5.

Administration of exogenous Sema3A (0.7 mg/kg) had no effect on bone volume, trabecular thickness, trabecular number, trabecular separation and trabecular pattern factor in the tumour-bearing femur as shown Figure 4.6.

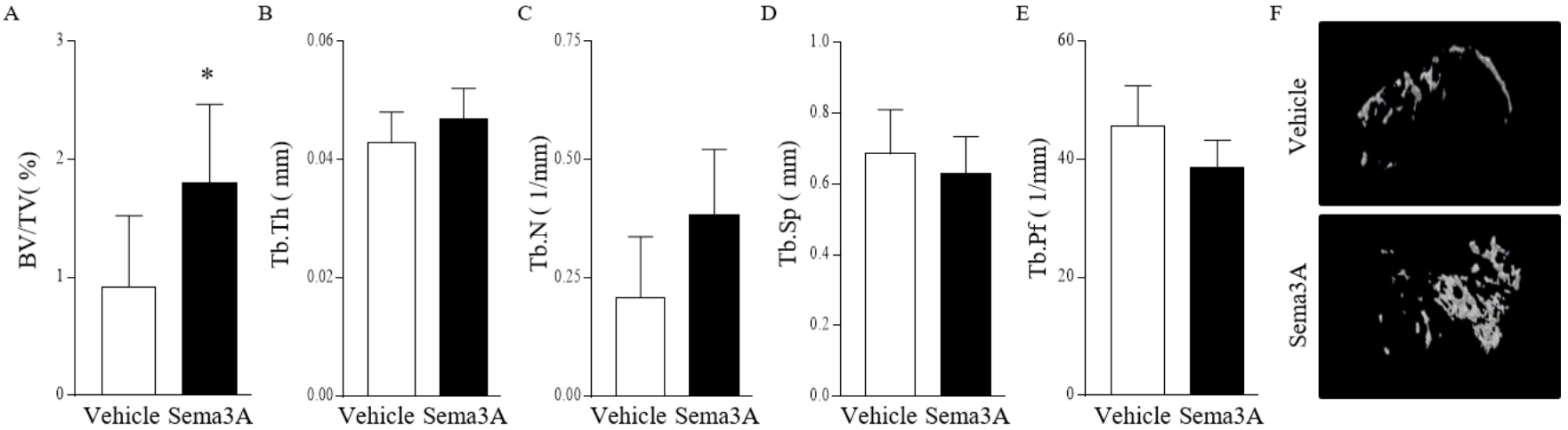

Figure 4.5. Treatment with exogenous Sema3A enhanced bone volume in the presence of osteosarcoma in the tibia.
Osteosarcoma tumours were induced by paratibial injection of KHOS osteosarcoma cells in female Rj: NMRI nude mice. Mice were treated with IP injections biweekly of vehicle (PBS) or recombinant Sema3A (0.7 mg/kg) for the duration of the experiment (21 days) to assess the effect of recombinant Sema3A on bone health. The osteosarcoma-bearing legs were analysed using microCT to assess the effects of recombinant Sema3A on the trabecular compartment of the osteosarcoma bearing tibia (Panel A-F). **A.** Quantification of Trabecular bone volume, **B.** Trabecular thickness, **C.** Trabecular number, **D.** Trabecular separation and **E.** Trabecular pattern factor of the tumour bearing tibia in mice treated with vehicle (PBS) or human recombinant Sema3A (0.7 mg/kg/2-weekly). **F.** 3D reconstruction images of tibia from the experiment described in panel A-E. Values in the graph are mean ± SD N=7. * $p < 0.05$

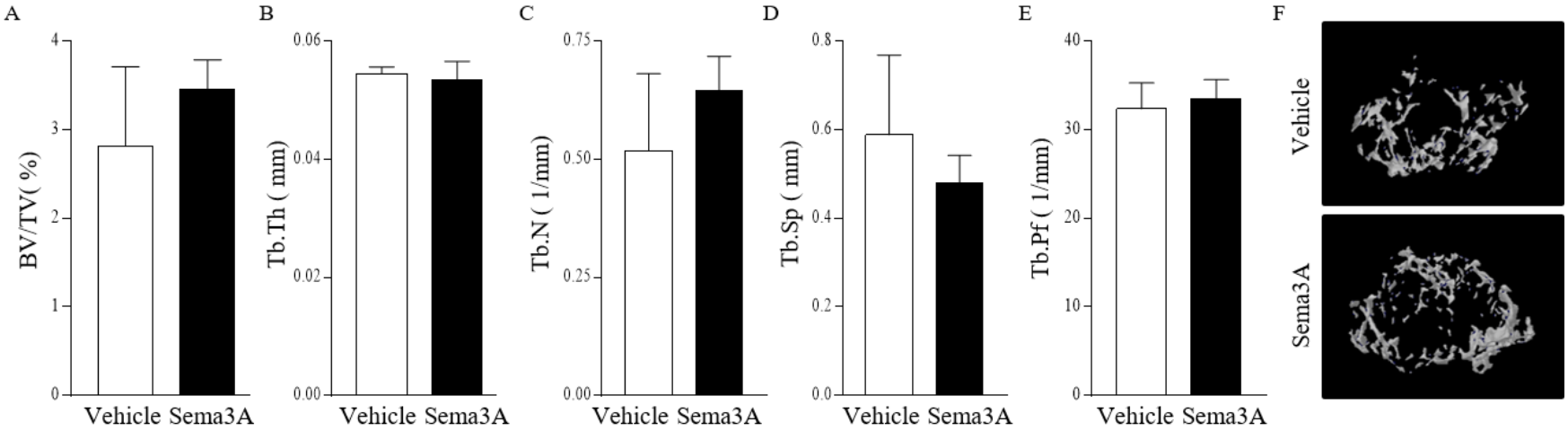

Figure 4.6. Sema3A treatment had no effect on bone volume of the tumour-bearing femur.
Osteosarcoma tumours were induced by paratibial injection of KHOS osteosarcoma cells in female Rj: NMRI nude mice. Mice were treated with IP injections biweekly of vehicle (PBS) or recombinant Sema3A (0.7 mg/kg) for the duration of the experiment (21 days) to assess the effect of recombinant Sema3A on bone health. The osteosarcoma-bearing legs were analysed using microCT to assess the effects of recombinant Sema3A on the trabecular compartment of the osteosarcoma-bearing femur (Panel A-F). **A.** Quantification of Trabecular bone volume, **B.** Trabecular thickness, **C.** Trabecular number, **D.** Trabecular separation and **E.** Trabecular pattern factor of the tumour bearing femur in mice treated with vehicle (PBS) or human recombinant Sema3A (0.7 mg/kg/2-weekly). **F.** 3D reconstruction images of femur from the experiment described in panel A-E. Values in the graph are mean ± SD N=7. * $p < 0.05$

Next, I analysed the cortical bone volume of the tumour-bearing tibia and femur. As shown in Figure 4.7, administration of exogenous Semaphorin3A had no effect on the cortical bone volume of the tumour-bearing tibia and femur.

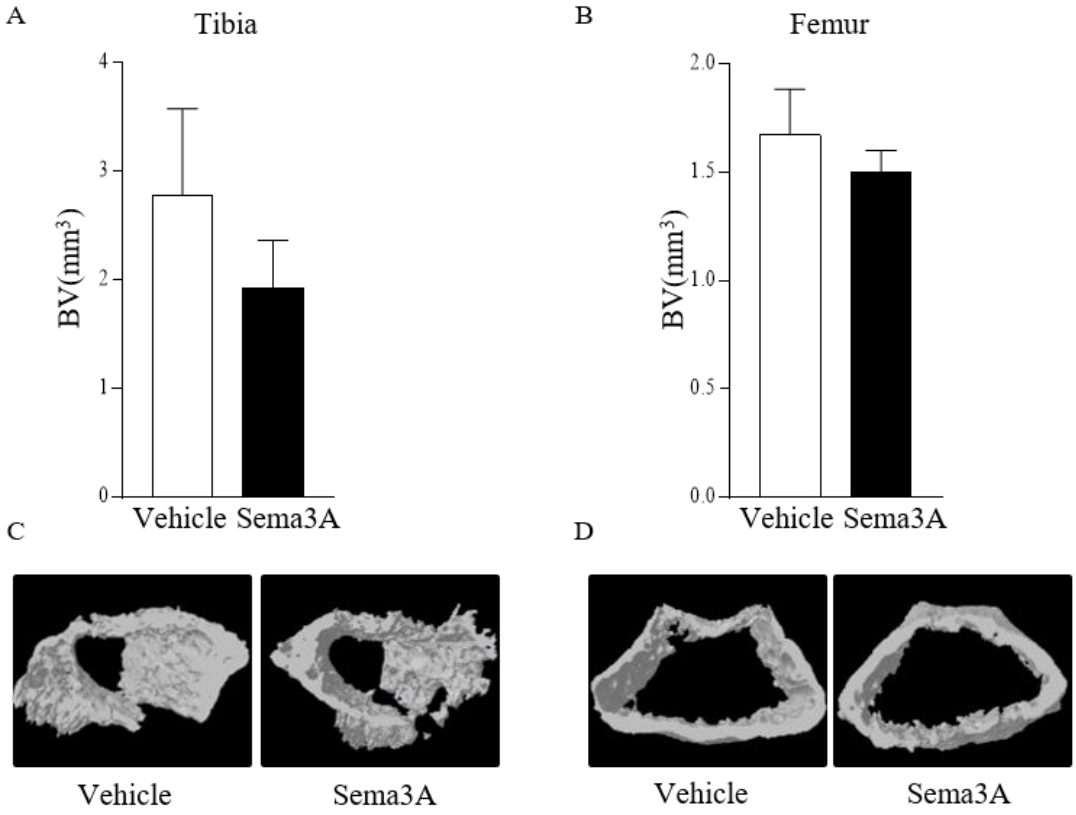

Figure 4.7. Sema3A treatment had no effect on cortical bone volume in the tumour-bearing leg. Osteosarcoma tumours were induced by paratibial injection of KHOS osteosarcoma cells in female Rj: NMRI nude mice. Mice were treated with IP injections biweekly of vehicle (PBS) or recombinant Sema3A (0.7 mg/kg) for the duration of the experiment (21 days) to assess the effect of recombinant Sema3A on bone health. The cortex of the osteosarcoma-bearing femur and tibia were analysed using microCT to assess the effect of recombinant Sema3A on cortical bone volume in the presence of osteosarcoma (Panel A-D). Quantification of cortical bone volume in the tumour bearing **A.** tibia and **B.** femur in mice treated with vehicle (PBS) or human recombinant Sema3A (0.7 mg/kg/2-weekly). **C.** 3D reconstruction images of tibia and **D.** femur from the experiment described in panel A-B. Values in the graph are mean ± SD N=7.

4.4.4 **Exogenous Sema3A showed a trend towards enhanced PINP and reduced CTX serum levels.**

Previous studies have suggested that serum markers of bone formation and bone resorption may have value in identifying osteosarcoma-associated changes in bone metabolism (Hu et al., 2015, Ambroszkiewicz et al., 2010). To investigate the systemic markers indicative of bone formation (PINP) and bone resorption (CTX), P1NP and CTX were measured in the serum of mice inoculated with osteosarcoma cells and treated with Sema3A or vehicle using ELISA kits. As shown in Figure 4.8, administration of Sema3A showed a trend towards a reduced serum level of CTX and an enhanced level of the bone formation marker PINP.

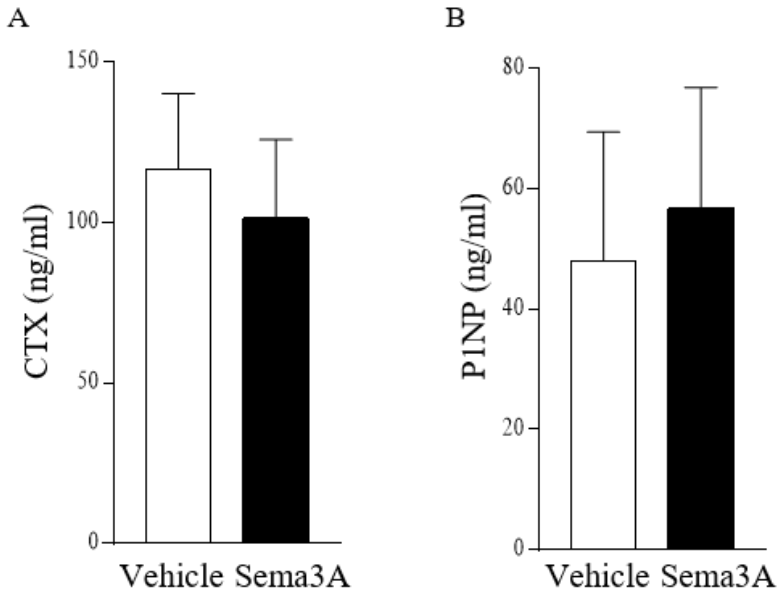

Figure 4.8. Exogenous Sema3A showed a trend towards reduced CTX and increased PINP. Osteosarcoma tumours were induced by paratibial injection of KHOS osteosarcoma cells in female Rj: NMRI nude mice. Mice were treated with IP injections biweekly of vehicle (PBS) or recombinant Sema3A (0.7 mg/kg) for the duration of the experiment (21 days) to assess the effect of recombinant Sema3A on bone health. Serum levels of bone turnover markers were assessed in osteosarcoma-bearing mice treated with vehicle or recombinant Sema3A. Serum levels of **A.** bone resorption marker C-terminal telopeptide crosslinks (CTX) and **B.** bone formation marker N-terminal propeptide of type 1 procollagen (P1NP) of mice inoculated with osteosarcoma tumours and treated with exogenous Sema3A or vehicle. Values are mean ± SD N=3.

4.4.5 **Semaphorin 3A showed a trend towards higher osteoblast number in osteosarcoma**

Mice administrated with exogenous Sema3A show enhanced bone volume with a corresponding reduction of osteoclast number and increased osteoblast surface (Hayashi et al., 2012). To assess the effects of Sema3A on osteoblast parameters in the tumour-bearing tibia, osteoblast histomorphometric analysis was performed on TRAcP stained slides of the osteosarcoma-bearing tibia (section 2.12.7). As shown in Figure 4.9, administration of exogenous Semaphorin3A (0.7 mg/kg) showed a trend towards higher osteoblast number and osteoblast surface in comparison to the vehicle treated osteosarcoma-bearing tibia.

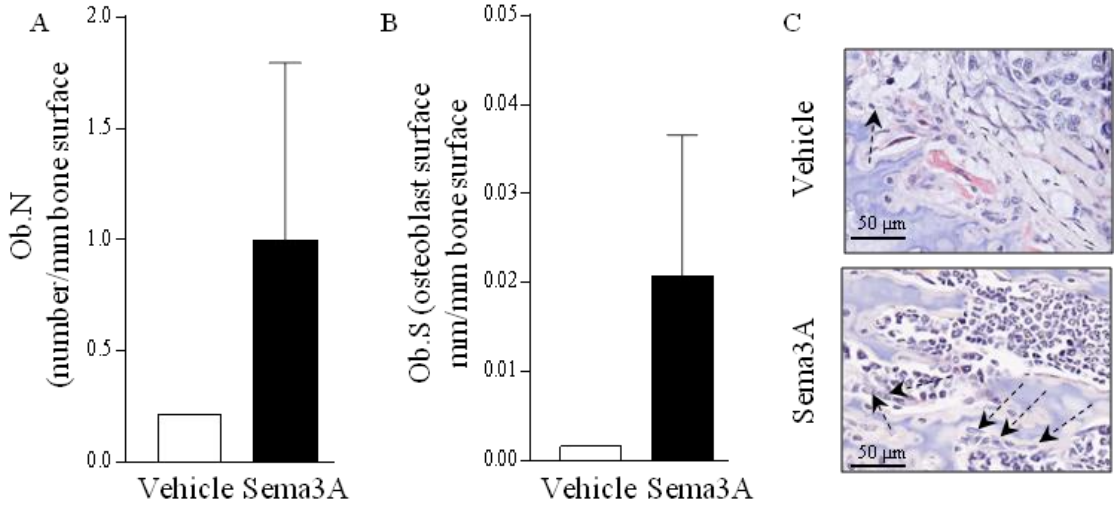

Figure 4.9. Sema3A showed a trend towards increased osteoblast number in the tumour-bearing tibia.
Osteosarcoma tumours were induced by paratibial injection of KHOS osteosarcoma cells in female Rj: NMRI nude mice. Mice were treated with IP injections biweekly of vehicle (PBS) or recombinant Sema3A (0.7 mg/kg) for the duration of the experiment (21 days) to assess the effect of recombinant Sema3A on bone health. Osteosarcoma-bearing tibia of mice were sectioned and TRAcP stained to assess the cellular parameters in the trabeculae to investigate the effect of recombinant Sema3A on osteoblast number and osteoblast surface. Histomorphometric analysis of **A** osteoblast number (Ob.N) **B.** osteoblast surface (Ob.S) of the tumour bearing tibia in mice treated with vehicle (PBS) or human recombinant Sema3A (0.7 mg/kg/2-weekly). **C.** Representative photomicrographs of osteoblasts indicated with dotted arrows from the experiment described in panel A-B. Scalebar in the bottom left of the images indicates 50 µm. Values in the graph are mean ± SD N=5.

4.4.6 **Semaphorin 3A showed a trend towards fewer osteoclasts in osteosarcoma**

Mice administrated with exogenous Sema3A show enhanced bone volume with a corresponding reduction of osteoclast number and increased osteoblast surface (Hayashi et al., 2012). To assess the effects of Sema3A on osteoclast parameters in the osteosarcoma-bearing tibia, osteoclast histomorphometric analysis was performed on TRAcP stained slides of the osteosarcoma-bearing tibia (section 2.12.7). As shown in Figure 4.10, administration of exogenous Semaphorin3A (0.7 mg/kg) showed a trend towards reduced osteoclast number and osteoclast surface in comparison to the vehicle treated osteosarcoma-bearing tibia (Figure 4.10).

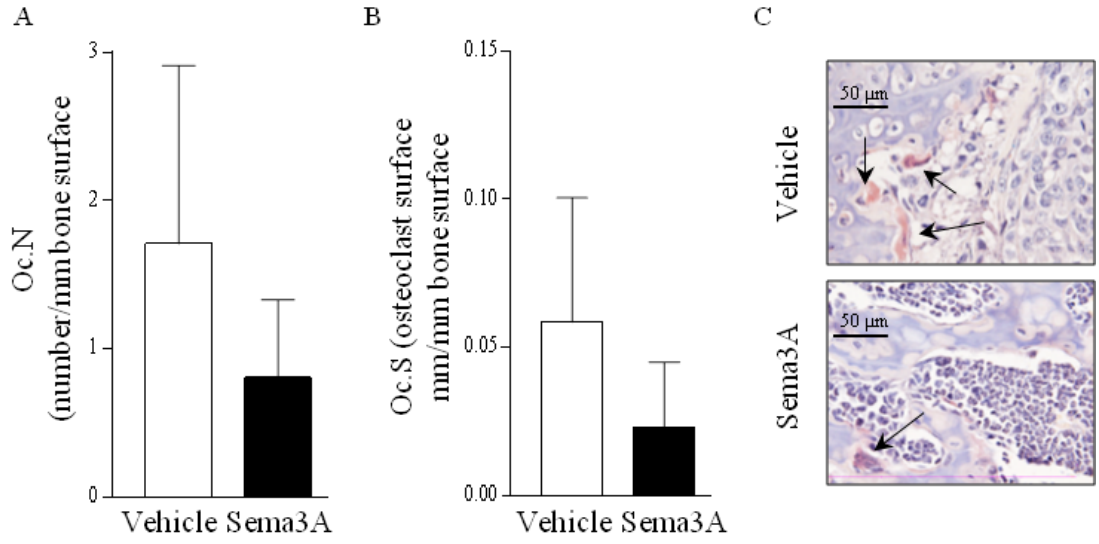

Figure 4.10 Sema3A showed a trend towards fewer osteoclasts in the tumour-bearing tibia. Osteosarcoma tumours were induced by paratibial injection of KHOS osteosarcoma cells in female Rj: NMRI nude mice. Mice were treated with IP injections biweekly of vehicle (PBS) or recombinant Sema3A (0.7 mg/kg) for the duration of the experiment (21 days) to assess the effect of recombinant Sema3A on bone health. Osteosarcoma-bearing tibia of mice were sectioned and TRAcP stained to assess the cellular parameters in the trabeculae to investigate the effect of recombinant Sema3A on osteoclast number and osteoclast surface. Histomorphometric analysis of **A** osteoclast number (Oc.N) **B.** osteoclast surface (Oc.S) of the tumour bearing tibia in mice treated with vehicle (PBS) or human recombinant Sema3A (0.7 mg/kg/2-weekly). **C.** Representative photomicrographs of TRAcP positive osteoclasts indicated with solid arrows from the experiment described in panel A-B. Scalebar in the top left of the images indicates 50 µm Values in the graph are mean ± SD N=5.

4.4.7 **Exogenous Sema3A reduced osteoclastogenesis in osteosarcoma-osteoclast cocultures *in vitro***

Previous studies have reported that Sema3A inhibits osteoclast formation and osteoclast activity (Hayashi et al., 2012, Fukuda et al., 2013, Teng et al., 2017). As observed in the previous section, Sema3A showed a trend towards fewer osteoclasts in the presence of osteosarcoma *in vivo*. To further investigate the effect of exogenous Sema3A on osteosarcoma-osteoclast interactions, I cultured a panel of osteosarcoma cell lines with osteoclast precursors *in vitro*. Briefly, RAW 264.7 or mouse bone marrow cultures were cultured 24 hours prior addition of low number of osteosarcoma cells and treatment with vehicle or Sema3A (300 ng/ml) as described in more detail in section 2.2.

Exogenous Sema3A significantly reduced osteoclastogenesis of RAW 264.7 - MG-63 cocultures by 19% ($p<0.01$). In mouse bone marrow- osteosarcoma cocultures, exogenous Sema3A significantly reduced osteoclastogenesis in the presence of Saos-2 (48% $p<0.001$), MNNG/HOS (51% $p<0.01$) and KHOS (48% $p<0.01$) osteosarcoma cells (Figure 4.11).

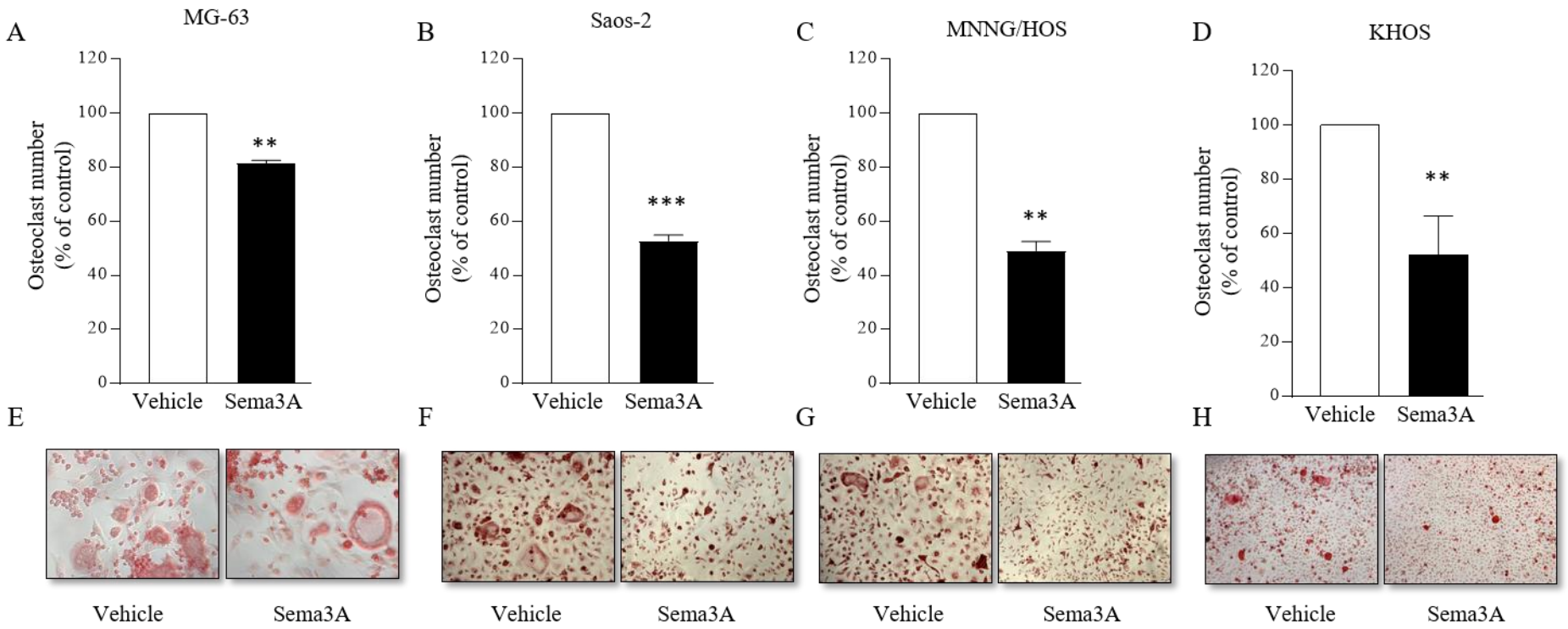

Figure 4.11. Exogenous Sema3A reduced osteoclastogenesis in mouse osteoclast-osteosarcoma cocultures.
The effect of exogenous Sema3A on osteoclast formation was assessed using cocultures of osteosarcoma cells with bone-marrow or RAW264.7 cells. The method of cocultures was chosen to investigate the effect of exogenous Sema3A in the presence of osteosarcoma to more closely mimic the tumour microenvironment *in vivo*. Cultures were treated for 7 days, after the culture period cultures were fixed and TRAcP stained for osteoclast quantification. Osteoclasts were counted when they were stained with TRAcP and contained >3 nuclei. **A**. Quantification of osteoclast number in RAW 264.7 coculture with MG-63 treated with vehicle (PBS) or exogenous Sema3A (300 ng/ml). Quantification of osteoclast number in M-CSF and RANKL stimulated mouse bone marrow cocultures with **B.** Saos-2 **C.** MNNG/HOS and **D.** KHOS osteosarcoma cells treated with vehicle (PBS) or exogenous Sema3A (300 ng/ml). **E.** Representative photomicrographs (10X) of MG-63-RAW 264.7 cocultures exposed to vehicle (PBS) or Sema3A (300 ng/ml) of experiments described in panel A. **F.** Representative photomicrographs (10X) of Saos-2- mouse bone marrow cocultures exposed to vehicle (PBS) or Sema3A (300 ng/ml) of experiments described in panel B. **G.** Representative photomicrographs (10X) of MNNG/HOS- mouse bone marrow cocultures exposed to vehicle (PBS) or Sema3A (300 ng/ml) of experiments described in panel C. **H.** Representative photomicrographs of (10X) KHOS- mouse bone marrow cocultures exposed to vehicle (PBS) or Sema3A (300 ng/ml) of experiments described in panel D. Values in the graph are mean ± SD and are obtained from 3 independent experiments ** $p < 0.01$, *** $p < 0.001$

Next, I investigated whether osteoclast formation was affected by exogenous Sema3A (300 ng/ml) in MC3T3-E1-RAW 264.7 cocultures cells. RAW264.7 cells were cultured 24 hours prior to addition of the MC3T3-E1 cells (section 2.2.3). As seen in Figure 4.12 exogenous Sema3A significantly reduced osteoclastogenesis in the presence of MC3T3-E1 cells (23%, $p<0.01$).

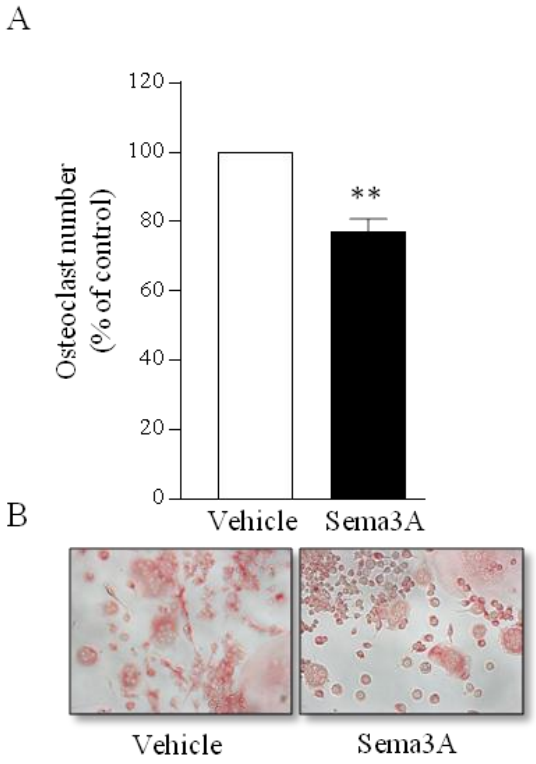

Figure 4.12. Exogenous Sema3A reduced osteoclast formation in MC3T3-E1-RAW264.7 cocultures.
Cultures were treated for 7 days, after the culture period cultures were fixed and TRAcP stained for osteoclast quantification. Osteoclasts were counted when they were stained with TRAcP and contained >3 nuclei. RAW264.7 cells were cocultured with MC3T3-E1 and treated with vehicle (PBS) or exogenous Sema3A (300 ng/ml). to assess the effect of Sema3A on osteoclast formation. **A.** Quantification of osteoclast number in RANKL (50 ng/ml) stimulated MC3T3-E1-RAW 264.7 co-cultures. **B.** Representative photomicrographs (10X) of cultures described in panel A. Values in the graph are mean ± SD and are obtained from 3 independent experiments ** $p < 0.01$.

4.5 Discussion

Previous studies have shown that Sema3A plays an important role in bone development, bone remodelling and cancer (Hayashi et al., 2012, Li et al., 2015a, Herman and Meadows, 2007, Zhou et al., 2014, Pan and Bachelder, 2010, Mishra et al., 2015b, Casazza et al., 2011, Chakraborty et al., 2012, Huang et al., 2017). To date little is known about the role of Sema3A in osteosarcoma-associated osteolysis. The neuropilins, the Sema3A coreceptors have been implicated in the prognosis and survival of osteosarcoma (Zhu et al., 2014, Boro et al., 2015). However, the observations in these studies may not be solely attributed to semaphorin class-3 signalling alone. Sema3A and VEGF are competitors for Nrp1 and Nrp2 binding and signaling (Guo and Vander Kooi, 2015, Miao et al., 1999, Bagnard et al., 2001). For that reason, involvement of VEGF signalling leading to a poorer prognosis in patients overexpressing the neuropilin receptors cannot be excluded. Altogether these findings suggest that the neuropilin coreceptor plays a role in osteosarcoma but the effects of Sema3A on osteosarcoma-associated bone disease is still unknown. The aim of this chapter was to investigate the effect of Sema3A administration on osteosarcoma-associated bone disease in mice.

The aim was achieved by administration of exogenous Sema3A in a xenograft osteosarcoma mouse model. Osteosarcoma was induced with a paratibial injection of the KHOS osteosarcoma cells and mice were given biweekly injections of vehicle or exogenous Sema3A until the experiment was terminated. As Sema3A is important in bone development, bone remodelling and osteoblast-osteoclast coupling (Hayashi et al., 2012), I first investigated the effects of exogenous Sema3A administration on bone parameters of non-inoculated tibia and femur of mice. Administration of exogenous Sema3A significantly increased trabecular bone volume, trabecular number, trabecular connectivity and reduced trabecular separation in the tibia. I observed similar effects of exogenous Sema3A in the femur where, in addition to the other bone parameters, the trabecular thickness was also significantly increased. Moreover, there was a modest but significant increase in the femoral cortical bone volume without any difference in the cortical bone volume of the tibia. Consistent with these effects, exogenous Sema3A enhanced osteoblast number and surface and reduced osteoclast number and osteoclast surface. These findings are in agreement

with the bone anabolic effect of Sema3A treatment as previously reported in wild-type and osteoporotic rodents (Hayashi et al., 2012, Li et al., 2015a).

The presence of osteosarcoma caused significant bone damage in both the tibia and the femur. Despite the severity of the osteosarcoma related trabecular bone loss in these mice, I demonstrated for the first time that administration of exogenous Sema3A enhanced the trabecular bone volume in the tibia, indicative of protection against osteosarcoma-associated osteolysis and bone destruction. While osteolysis was observed in the femur as evidenced by a reduced BV/TV in comparison to the non-inoculated control, there were no changes detected in the femoral trabecular bone volume. Consistent with the increase in trabecular bone volume of the tibia by Sema3A in the presence and absence of osteosarcoma I observed a trend towards reduced serum level of the bone resorption marker CTX and enhanced level of the bone formation marker PINP. Furthermore, exogenous Sema3A showed a trend towards less osteoclasts and more osteoblasts in the tumour-bearing tibia which is in agreement with the inhibitory effect of Sema3A on osteoclasts and enhanced osteoblast differentiation as reported in Chapter 3 and previous studies (Hayashi et al., 2012).

Osteosarcoma tumours often present as a mixture of osteoblastic and osteolytic lesions (Geller and Gorlick, 2010). Benign multinucleated giant cells that resemble osteoclasts are present in 25% of osteosarcoma cases (Klein and Siegal, 2006). To further investigate the observed trend towards fewer osteoclasts *in vivo*, I investigated whether Sema3A is able to inhibit osteoclast formation in the presence of osteosarcoma cells using osteoclast-osteosarcoma cocultures. In this chapter I showed that regardless of the presence of osteoblasts or osteosarcoma cells in osteoclast precursor cultures, Sema3A was effective in inhibiting osteoclast formation *in vitro*. As described in previous chapters Sema3A had no effect on osteosarcoma cell viability and previous work in our lab showed that Sema3A inhibited RANKL-induced osteoclast formation. These results imply that Sema3A has a direct effect on the osteoclasts rather than an indirect effect via the osteosarcoma cells present in the cultures. This is consistent with previous studies (Hayashi et al., 2012, Fukuda et al., 2013).

Several studies have shown that genetic modulation of Sema3A inhibits tumour growth *in vivo* suggesting that exogenous Sema3A may be of therapeutic value in the treatment of cancer (Casazza et al., 2011, Chakraborty et al., 2012, Huang et al., 2017). Cassaza and colleagues also showed that lentiviral activation of Sema3A injected systemically reduced tumour growth. In contrast, I observed no effect of exogenous Sema3A on tumour growth in the KHOS model of human osteosarcoma.

In summary, administration of exogenous Sema3A significantly enhanced bone volume in the absence and presence of osteosarcoma and showed a trend towards fewer osteoclasts and more osteoblasts in the osteosarcoma-bearing tibia. (Figure 4.13).

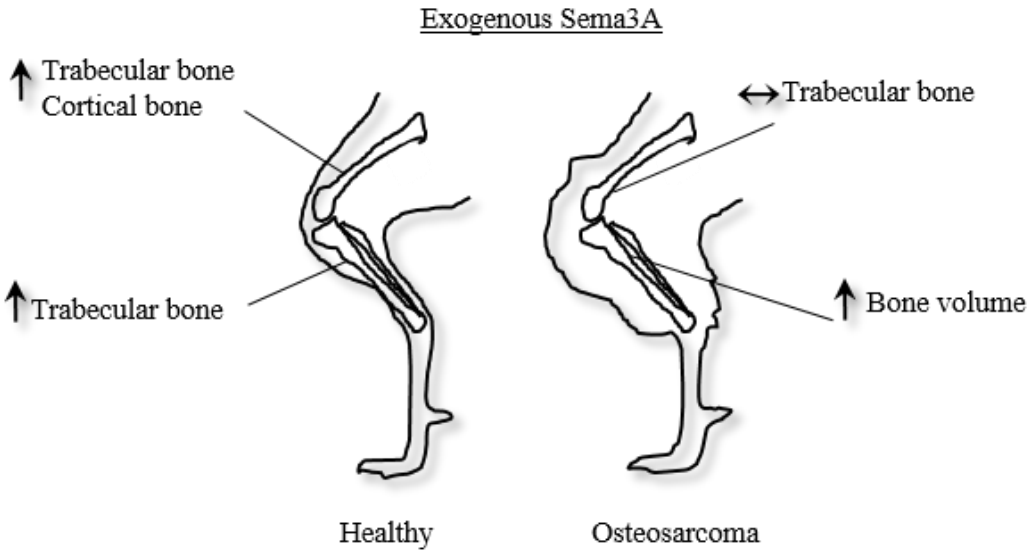

Figure 4.13. Schematic representation of the effects of exogenous Sema3A on bone *in vivo*. Recombinant Sema3A treatment in mice enhanced trabecular and cortical bone volume of the femur and enhanced trabecular bone volume of the healthy tibia. In the osteosarcoma-bearing leg Sema3A enhanced bone volume in the tibia but had not effect on trabecular bone volume of the femur.

CHAPTER FIVE

Role of osteosarcoma-derived Sema3A on tumour growth and lung metastasis

5 CHAPTER FIVE

5.1 Summary

Sema3A expression has been correlated with patient survival in several types of cancers and overexpression of Sema3A in breast cancer, melanoma and oral cancer cells significantly reduced tumour growth. However, the role of tumour-derived Sema3A in osteosarcoma is unknown. Exogenous Sema3A enhanced alkaline phosphatase activity and reduced migration in a panel of osteosarcoma cells as described in chapter 3. Based on these previous studies, I overexpressed Sema3A in the KHOS osteosarcoma cell line and investigated the effect of Sema3A overexpression on metastatic characteristics of the KHOS osteosarcoma cells *in vitro* and *in vivo*.

The KHOS osteosarcoma cells successfully and stably overexpressed and secreted Sema3A with the use of lentiviral activation particles. Overexpression of Sema3A in the KHOS osteosarcoma cells decreased cell viability *in vitro*. Sema3A overexpression also reduced directed migration, random single cell migration and invasion *in vitro* indicative of anti-metastatic effects. However, Sema3A overexpression had no effect on tumour growth or lung metastasis *in vivo*. Overall this chapter showed that overexpression of Sema3A was effective in reducing osteosarcoma cell viability and motility *in vitro* but showed a lack of effect on tumour growth and lung metastases *in vivo*.

5.2 Introduction

Sema3A has been shown to modulate tumour cell behaviour in a variety of cell types (Table 1.3). A decreased Sema3A expression was correlated with a poor survival rate in gastric carcinoma and non-small cell lung cancer patients (Zhou et al., 2014, Tang et al., 2014). Overexpression of Sema3A was shown to inhibit breast cancer cell motility and prostate cancer cell invasion and tumour-specific Sema3A expression in several breast cancer cell lines, different melanoma cell lines and oral cancer significantly reduced tumour growth *in vivo* (Pan and Bachelder, 2010, Mishra et al., 2015b, Herman and Meadows, 2007, Casazza et al., 2011, Chakraborty et al., 2012, Huang et al., 2017). In osteosarcoma, overexpression of the Sema3A receptor Nrp1 was shown to be a predicting factor of patient prognosis (Zhu et al., 2014). Another study reported that patients with Nrp2 but not Nrp1 positive osteosarcoma have a significantly shorter overall survival (Boro et al., 2015). However, the role of tumour-derived Sema3A on osteosarcoma growth and lung metastases is unknown.

As described in the previous chapter, exogenous Sema3A enhanced alkaline phosphatase activity, inhibited osteoclast formation and reduced migration in a panel of osteosarcoma cells. Furthermore, exogenous Sema3A enhanced bone volume in the absence and presence of osteosarcoma and showed a trend towards fewer and smaller lung metastases in comparison to the control without affecting tumour growth *in vivo*.

Based on the aforementioned studies and the effects of exogenous Sema3A reported in chapter 3 and 4, I hypothesized that overexpression of Sema3A in the human KHOS osteosarcoma cell line inhibits osteosarcoma viability and motility *in vitro* and inhibits osteosarcoma tumour growth and lung metastases *in vivo*.

5.3 Aim

The aim of this chapter was to investigate the role of Sema3A overexpression in human osteosarcoma cancer cell behaviour *in vitro* and *in vivo*. The aim was achieved by overexpressing Sema3A in the highly metastatic human osteosarcoma cell line KHOS. Next I investigated the effect of osteosarcoma-derived Sema3A on osteosarcoma viability, migration and invasion *in vitro* and tumour growth and lung metastasis *in vivo*.

5.4 Results

5.4.1 **Successful overexpression of Sema3A in KHOS osteosarcoma cells**

To investigate the role of tumour-derived Sema3A, I overexpressed it in the highly metastatic human KHOS osteosarcoma cells with the use of Sema3A lentiviral activation particles (section 2.5). Western blot was used to assess protein expression of Sema3A in the cell lysates and the production of secreted Sema3A was detected in the cell medium. Sema3A in the conditioned medium was quantified using a standard of recombinant Sema3A ran in the same western blot. Semaphorin 3A was successfully overexpressed in the cells by 2.5 fold ($p<0.05$) as assessed by Sema3A 95kDa expression. Sema3A was also secreted 6.5 fold more by Sema3A overexpressing KHOS cells than the mock control ($p<0.05$) as assessed by amount of Sema3A 95kDa detected in the conditioned medium in comparison to mock control as shown in Figure 5.1.

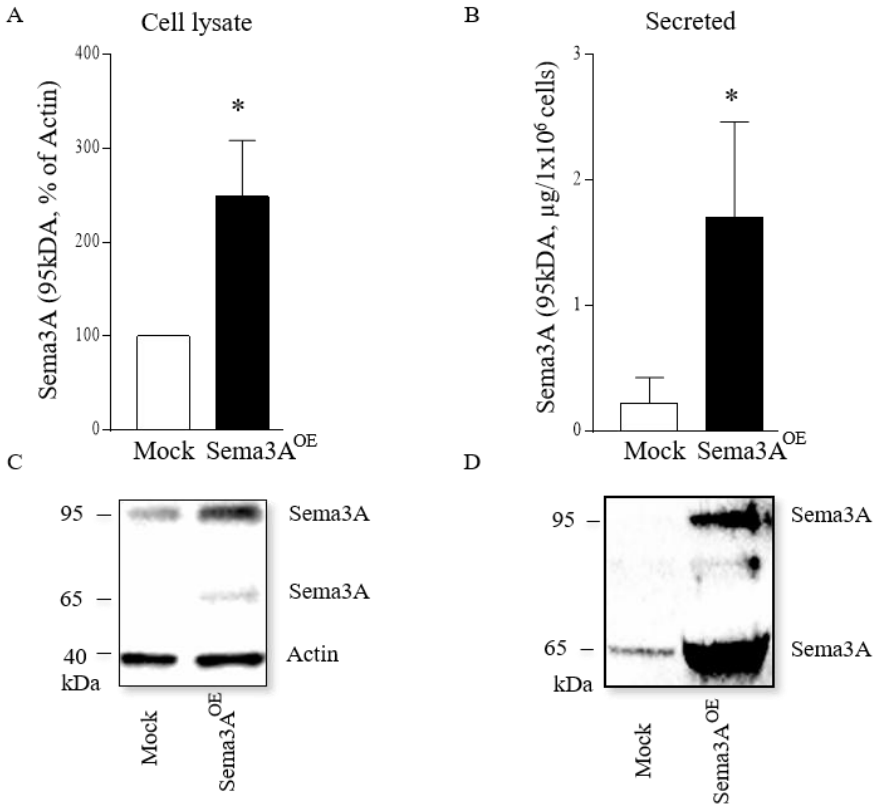

Figure 5.1. Sema3A was successfully overexpressed in the human KHOS osteosarcoma cells.
To confirm the Sema3A overexpression by lentiviral activation particles the protein levels of Sema3A were measured in the cell lysates and conditioned medium by western blot. **A.** Quantification of Sema3A expression in the cell lysate of KHOS mock and Sema3A overexpressing KHOS ($Sema3A^{OE}$) cells. **B.** Quantification of Sema3A in the cell medium of mock and Sema3A overexpressing KHOS cells. Quantification of Sema3a protein expression in the conditioned medium was achieved using a standard of recombinant Sema3A (2 µg) in the western blot. **C.** Representative photomicrograph of the western blot experiment described in panel A. **D.** Representative photomicrograph of a western blot experiment

described in panel B. Values in the graph are mean ± SD and are obtained from 3 independent experiments. * $p < 0.05$

5.4.2 **Sema3A overexpression reduced osteosarcoma cell viability *in vitro***

After successful generation of stable Sema3A overexpression in human KHOS osteosarcoma cells, I performed functional assays to assess the effect of tumour-specific Sema3A overexpression on osteosarcoma cell viability, migration and invasion. First, I investigated the effect of tumour-specific Sema3A overexpression on the viability of KHOS osteosarcoma cells *in vitro*. As shown in Figure 5.2, Sema3A overexpression significantly reduced cell growth by 40% ($p<0.01$) after 48 hours.

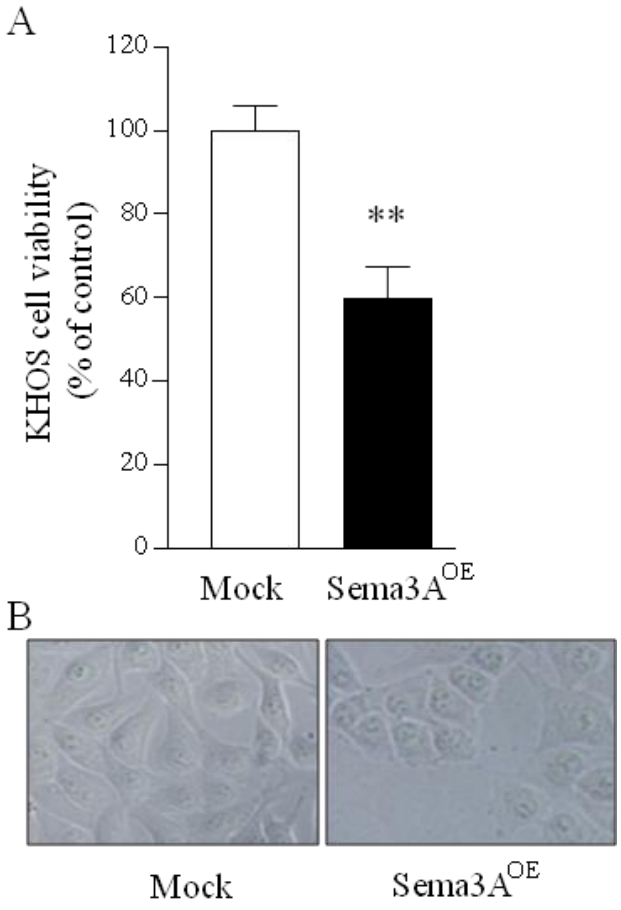

Figure 5.2. Sema3A overexpression reduced KHOS osteosarcoma cell viability in the absence of FCS.
KHOS cell viability was measured using the AlamarBlue assay to investigate the effects of Sema3A overexpression on cell viability. **A**. Quantification of KHOS osteosarcoma mock or Sema3A overexpressing cells ($Sema3A^{OE}$) after 48 hours in Serum free medium. **B.** Representative photomicrographs of KHOS osteosarcoma mock or Sema3A overexpressing cells of the experiment described in panel A. Values in the graphs are mean ± SD and are obtained from 3 independent experiments. ** $p<0.01$

5.4.3 **Sema3A overexpression reduced osteosarcoma cell motility *in vitro***

Overexpression of Sema3A has been shown to affect tumour cell migration and invasion in a variety of different cancer cell types (Muller et al., 2007, Bagci et al., 2009, Bachelder et al., 2003). To assess the role of tumour-derived Sema3A on migration, I assessed wound closure and tracked distance and velocity of single cells (section 2.9.1 and section 2.9.2). Overexpression of Sema3A significantly reduced 2D directed migration (24%, $p<0.001$). Furthermore, KHOS osteosarcoma cells overexpressing Sema3A travelled a shorter distance at a slower pace as assessed by single cell velocity and distance over a period of 8 hours (50%, $p<0.05$) (Figure 5.3).

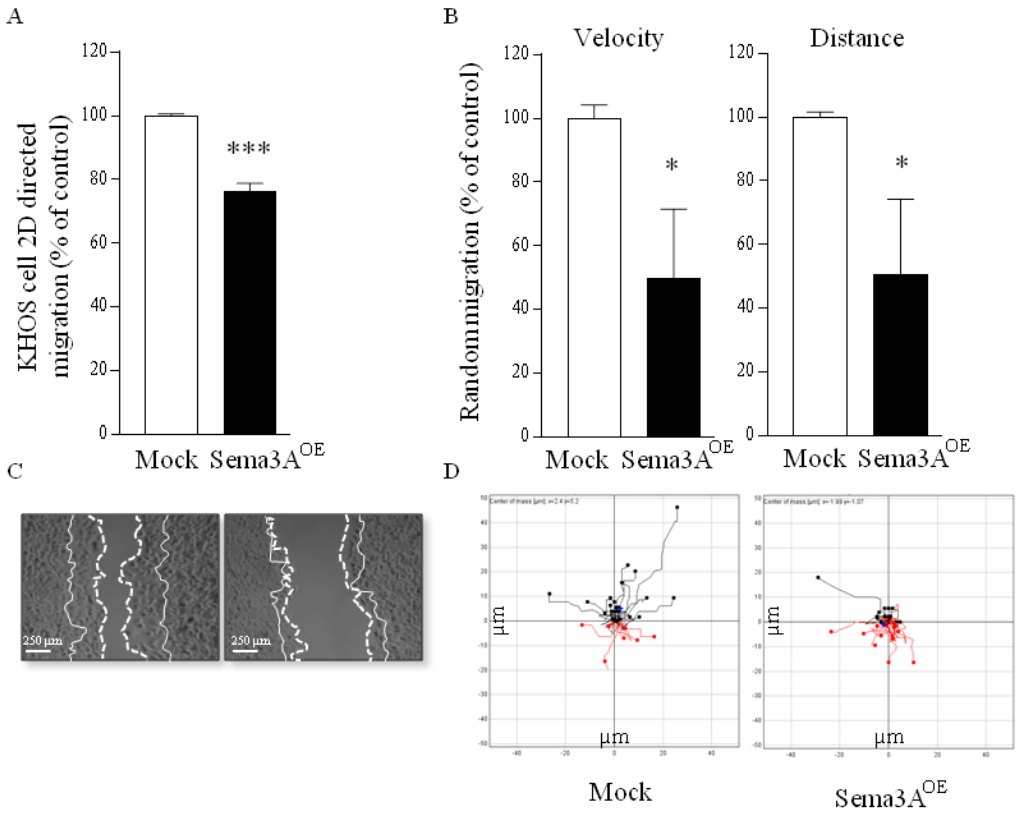

Figure 5.3. Sema3A overexpression reduced KHOS osteosarcoma cell 2D and random migration. The effect of Sema3A overexpression on KHOS cell migration was assessed using the wound healing assay and the random single cell migration. **A**. Quantification of KHOS osteosarcoma mock or Sema3A overexpressing cell (Sema3A^{OE}) 2D directed migration at 4 hours. **B.** Quantification of random migration velocity and distance of KHOS osteosarcoma mock or Sema3A overexpressing single cells over a period of 8 hours. **C.** Representative photomicrographs of 2D directed migration of KHOS osteosarcoma mock or Sema3A overexpressing cells of the experiment described in panel A. Solid thick white lines represent the cell front at the timepoint that was analysed, thin white lines represent the cell front at 0 hours. **D.** Representative plots of single cell random migration experiments described in panel B. Each plot represents a cell's travelled path. Black lines represent cells travelling in a northward direction while red lines represent cells travelled southward on the 2D plane. Scalebar in the bottom left of the migration images indicates 250 µm Values in the graphs are mean ± SD and are obtained from 3 independent experiments * $p< 0.05$, *** $p < 0.001$.

5.4.4 **Overexpression of Sema3A reduced KHOS cell invasion *in vitro***

Next the effect of tumour-specific Sema3A overexpression on cell invasion was assessed by the Matrigel transwell insert assay. In short, cells were pipetted onto the Matrigel insert in serum free medium and an FCS gradient was created by using standard DMEM containing 10% FCS in the well underneath the insert (section 2.9.3). As shown in Figure 5.4, Sema3A overexpression significantly reduced KHOS osteosarcoma cell invasion 77% ($p<0.001$).

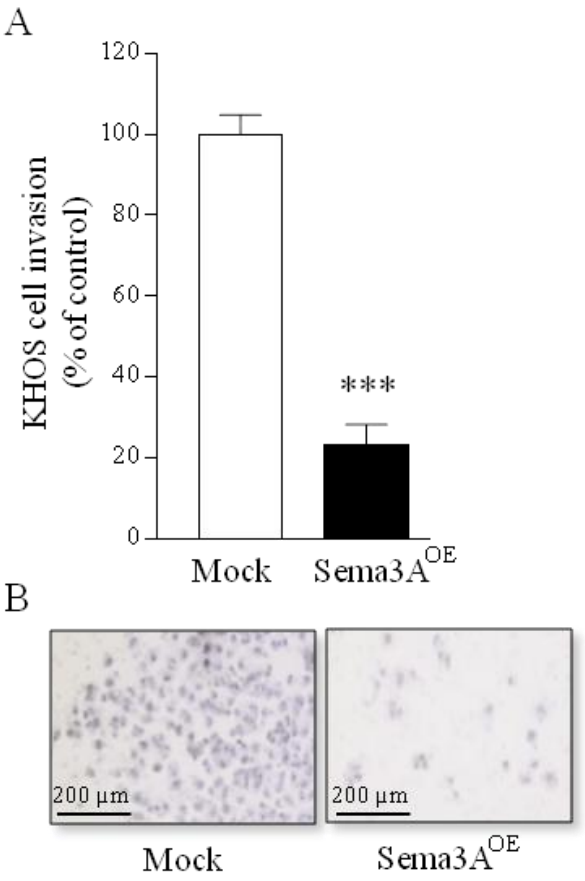

Figure 5.4. Sema3A overexpression reduced KHOS osteosarcoma cell invasion.
This figure describes the effect of Sema3A overexpression on KHOS cell invasion using the Matrigel assay with an FCS gradient. **A**. Quantification of KHOS osteosarcoma mock or Sema3A overexpressing cells ($Sema3A^{OE}$) invasion after 72 hours. **B.** Representative photomicrographs of KHOS osteosarcoma mock or Sema3A overexpressing cells of the experiment described in panel A. Scalebar in the bottom left of the images indicates 200 µm Values in the graphs are mean ± SD and are obtained from 3 independent experiments. *** $p<0.001$

5.4.5 **Sema3A overexpression had no effect on osteosarcoma tumour growth *in vivo***

Previous studies in different types of cancer have shown that Sema3A overexpression reduced tumour growth *in vivo* (Mishra et al., 2015b, Casazza et al., 2011). Based on these studies and encouraged by the results of Sema3A overexpression in osteosarcoma *in vitro*, I tested the effects of Sema3A overexpression on tumour growth *in vivo*. Briefly, mice were paratibially injected with KHOS mock or KHOS Sema3A overexpressing cells and tumour growth was monitored throughout the experiment until the mice were sacrificed at day 16. As shown in Figure 5.5, mice inoculated with mock control and Sema3A overexpressing KHOS cells developed tumours. There was no difference in tumour growth in mice inoculated with KHOS mock or Sema3A overexpressing cells. The above described experiment was performed in full by Dr Nathalie Renema in France.

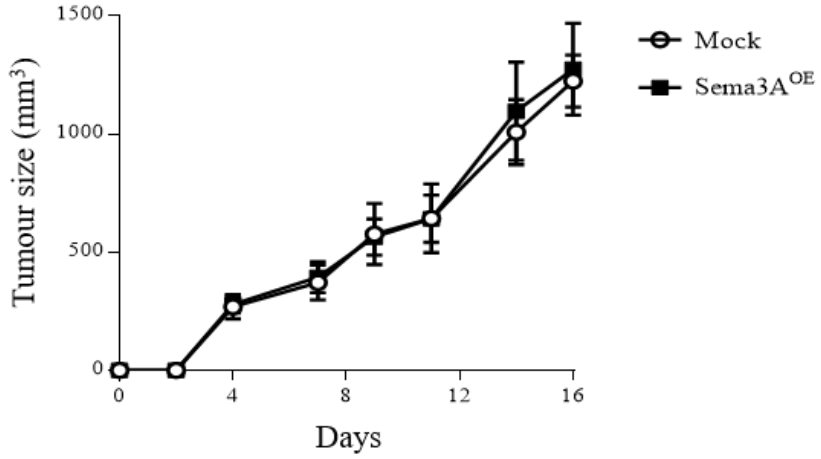

Figure 5.5. Sema3A overexpression had no effect on osteosarcoma tumour growth *in vivo*. Osteosarcoma tumours were induced by paratibial injection of KHOS mock or Sema3A overexpressing osteosarcoma cells in female Rj: NMRI nude mice and the osteosarcoma tumours were allowed to grow until mice were sacrificed at day 16. This figure describes the effect of Sema3A overexpression on the growth of osteosarcoma tumours *in vivo* in mice inoculated with osteosarcoma mock or Sema3A overexpressing cells. Tumour growth was monitored throughout the experiment using callipers. Tumour growth throughout the duration of the experiment in which mice were inoculated with KHOS mock and Sema3A overexpressing osteosarcoma cells ($Sema3A^{OE}$). N = 10. Values are mean ± SD.

5.4.6 **Sema3A overexpression has no effect on lung metastasis *in vivo***

Lung metastasis are a common feature of osteosarcoma (Mutsaers and Walkley, 2014, Bielack et al., 2009). Lungs of mice inoculated with KHOS mock or KHOS Sema3A overexpressing cells were embedded in paraffin, sectioned and stained with H&E. Metastatic nodules were counted and the total tumour area for metastatic nodules was measured using the Osteomeasure system at each depth at three separate depths per sample (section 2.12.5). Of the 10 mice in each group, 4/10 mock inoculated mice and 2/10 mice inoculated with KHOS Sema3A overexpressing cells showed evidence of microscopic lung metastasis. There was no difference in the size of metastatic nodules of the lungs between the mice inoculated with KHOS mock or KHOS Sema3A overexpressing cells.

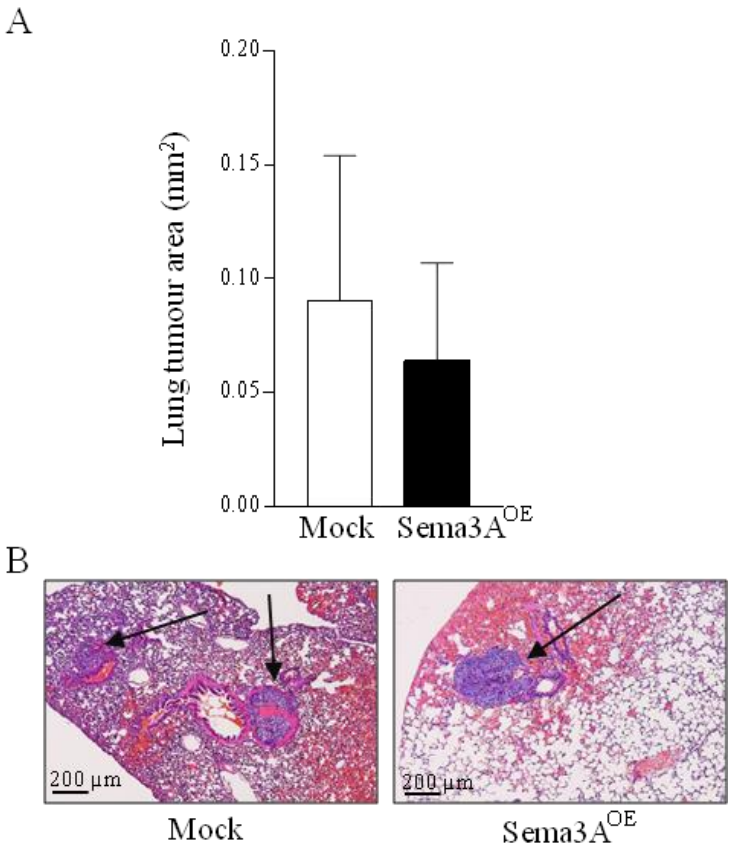

Figure 5.6. Sema3A Overexpression had no effect on lung metastasis *in vivo*
Osteosarcoma tumours were induced by paratibial injection of KHOS mock or Sema3A overexpressing osteosarcoma cells in female Rj: NMRI nude mice and the osteosarcoma tumours were allowed to grow until mice were sacrificed at day 16. The lungs were sectioned and stained with H&E to assess the effect of tumour-specific Sema3A overexpression on the size and number of metastatic nodules in the lungs. Metastatic nodules were counted at three different depths per mouse and size of metastatic nodules was assessed using the Osteomeasure. **A.** Quantification of the size of metastatic nodules in the lungs of mice inoculated with KHOS mock or KHOS Sema3A overexpressing cells. **B**. Representative microphotographs (10X) of tumour nodules in lungs of mice from the experiment described in panel A. Black arrows indicate nodules. Scalebar in the bottom corner of the images indicates 200 µm. Values in the graph are mean ± SD N=10.

5.5 Discussion

Sema3A has been implicated to play a role in tumour growth and progression in a variety of different cell types (Tamagnone, 2012). There is conflicting data that reported the Sema3A receptor Nrp1 as an indicator for patient prognosis (Boro et al., 2015, Zhu et al., 2014). Previous studies have shown that osteosarcoma cells express Nrp1 and produce Sema3A after a RANKL stimulus (Mori et al., 2007, Yue et al., 2014). However, the role of tumour-derived Sema3A in osteosarcoma growth and motility is still unknown. The aim of this chapter was to investigate the role of tumour-derived Sema3A on osteosarcoma cell viability, migration and invasion *in vitro* and tumour growth and lung metastasis *in vivo*.

To achieve this aim, first I overexpressed Sema3A in the human KHOS osteosarcoma cells by a lentiviral expression vector. As a result, Sema3A protein levels in the cell lysates and in the conditioned medium were significantly increased in comparison to the mock control. Overexpression of Sema3A reduced the viability of the tumour cells. This is in contrast to the lack of effect of exogenous Sema3A on osteosarcoma cell viability as described in chapter 3. Additionally, the reduction in cell viability by overexpression of Sema3A is in contrast to previous studies that have indicated that tumour-specific Sema3A expression had no effect on breast cancer and melanoma cell growth *in vitro* (Casazza et al., 2011). The discrepancy between exogenous Sema3A and Sema3A overexpression may be due to off target effects by the lentiviral vector. Additionally, Sema3A overexpression results into a continuous exposure of the osteosarcoma cells to Sema3A which might explain why exogenous Sema3A does not have an effect on viability in contrast to Sema3A overexpression. Next I investigated the effects of Sema3A overexpression on the migration and invasion of the KHOS osteosarcoma cells. Sema3A overexpression significantly reduced KHOS osteosarcoma cell directed and random migration. Overexpression of Sema3A also reduced invasion of these osteosarcoma cells. This is in confirmation with previous studies that reported that tumour-specific Sema3A expression affects cancer cell migration and invasion depending on the investigated cell type (Muller et al., 2007, Bagci et al., 2009, Pan and Bachelder, 2010, Herman and Meadows, 2007, Mishra et al., 2015b). These results imply that in osteosarcoma, tumour-specific Sema3A expression has osteosarcoma suppressive effects *in vitro*.

The next step was to investigate whether Sema3A overexpression conveys anti-tumorigenic properties *in vivo*. Several studies have shown that although Sema3A overexpression had no effect on tumour cell growth *in vitro,* Sema3A overexpression reduced tumour growth *in vivo* in melanoma, breast and oral cancer (Chakraborty et al., 2012, Mishra et al., 2015a, Casazza et al., 2011). To investigate whether Sema3A overexpression had an effect on osteosarcoma tumour growth, mice were given paratibial injections of KHOS mock or KHOS Sema3A overexpressing cells to induce tumours. To our surprise and in contrast to the effect on viability *in vitro*, Sema3A overexpression had no effect on osteosarcoma tumour growth *in vivo*. As previously mentioned in Chapter 4, one of the drawbacks of this xenograft model is its aggressive nature and rapid tumour growth which may explain the lack of effect on tumour growth *in vivo*. There was no significant reduction in lung metastasis between the mock and Sema3A overexpression group. In this particular osteosarcoma mouse model, metastasis tend to develop in the 3rd week after inoculation, the endpoint of day 16 may have been premature to provide a definitive conclusion on the effect of tumour-specific overexpression of Sema3A on lung metastasis.

To summarise, overexpression of Sema3A in the KHOS osteosarcoma cells significantly inhibited osteosarcoma viability *in vitro.* Furthermore, overexpression of Sema3A significantly inhibited directed and random migration and inhibited osteosarcoma cell invasion *in vitro*. Despite the effects observed *in vitro,* there was no effect of Sema3A overexpression on tumour growth or lung metastasis *in vivo* (Figure 5.7).

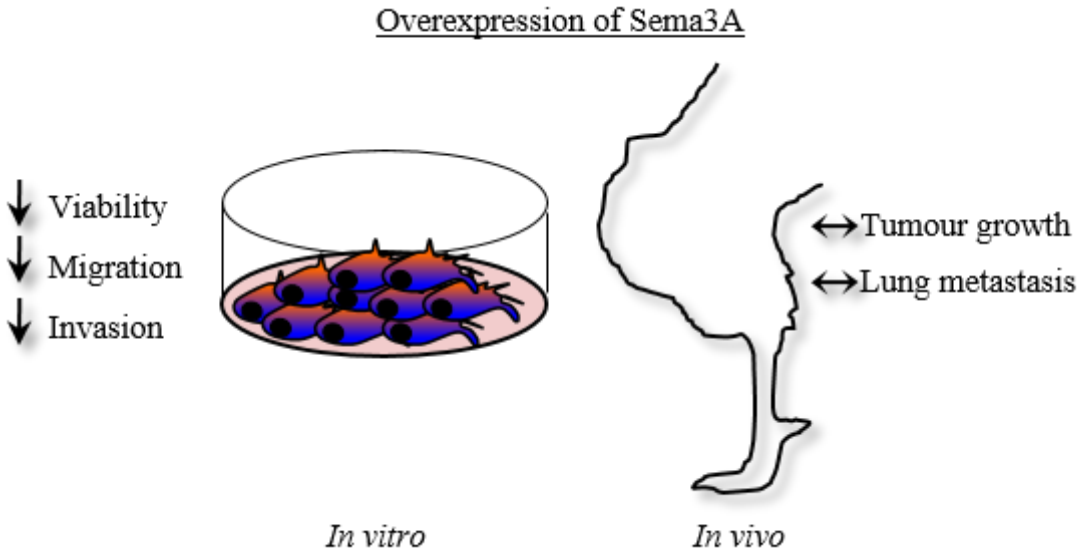

Figure 5.7. Schematic representation of the effects of overexpression of Sema3A on the KHOS osteosarcoma cells *in vitro* and *in vivo*. Overexpression of Sema3A reduced KHOS cell viability, migration and invasion *in vitro* but had no effect on tumour growth or lung metastasis *in vivo*.

CHAPTER SIX

Effects of osteosarcoma-derived Sema3A on osteolysis *in vivo*

6 CHAPTER SIX

6.1 Summary

One of the common features of osteosarcoma is osteolysis. In 25% of osteosarcoma cases, multinucleated giant cells that resemble osteoclasts are present in close proximity to the tumour. Osteoclasts are known to express the semaphorin 3A receptors and Sema3A is known to inhibit osteoclast formation and osteoclast activity. However, the effect of tumour-derived Sema3A on osteoclast formation and osteolysis is unknown. This chapter reports the effects of osteosarcoma-derived Sema3A on osteolysis and bone damage of osteosarcoma-bearing tibia and femurs.

In vitro, *c*onditioned medium from KHOS Sema3A overexpressing cells inhibited osteoclast formation *in vitro* in comparison to conditioned medium from the mock control. To investigate whether osteosarcoma-derived Sema3A also affects osteoclast formation *in vivo,* histomorphometric analysis was performed on TRAcP stained slides of the osteosarcoma-bearing tibia. Osteosarcoma-derived Sema3A significantly reduced osteoclast number and osteoclast surface *in vivo*. In contrast, osteosarcoma-derived Sema3A only showed a trend towards protection against osteosarcoma-associated trabecular osteolysis of the tibia. This chapter showed that osteosarcoma-derived Sema3A inhibited osteoclast formation *in vitro* and *in vivo* but these effects were insufficient to protect the bone from osteosarcoma-associated osteolysis.

6.2 Introduction

One of the common features of osteosarcoma is osteolytic bone damage (Geller and Gorlick, 2010). Osteoclasts have been shown to express the Sema3A receptors plexin-A1, plexin-A2 and Nrp1 but have no Sema3A expression (Gomez et al., 2005). Plexin-A1 is constitutively associated with Nrp1, when Nrp1 is downregulated, plexin-A1 is released to associate with the TREM2-DAP12 complex to stimulate osteoclastogenesis (Takahashi and Strittmatter, 2001, Takegahara et al., 2006). Hayashi and colleagues showed that, upon RANKL stimulation, osteoclast precursors downregulate Nrp1 thereby releasing the plexin-A1 from the Nrp1-plexin-A1 complex. Therefore, osteoblast derived Sema3A only inhibits osteoclast formation in the absence of a previous RANKL stimulus (Hayashi et al., 2012). This is in confirmation with previous studies that confirmed that treatment of osteoclast precursors with Sema3A inhibits osteoclastogenesis (Fukuda et al., 2013, Teng et al., 2017) and unpublished work from our laboratories (de Ridder MSc thesis unpublished data, 2014). Sema3A deficient mice exhibit increased bone resorption that is accompanied by an increase in osteoclast numbers (Hayashi et al., 2012). A similar phenotype is observed in Nrp^{sema-} knock-in mice. These mice have a functional neuropilin receptor that is unable to bind Sema3A due to deletion of the semaphorin binding domain and therefore only lacks semaphorin signalling whereas the other pathways such as VEGF signalling are not impaired. Furthermore, Sema3A was also found to inhibit osteoclast activity *in vitro* (Teng et al., 2017).

Previous unpublished work from our laboratories showed that knockdown of Sema3A in breast cancer cells significantly enhanced breast cancer induced osteoclastogenesis *in vitro* (de Ridder MSc thesis unpublished data, 2014). There is to date no published research on the effect of tumour-specific Sema3A expression on tumour cell-osteoclast interactions. This chapter investigated the effects of osteosarcoma-derived Sema3A on osteosarcoma-associated osteolysis and osteoclast formation.

6.3 Aim

The aim of this chapter was to investigate the role of tumour-derived Sema3A in human osteosarcoma cell-osteoclast crosstalk *in vitro* and *in vivo*. The aim was achieved by exposure of osteoclasts to conditioned medium from Sema3A overexpressing KHOS osteosarcoma cells and assess osteoclast formation *in vitro* and *in vivo* and osteolysis in Sema3A overexpressing tumours in mice.

6.4 Results

6.4.1 **Osteosarcoma-derived Sema3A reduced osteoclast formation *in vitro*.**

As reported in Chapter 3 and in confirmation with several studies, Sema3A inhibits osteoclast formation (Hayashi et al., 2012, Fukuda et al., 2013, Teng et al., 2017). To investigate whether osteosarcoma-derived Sema3A has similar effects on osteoclast formation, mouse bone marrow cultures were exposed to conditioned medium 20% (v/v) from KHOS mock or KHOS Sema3A overexpressing cells. Cultures treated with conditioned medium of KHOS Sema3A overexpressing cells showed a significantly reduced osteoclast formation as compared to cultures exposed to conditioned medium from KHOS mock cells (37%, $p<0.001$)(Figure 6.1).

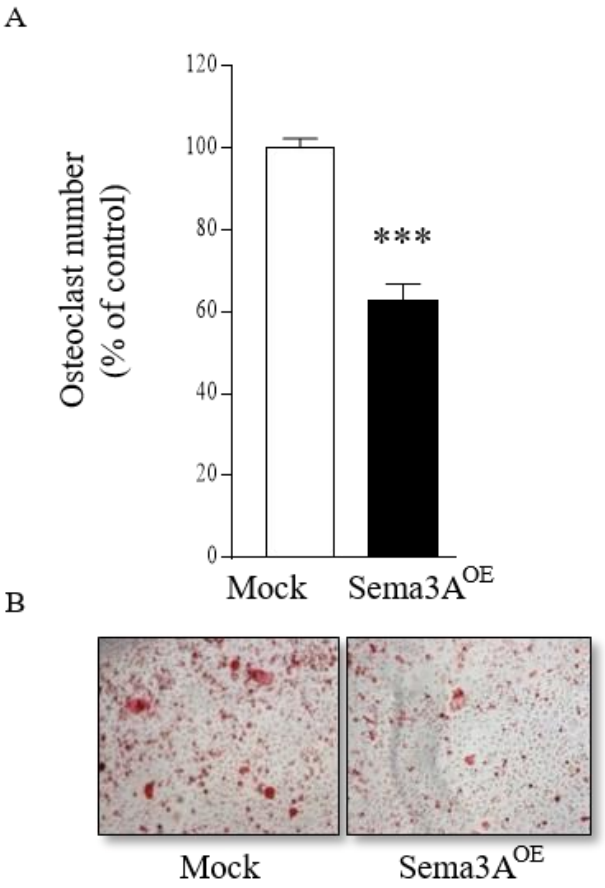

Figure 6.1. Osteosarcoma-derived Sema3A reduced osteosarcoma associated osteoclast formation.
To assess the effect of tumour-derived Sema3A on osteoclast formation, bone-marrow cultures were exposed to conditioned medium from KHOS Mock or Sema3A overexpressing cells. Cultures were exposed for 7 days, fixed and then stained with TRAcP. Osteoclasts were counted when they were stained with TRAcP and contained >3 nuclei. **A.** Quantification of osteoclast number in mouse bone marrow cultures treated with 20% conditioned medium (v/v) of KHOS mock or KHOS Sema3A overexpressing cells ($Sema3A^{OE}$). **B.** Representative photomicrographs (10X) of cultures described in panel A. Values in the graph are mean ± SD and are obtained from 3 independent experiments *** $p<0.001$.

6.4.2 **Osteosarcoma-derived Sema3A showed a trend towards reduction of osteolysis**

Sema3A treatment was shown to increase bone volume and increased bone fracture healing (Hayashi et al., 2012, Li et al., 2015a). In order to investigate the effect of osteosarcoma-derived Sema3A on bone metabolism *in vivo*, legs of mice were paratibially injected with KHOS mock or KHOS Sema3A overexpressing cells to induce osteosarcoma. The bone parameters of the tumour-bearing tibia and femur were then analysed using microCT (section 02.11). As shown in Figure 6.2, osteosarcoma-derived Sema3A showed a trend towards an osteoprotective effect in the tumour-bearing tibia but had no significant effect on bone volume, trabecular thickness, trabecular number, trabecular separation and trabecular pattern factor. Further microCT analysis of the femur showed that osteosarcoma-derived Sema3A had no effect on bone volume, trabecular thickness, trabecular number, trabecular separation and trabecular pattern factor in the tumour-bearing femur (Figure 6.3).

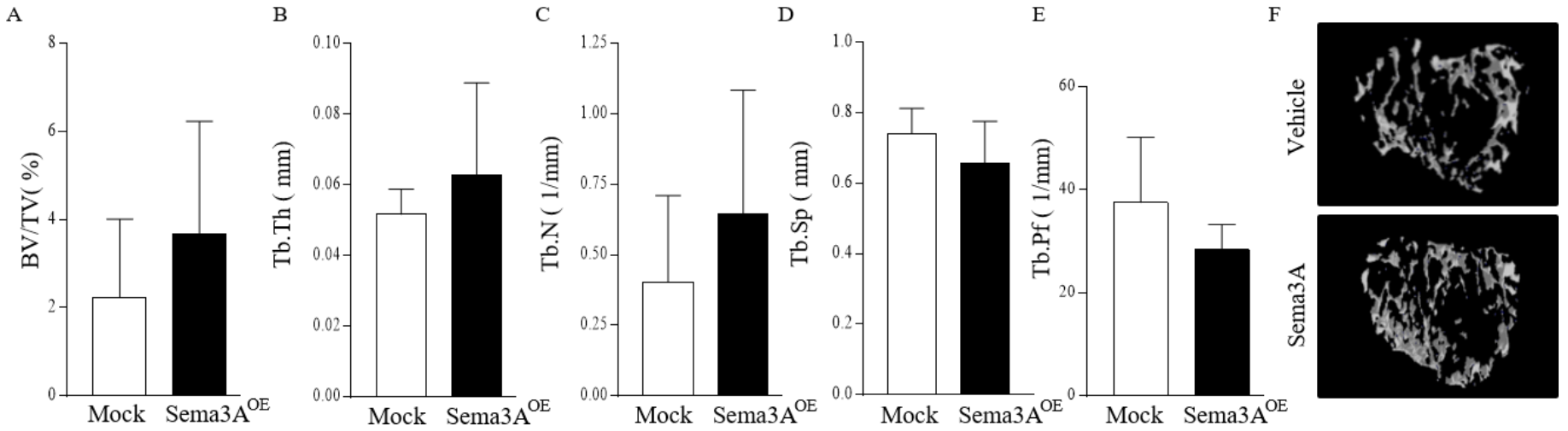

Figure 6.2. Osteosarcoma-derived Sema3A showed a trend towards more bone volume in the tibia.
Osteosarcoma tumours were induced by paratibial injection of KHOS mock or Sema3A overexpressing osteosarcoma cells in female Rj: NMRI nude mice and the osteosarcoma tumours were allowed to grow until mice were sacrificed and legs organs were collected for analysis at day 16. This figure describes the effect of tumour-specific Sema3A overexpression on the trabecular compartment of the osteosarcoma-bearing tibia analysed by microCT. **A.** Quantification of Trabecular bone volume, **B.** Trabecular thickness, **C.** Trabecular number, **D.** Trabecular separation and **E.** Trabecular pattern factor of the tumour-bearing tibia of mice inoculated with KHOS mock or KHOS Sema3A overexpressing cells (Sema3A^{OE}). **F.** 3D reconstruction images of the tibia from the experiment described in panel A-E. Values in the graph are mean ± SD N=10.

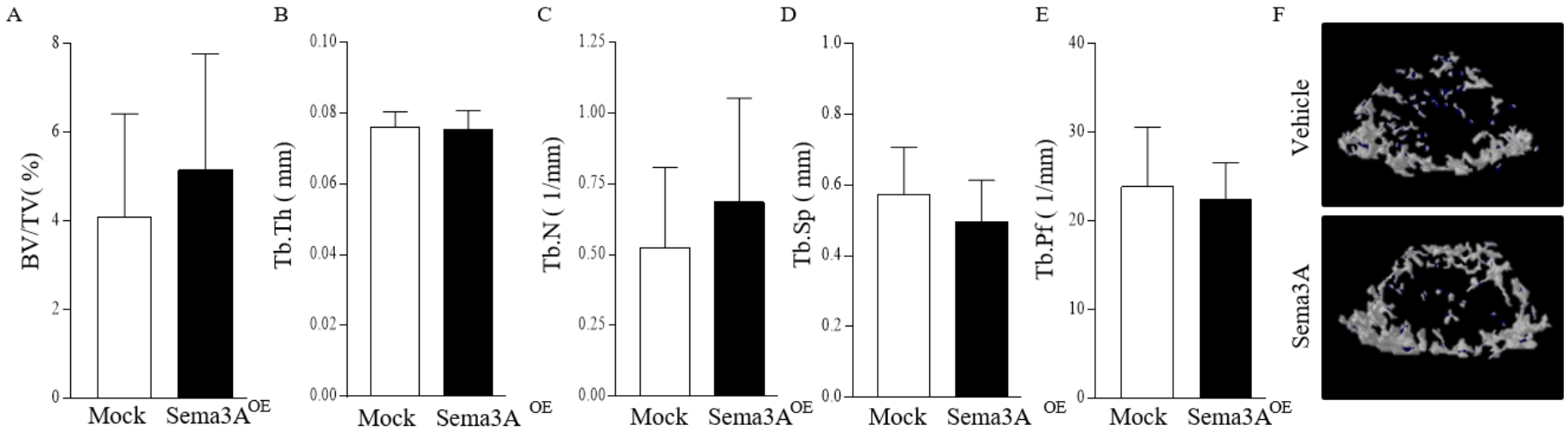

Figure 6.3. Osteosarcoma-derived Sema3A had no effect on femoral bone parameters.
Osteosarcoma tumours were induced by paratibial injection of KHOS mock or Sema3A overexpressing osteosarcoma cells in female Rj: NMRI nude mice and the osteosarcoma tumours were allowed to grow until mice were sacrificed and legs and organs were collected for analysis at day 16. This figure describes the effect of tumour-specific Sema3A overexpression on the trabecular compartment of the osteosarcoma-bearing femur analysed by microCT. **A.** Quantification of Trabecular bone volume, **B.** Trabecular thickness, **C.** Trabecular number, **D.** Trabecular separation and **E.** Trabecular pattern factor of the tumour bearing femur in mice inoculated with KHOS mock or KHOS Sema3A overexpressing cells (Sema3A^{OE}). **F.** 3D reconstruction images of femur from the experiment described in panel A-E. Values in the graph are mean ± SD N=10.

Consistent with the results described above, osteosarcoma-derived Sema3A had no effect on cortical bone volume of the tumour-bearing tibia or femur as shown in Figure 6.4.

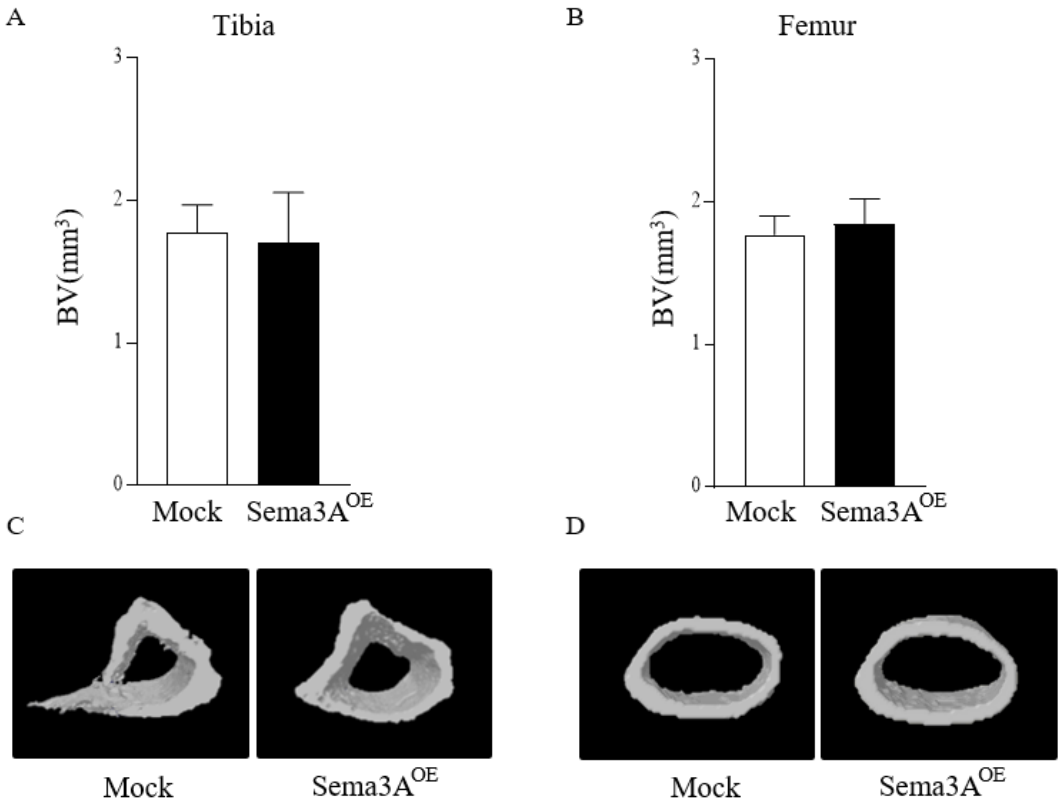

Figure 6.4. Osteosarcoma-derived Sema3A had no effect on cortical bone volume in the tumour-bearing leg.
Osteosarcoma tumours were induced by paratibial injection of KHOS mock or Sema3A overexpressing osteosarcoma cells in female Rj: NMRI nude mice and the osteosarcoma tumours were allowed to grow until mice were sacrificed and legs and organs were collected for analysis at day 16. This figure describes the effect of tumour-specific Sema3A overexpression on the cortical bone volume of the osteosarcoma-bearing tibia and femur analysed by microCT. Quantification of cortical bone volume in the tumour-bearing **A.** tibia and **B.** femur in mice inoculated with KHOS mock or KHOS Sema3A overexpressing cells (Sema3A^{OE}). **C.** 3D reconstruction images of tibia and **D.** femur from the experiment described in panel A-B. Values in the graph are mean ± SD N=10.

6.4.3 **Osteosarcoma-derived Sema3A reduced osteoclast formation *in vivo*.**

Sema3A deficient mice have an increased osteoclast number and resorption whereas treatment with Sema3A inhibited bone resorption in mice with ovariectomy induced osteoporosis (Hayashi et al., 2012). To investigate whether osteosarcoma-derived Sema3A has any effects on osteoclast formation *in vivo*, I performed bone histomorphometry on the tibia of the tumour-bearing legs of the mice inoculated with KHOS mock or KHOS Sema3A overexpressing cells. As shown in Figure 6.5 mice injected with KHOS cells overexpressing Sema3A showed a significantly reduced osteoclast number 42% ($p<0.05$) and osteoclast surface 52% ($p<0.05$) in the tumour-bearing tibia *in vivo.*

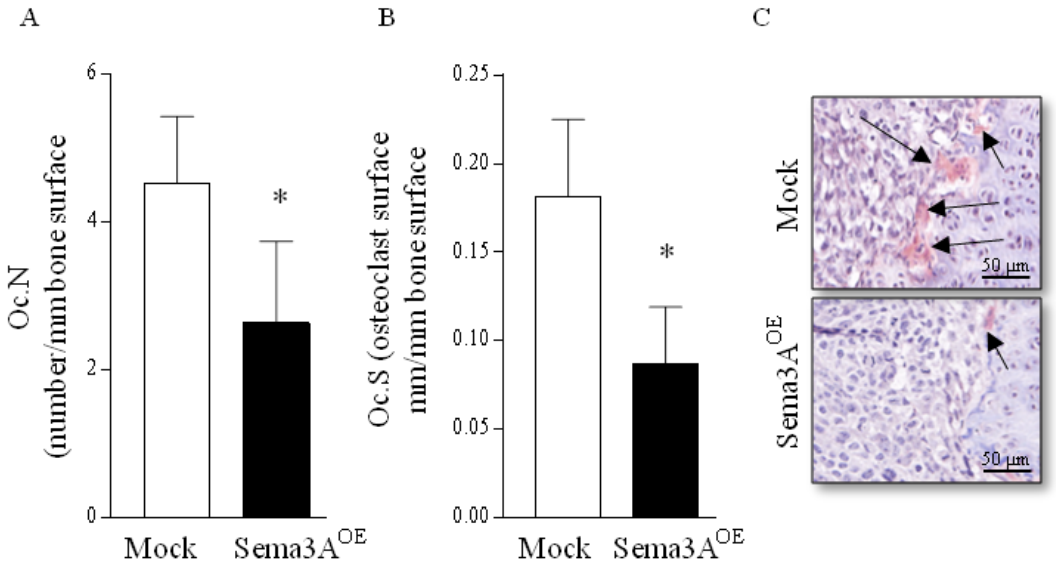

Figure 6.5. Osteosarcoma-derived Sema3A reduced osteoclast formation *in vivo*.
Osteosarcoma tumours were induced by paratibial injection of KHOS mock or Sema3A overexpressing osteosarcoma cells in female Rj: NMRI nude mice and the osteosarcoma tumours were allowed to grow until mice were sacrificed and legs and organs were collected for analysis at day 16. Osteosarcoma-bearing tibia were sectioned and TRAcP stained to assess the cellular parameters in the trabeculae to assess the effect of tumour-specific overexpression of Sema3A on osteoclast number and osteoclast surface. **A.** Quantification of osteoclast number in the tibia inoculated with KHOS mock or KHOS Sema3A overexpressing cells ($Sema3A^{OE}$). **B.** Quantification of osteoclast surface in the tibia inoculated with KHOS mock or KHOS Sema3A overexpressing cells. **C.** Representative photomicrographs of TRAcP stained tibia from experiments described in panel A and B. Arrows indicate TRAcP positive osteoclasts. Scalebar in the bottom right indicates 50µm. Values in the graph are mean ± SD, N=5 * $p<0.05$.

6.4.4 **Osteosarcoma-derived Sema3A showed a trend towards more osteoblasts in vivo**

Mice administrated with exogenous Sema3A show enhanced bone volume with a corresponding increase in osteoblasts and osteoblast surface (Hayashi et al., 2012). To investigate whether osteosarcoma-derived Sema3A had an effect on osteoblasts *in vivo*, osteoblast number and osteoblast surface in the tumour-bearing tibia of mice inoculated with KHOS mock or KHOS Sema3A overexpressing cells was analysed using histomorphometry. As shown in Figure 6.6, osteosarcoma-derived Sema3A showed a trend towards increased osteoblast number and osteoblast surface but these changes were not significant.

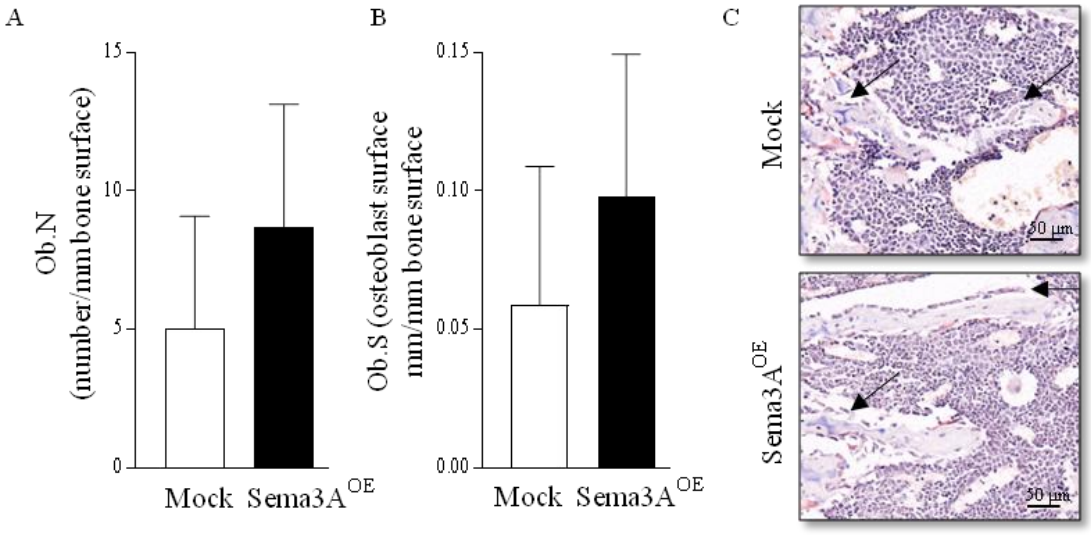

Figure 6.6. Osteosarcoma-derived Sema3A showed a trend towards more osteoblasts.
Osteosarcoma tumours were induced by paratibial injection of KHOS mock or Sema3A overexpressing osteosarcoma cells in female Rj: NMRI nude mice and the osteosarcoma tumours were allowed to grow until mice were sacrificed and legs and organs were collected for analysis at day 16. Osteosarcoma-bearing tibia were sectioned and TRAcP stained to assess the cellular parameters in the trabeculae to assess the effect of tumour-specific overexpression of Sema3A on osteoblast number and osteoblast surface **A.** Quantification of osteoblast number (Ob.N) in the tibia inoculated with KHOS mock or KHOS Sema3A overexpressing cells ($Sema3A^{OE}$). **B.** Quantification of osteoblast surface (Ob.S) in the tibia inoculated with KHOS mock or KHOS Sema3A overexpressing cells. **C.** Representative photomicrographs of TRAcP stained tibia of experiments described in panel A and B. Arrows indicate osteoblasts.Scalebar in the bottom right of the images indicates 50µm. Values in the graph are mean ± SD, N=5.

6.5 Discussion

A number of studies have shown that Sema3A enhanced bone volume, protected against ovariectomy induced bone loss, enhanced osteoblast differentiation as well as inhibited osteoclast formation and osteoclast activity (Hayashi et al., 2012, Fukuda et al., 2013, Teng et al., 2017). These findings suggest that osteosarcoma-derived Sema3A may play a role in osteoclast formation and osteosarcoma-associated osteolysis. In this chapter we hypothesized that osteosarcoma-derived Sema3A reduces osteosarcoma-induced osteoclastogenesis and osteolysis.

To investigate this hypothesis, I first tested whether osteosarcoma-derived Sema3A had any effect on osteoclast formation *in vitro*. Similar to the inhibitory effect of exogenous Sema3A on osteoclast formation as described in Chapter 3 and reported by previous studies (Hayashi et al., 2012, Fukuda et al., 2013, Teng et al., 2017), osteosarcoma-derived Sema3A significantly reduced RANKL-induced osteoclast formation *in vitro*. A reduction of osteoclast number and osteoclast surface was also found in the tumour-bearing tibia of mice inoculated with KHOS Sema3A overexpressing cells in comparison to the mock control. The trabecular bone of Sema3A overexpressing tumours showed a trend towards more osteoblasts. These observations are similar to exogenous Sema3A that enhanced osteoblast number and osteoblast surface in the absence of cancer and showed a trend towards more osteoblasts in the tumour bearing leg as described in chapter 4, suggesting that tumour-specific Sema3A expression exhibits the same effects on osteoclast formation as would treatment with exogenous Sema3A (Hayashi 2012).

To our surprise, despite a significant reduction in osteoclast formation *in vivo*, osteosarcoma-derived Sema3A only showed a trend towards enhanced bone volume. There were no significant effects of osteosarcoma-derived Sema3A on trabecular bone volume, trabecular number, trabecular separation or trabecular connectivity in the tumour-bearing tibia or the tumour-bearing femur. In addition, there was no effect of osteosarcoma-derived Sema3A on the cortex of the tibia or the femur in the tumour-bearing leg.

There are several elements that may have contributed to the lack of effect of osteosarcoma-derived Sema3A on the osteosarcoma-associated osteolysis in this model. As described in Chapter 5, there was no effect on tumour growth by Sema3A overexpression this is in contrast to other studies that found that Sema3A overexpression reduced tumour growth (Chakraborty et al., 2012, Mishra et al., 2015b, Casazza et al., 2011). The lack of effect of osteosarcoma-derived Sema3A on tumour growth may explain why there is no significant protection against bone loss in the Sema3A overexpressing tumours. In addition, the other factors secreted by the tumour may play a role in the bone microenvironment and a continuous stimulation of the bone environment with Sema3A differs from the intermittent exposure that is achieved with administration of exogenous Sema3A. The difference in exposure time may contribute to the differences on the trabecular compartment between exogenous and osteosarcoma-derived Sema3A.

In summary, osteosarcoma-derived Sema3A significantly inhibited osteoclast formation *in vitro* and reduced osteoclast number and osteoclast surface *in vivo.* In addition, there was a trend towards more osteoblast surface and number of osteoblasts but osteosarcoma-derived Sema3A had no significant effect on the bone volume of the tumour-bearing tibia or femur.

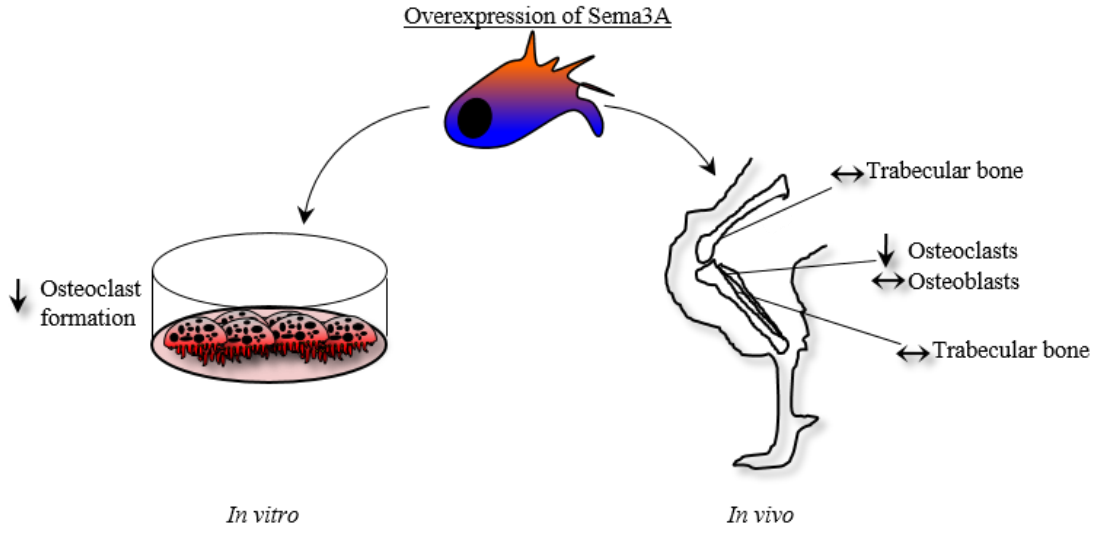

Figure 6.7. Schematic representation of the effects of osteosarcoma-derived Sema3A on osteoclasts *in vitro* and osteoclasts, osteoblasts and osteolysis *in vivo*. Tumour-specific overexpression of Sema3A reduced osteoclast formation *in vitro* and *in vivo* but had no effect on the trabecular bone of the osteosarcoma-bearing tibia or femur.

CHAPTER SEVEN

Effects of osteosarcoma-derived Sema3A on ectopic bone formation

7 CHAPTER SEVEN

7.1 Summary

Ectopic bone is a common feature in osteosarcoma. Recent studies reported that osteoblasts express the Sema3A receptors and produce and secrete Sema3A. Sema3A was shown to enhance osteoblast differentiation via activation of the canonical Wnt/β-catenin pathway. This chapter describes the role of tumour-derived Sema3A in human osteosarcoma cancer cell-osteoblast crosstalk *in vitro* and *in vivo*.

Osteosarcoma tumours overexpressing Sema3A showed a reduction in ectopic bone formation. In contrast, there was no effect on ectopic bone formation in mice administrated with exogenous Sema3A. To investigate the effect on ectopic bone formation further, Saos-2 cells were exposed to conditioned medium from KHOS mock or KHOS Sema3A overexpressing cells for a continuous and intermittent period. Continuous exposure to osteosarcoma-derived Sema3A reduced mineralization without affecting alkaline phosphatase activity, whereas intermittent exposure enhanced alkaline phosphatase activity without affecting mineralization. Osteoblast viability was not affected by exposure to osteosarcoma-derived Sema3A but enhanced osteoblast alkaline phosphatase activity. The Wnt/β-catenin signalling pathway in MC3T3-E1 osteoblasts was inhibited when treated with conditioned medium from KHOS overexpressing Sema3A. This effect may be attributed to the enhanced expression of DKK1 by the Sema3A overexpressing cells.

Altogether these results indicate that osteosarcoma-derived Sema3A affects osteoblast viability and alkaline phosphatase activity in similar ways as recombinant Sema3A. Conditioned medium from KHOS Sema3A overexpressing cells inhibited Wnt/β-catenin signalling which may be attributed to differential expression of other cytokines such as DKK1. This mechanism may have contributed to the reduction of ectopic bone formation by osteosarcoma-derived Sema3A.

7.2 Introduction

Osteosarcomas are known to have an aggressive clinical course, characterized by local bone, muscle and soft tissue destruction. Furthermore, osteosarcoma is characterized by a high propensity for distant metastasis to the lungs (Mutsaers and Walkley, 2014). One of the common features of osteosarcoma besides osteolytic bone damage is the formation of ectopic bone in a typical sunburst pattern (Geller and Gorlick, 2010).

Recently, Sema3A was shown to signal at least in part via the Wnt/β-catenin pathway in osteoblasts. Sema3A enhanced osteoblast differentiation via stimulation of the Wnt/β-catenin pathway through FARP2 induced Rac activation thereby enhancing osteoblast differentiation and inhibition of adipocyte differentiation (Hayashi et al., 2012). Moreover, Sema3A deficiency resulted in a suppressed wnt3a induced β-catenin accumulation and an inhibited wnt3a induced activation of Rac but not Rhoa in calvarial cells (Hayashi et al., 2012). The detailed molecular mechanisms of Sema3A signalling in osteoblasts remains to be elucidated.

Together these previous studies suggest that Sema3A enhances osteoblast differentiation at least in part via the Wnt/β-catenin pathway. The effects of tumour-specific Sema3A expression on the Wnt/β-catenin pathway in osteoblasts is still unknown. This chapter describes the effects of osteosarcoma-derived Sema3A on osteoblasts and osteosarcoma-associated ectopic bone formation. Additionally, this chapter describes a potential mechanism of action for osteosarcoma-derived Sema3A on osteoblast differentiation and activity.

7.3 Aim

The aim of this chapter was to investigate the role of tumour-derived Sema3A in human osteosarcoma cancer cell-osteoblast crosstalk *in vitro* and *in vivo*. The aim was achieved by (a) investigating the effects of osteosarcoma-derived Sema3A on ectopic bone formation *in vivo*, osteoblast viability, activity and Wnt/β-catenin signalling *in vitro* and (b) investigate the effects of overexpression of Sema3A on Wnt/β-catenin signalling in the KHOS osteosarcoma cells.

7.4 Results

7.4.1 **Osteosarcoma-derived Sema3A reduced ectopic bone formation *in vivo***

Ectopic bone is a common feature in osteosarcoma and has been reported previously in mouse models of osteosarcoma (Geller and Gorlick, 2010, Lamoureux et al., 2014). Ectopic bone formation was analysed by total bone volume of the tibia and fibula normalised against the corresponding bone in the contralateral leg (section 2.11.3). As shown in Figure 7.1, osteosarcoma-derived Sema3A significantly reduced ectopic bone formation of the tibia by 15% ($p<0.05$) and fibula by 67% ($p<0.01$).

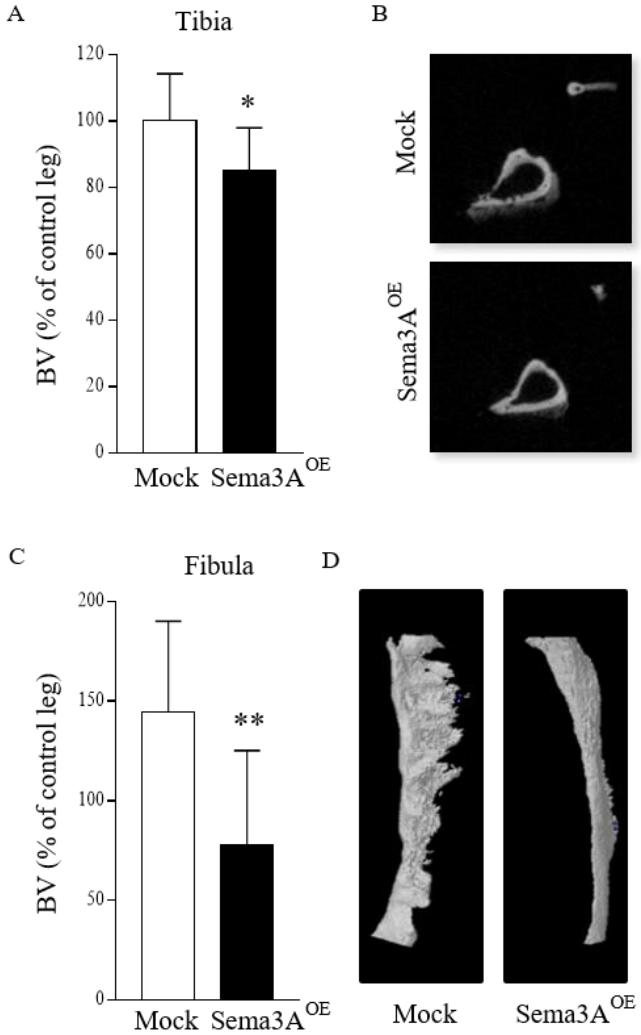

Figure 7.1. Osteosarcoma-derived Sema3A reduced osteosarcoma-associated ectopic bone formation. This figure describes the effect of tumour-specific overexpression of Sema3A on the formation of ectopic bone volume by the osteosarcoma tumours. Osteosarcoma tumours were induced by paratibial injection of KHOS mock or Sema3A overexpressing osteosarcoma cells in female Rj: NMRI nude mice and the osteosarcoma tumours were allowed to grow until mice were sacrificed and legs organs were collected for analysis at day 16. Ectopic bone volume was calculated by measuring the total bone volume in the tumour bearing tibia or fibula and normalizing that to the total bone volume of the contralateral tibia and fibula. **A.** Quantification of bone volume of the tumour-bearing tibia in mice inoculated with KHOS mock or KHOS Sema3A overexpressing cells ($Sema3A^{OE}$). **B.** 2D reconstructed images of the experiment described in panel A. **C.** Quantification of bone volume of the tumour-bearing in mice inoculated with KHOS mock or KHOS Sema3A overexpressing cells. **D.** 3D reconstructed images of tumour-bearing fibula of the experiment described in panel C. Values in the graph are mean ± SD N=10. * $p < 0.05$, ** $p < 0.01$

7.4.2 **Exogenous Semaphorin 3A had no effect on ectopic bone formation**

To analyse the effects of exogenous Sema3A on ectopic bone formation, the total bone volume of the tibia and the fibula was normalised with the total bone volume of the corresponding bone in the contralateral leg (section 2.11.3). Administration of exogenous Semaphorin3A (0.7 mg/kg) had no effect on the ectopic bone formation in the tibia or the fibula of the tumour-bearing leg (Figure 7.2).

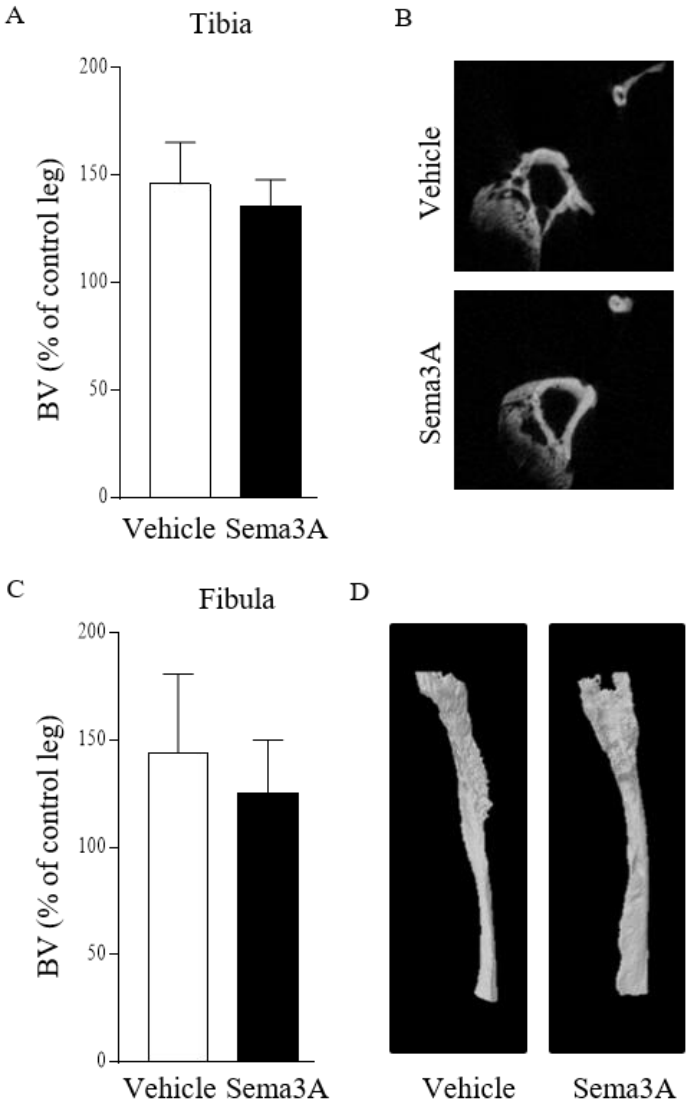

Figure 7.2. Sema3A treatment had no effect on osteosarcoma-associated ectopic bone formation. This figure describes the effect of recombinant Sema3A on the formation of ectopic bone volume by the osteosarcoma tumours. Osteosarcoma tumours were induced by paratibial injection of KHOS osteosarcoma cells in female Rj: NMRI nude mice. Mice were treated with IP injections biweekly of vehicle (PBS) or recombinant Sema3A (0.7 mg/kg) for the duration of the experiment (21 days). Ectopic bone volume was calculated by measuring the total bone volume in the tumour bearing tibia or fibula and normalizing that to the total bone volume of the contralateral tibia and fibula. **A.** Quantification of bone volume of the tumour bearing tibia by normalization of the tibia in mice treated with vehicle (PBS) or human recombinant Sema3A (0.7 mg/kg/2-weekly). **B.** 2D reconstructed images of the experiment described in panel A. **C.** Quantification of bone volume of the tumour bearing fibula by normalization of the fibula in mice treated with vehicle (PBS) or human recombinant Sema3A (0.7 mg/kg/2-weekly). **D.** 3D reconstructed images of tumour bearing fibula of the experiment described in panel C. Values in the graph are mean ± SD N=7.

7.4.3 **Osteosarcoma-derived Sema3A had no effect on osteoblast viability**

First, I investigated the effect of osteosarcoma-derived Sema3A on the viability of a panel of osteoblasts like cells, mouse primary osteoblasts, mouse osteoblast-like MC3T3-E1 cells and human osteoblast-like Saos-2 osteosarcoma cells. Cells were exposed to 20% conditioned medium (v/v) for a short period (48 hours) after which viability was measured using the AlamarBlue assay, (section 2.3.4). As shown in Figure 7.3, exposure to osteosarcoma-derived Sema3A had no effect on the viability of mouse primary osteoblasts, mouse MC3T3-E1 osteoblast-like cells or human osteoblast-like osteosarcoma cells Saos-2.

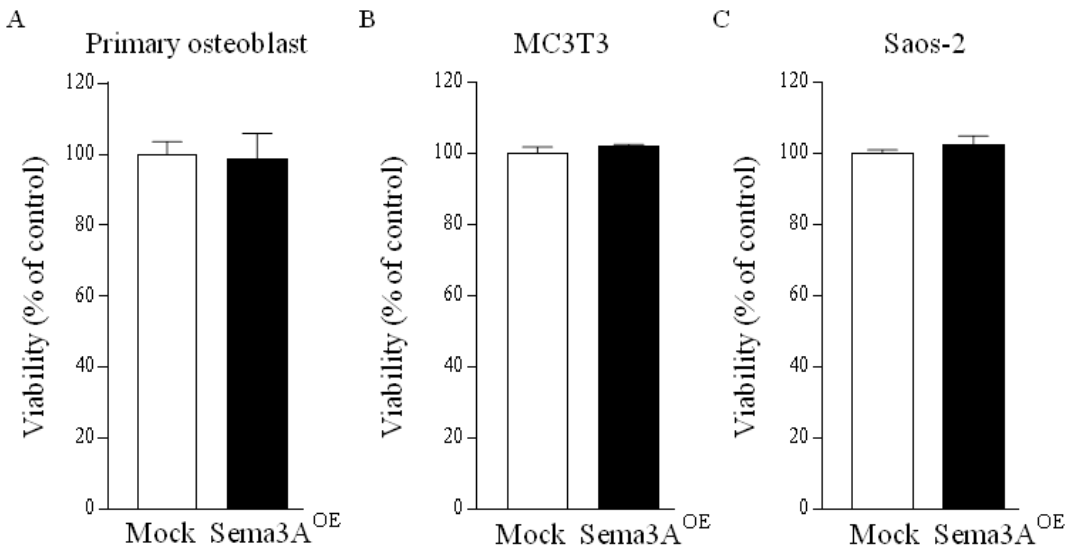

Figure 7.3. Osteoblast viability was not affected after short term exposure to osteosarcoma-derived Sema3A.
This experiment was performed to assess the effect of short term exposure on osteoblast viability to osteosarcoma-derived Sema3A using the AlamarBlue assay. Cultures were exposed to conditioned medium 24 hours after plating. **A.** Quantification of viability of mouse primary osteoblasts after exposure to 20% conditioned medium (v/v) of KHOS mock or KHOS Sema3A overexpressing cells ($Sema3A^{OE}$) for 48 hours **B.** Quantification of viability of mouse MC3T3-E1 osteoblasts after exposure to 20% conditioned medium (v/v) of KHOS mock or KHOS ($Sema3A^{OE}$) for 48 hours **C.** Quantification of viability of human Saos-2 osteoblast-like osteosarcoma cell after exposure to 20% conditioned medium (v/v) of KHOS mock or KHOS ($Sema3A^{OE}$) for 48 hours. Values in the graph are mean ± SD and are obtained from 3 independent experiments.

To assess the effects of long term exposure to osteosarcoma-derived Sema3A, mouse primary osteoblasts, mouse MC3T3-E1 cells and human Saos-2 cells were treated with 20% conditioned medium (v/v) for a prolonged period (up to 28 days) and viability was assessed. As shown in Figure 7.4, prolonged exposure of mouse primary osteoblasts, mouse MC3T3-E1 cells and human Saos-2 cells to osteosarcoma-derived Sema3A had no effect on the osteoblast viability.

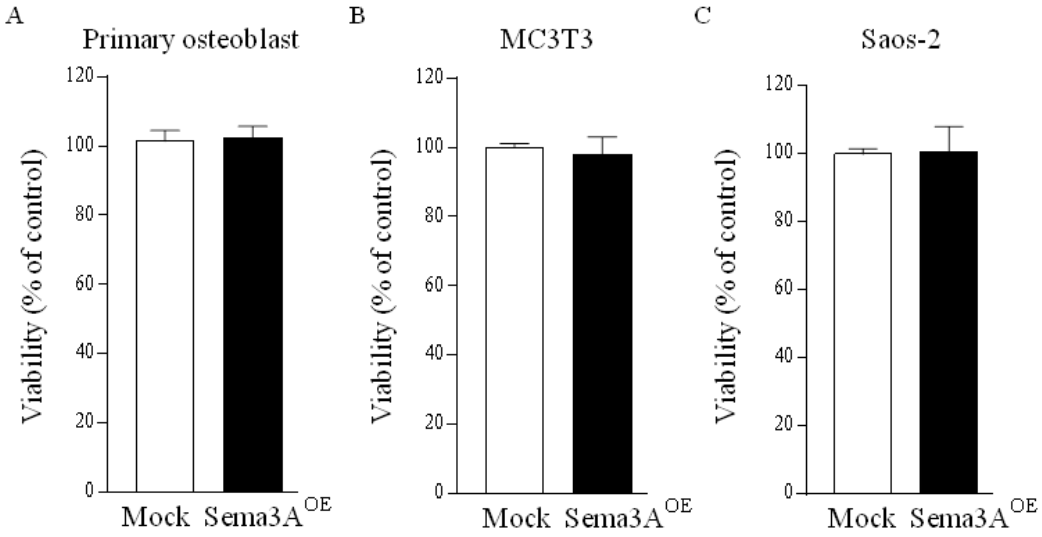

Figure 7.4. Osteoblast viability was not affected after long term exposure to osteosarcoma-derived Sema3A.
This experiment was performed to assess the effect of long term exposure on osteoblast viability to osteosarcoma-derived Sema3A using the AlamarBlue assay. Cultures were exposed to conditioned medium 24 hours after plating. **A.** Quantification of viability of mouse primary osteoblasts after exposure to 20% conditioned medium (v/v) of KHOS mock or KHOS Sema3A overexpressing cells ($Sema3A^{OE}$) for 28 days. **B.** Quantification of viability of mouse MC3T3-E1 osteoblasts after exposure to 20% conditioned medium (v/v) of KHOS mock or KHOS ($Sema3A^{OE}$) for 25 days **C.** Quantification of viability of human Saos-2 osteoblast-like osteosarcoma cell after exposure to 20% conditioned medium (v/v) of KHOS mock or KHOS ($Sema3A^{OE}$) for 9 days. Values in the graph are mean ± SD and are obtained from 3 independent experiments.

7.4.4 **Osteosarcoma-derived Sema3A enhanced alkaline phosphatase activity of osteoblasts**

Sema3A has previously been reported to enhance alkaline phosphatase activity of osteoblasts (Hayashi et al., 2012). Alkaline phosphatase activity was measured after short term exposure of mouse primary osteoblasts, mouse MC3T3-E1 cells and human Saos-2 cells to conditioned medium from KHOS mock or KHOS Sema3A overexpressing cells. Short term exposure of mouse primary osteoblast and mouse MC3T3-E1 osteoblasts significantly increased alkaline phosphatase activity (31%, $p<0.01$ and 26%, $p<0.05$ respectively), while alkaline phosphatase activity of Saos-2 cells was not significantly enhanced in response to osteosarcoma-derived Sema3A (Figure 7.5).

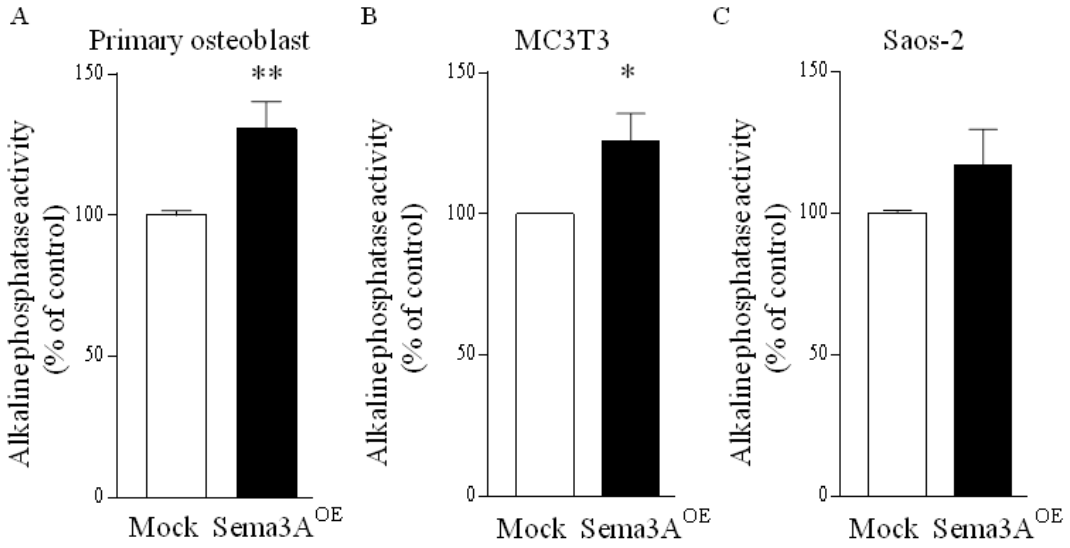

Figure 7.5. Osteosarcoma-derived Sema3A increased osteoblast alkaline phosphatase activity after short term exposure.
This experiment was performed to assess the effect of short term exposure of osteoblast cells to osteosarcoma-derived Sema3A on the alkaline phosphatase activity using the alkaline phosphatase activity assay. Cultures were exposed to conditioned medium 24 hours after plating. **A.** Quantification of alkaline phosphatase activity of mouse primary osteoblasts after exposure to 20% conditioned medium (v/v) of KHOS mock or KHOS Sema3A overexpressing cells ($Sema3A^{OE}$) for 48 hours. **B.** Quantification of alkaline phosphatase activity of mouse MC3T3-E1 osteoblasts after exposure to 20% conditioned medium (v/v) of KHOS mock or KHOS ($Sema3A^{OE}$) for 48 hours. **C.** Quantification of alkaline phosphatase activity of human Saos-2 osteoblast-like osteosarcoma cells after exposure to 20% conditioned medium (v/v) of KHOS mock or KHOS ($Sema3A^{OE}$) for 48 hours. Values in the graph are mean ± SD and are obtained from 3 independent experiments. * $p<0.05$, ** $p<0.01$

7.4.5 **Osteosarcoma-derived Sema3A reduced bone nodule formation after long term continuous exposure**

As shown earlier in this chapter, osteosarcoma-derived Sema3A reduced ectopic bone formation. To investigate the mineralization and alkaline phosphatase activity of osteoblast-like osteosarcoma Saos-2 cells in response to continuous and intermittent exposure of 20% (v/v) conditioned medium from KHOS mock and KHOS Sema3A overexpressing cells, Saos-2 cells were plated and exposed to conditioned medium for different time periods. First to assess the effect of continuous exposure, the osteoblast-like Saos-2 osteosarcoma cells were exposed to conditioned medium from KHOS mock and KHOS Sema3A overexpressing cells 20% (v/v) in osteogenic medium and the medium was refreshed every two days and the experiment was terminated at 9 days (section 2.3.6). As shown in Figure 7.6, long term continuous exposure of Saos-2 osteosarcoma cells to tumour-derived Sema3A had no effect on alkaline phosphatase activity. In contrast, continuous exposure of Saos-2 to tumour-derived Sema3A significantly reduced bone nodule formation by 32% ($p<0.01$).

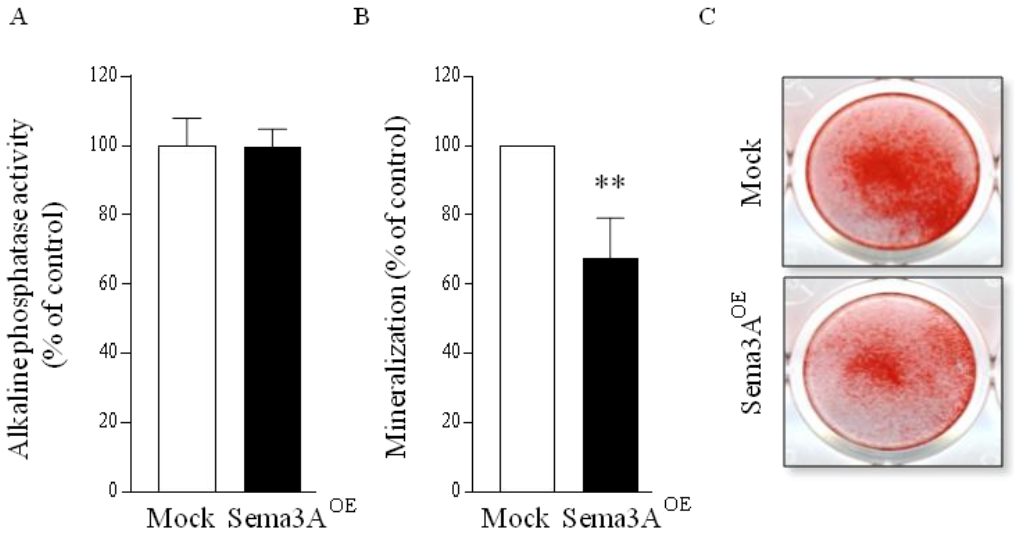

Figure 7.6. Continuous exposure osteosarcoma-derived Sema3A reduced bone nodule formation. Saos-2 cells were continuously exposed to conditioned medium from KHOS cells to assess the effect of osteosarcoma-derived Sema3A on alkaline phosphatase activity and mineralization at the end of the 9 day culture period. Cultures were exposed to conditioned medium 24 hours after plating. After the culture period, cultures were either lysed with alkaline phosphatase lysing buffer or stained with Alizarin red to quantify mineraliazation using destaining solution (section 2.3.8). Quantification of human Saos-2 osteoblast-like osteosarcoma cell **A.** alkaline phosphatase activity and **B.** bone nodule formation after continuous exposure to 20% conditioned medium (v/v) of KHOS mock or KHOS Sema3A overexpressing cells ($Sema3A^{OE}$) for 9 days. **C.** Representative images of bone nodule formation of the cultures described in panel A and B. Values in the graph are mean ± SD and are obtained from 3 independent experiments. ** $p<0.01$

7.4.6 **Osteosarcoma-derived Sema3A increased alkaline phosphatase activity after long term intermittent exposure**

Next, I investigated the effect of intermittent exposure of osteoblast-like Saos-2 osteosarcoma cells to tumour-derived Sema3A *in vitro*. Saos-2 cells were exposed to conditioned medium in osteogenic medium from KHOS mock and KHOS Sema3A overexpressing cells 20% (v/v) for 6 hours of each 48 hour cycle. The Saos-2 cells were exposed to conditioned medium 20% (v/v) in osteogenic medium for 6 hours and after 6 hours the medium was removed and replaced for regular osteogenic medium. This was repeated every 48 hours until the experiment was terminated at 9 days (section 2.3.6). Intermittent exposure of osteoblast-like Saos-2 osteosarcoma cells to 20% (v/v) conditioned medium showed from KHOS mock and KHOS Sema3A overexpressing cells had no effect on bone nodule formation. However, exposure to tumour-derived Sema3A significantly increased the alkaline phosphatase activity of these cultures (36%, $p<0.01$ Figure 7.7)

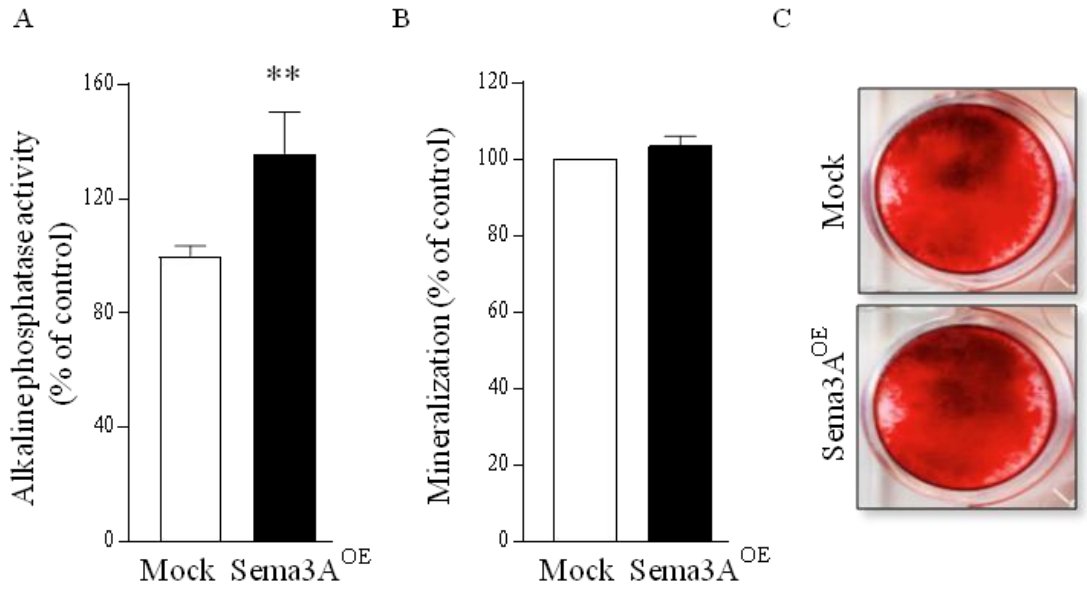

Figure 7.7. Intermittent exposure to osteosarcoma-derived Sema3A increased alkaline phosphatase activity.
Saos-2 cells were intermittently exposed to conditioned medium from KHOS cells for 6 hours out of each 48 hour cycle to assess the effect of osteosarcoma-derived Sema3A on alkaline phosphatase activity and mineralization at the end of the 9 day culture period. Cultures were exposed to conditioned medium 24 hours after plating. After the culture period, cultures were either lysed with alkaline phosphatase lysing buffer or stained with Alizarin red to quantify mineraliazation using destaining solution (section 2.3.8). Quantification of human Saos-2 osteoblast-like osteosarcoma cell **A.** alkaline phosphatase activity and **B.** bone nodule formation after intermittent exposure to 20% conditioned medium (v/v) of KHOS mock or KHOS Sema3A overexpressing cells ($Sema3A^{OE}$) for 9 days. **C.** Representative images of bone nodule formation of the cultures described in panel A and B. Values in the graph are mean ± SD and are obtained from 3 independent experiments. ** $p<0.01$

7.4.7 Osteosarcoma-derived Sema3A reduced phosphorylation of GSK3β, nuclear translocation of β-catenin and total β-catenin expression

Semaphorin 3A is known to influence the Wnt/β-catenin in osteoblasts (Hayashi et al., 2012). To investigate whether osteosarcoma-derived Sema3A affects the Wnt/β-catenin pathway, I examined the level of phosphorylation of GSK3β, nuclear translocation of β-catenin and total β-catenin expression in mouse osteoblast-like MC3T3-E1 cells after exposure to conditioned medium from KHOS mock and KHOS Sema3A overexpressing cells 20% (v/v).

The osteoblast-like MC3T3-E1 cells were incubated in serum free medium overnight and exposed to conditioned medium from KHOS mock and KHOS Sema3A overexpressing cells 20% (v/v) in serum free medium for 15 minutes. Cell lysates were collected and protein expression was measured using western blot (section 0). Exposure to conditioned medium from KHOS Sema3A overexpressing cells modestly but significantly reduced the phosphorylation of GSK3β in MC3T3-E1 by 7% ($p<0.05$).

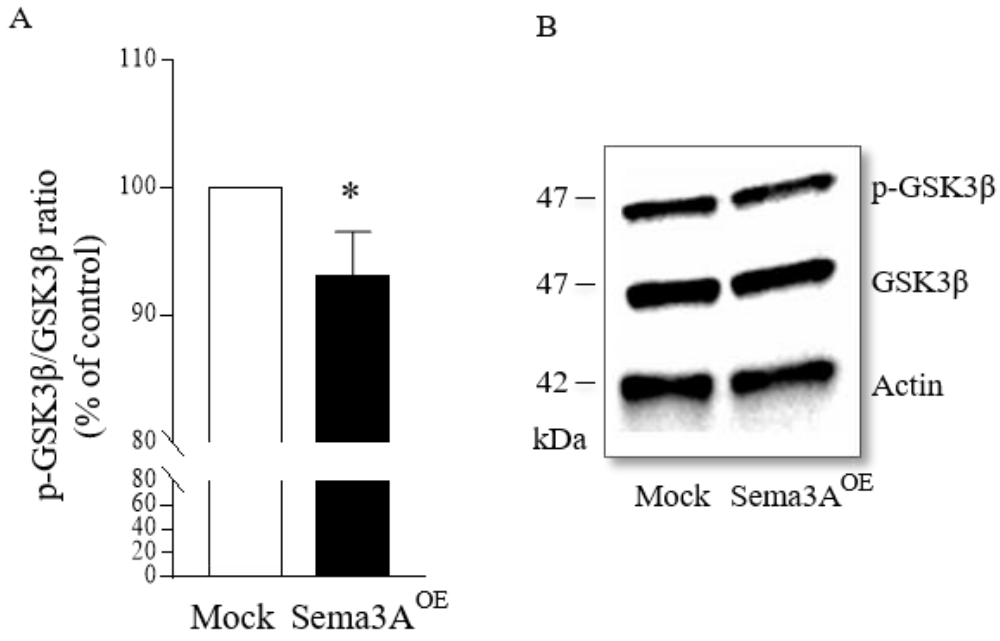

Figure 7.8. Osteosarcoma-derived Sema3A inhibited phosphorylation of GSK3β.
To assess the effect of osteosarcoma-derived Sema3A on activation of the Wnt/β-catenin pathway MC3T3-E1 cells were exposed to conditioned medium from KHOS mock and KHOS Sema3A overexpressing cells and the ratio of GSK3β/Total GSK3β was measured using western blot. **A.** Quantification of the ratio of phosphorylated GSK3β/Total GSK3β in MC3T3-E1 cells exposed to conditioned medium from KHOS mock or KHOS Sema3A overexpressing cells ($Sema3A^{OE}$) for 15 minutes. **B.** Representative photomicrograph of a western blot described in panel A. Values in the graph are mean ± SD and are obtained from 3 independent experiments. * $p<0.05$

Next I investigated whether exposure of MC3T3-E1 to conditioned medium from KHOS Sema3A overexpressing cells had an effect on the nuclear translocation of β-catenin and total β-catenin expression. Nuclear translocation was reduced by 38% ($p<0.05$) after 45 minutes of exposure and total β-catenin expression modestly but significantly reduced by 7% ($p<0.05$) after 24 hours of exposure.

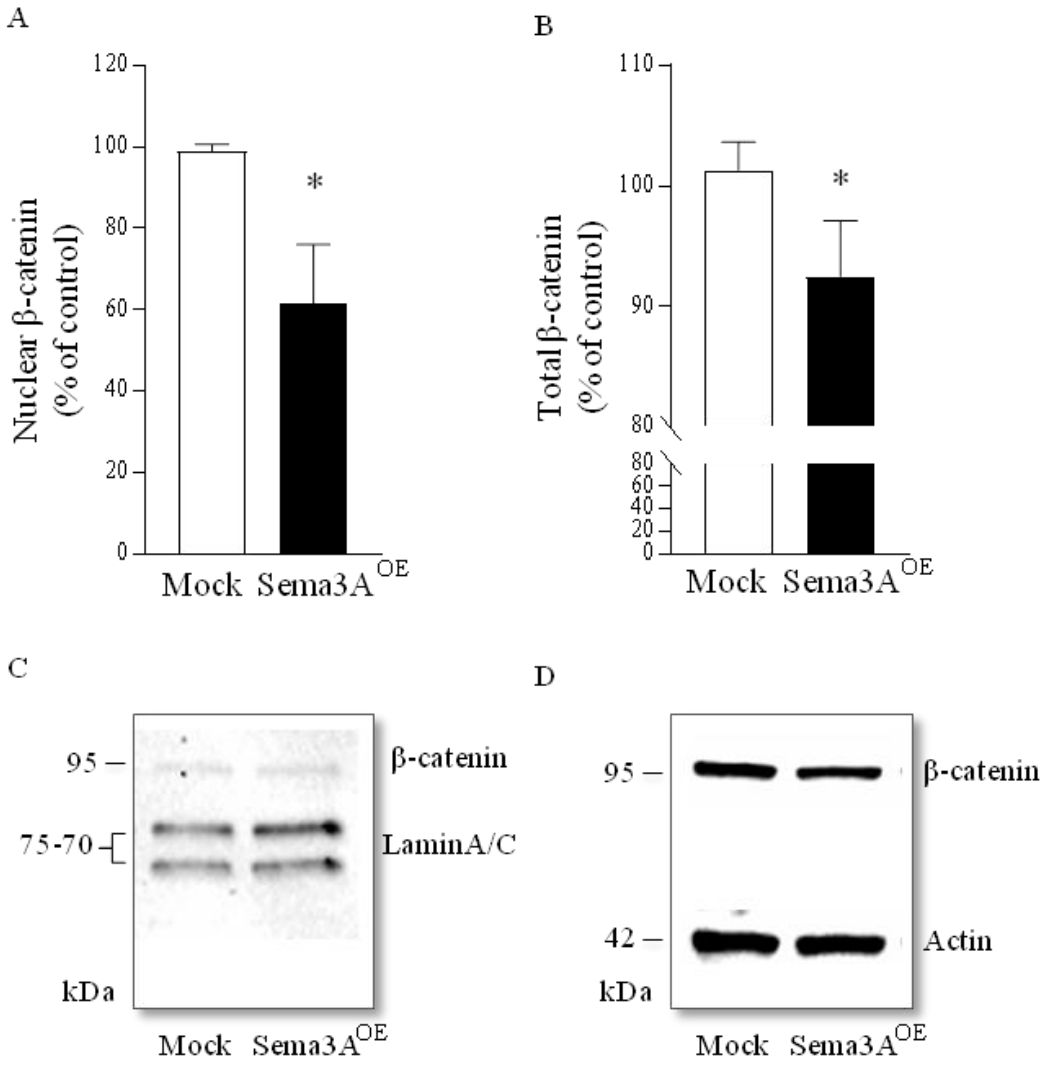

Figure 7.9 Osteosarcoma-derived Sema3A reduced nuclear localization and total β-catenin expression.
To assess the effect of osteosarcoma-derived Sema3A on activation of the Wnt/β-catenin pathway MC3T3-E1 cells were exposed to conditioned medium from KHOS mock and KHOS Sema3A overexpressing cells and β-catenin protein expression was measured using western blot. Loading controls were probed on the same westen blot as target proteins. **A.** Quantification of nuclear β-catenin in MC3T3-E1 cells exposed to conditioned medium from KHOS mock or KHOS Sema3A overexpressing cells ($Sema3A^{OE}$) for 45 minutes. Nuclear β-catenin was normalized to LaminA/C a loading control for nuclear protein. **B.** Quantification of total β-catenin expression in MC3T3-E1 cells exposed to conditioned medium from KHOS mock or KHOS ($Sema3A^{OE}$) for 24 hours. Total β-catenin was normalized using Actin as loading control and was analyzed using total protein lysates. **C.** Representative photomicrograph of a western blot described in panel A. **D.** Representative photomicrograph of a western blot described in panel B. Values in the graph are mean ± SD and are obtained from 3 independent experiments. * $p<0.05$

7.4.8 **Cytokine secretion by KHOS Sema3A overexpressing cells**

Exogenous Sema3A enhances osteoblast differentiation via activation of the Wnt/β-catenin pathway (Hayashi et al., 2012). To investigate whether overexpression of Sema3A in the KHOS osteosarcoma cells had an effect on the expression of other secreted proteins, the conditioned medium from KHOS mock and KHOS Sema3A overexpressing cells was examined using the Proteome Profiler Human XL Cytokine Array Kit R&D systems, which measures the levels of 102 human cytokines (section 2.7).

Of the 102 panel of factors tested, 19 factors were found in the conditioned medium. Of the cytokines expressed, 5 were found to be upregulated and 5 were found to be downregulated in the conditioned medium from KHOS Sema3A overexpressing cells in comparison to conditioned medium from the control (Figure 7.10). Amongst the upregulated cytokines in the conditioned medium from KHOS Sema3A overexpressing cells were dickkopf WNT signalling pathway inhibitor 1 (DKK-1, 254%), chemokine C-X-C motif ligand 5 (CXCL5, 311%), fms related tyrosine kinase 3 ligand (Flt-3 ligand, 305%), Interleukin-17A (IL-17A, 256%) and Osteopontin (661%). The cytokines that were downregulated by the KHOS Sema3A overexpressing cells were Macrophage migration inhibitory factor (MIF, 55%), Pentatraxin 3 (31%), Resistin (73%), ST2 (35%) and Thrombospondin-1 (24%).

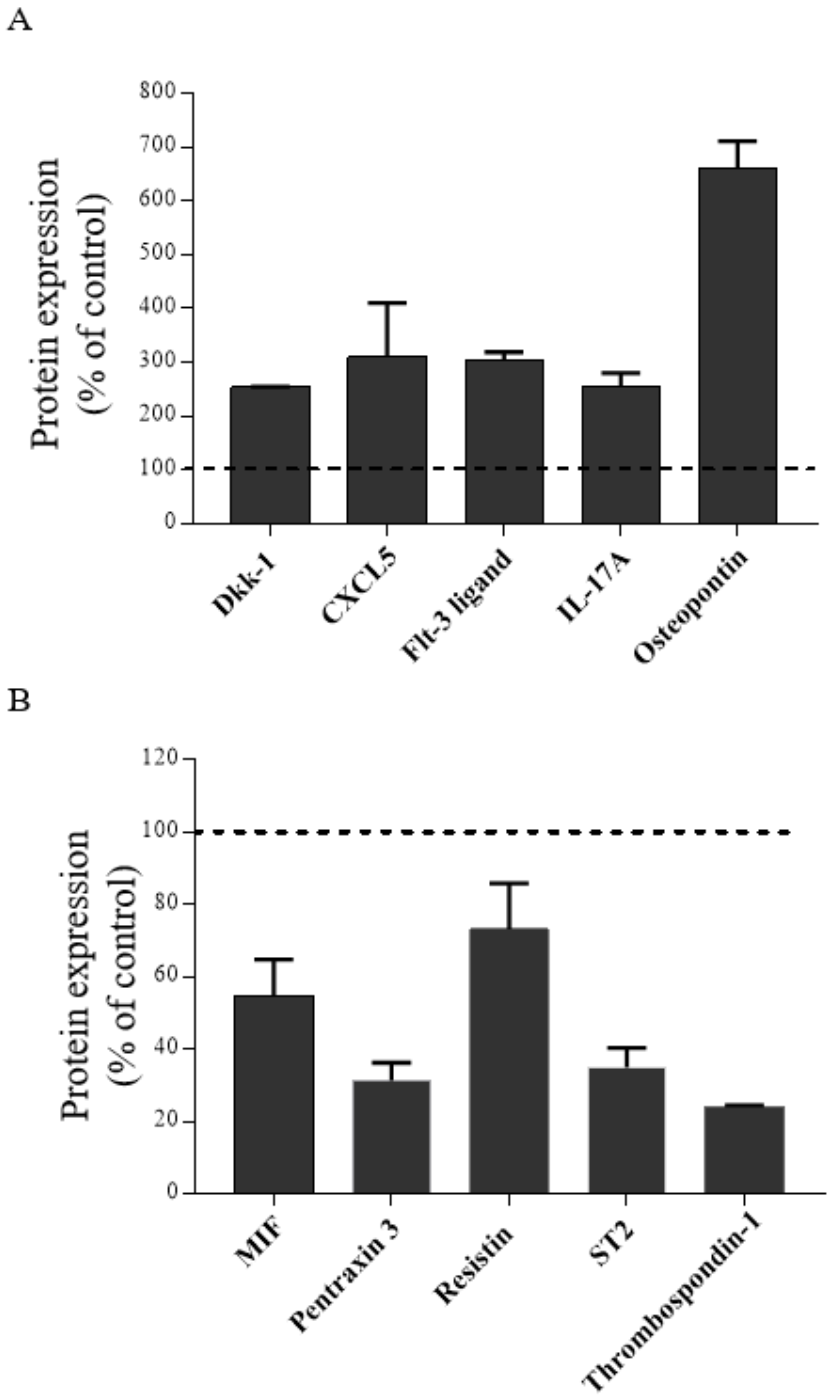

Figure 7.10. Differential levels of cytokines in the conditioned medium of KHOS Sema3A expressing cells.

The cytokine expression of KHOS mock and KHOS Sema3A overexpressing cells was measured in the conditioned medium using the human cytokine array kit on a chemidoc by densitometry analysis. KHOS mock cytokine expression represents a 100% Cells were counted and plated at $0.2x10^6$ left to adhere overnight and then supplemented with serum free medium. Conditioned medium was collected after 16 hours of culture. **A.** Quantification of cytokine expression higher expressed in the KHOS Sema3A expressing cells ($Sema3A^{OE}$) in comparison to the KHOS mock control. **B.** Quantification of cytokine expression that are less expressed in the KHOS ($Sema3A^{OE}$). The experiment was performed using a Proteome Profiler Human XL Cytokine Array Kit.

7.5 Discussion

Osteoblasts express the Sema3A receptors and produce Sema3A which is known to enhance osteoblast differentiation (Gomez et al., 2005, Hayashi et al., 2012). By its dual effect on stimulating osteoblasts and inhibiting osteoclasts, Sema3A enhances bone volume and reduces bone resorption thereby increasing bone volume and protects against bone loss (Hayashi et al., 2012). Previous mechanistic studies in osteoblasts have shown that Sema3A activates the canonical Wnt/β-catenin pathway and as a result enhances osteoblast differentiation (Hayashi et al., 2012). The aim of this chapter was to investigate the role of tumour-derived Sema3A in human osteosarcoma cancer cell-osteoblast crosstalk *in vitro* and whether tumour-derived Sema3A affects the development of osteosarcoma-associated ectopic bone formation in mice.

One of the hallmarks of osteosarcoma is the formation of ectopic bone and this has previously been reported in mouse models of osteosarcoma (Geller and Gorlick, 2010, Lamoureux et al., 2014). Here, I investigated whether osteosarcoma-derived Sema3A had any effect on ectopic bone formation of the tibia and fibula in the xenograft mouse model of osteosarcoma. Inoculation of KHOS mock cells caused ectopic bone formation and surprisingly, mice injected with KHOS cell overexpressing Sema3A showed a significant reduction in ectopic bone formation. In contrast, administration of exogenous Sema3A had no significant effect on the ectopic bone formation. It is important to note that exogenous Sema3A was only administrated twice a week leading to intermittent exposure whereas we anticipate osteosarcoma cells overexpressing Sema3A to continuously secrete it in the bone microenvironment. Thus we hypothesized that this discrepancy in ectopic bone formation may be attributed to the sustained exposure to tumour-derived Sema3A that reduced the ability of osteosarcoma cells and osteoblasts to form new bone.

In an attempt to further examine this hypothesis, I assessed whether osteosarcoma-derived Sema3A affected osteoblast viability and differentiation, using a panel of osteoblast-like cells, mouse primary osteoblasts, mouse MC3T3-E1 cells and human osteoblast-like osteosarcoma Saos-2 cells. Short and sustained exposure of these cells to conditioned medium from Sema3A overexpressing KHOS cells had no effect on their viability. This suggests that the inhibitory effect of osteosarcoma-derived

Sema3A is not attributed to a reduction in osteoblasts. However, exposure to tumour-derived Sema3A significantly increased the alkaline phosphatase activity of primary osteoblasts and MC3T3-E1 but not in the osteoblastic Saos-2 osteosarcoma cells. The increase in alkaline phosphatase activity in the panel of osteoblast-like cells is in confirmation with previous studies (Hayashi et al., 2012) and the effect of exogenous Sema3A as described in Chapter 3.

To investigate whether the reduction in ectopic bone could be due to sustained exposure to osteosarcoma-derived Sema3A, I investigated whether continuous or intermittent exposure of Saos-2 osteoblastic osteosarcoma cells had an effect on mineralization *in vitro*. Continuous exposure to osteosarcoma-derived Sema3A had no effect on alkaline phosphatase activity but significantly inhibited mineralization. Interestingly, intermittent exposure increased alkaline phosphatase activity and did not affect mineralization. These effects imply that the duration of Sema3A exposure may indeed play a role in the differential effects on the trabecular compartment and osteosarcoma-associated ectopic bone formation.

Sema3A has been shown to enhance osteoblast differentiation at least in part by activating the Wnt/β-catenin pathway through FARP2 induced Rac activation (Hayashi et al., 2012). The canonical Wnt/β-catenin pathway is an important factor in osteoblast differentiation (Krishnan et al., 2006, Cawthorn et al., 2012, Day et al., 2005). Without an activating signal, β-catenin is phosphorylated by CKI and GSK3-β, after phosphorylation β-catenin is degraded by a destruction complex (Reya and Clevers, 2005). Therefore, to investigate whether osteosarcoma-derived Sema3A had any effect on osteoblast Wnt/β-catenin signalling, MC3T3-E1 osteoblast-like cells were exposed to conditioned medium from KHOS Sema3A overexpressing cells. Surprisingly, conditioned medium from the Sema3A overexpressing cells modestly but significantly reduced phosphorylation of GSK3β, total β-catenin expression and nuclear translocation of β-catenin. Suggesting that conditioned medium from Sema3A overexpressing osteosarcoma cells inhibits osteoblastic canonical Wnt/β-catenin signalling. This is in contrast with the effects of Sema3A on Wnt/β-catenin signalling in osteoblasts as described previously by Hayashi and colleagues (Hayashi 2012). Evidently, Sema3A is not the only factor produced by the tumour cells as the

conditioned medium contains a cocktail of secreted factors. Therefore, contribution of other factors secreted by the tumour cells aside from Sema3A cannot be excluded.

To test this hypothesis, 102 different cytokines were measured simultaneously in the conditioned medium of the KHOS mock and KHOS Sema3A overexpressing cells using the Proteome Profiler Human XL Cytokine Array Kit. Out of the 19 secreted factors detected, 10 were differentially expressed in the Sema3A overexpressing conditioned medium in comparison to the conditioned medium from the KHOS mock control. Of these 10, the following 5 factors were upregulated by the Sema3A overexpressing KHOS cells, DKK1, CXCL5, Flt-3 ligand, IL17A and Osteopontin. Furthermore, 5 factors, MIF, Pentatraxin, Resistin, ST2 and thrombospondin-1 were downregulated. Most of these cytokines have been shown to be involved in osteoblast differentiation, osteoclast formation and have been implicated to play a role in osteosarcoma cells (Table 7.1).

The factors of main interest that were secreted at higher levels by the KHOS cells overexpressing Sema3A are DKK1, IL-17A and osteopontin because of their involvement in pathways affecting osteoblast differentiation. Acting as a Wnt/β-catenin antagonist, DKK1 is a Wnt/β-catenin signalling antagonist and by inhibiting the Wnt/β-catenin pathway, DKK1 inhibits osteoblast differentiation which also leads to a decrease in OPG that in turns leads to more osteoclast formation (Qiang et al., 2008, Diarra et al., 2007). In osteosarcoma, anti-DKK1 treatment reduced tumour growth and metastasis indicating that active Wnt signalling is involved in osteosarcoma and that by inhibiting the Wnt signalling pathway, DKK1 enhances osteosarcoma (Goldstein et al., 2016). Higher levels of DKK1 in conditioned medium from KHOS cells overexpressing Sema3A may explain the modest inhibition on the Wnt/β-catenin pathway in the osteoblasts and may also have contributed to the reduction in ectopic bone formation *in vivo*. Another factor that was upregulated by the KHOS cells overexpressing Sema3A was IL17A. IL17A also inhibits osteogenic differentiation of bone mesenchymal stem cells most likely by downregulation of Wnt molecules (Wang et al., 2017c). Furthermore, higher IL17A levels were associated with metastasis and clinical stage and enhanced osteosarcoma associated metastasis *in vivo* (Wang et al., 2013) which may in part be due to the effect of IL17A on Wnt production in bone mesenchymal stem cells.

Table 7.1 Involvement of differentially expressed cytokines in osteosarcoma and bone cells.

Protein	Osteosarcoma	Osteoclast	Osteoblast	Reference
CXC Motif Chemokine Ligand 5 (CXCL5)	↑	-	-	(Dang et al., 2017)
Dickkopf WNT inhibitor1 (DKK1)	↑	↑	↓	(Qiang et al., 2008), (Diarra et al., 2007), (Goldstein et al., 2016).
Fms-related tyrosine kinase 3 (FLT3) ligand	↑	↑	-	(Flores et al., 2017, Lean et al., 2001)
IL17A	↑	↓	↓	(Balani et al., 2013) (Wang et al., 2017c) (Wang et al., 2013)
Osteopontin	↔	↓	↑	(Holm et al., 2014) (Chellaiah et al., 2003) (Li et al., 2015b)
Pentraxin-related protein 3 (PTX3)	-	↔	↔	(Lee et al., 2014)
ST2	-	-	-	
Macrophage migration inhibitory factor (MIF)	↑	↑	-	(Wang et al., 2017a) (Madeira et al., 2012)
Resistin	-	↑	↑	(Thommesen et al., 2006)
Thrombospondin-1 (TSP1)	↑	↑	↓	(Hu et al., 2017) (Amend et al., 2015, Bailey Dubose et al., 2012)

↑ Enhancement in metastatic properties of osteosarcoma, increase in osteoclast formation or enhanced osteoblast differentiation and/or function. ↔ Inconclusive data or no effect. ↓ Reduction of metastatic properties, reduction of osteoclast formation or reduction in osteoblast differentiation and/or function. – No known effect.

Osteopontin was also upregulated in the conditioned medium from KHOS Sema3A overexpressing cells. Osteopontin one of the organic components of bone is produced by osteoblasts and is an important mediator of mineralization by osteoblasts but seems to have no role in osteoblast differentiation (Katagiri and Takahashi, 2002, Holm et al., 2014). Osteopontin deficiency has been shown to lead to a dysfunction in osteoclasts (Chellaiah et al., 2003). There is conflicting data regarding the role of osteopontin in osteosarcoma. Osteopontin is a marker of osteogenic differentiation, a lower level of osteopontin may therefore indicate an undifferentiated state of the osteosarcoma cell. Altered levels of osteopontin may play a role in osteosarcoma progression and metastasis (Li et al., 2015b). As osteopontin is a marker for osteogenic differentiation an increase in osteopontin may indicate that overexpression of Sema3A in the osteosarcoma cells leads to a more differentiated osteoblastic state.

Whilst the exact mechanism by which tumour-derived Sema3A regulates the differentiation of osteoblasts and osteosarcoma cells remains to be explored, the results in this chapter showed that tumour-derived Sema3A increases osteoblast alkaline phosphatase activity without affecting osteoblast viability. Furthermore, conditioned medium from Sema3A overexpressing cells reduced Wnt/β-catenin signalling. DKK1 and IL17A were upregulated by KHOS Sema3A overexpressing cells which may have contributed to the reduction of osteoblastic β-catenin signalling and the reduction in ectopic bone formation seen in the Sema3A overexpressing tumours (Figure 7.11).

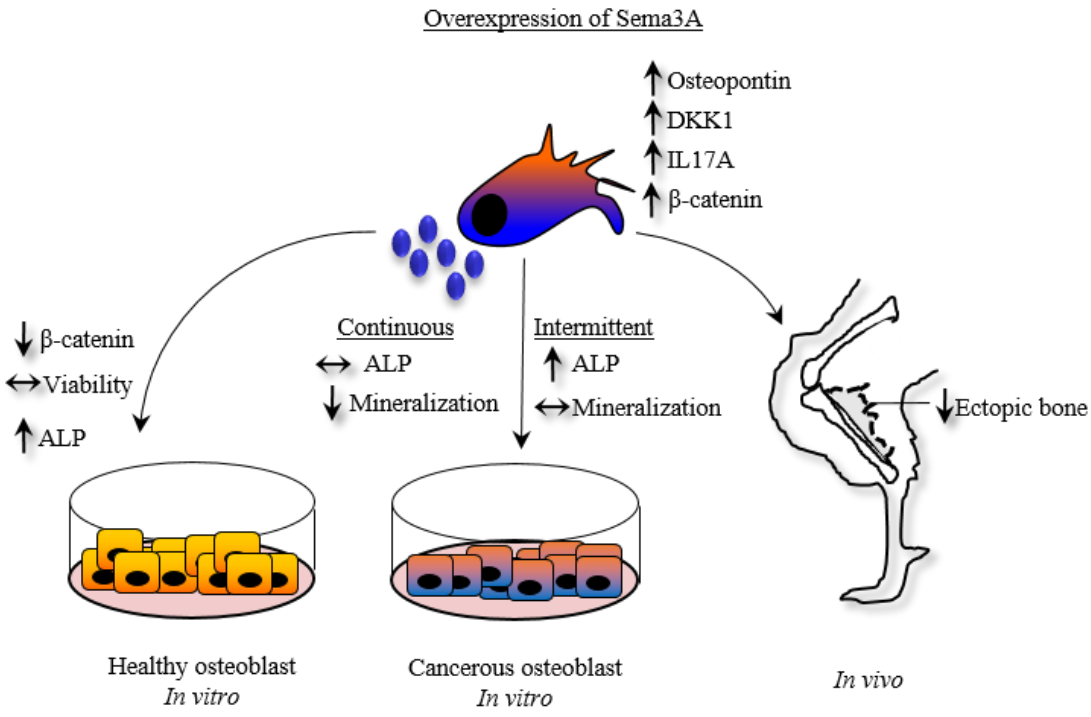

Figure 7.11 Schematic summary of the effect of Sema3A overexpression in KHOS osteosarcoma cells on osteoblasts.
Tumour-derived Sema3A reduced wnt signalling in osteoblasts and enhanced alkaline phosphatase activity without affecting viability. In Saos-2 osteosarcoma cells, conditioned medium from KHOS Sema3A overexpressing cells reduced mineralization *in vitro* and ectopic bone formation *in vivo*. Additionally, overexpression of Sema3A enhanced expression of osteopontin, DKK1 and IL17A in the KHOS osteosarcoma cells. For detailed information see text. ALP, Alkaline phosphatase activity. DKK1, dickkopf WNT signalling pathway inhibitor 1. IL17A, Interleuking-17A

CHAPTER EIGHT

General discussion

8 General discussion

Osteosarcoma is the most common malignant primary bone tumour, the disease mainly affects children and young adults and is more common in males than females (Meyers and Gorlick, 1997). Osteosarcoma is characterized by severe chromosomal instability at the time of diagnosis (Bousquet et al., 2016), this is one of the underlying challenges in finding a treatment that benefits the majority of patients. Since the introduction of chemotherapy the survival rate for osteosarcoma patients has not improved, the 5-year survival rate for metastatic osteosarcoma patients is particularly poor and remains around 25-30% (Allison et al., 2012), illustrating the need to identify new therapeutic targets.

Osteosarcoma is thought to arise from the mesenchymal stem cell lineage or a more differentiated form of mesenchymal derived osteogenic precursors (Mohseny et al., 2009, Xiao et al., 2013, Mutsaers and Walkley, 2014). In 2012, Sema3A was identified as an osteoblast derived factor that influences both osteoblasts and osteoclasts and enhances bone formation (Hayashi et al., 2012). However, the role of Sema3A in osteosarcoma is still unknown. Sema3A is a member of the semaphorin class-3 secreted signalling proteins. Initially Sema3A was found to be important for the development of the bone, heart and nervous system (Behar et al., 1996). More recently, Sema3A was found to be important in osteoblast-osteoclast coupling, bone development and bone metabolism (Adams et al., 1997, Behar et al., 1996, Hayashi et al., 2012). Both osteoclasts and osteoblasts express the Sema3A receptors, neuropilins and plexins, and osteoblasts produce and secrete Sema3A (Gomez et al., 2005). Over the years Sema3A has been implicated in cancer and depending on the type of cancer, Sema3A exhibits tumour promoting or tumour suppressive effects (Table 1.3) (Casazza et al., 2011, Zhou et al., 2014, Muller et al., 2007, Bagci et al., 2009, Hu et al., 2016, Mishra et al., 2015b, Chakraborty et al., 2012, Huang et al., 2017). Moreover Nrp1 and Nrp2, the receptors for the semaphorin class-3 proteins, have been implicated in osteosarcoma (Ji et al., 2015, Handa et al., 2000, Boro et al., 2015, Zhu et al., 2014). Altogether, these studies suggest that Sema3A might play a role in osteosarcoma and may be of value for the treatment of osteosarcoma. The aim of this thesis was to examine the effects of exogenous and osteosarcoma-derived Sema3A *in vitro* and xenograft mouse models of osteosarcoma.

Previous studies have shown that administration of Sema3A increases the number of osteoblasts, enhances bone formation, protects against ovariectomy induced osteoporosis and stimulated fracture healing suggesting Sema3A acts as a bone anabolic (Hayashi et al., 2012, Li et al., 2015a). In agreement with these previous studies, administration of exogenous Sema3A significantly enhanced bone volume of the trabeculae in the tibia. This effect was accompanied by an increase in osteoblast number. Furthermore, administration of exogenous Sema3A also enhanced trabecular and cortical bone volume of the femur and showed a corresponding trend in enhanced P1NP and reduced CTX serum markers. Whilst these findings confirm that Sema3A exhibits bone anabolic activity and may be of use in osteolytic bone diseases, caution is required as present and previous studies (Hayashi et al., 2012, Li et al., 2015a), are limited to a treatment regimen of a single or double dose a week and the effect of continuous Sema3A treatment on bone is unknown.

One of the common features of osteosarcoma is the formation of ectopic bone (Geller and Gorlick, 2010). Consistent with the anabolic activity of Sema3A observed in the healthy leg, I detected a significant increase in bone volume in the tumour-bearing tibia of the mice that received exogenous Sema3A. In agreement with previous data (Fukuda et al., 2013, Hayashi et al., 2012) exogenous Sema3A enhanced alkaline phosphatase activity in osteoblasts, these effects were also observed by exposure to osteosarcoma-derived Sema3A. Moreover, exogenous Sema3A also enhanced the alkaline phosphatase activity of the low metastatic osteosarcoma cell lines but had no effect on the alkaline phosphatase activity of the highly metastatic MNNG/HOS osteosarcoma cell line. These results suggest that the effects of Sema3A on the low metastatic osteosarcoma cell lines *in vitro* are comparable with the effects of Sema3A on calvarial osteoblasts as reported by Hayashi and colleagues (Hayashi et al., 2012). Surprisingly administration of exogenous Sema3A had no effect on osteosarcoma-associated ectopic bone formation. This indicates that Sema3A could be used in osteosarcoma patients to protect the bone without exacerbating the ectopic bone formation. This may especially be useful in patients where the tumour cannot be removed by surgery.

Previous studies have shown that osteoblasts produce Sema3A (Hayashi et al., 2012, Li et al., 2015a) and the Sema3A receptor Nrp1 has been implicated in osteosarcoma

(Boro et al., 2015). Tumour specific expression of Sema3A in the primary tumour microenvironment may have several effects. Sema3A could inhibit the migration and invasion of the tumour into the tissue surrounding the tumour by its effect on cell motility. Furthermore, Sema3A is a known factor to inhibit angiogenesis and may contribute to a reduction in tumour growth due to a reduction in tumour vascularisation. To assess the effects of tumour-specific Sema3A expression in osteosarcoma, I overexpressed Sema3A in the metastatic human KHOS osteosarcoma cells and examined the effects of tumour-derived Sema3A on osteosarcoma growth, osteolysis and lung metastasis. In contrast to the administration of exogenous Sema3A, tumour-derived Sema3A had no effect on the bone volume of the tumour-bearing tibia or femur despite a significant increase in osteoblast differentiation *in vitro* by conditioned medium from these cells and a trend towards increased osteoblast number in mice. Surprisingly tumour-derived Sema3A significantly reduced ectopic bone formation. My *in vitro* studies have indicated that the discrepancy in the effect of exogenous Sema3A and tumour-derived Sema3A on ectopic bone formation may be due to the inhibition of osteoblast differentiation – but not viability - due to sustained exposure to tumour-derived Sema3A and other factors present in the conditioned medium from KHOS overexpressing Sema3A cells.

Sema3A is known to stimulate osteoblast differentiation by engaging the canonical Wnt/β-catenin pathway (Hayashi et al., 2012). Surprisingly, despite an enhanced alkaline phosphatase activity in osteoblasts, conditioned medium from the KHOS Sema3A overexpressing cells significantly reduced phosphorylation of GSK3β, nuclear translocation of β-catenin and total β-catenin expression. This suggests that, in contrast with previous studies with exogenous Sema3A (Hayashi et al., 2012), conditioned medium from KHOS cells overexpressing Sema3A inhibits canonical Wnt/β-catenin signalling. Interestingly, continuous exposure of osteoblast-like Saos-2 cells to tumour-derived Sema3A significantly reduced mineralization without affecting alkaline phosphatase activity *in vitro*, while intermittent exposure had no effect on mineralization but enhanced alkaline phosphatase activity. Evidently, the conditioned medium from osteosarcoma consists of a variety of factors that may play a role in the reduction in osteoblastic Wnt/β-catenin signalling and mineralization *in vitro*.

Ten secreted factors were found to be differentially expressed in the Sema3A overexpressing osteosarcoma cells compared to the control. Of these 10, DKK1, osteopontin and IL17A were upregulated and of specific interest because of their role in osteoblasts. DKK1 is a Wnt signalling antagonist that inhibits osteoblastic differentiation and IL17A inhibits osteogenic differentiation at least in part by downregulating Wnt signalling (Wang et al., 2017c, Diarra et al., 2007, Qiang et al., 2008). The upregulation of DKK1 and IL17A could explain the modest inhibition seen on the Wnt/β-catenin pathway in the osteoblasts. The upregulation of these 2 factors most likely also contributed to the reduction of mineralization *in vitro* and inhibition of ectopic bone formation *in vivo*. The other protein of interest that was upregulated in the conditioned medium from KHOS Sema3A overexpressing cells was osteopontin. Osteopontin is a marker for mature osteoblasts and an important protein in mineralization by osteoblasts (Katagiri and Takahashi, 2002, Holm et al., 2014). An increase in osteopontin may indicate that overexpression of Sema3A in the osteosarcoma cells leads to a more differentiated osteoblastic state. In summary, both the duration of exposure to Sema3A and the production of DKK1 and IL17A may play a role in the reduction of ectopic bone formation in mice. Whilst these findings are interesting, the involvement of these osteosarcoma-derived factors, besides tumour-derived Sema3A, on the inhibition of ectopic bone formation warrants further investigation. Incidentally, previous studies have shown that parathyroid hormone (PTH) exerts a bone anabolic effect when given intermittently but continuous treatment has been found to be detrimental to bone health (Potts and Gardella, 2007, Iida-Klein et al., 2005). Thus, further testing of intermittent and continuous dosing of exogenous Sema3A in preclinical models of bone diseases is needed.

Previous studies including research conducted in our laboratories (MSc thesis de Ridder unpublished data, 2014) have shown that Sema3A inhibited RANKL induced osteoclast formation *in vitro* (Fukuda et al., 2013, Hayashi et al., 2012). Exogenous Sema3A and tumour-derived Sema3A significantly reduced osteoclast formation in osteosarcoma-osteoclast cocultures *in vitro*. *In vivo*, exogenous Sema3A significantly reduced osteoclast numbers in the healthy mouse tibia. Consistent with these observations, exogenous Sema3A showed a trend towards a reduction in osteoclasts in the tumour-bearing tibia whereas tumour-derived Sema3A significantly reduced osteoclast numbers in the tumour-bearing tibia. Immunostaining of Sema3A would

have added additional information to where Sema3A was expressed and to what extent the overexpresssion was efficicent within the tumour microenvironment. One of the limitations of this model is the rapid tumour growth which may have contributed to the limited effects on preservation of bone volume despite the inhibition of osteoclast number.

Sema3A overexpression has been reported to reduce tumour growth *in vivo* in a variety of cancer cell types including breast cancer, melanoma and oral cancer (Chakraborty et al., 2012, Mishra et al., 2015a, Casazza et al., 2011). Furthermore, tumour specific expression of Sema3A has been shown to affect cancer cell migration and invasion in a variety of cancer cells (Muller et al., 2007, Bagci et al., 2009, Pan and Bachelder, 2010, Herman and Meadows, 2007, Mishra et al., 2015b, Casazza et al., 2011). Here, I showed for the first time that both exogenous Sema3A and tumour-derived Sema3A inhibited osteosarcoma cell motility *in vitro*. Treatment with exogenous Sema3A had no effect on the viability of any of the osteosarcoma cell lines tested but overexpression of Sema3A reduced the viability of the KHOS osteosarcoma cells. My results indicate that this difference may be explained by the differential expression of the other tumour-derived factors listed above. Furthermore, exogenous Sema3A administration had no effect on osteosarcoma tumour growth although there was a trend towards less lung metastasis. These *in vivo* observations are in agreement with the results I reported *in vitro* where exogenous Sema3A inhibited osteosarcoma cell motility without affecting viability. Interestingly, in contrast to previous studies in other cancers (Chakraborty et al., 2012, Mishra et al., 2015a, Casazza et al., 2011), tumour-specific overexpression of Sema3A had no effect on tumour growth.

One of the challenges of this osteosarcoma xenograft model is its aggressive nature which may have limited the effects of Sema3A on tumour growth and metastasis. Another limitation of this xenograft model is the immunodeficiency. Sema3A has previously been shown to enhance the macrophage M1 phenotype which enhanced natural killer cells and CD8 T cell recruitment to the tumour (Wallerius et al., 2016), highlighting the importance of Sema3A in anti-tumour immunity. Furthermore, osteosarcoma are highly heterogeneous and the main limitation of osteosarcoma research in general is the limited availability of cell lines and models (Peterse et al.,

2017, Bousquet et al., 2016). To provide a definitive conclusion on the efficacy of Sema3A on osteosarcoma growth and metastasis, future studies should test the effect of Sema3A on osteosarcoma tumours in syngeic immunocompetent models, such as MOS-J, and investigate the effects of Sema3A on the development and progression of osteosarcoma in spontaneous osteosarcoma models (Grigoriadis et al., 1993, Walkley et al., 2008, Entz-Werle et al., 2010).

In conclusion, my present findings, when combined with previous studies, administration of exogenous Sema3A significantly enhanced bone volume in mice. The bone anabolic nature of administration of Sema3A may provide an alternative approach to osteoporosis treatment due to its coupled effect on bone resorption and bone formation. We caution however that the treatment regimen has to be investigated in more detail as long term continuous exposure to Sema3A may inhibit bone formation. In osteosarcoma models, I have shown for the first time that exogenous Sema3A enhanced bone volume in mice bearing human osteosarcoma, and tumour-derived Sema3A, but not exogenous Sema3A, reduced osteosarcoma-associated ectopic bone formation. Both exogenous and osteosarcoma-derived Sema3A act as a tumour inhibitor on osteosarcoma *in vitro* and despite a lack of effect on tumour growth showed a trend towards fewer lung metastases *in vivo*. Current osteosarcoma treatment consists of chemotherapy followed by removal of the tumour and adjuvant chemotherapy. Therefore, the protective effect on bone by exogenous Sema3A administration may provide an option to preserve bone without exacerbating ectopic bone formation in an adjuvant setting in the osteosarcoma tumours that are inaccessible for surgery.

Bibliography

9 References

1999. Unified nomenclature for the semaphorins/collapsins. Semaphorin Nomenclature Committee. *Cell.* United states.

ADAMS, R. H., LOHRUM, M., KLOSTERMANN, A., BETZ, H. & PUSCHEL, A. W. 1997. The chemorepulsive activity of secreted semaphorins is regulated by furin-dependent proteolytic processing. *Embo j,* 16**,** 6077-86.

AIZAWA, H., WAKATSUKI, S., ISHII, A., MORIYAMA, K., SASAKI, Y., OHASHI, K., SEKINE-AIZAWA, Y., SEHARA-FUJISAWA, A., MIZUNO, K., GOSHIMA, Y. & YAHARA, I. 2001. Phosphorylation of cofilin by LIM-kinase is necessary for semaphorin 3A-induced growth cone collapse. *Nat Neurosci,* 4**,** 367-73.

AKIYAMA, H., CHABOISSIER, M. C., MARTIN, J. F., SCHEDL, A. & DE CROMBRUGGHE, B. 2002. The transcription factor Sox9 has essential roles in successive steps of the chondrocyte differentiation pathway and is required for expression of Sox5 and Sox6. *Genes Dev,* 16**,** 2813-28.

ALFRANCA, A., MARTINEZ-CRUZADO, L., TORNIN, J., ABARRATEGI, A., AMARAL, T., DE ALAVA, E., MENENDEZ, P., GARCIA-CASTRO, J. & RODRIGUEZ, R. 2015. Bone microenvironment signals in osteosarcoma development. *Cell Mol Life Sci,* 72**,** 3097-113.

ALLISON, D. C., CARNEY, S. C., AHLMANN, E. R., HENDIFAR, A., CHAWLA, S., FEDENKO, A., ANGELES, C. & MENENDEZ, L. R. 2012. A meta-analysis of osteosarcoma outcomes in the modern medical era. *Sarcoma,* 2012**,** 704872.

AMBROSZKIEWICZ, J., GAJEWSKA, J., KLEPACKA, T., CHELCHOWSKA, M., LASKOWSKA-KLITA, T. & WOZNIAK, W. 2010. Clinical utility of biochemical bone turnover markers in children and adolescents with osteosarcoma. *Adv Med Sci,* 55**,** 266-72.

AMEND, S. R., ULUCKAN, O., HURCHLA, M., LEIB, D., NOVACK, D. V., SILVA, M., FRAZIER, W. & WEILBAECHER, K. N. 2015. Thrombospondin-1 regulates bone homeostasis through effects on bone matrix integrity and nitric oxide signaling in osteoclasts. *J Bone Miner Res,* 30**,** 106-15.

ANDO, K., HEYMANN, M. F., STRESING, V., MORI, K., REDINI, F. & HEYMANN, D. 2013. Current therapeutic strategies and novel approaches in osteosarcoma. *Cancers (Basel),* 5**,** 591-616.

AUNG, L., GORLICK, R., HEALEY, J. H., SHI, W., THALER, H. T., SHORTER, N. A., HUVOS, A. G. & MEYERS, P. A. 2003. Metachronous skeletal osteosarcoma in patients treated with adjuvant and neoadjuvant chemotherapy for nonmetastatic osteosarcoma. *J Clin Oncol,* 21**,** 342-8.

BACCI, G., LONGHI, A., BERTONI, F., BRICCOLI, A., VERSARI, M., PIGNOTTI, E. & PICCI, P. 2006a. Bone metastases in osteosarcoma patients treated with neoadjuvant or adjuvant chemotherapy: the Rizzoli experience in 52 patients. *Acta Orthop,* 77**,** 938-43.

BACCI, G., LONGHI, A., VERSARI, M., MERCURI, M., BRICCOLI, A. & PICCI, P. 2006b. Prognostic factors for osteosarcoma of the extremity treated with neoadjuvant chemotherapy: 15-year experience in 789 patients treated at a single institution. *Cancer,* 106**,** 1154-61.

BACHELDER, R. E., LIPSCOMB, E. A., LIN, X., WENDT, M. A., CHADBORN, N. H., EICKHOLT, B. J. & MERCURIO, A. M. 2003. Competing autocrine

pathways involving alternative neuropilin-1 ligands regulate chemotaxis of carcinoma cells. *Cancer Res,* 63**,** 5230-3.

BAGCI, T., WU, J. K., PFANNL, R., ILAG, L. L. & JAY, D. G. 2009. Autocrine semaphorin 3A signaling promotes glioblastoma dispersal. *Oncogene,* 28**,** 3537-50.

BAGNARD, D., VAILLANT, C., KHUTH, S. T., DUFAY, N., LOHRUM, M., PUSCHEL, A. W., BELIN, M. F., BOLZ, J. & THOMASSET, N. 2001. Semaphorin 3A-vascular endothelial growth factor-165 balance mediates migration and apoptosis of neural progenitor cells by the recruitment of shared receptor. *J Neurosci,* 21**,** 3332-41.

BAILEY DUBOSE, K., ZAYZAFOON, M. & MURPHY-ULLRICH, J. E. 2012. Thrombospondin-1 inhibits osteogenic differentiation of human mesenchymal stem cells through latent TGF-beta activation. *Biochem Biophys Res Commun,* 422**,** 488-93.

BALANI, D., AEBERLI, D., HOFSTETTER, W. & SEITZ, M. 2013. Interleukin-17A stimulates granulocyte-macrophage colony-stimulating factor release by murine osteoblasts in the presence of 1,25-dihydroxyvitamin D(3) and inhibits murine osteoclast development in vitro. *Arthritis Rheum,* 65**,** 436-46.

BAR-SHAVIT, Z. 2007. The osteoclast: a multinucleated, hematopoietic-origin, bone-resorbing osteoimmune cell. *J Cell Biochem,* 102**,** 1130-9.

BARRESI, V. & TUCCARI, G. 2010. Increased ratio of vascular endothelial growth factor to semaphorin3A is a negative prognostic factor in human meningiomas. *Neuropathology,* 30**,** 537-46.

BEHAR, O., GOLDEN, J. A., MASHIMO, H., SCHOEN, F. J. & FISHMAN, M. C. 1996. Semaphorin III is needed for normal patterning and growth of nerves, bones and heart. *Nature,* 383**,** 525-8.

BERMAN, S. D., CALO, E., LANDMAN, A. S., DANIELIAN, P. S., MILLER, E. S., WEST, J. C., FONHOUE, B. D., CARON, A., BRONSON, R., BOUXSEIN, M. L., MUKHERJEE, S. & LEES, J. A. 2008. Metastatic osteosarcoma induced by inactivation of Rb and p53 in the osteoblast lineage. *Proc Natl Acad Sci U S A,* 105**,** 11851-6.

BIELACK, S., CARRLE, D. & CASALI, P. G. 2009. Osteosarcoma: ESMO clinical recommendations for diagnosis, treatment and follow-up. *Ann Oncol,* 20 Suppl 4**,** 137-9.

BIELACK, S. S., HECKER-NOLTING, S., BLATTMANN, C. & KAGER, L. 2016. Advances in the management of osteosarcoma. *F1000Res,* 5**,** 2767.

BIELACK, S. S., KEMPF-BIELACK, B., DELLING, G., EXNER, G. U., FLEGE, S., HELMKE, K., KOTZ, R., SALZER-KUNTSCHIK, M., WERNER, M., WINKELMANN, W., ZOUBEK, A., JURGENS, H. & WINKLER, K. 2002. Prognostic factors in high-grade osteosarcoma of the extremities or trunk: an analysis of 1,702 patients treated on neoadjuvant cooperative osteosarcoma study group protocols. *J Clin Oncol,* 20**,** 776-90.

BOLLARD, J., MASSOMA, P., VERCHERAT, C., BLANC, M., LEPINASSE, F., GADOT, N., COUDERC, C., PONCET, G., WALTER, T., JOLY, M. O., HERVIEU, V., SCOAZEC, J. Y. & ROCHE, C. 2015. The axon guidance molecule semaphorin 3F is a negative regulator of tumor progression and proliferation in ileal neuroendocrine tumors. *Oncotarget,* 6**,** 36731-45.

BORO, A., ARLT, M. J., LENGNICK, H., ROBL, B., HUSMANN, M., BERTZ, J., BORN, W. & FUCHS, B. 2015. Prognostic value and in vitro biological

relevance of Neuropilin 1 and Neuropilin 2 in osteosarcoma. *Am J Transl Res,* 7**,** 640-53.

BOTTER, S. M., NERI, D. & FUCHS, B. 2014. Recent advances in osteosarcoma. *Curr Opin Pharmacol,* 16**,** 15-23.

BOUGEARD, G., RENAUX-PETEL, M., FLAMAN, J. M., CHARBONNIER, C., FERMEY, P., BELOTTI, M., GAUTHIER-VILLARS, M., STOPPA-LYONNET, D., CONSOLINO, E., BRUGIERES, L., CARON, O., BENUSIGLIO, P. R., BRESSAC-DE PAILLERETS, B., BONADONA, V., BONAITI-PELLIE, C., TINAT, J., BAERT-DESURMONT, S. & FREBOURG, T. 2015. Revisiting Li-Fraumeni Syndrome From TP53 Mutation Carriers. *J Clin Oncol,* 33**,** 2345-52.

BOUSQUET, M., NOIROT, C., ACCADBLED, F., SALES DE GAUZY, J., CASTEX, M. P., BROUSSET, P. & GOMEZ-BROUCHET, A. 2016. Whole-exome sequencing in osteosarcoma reveals important heterogeneity of genetic alterations. *Ann Oncol,* 27**,** 738-44.

BROWN, C. B., FEINER, L., LU, M. M., LI, J., MA, X., WEBBER, A. L., JIA, L., RAPER, J. A. & EPSTEIN, J. A. 2001. PlexinA2 and semaphorin signaling during cardiac neural crest development. *Development,* 128**,** 3071-80.

BROWN, H. K., SCHIAVONE, K., GOUIN, F., HEYMANN, M. F. & HEYMANN, D. 2018. Biology of Bone Sarcomas and New Therapeutic Developments. *Calcif Tissue Int,* 102**,** 174-195.

CAMPBELL, G. M. & SOPHOCLEOUS, A. 2014. Quantitative analysis of bone and soft tissue by micro-computed tomography: applications to ex vivo and in vivo studies. *Bonekey Rep,* 3**,** 564.

CANCERRESEARCHUK. 2018. *Bone sarcoma incidence statistics* [Online]. Available: https://www.cancerresearchuk.org/health-professional/cancer-statistics/statistics-by-cancer-type/bone-sarcoma/incidence#heading-Zero [Accessed 05-10-2018 2018].

CARRLE, D. & BIELACK, S. S. 2006. Current strategies of chemotherapy in osteosarcoma. *Int Orthop,* 30**,** 445-51.

CASAZZA, A., FINISGUERRA, V., CAPPARUCCIA, L., CAMPERI, A., SWIERCZ, J. M., RIZZOLIO, S., ROLNY, C., CHRISTENSEN, C., BERTOTTI, A., SAROTTO, I., RISIO, M., TRUSOLINO, L., WEITZ, J., SCHNEIDER, M., MAZZONE, M., COMOGLIO, P. M. & TAMAGNONE, L. 2010. Sema3E-Plexin D1 signaling drives human cancer cell invasiveness and metastatic spreading in mice. *J Clin Invest,* 120**,** 2684-98.

CASAZZA, A., FU, X., JOHANSSON, I., CAPPARUCCIA, L., ANDERSSON, F., GIUSTACCHINI, A., SQUADRITO, M. L., VENNERI, M. A., MAZZONE, M., LARSSON, E., CARMELIET, P., DE PALMA, M., NALDINI, L., TAMAGNONE, L. & ROLNY, C. 2011. Systemic and targeted delivery of semaphorin 3A inhibits tumor angiogenesis and progression in mouse tumor models. *Arterioscler Thromb Vasc Biol,* 31**,** 741-9.

CASAZZA, A., KIGEL, B., MAIONE, F., CAPPARUCCIA, L., KESSLER, O., GIRAUDO, E., MAZZONE, M., NEUFELD, G. & TAMAGNONE, L. 2012. Tumour growth inhibition and anti-metastatic activity of a mutated furin-resistant Semaphorin 3E isoform. *EMBO Mol Med,* 4**,** 234-50.

CASTRO-RIVERA, E., RAN, S., BREKKEN, R. A. & MINNA, J. D. 2008. Semaphorin 3B inhibits the phosphatidylinositol 3-kinase/Akt pathway through neuropilin-1 in lung and breast cancer cells. *Cancer Res,* 68**,** 8295-303.

CASTRO-RIVERA, E., RAN, S., THORPE, P. & MINNA, J. D. 2004. Semaphorin 3B (SEMA3B) induces apoptosis in lung and breast cancer, whereas VEGF165 antagonizes this effect. *Proc Natl Acad Sci U S A,* 101**,** 11432-7.

CATALANO, A., CAPRARI, P., MORETTI, S., FARONATO, M., TAMAGNONE, L. & PROCOPIO, A. 2006. Semaphorin-3A is expressed by tumor cells and alters T-cell signal transduction and function. *Blood,* 107**,** 3321-9.

CATALANO, A., CAPRARI, P., RODILOSSI, S., BETTA, P., CASTELLUCCI, M., CASAZZA, A., TAMAGNONE, L. & PROCOPIO, A. 2004. Cross-talk between vascular endothelial growth factor and semaphorin-3A pathway in the regulation of normal and malignant mesothelial cell proliferation. *Faseb j,* 18**,** 358-60.

CAWTHORN, W. P., BREE, A. J., YAO, Y., DU, B., HEMATI, N., MARTINEZ-SANTIBANEZ, G. & MACDOUGALD, O. A. 2012. Wnt6, Wnt10a and Wnt10b inhibit adipogenesis and stimulate osteoblastogenesis through a beta-catenin-dependent mechanism. *Bone,* 50**,** 477-89.

CHAKRABORTY, G., KUMAR, S., MISHRA, R., PATIL, T. V. & KUNDU, G. C. 2012. Semaphorin 3A suppresses tumor growth and metastasis in mice melanoma model. *PLoS One,* 7**,** e33633.

CHEDOTAL, A., DEL RIO, J. A., RUIZ, M., HE, Z., BORRELL, V., DE CASTRO, F., EZAN, F., GOODMAN, C. S., TESSIER-LAVIGNE, M., SOTELO, C. & SORIANO, E. 1998. Semaphorins III and IV repel hippocampal axons via two distinct receptors. *Development,* 125**,** 4313-23.

CHELLAIAH, M. A., KIZER, N., BISWAS, R., ALVAREZ, U., STRAUSS-SCHOENBERGER, J., RIFAS, L., RITTLING, S. R., DENHARDT, D. T. & HRUSKA, K. A. 2003. Osteopontin deficiency produces osteoclast dysfunction due to reduced CD44 surface expression. *Mol Biol Cell,* 14**,** 173-89.

CHEN, H., CHEDOTAL, A., HE, Z., GOODMAN, C. S. & TESSIER-LAVIGNE, M. 1997. Neuropilin-2, a novel member of the neuropilin family, is a high affinity receptor for the semaphorins Sema E and Sema IV but not Sema III. *Neuron,* 19**,** 547-59.

CHEN, H., XIE, G. H., WANG, W. W., YUAN, X. L., XING, W. M., LIU, H. J., CHEN, J., DOU, M. & SHEN, L. S. 2015. Epigenetically downregulated Semaphorin 3E contributes to gastric cancer. *Oncotarget,* 6**,** 20449-65.

CIONI, J. M., TELLEY, L., SAYWELL, V., CADILHAC, C., JOURDAN, C., HUBER, A. B., HUANG, J. Z., JAHANNAULT-TALIGNANI, C. & ANGO, F. 2013. SEMA3A signaling controls layer-specific interneuron branching in the cerebellum. *Curr Biol,* 23**,** 850-61.

CLARKE, B. 2008. Normal bone anatomy and physiology. *Clin J Am Soc Nephrol,* 3 Suppl 3**,** S131-9.

COULTAS, L., CHAWENGSAKSOPHAK, K. & ROSSANT, J. 2005. Endothelial cells and VEGF in vascular development. *Nature,* 438**,** 937-45.

DANG, H., WU, W., WANG, B., CUI, C., NIU, J., CHEN, J., CHEN, Z. & LIU, Y. 2017. CXCL5 Plays a Promoting Role in Osteosarcoma Cell Migration and Invasion in Autocrine- and Paracrine-Dependent Manners. *Oncol Res,* 25**,** 177-186.

DAY, T. F., GUO, X., GARRETT-BEAL, L. & YANG, Y. 2005. Wnt/beta-catenin signaling in mesenchymal progenitors controls osteoblast and chondrocyte differentiation during vertebrate skeletogenesis. *Dev Cell,* 8**,** 739-50.

DE RIDDER, D., MARINO, S., BISHOP, R. T., RENEMA, N., CHENU, C., HEYMANN, D. & IDRIS, A. I. 2018. Bidirectional regulation of bone formation by exogenous and osteosarcoma-derived Sema3A. *Sci Rep,* 8**,** 6877.

DEGENHARDT, K., SINGH, M. K., AGHAJANIAN, H., MASSERA, D., WANG, Q., LI, J., LI, L., CHOI, C., YZAGUIRRE, A. D., FRANCEY, L. J., GALLANT, E., KRANTZ, I. D., GRUBER, P. J. & EPSTEIN, J. A. 2013. Semaphorin 3d signaling defects are associated with anomalous pulmonary venous connections. *Nat Med,* 19**,** 760-5.

DIARRA, D., STOLINA, M., POLZER, K., ZWERINA, J., OMINSKY, M. S., DWYER, D., KORB, A., SMOLEN, J., HOFFMANN, M., SCHEINECKER, C., VAN DER HEIDE, D., LANDEWE, R., LACEY, D., RICHARDS, W. G. & SCHETT, G. 2007. Dickkopf-1 is a master regulator of joint remodeling. *Nat Med,* 13**,** 156-63.

DING, J. B., OH, W. J., SABATINI, B. L. & GU, C. 2011. Semaphorin 3E-Plexin-D1 signaling controls pathway-specific synapse formation in the striatum. *Nat Neurosci,* 15**,** 215-23.

DOCI, C. L., MIKELIS, C. M., LIONAKIS, M. S., MOLINOLO, A. A. & GUTKIND, J. S. 2015. Genetic Identification of SEMA3F as an Antilymphangiogenic Metastasis Suppressor Gene in Head and Neck Squamous Carcinoma. *Cancer Res,* 75**,** 2937-48.

DONTCHEV, V. D. & LETOURNEAU, P. C. 2002. Nerve growth factor and semaphorin 3A signaling pathways interact in regulating sensory neuronal growth cone motility. *J Neurosci,* 22**,** 6659-69.

DUCY, P. 2000. Cbfa1: a molecular switch in osteoblast biology. *Dev Dyn,* 219**,** 461-71.

EASTELL, R., REID, D. M., COMPSTON, J., COOPER, C., FOGELMAN, I., FRANCIS, R. M., HOSKING, D. J., PURDIE, D. W., RALSTON, S. H., REEVE, J., RUSSELL, R. G., STEVENSON, J. C. & TORGERSON, D. J. 1998. A UK Consensus Group on management of glucocorticoid-induced osteoporosis: an update. *J Intern Med,* 244**,** 271-92.

EICKHOLT, B. J., WALSH, F. S. & DOHERTY, P. 2002. An inactive pool of GSK-3 at the leading edge of growth cones is implicated in Semaphorin 3A signaling. *J Cell Biol,* 157**,** 211-7.

ENG, C., LI, F. P., ABRAMSON, D. H., ELLSWORTH, R. M., WONG, F. L., GOLDMAN, M. B., SEDDON, J., TARBELL, N. & BOICE, J. D., JR. 1993. Mortality from second tumors among long-term survivors of retinoblastoma. *J Natl Cancer Inst,* 85**,** 1121-8.

ENTZ-WERLE, N., CHOQUET, P., NEUVILLE, A., KUCHLER-BOPP, S., CLAUSS, F., DANSE, J. M., SIMO-NOUMBISSIE, P., GUERIN, E., GAUB, M. P., FREUND, J. N., BOEHM, N., CONSTANTINESCO, A., LUTZ, P., GUENOT, D. & PERRIN-SCHMITT, F. 2010. Targeted apc;twist double-mutant mice: a new model of spontaneous osteosarcoma that mimics the human disease. *Transl Oncol,* 3**,** 344-53.

ERBEN, R. G. & GLOSMANN, M. 2012. Histomorphometry in rodents. *Methods Mol Biol,* 816**,** 279-303.

ESMO 2014. Bone sarcomas: ESMO Clinical Practice Guidelines for diagnosis, treatment and follow-up. *Ann Oncol,* 25 Suppl 3**,** iii113-23.

FALK, J., BECHARA, A., FIORE, R., NAWABI, H., ZHOU, H., HOYO-BECERRA, C., BOZON, M., ROUGON, G., GRUMET, M., PUSCHEL, A. W., SANES, J. R. & CASTELLANI, V. 2005. Dual functional activity of

semaphorin 3B is required for positioning the anterior commissure. *Neuron,* 48**,** 63-75.

FEINER, L., KOPPEL, A. M., KOBAYASHI, H. & RAPER, J. A. 1997. Secreted chick semaphorins bind recombinant neuropilin with similar affinities but bind different subsets of neurons in situ. *Neuron,* 19**,** 539-45.

FEINER, L., WEBBER, A. L., BROWN, C. B., LU, M. M., JIA, L., FEINSTEIN, P., MOMBAERTS, P., EPSTEIN, J. A. & RAPER, J. A. 2001. Targeted disruption of semaphorin 3C leads to persistent truncus arteriosus and aortic arch interruption. *Development,* 128**,** 3061-70.

FENSTERMAKER, V., CHEN, Y., GHOSH, A. & YUSTE, R. 2004. Regulation of dendritic length and branching by semaphorin 3A. *J Neurobiol,* 58**,** 403-12.

FLETCHER, C. D. M. 2013. *WHO classification of Tumours of Soft Tissue and Bone,* Lyon, IARC.

FLORES, R. J., KELLY, A. J., LI, Y., NAKKA, M., BARKAUSKAS, D. A., KRAILO, M., WANG, L. L., PERLAKY, L., LAU, C. C., HICKS, M. J. & MAN, T. K. 2017. A novel prognostic model for osteosarcoma using circulating CXCL10 and FLT3LG. *Cancer,* 123**,** 144-154.

FOLEY, K., RUCKI, A. A., XIAO, Q., ZHOU, D., LEUBNER, A., MO, G., KLEPONIS, J., WU, A. A., SHARMA, R., JIANG, Q., ANDERS, R. A., IACOBUZIO-DONAHUE, C. A., HAJJAR, K. A., MAITRA, A., JAFFEE, E. M. & ZHENG, L. 2015. Semaphorin 3D autocrine signaling mediates the metastatic role of annexin A2 in pancreatic cancer. *Sci Signal,* 8**,** ra77.

FRITZSCHE, H., SCHASER, K. D. & HOFBAUER, C. 2017. [Benign tumours and tumour-like lesions of the bone : General treatment principles]. *Orthopade,* 46**,** 484-497.

FUKUDA, T., TAKEDA, S., XU, R., OCHI, H., SUNAMURA, S., SATO, T., SHIBATA, S., YOSHIDA, Y., GU, Z., KIMURA, A., MA, C., XU, C., BANDO, W., FUJITA, K., SHINOMIYA, K., HIRAI, T., ASOU, Y., ENOMOTO, M., OKANO, H., OKAWA, A. & ITOH, H. 2013. Sema3A regulates bone-mass accrual through sensory innervations. *Nature,* 497**,** 490-3.

FUTAMURA, M., KAMINO, H., MIYAMOTO, Y., KITAMURA, N., NAKAMURA, Y., OHNISHI, S., MASUDA, Y. & ARAKAWA, H. 2007. Possible role of semaphorin 3F, a candidate tumor suppressor gene at 3p21.3, in p53-regulated tumor angiogenesis suppression. *Cancer Res,* 67**,** 1451-60.

GALSON, D. L. & ROODMAN, G. D. 2014. Pathobiology of Paget's Disease of Bone. *J Bone Metab,* 21**,** 85-98.

GEBACK, T., SCHULZ, M. M., KOUMOUTSAKOS, P. & DETMAR, M. 2009. TScratch: a novel and simple software tool for automated analysis of monolayer wound healing assays. *Biotechniques,* 46**,** 265-74.

GELLER, D. S. & GORLICK, R. 2010. Osteosarcoma: a review of diagnosis, management, and treatment strategies. *Clin Adv Hematol Oncol,* 8**,** 705-18.

GERETTI, E., SHIMIZU, A. & KLAGSBRUN, M. 2008. Neuropilin structure governs VEGF and semaphorin binding and regulates angiogenesis. *Angiogenesis,* 11**,** 31-9.

GERHARDT, H., RUHRBERG, C., ABRAMSSON, A., FUJISAWA, H., SHIMA, D. & BETSHOLTZ, C. 2004. Neuropilin-1 is required for endothelial tip cell guidance in the developing central nervous system. *Dev Dyn,* 231**,** 503-9.

GIANFERANTE, D. M., MIRABELLO, L. & SAVAGE, S. A. 2017. Germline and somatic genetics of osteosarcoma - connecting aetiology, biology and therapy. *Nat Rev Endocrinol,* 13**,** 480-491.

GIGER, R. J., CLOUTIER, J. F., SAHAY, A., PRINJHA, R. K., LEVENGOOD, D. V., MOORE, S. E., PICKERING, S., SIMMONS, D., RASTAN, S., WALSH, F. S., KOLODKIN, A. L., GINTY, D. D. & GEPPERT, M. 2000. Neuropilin-2 is required in vivo for selective axon guidance responses to secreted semaphorins. *Neuron,* 25**,** 29-41.

GOLDRING, M. B. 2012. Chondrogenesis, chondrocyte differentiation, and articular cartilage metabolism in health and osteoarthritis. *Ther Adv Musculoskelet Dis,* 4**,** 269-85.

GOLDSTEIN, S. D., TRUCCO, M., BAUTISTA GUZMAN, W., HAYASHI, M. & LOEB, D. M. 2016. A monoclonal antibody against the Wnt signaling inhibitor dickkopf-1 inhibits osteosarcoma metastasis in a preclinical model. *Oncotarget,* 7**,** 21114-23.

GOMEZ, C., BURT-PICHAT, B., MALLEIN-GERIN, F., MERLE, B., DELMAS, P. D., SKERRY, T. M., VICO, L., MALAVAL, L. & CHENU, C. 2005. Expression of Semaphorin-3A and its receptors in endochondral ossification: potential role in skeletal development and innervation. *Dev Dyn,* 234**,** 393-403.

GRIGORIADIS, A. E., SCHELLANDER, K., WANG, Z. Q. & WAGNER, E. F. 1993. Osteoblasts are target cells for transformation in c-fos transgenic mice. *J Cell Biol,* 122**,** 685-701.

GU, C., RODRIGUEZ, E. R., REIMERT, D. V., SHU, T., FRITZSCH, B., RICHARDS, L. J., KOLODKIN, A. L. & GINTY, D. D. 2003. Neuropilin-1 conveys semaphorin and VEGF signaling during neural and cardiovascular development. *Dev Cell,* 5**,** 45-57.

GU, C., YOSHIDA, Y., LIVET, J., REIMERT, D. V., MANN, F., MERTE, J., HENDERSON, C. E., JESSELL, T. M., KOLODKIN, A. L. & GINTY, D. D. 2005. Semaphorin 3E and plexin-D1 control vascular pattern independently of neuropilins. *Science,* 307**,** 265-8.

GUO, H. F. & VANDER KOOI, C. W. 2015. Neuropilin Function as an Essential Cell Surface Receptor. *J Biol Chem.*

HADJIDAKIS, D. J. & ANDROULAKIS, II 2006. Bone remodeling. *Ann N Y Acad Sci,* 1092**,** 385-96.

HAKIM, D. N., PELLY, T., KULENDRAN, M. & CARIS, J. A. 2015. Benign tumours of the bone: A review. *J Bone Oncol,* 4**,** 37-41.

HANDA, A., TOKUNAGA, T., TSUCHIDA, T., LEE, Y. H., KIJIMA, H., YAMAZAKI, H., UEYAMA, Y., FUKUDA, H. & NAKAMURA, M. 2000. Neuropilin-2 expression affects the increased vascularization and is a prognostic factor in osteosarcoma. *Int J Oncol,* 17**,** 291-5.

HAYASHI, M., KAMIYA, Y., ITOH, H., HIGASHI, T., MIYAZAKI, T., FUNAKOSHI, K., YAMASHITA, N., GOSHIMA, Y., ANDOH, T., YAMADA, Y. & GOTO, T. 2011. Intrathecally administered Sema3A protein attenuates neuropathic pain behavior in rats with chronic constriction injury of the sciatic nerve. *Neurosci Res,* 69**,** 17-24.

HAYASHI, M., NAKASHIMA, T., TANIGUCHI, M., KODAMA, T., KUMANOGOH, A. & TAKAYANAGI, H. 2012. Osteoprotection by semaphorin 3A. *Nature,* 485**,** 69-74.

HERMAN, J. G. & MEADOWS, G. G. 2007. Increased class 3 semaphorin expression modulates the invasive and adhesive properties of prostate cancer cells. *Int J Oncol,* 30**,** 1231-8.

HEYMANN, D., ORY, B., BLANCHARD, F., HEYMANN, M. F., COIPEAU, P., CHARRIER, C., COUILLAUD, S., THIERY, J. P., GOUIN, F. & REDINI, F.

2005. Enhanced tumor regression and tissue repair when zoledronic acid is combined with ifosfamide in rat osteosarcoma. *Bone,* 37**,** 74-86.

HEYMANN, M. F., BROWN, H. K. & HEYMANN, D. 2016. Drugs in early clinical development for the treatment of osteosarcoma. *Expert Opin Investig Drugs,* 25**,** 1265-1280.

HOLM, E., GLEBERZON, J. S., LIAO, Y., SORENSEN, E. S., BEIER, F., HUNTER, G. K. & GOLDBERG, H. A. 2014. Osteopontin mediates mineralization and not osteogenic cell development in vitro. *Biochem J,* 464**,** 355-64.

HOU, S. T., NILCHI, L., LI, X., GANGARAJU, S., JIANG, S. X., AYLSWORTH, A., MONETTE, R. & SLINN, J. 2015. Semaphorin3A elevates vascular permeability and contributes to cerebral ischemia-induced brain damage. *Sci Rep,* 5**,** 7890.

HU, C., WEN, J., GONG, L., CHEN, X., WANG, J., HU, F., ZHOU, Q., LIANG, J., WEI, L., SHEN, Y. & ZHANG, W. 2017. Thrombospondin-1 promotes cell migration, invasion and lung metastasis of osteosarcoma through FAK dependent pathway. *Oncotarget,* 8**,** 75881-75892.

HU, T., YANG, Q., XU, J., ZHANG, Z., HE, N. & DU, Y. 2015. Role of beta-isomerized C-terminal telopeptides (beta-CTx) and total procollagen type 1 amino-terminal propeptide (tP1NP) as osteosarcoma biomarkers. *Int J Clin Exp Med,* 8**,** 890-6.

HU, Z. Q., ZHOU, S. L., ZHOU, Z. J., LUO, C. B., CHEN, E. B., ZHAN, H., WANG, P. C., DAI, Z., ZHOU, J., FAN, J. & HUANG, X. W. 2016. Overexpression of semaphorin 3A promotes tumor progression and predicts poor prognosis in hepatocellular carcinoma after curative resection. *Oncotarget,* 7**,** 51733-51746.

HUANG, C., WANG, Y., HUANG, J. H. & LIU, W. 2017. Sema3A drastically suppresses tumor growth in oral cancer Xenograft model of mice. *BMC Pharmacol Toxicol,* 18**,** 55.

HUGHES, A., KLEINE-ALBERS, J., HELFRICH, M. H., RALSTON, S. H. & ROGERS, M. J. 2012. A class III semaphorin (Sema3e) inhibits mouse osteoblast migration and decreases osteoclast formation in vitro. *Calcif Tissue Int,* 90**,** 151-62.

IDRIS, A. I. 2012. Analysis of signalling pathways by western blotting and immunoprecipitation. *Methods Mol Biol,* 816**,** 223-32.

IEDA, M., KANAZAWA, H., KIMURA, K., HATTORI, F., IEDA, Y., TANIGUCHI, M., LEE, J. K., MATSUMURA, K., TOMITA, Y., MIYOSHI, S., SHIMODA, K., MAKINO, S., SANO, M., KODAMA, I., OGAWA, S. & FUKUDA, K. 2007. Sema3a maintains normal heart rhythm through sympathetic innervation patterning. *Nat Med,* 13**,** 604-12.

IIDA-KLEIN, A., LU, S. S., KAPADIA, R., BURKHART, M., MORENO, A., DEMPSTER, D. W. & LINDSAY, R. 2005. Short-term continuous infusion of human parathyroid hormone 1-34 fragment is catabolic with decreased trabecular connectivity density accompanied by hypercalcemia in C57BL/J6 mice. *J Endocrinol,* 186**,** 549-57.

ISAKOFF, M. S., BIELACK, S. S., MELTZER, P. & GORLICK, R. 2015. Osteosarcoma: Current Treatment and a Collaborative Pathway to Success. *J Clin Oncol,* 33**,** 3029-35.

J.FAVUS, M. 2006. *Primer on the Metabolic Bone Diseases and Disorders of MineralMetabolism (Fifth Edition).* The American Society for Bone and Mineral Research.

JACQUES, C., RENEMA, N., LEZOT, F., ORY, B., WALKLEY, C. R., GRIGORIADIS, A. E. & HEYMANN, D. 2018. Small animal models for the study of bone sarcoma pathogenesis:characteristics, therapeutic interests and limitations. *J Bone Oncol,* 12**,** 7-13.

JAIN, D., JAIN, V. K., VASISHTA, R. K., RANJAN, P. & KUMAR, Y. 2008. Adamantinoma: a clinicopathological review and update. *Diagn Pathol,* 3**,** 8.

JI, T., GUO, Y., KIM, K., MCQUEEN, P., GHAFFAR, S., CHRIST, A., LIN, C., ESKANDER, R., ZI, X. & HOANG, B. H. 2015. Neuropilin-2 expression is inhibited by secreted Wnt antagonists and its down-regulation is associated with reduced tumor growth and metastasis in osteosarcoma. *Mol Cancer,* 14**,** 86.

JONES, E. A., YUAN, L., BREANT, C., WATTS, R. J. & EICHMANN, A. 2008. Separating genetic and hemodynamic defects in neuropilin 1 knockout embryos. *Development,* 135**,** 2479-88.

JOSEPH, D., HO, S. M. & SYED, V. 2010. Hormonal regulation and distinct functions of semaphorin-3B and semaphorin-3F in ovarian cancer. *Mol Cancer Ther,* 9**,** 499-509.

KARNER, C. M. & LONG, F. 2017. Wnt signaling and cellular metabolism in osteoblasts. *Cell Mol Life Sci,* 74**,** 1649-1657.

KARPANEN, T., HECKMAN, C. A., KESKITALO, S., JELTSCH, M., OLLILA, H., NEUFELD, G., TAMAGNONE, L. & ALITALO, K. 2006. Functional interaction of VEGF-C and VEGF-D with neuropilin receptors. *Faseb j,* 20**,** 1462-72.

KARSENTY, G. & WAGNER, E. F. 2002. Reaching a genetic and molecular understanding of skeletal development. *Dev Cell,* 2**,** 389-406.

KATAGIRI, T. & TAKAHASHI, N. 2002. Regulatory mechanisms of osteoblast and osteoclast differentiation. *Oral Dis,* 8**,** 147-59.

KAWASAKI, T., KITSUKAWA, T., BEKKU, Y., MATSUDA, Y., SANBO, M., YAGI, T. & FUJISAWA, H. 1999. A requirement for neuropilin-1 in embryonic vessel formation. *Development,* 126**,** 4895-902.

KEMPF-BIELACK, B., BIELACK, S. S., JURGENS, H., BRANSCHEID, D., BERDEL, W. E., EXNER, G. U., GOBEL, U., HELMKE, K., JUNDT, G., KABISCH, H., KEVRIC, M., KLINGEBIEL, T., KOTZ, R., MAAS, R., SCHWARZ, R., SEMIK, M., TREUNER, J., ZOUBEK, A. & WINKLER, K. 2005. Osteosarcoma relapse after combined modality therapy: an analysis of unselected patients in the Cooperative Osteosarcoma Study Group (COSS). *J Clin Oncol,* 23**,** 559-68.

KENKRE, J. S. & BASSETT, J. 2018. The bone remodelling cycle. *Ann Clin Biochem,* 55**,** 308-327.

KESSLER, O., SHRAGA-HELED, N., LANGE, T., GUTMANN-RAVIV, N., SABO, E., BARUCH, L., MACHLUF, M. & NEUFELD, G. 2004. Semaphorin-3F is an inhibitor of tumor angiogenesis. *Cancer Res,* 64**,** 1008-15.

KITSUKAWA, T., SHIMIZU, M., SANBO, M., HIRATA, T., TANIGUCHI, M., BEKKU, Y., YAGI, T. & FUJISAWA, H. 1997. Neuropilin-semaphorin III/D-mediated chemorepulsive signals play a crucial role in peripheral nerve projection in mice. *Neuron,* 19**,** 995-1005.

KLEIN, M. J. & SIEGAL, G. P. 2006. Osteosarcoma: anatomic and histologic variants. *Am J Clin Pathol,* 125**,** 555-81.

KLEIN-NULEND, J., NIJWEIDE, P. J. & BURGER, E. H. 2003. Osteocyte and bone structure. *Curr Osteoporos Rep,* 1**,** 5-10.

KLOSTERMANN, A., LOHRUM, M., ADAMS, R. H. & PUSCHEL, A. W. 1998. The chemorepulsive activity of the axonal guidance signal semaphorin D requires dimerization. *J Biol Chem,* 273**,** 7326-31.

KOLODKIN, A. L., LEVENGOOD, D. V., ROWE, E. G., TAI, Y. T., GIGER, R. J. & GINTY, D. D. 1997. Neuropilin is a semaphorin III receptor. *Cell,* 90**,** 753-62.

KOLODKIN, A. L., MATTHES, D. J. & GOODMAN, C. S. 1993. The semaphorin genes encode a family of transmembrane and secreted growth cone guidance molecules. *Cell,* 75**,** 1389-99.

KOMORI, T. 2018. Runx2, an inducer of osteoblast and chondrocyte differentiation. *Histochem Cell Biol*.

KRISHNAN, V., BRYANT, H. U. & MACDOUGALD, O. A. 2006. Regulation of bone mass by Wnt signaling. *J Clin Invest,* 116**,** 1202-9.

KRUGER, R. P., AURANDT, J. & GUAN, K. L. 2005. Semaphorins command cells to move. *Nat Rev Mol Cell Biol,* 6**,** 789-800.

KUMANOGOH, A. & KIKUTANI, H. 2013. Immunological functions of the neuropilins and plexins as receptors for semaphorins. *Nat Rev Immunol,* 13**,** 802-14.

LABRINIDIS, A., HAY, S., LIAPIS, V., FINDLAY, D. M. & EVDOKIOU, A. 2010. Zoledronic acid protects against osteosarcoma-induced bone destruction but lacks efficacy against pulmonary metastases in a syngeneic rat model. *Int J Cancer,* 127**,** 345-54.

LAMOUREUX, F., BAUD'HUIN, M., RODRIGUEZ CALLEJA, L., JACQUES, C., BERREUR, M., REDINI, F., LECANDA, F., BRADNER, J. E., HEYMANN, D. & ORY, B. 2014. Selective inhibition of BET bromodomain epigenetic signalling interferes with the bone-associated tumour vicious cycle. *Nat Commun,* 5**,** 3511.

LEAN, J. M., FULLER, K. & CHAMBERS, T. J. 2001. FLT3 ligand can substitute for macrophage colony-stimulating factor in support of osteoclast differentiation and function. *Blood,* 98**,** 2707-13.

LEE, E. J., SONG, D. H., KIM, Y. J., CHOI, B., CHUNG, Y. H., KIM, S. M., KOH, J. M., YOON, S. Y., SONG, Y., KANG, S. W. & CHANG, E. J. 2014. PTX3 stimulates osteoclastogenesis by increasing osteoblast RANKL production. *J Cell Physiol,* 229**,** 1744-52.

LEE, J., SHIN, Y. J., LEE, K., CHO, H. J., SA, J. K., LEE, S. Y., KIM, S. H., YOON, Y. & NAM, D. H. 2017. Anti-SEMA3A Antibody: A Novel Therapeutic Agent to Suppress GBM Tumor Growth. *Cancer Res Treat*.

LERNER, U. H. 2006. Bone remodeling in post-menopausal osteoporosis. *J Dent Res,* 85**,** 584-95.

LI, Y., YANG, L., HE, S. & HU, J. 2015a. The effect of semaphorin 3A on fracture healing in osteoporotic rats. *J Orthop Sci*.

LI, Y. S., DENG, Z. H., ZENG, C. & LEI, G. H. 2015b. Role of osteopontin in osteosarcoma. *Med Oncol,* 32**,** 449.

LIN, P. P., PANDEY, M. K., JIN, F., RAYMOND, A. K., AKIYAMA, H. & LOZANO, G. 2009. Targeted mutation of p53 and Rb in mesenchymal cells of the limb bud produces sarcomas in mice. *Carcinogenesis,* 30**,** 1789-95.

LIU, F., SHEN, W., QIU, H., HU, X., ZHANG, C. & CHU, T. 2015. Prostate cancer cells induce osteoblastic differentiation via semaphorin 3A. *Prostate,* 75**,** 370-80.

LOGAN, J. G., SOPHOCLEOUS, A., MARINO, S., MUIR, M., BRUNTON, V. G. & IDRIS, A. I. 2013. Selective tyrosine kinase inhibition of insulin-like growth factor-1 receptor inhibits human and mouse breast cancer-induced bone cell activity, bone remodeling, and osteolysis. *J Bone Miner Res,* 28**,** 1229-42.

LOHMANN, D. 2010. Retinoblastoma. *Adv Exp Med Biol,* 685**,** 220-7.

LUCHINO, J., HOCINE, M., AMOUREUX, M. C., GIBERT, B., BERNET, A., ROYET, A., TREILLEUX, I., LECINE, P., BORG, J. P., MEHLEN, P., CHAUVET, S. & MANN, F. 2013. Semaphorin 3E suppresses tumor cell death triggered by the plexin D1 dependence receptor in metastatic breast cancers. *Cancer Cell,* 24**,** 673-85.

LUETKE, A., MEYERS, P. A., LEWIS, I. & JUERGENS, H. 2014. Osteosarcoma treatment - where do we stand? A state of the art review. *Cancer Treat Rev,* 40**,** 523-32.

LUO, Y., RAIBLE, D. & RAPER, J. A. 1993. Collapsin: a protein in brain that induces the collapse and paralysis of neuronal growth cones. *Cell,* 75**,** 217-27.

MADEIRA, M. F., QUEIROZ-JUNIOR, C. M., COSTA, G. M., SANTOS, P. C., SILVEIRA, E. M., GARLET, G. P., CISALPINO, P. S., TEIXEIRA, M. M., SILVA, T. A. & SOUZA DDA, G. 2012. MIF induces osteoclast differentiation and contributes to progression of periodontal disease in mice. *Microbes Infect,* 14**,** 198-206.

MAEDA, T., YAMADA, D. & KAWAHARA, K. 2016. Cancer pain relief achieved by disrupting tumor-driven semaphorin 3A signaling in mice. *Neurosci Lett,* 632**,** 147-51.

MAEJIMA, R., TAMAI, K., SHIROKI, T., YOKOYAMA, M., SHIBUYA, R., NAKAMURA, M., YAMAGUCHI, K., ABUE, M., OIKAWA, T., NOGUCHI, T., MIURA, K., FUJIYA, T., SATO, I., IIJIMA, K., SHIMOSEGAWA, T., TANAKA, N. & SATOH, K. 2016. Enhanced expression of semaphorin 3E is involved in the gastric cancer development. *Int J Oncol,* 49**,** 887-94.

MAIONE, F., CAPANO, S., REGANO, D., ZENTILIN, L., GIACCA, M., CASANOVAS, O., BUSSOLINO, F., SERINI, G. & GIRAUDO, E. 2012. Semaphorin 3A overcomes cancer hypoxia and metastatic dissemination induced by antiangiogenic treatment in mice. *J Clin Invest,* 122**,** 1832-48.

MALIK, M. F., YE, L. & JIANG, W. G. 2015. Reduced expression of semaphorin 4D and plexin-B in breast cancer is associated with poorer prognosis and the potential linkage with oestrogen receptor. *Oncol Rep,* 34**,** 1049-57.

MANOLAGAS, S. C. 2000. Birth and death of bone cells: basic regulatory mechanisms and implications for the pathogenesis and treatment of osteoporosis. *Endocr Rev,* 21**,** 115-37.

MARINO, S., LOGAN, J. G., MELLIS, D. & CAPULLI, M. 2014. Generation and culture of osteoclasts. *Bonekey Rep,* 3**,** 570.

MASUDA, T., TANIGUCHI, M., SAKUMA, C., YAMAGISHI, T., UEDA, S., KAWAGUCHI, M. & YAGINUMA, H. 2013. Development of the dorsal ramus of the spinal nerve in the mouse embryo: involvement of semaphorin 3A in dorsal muscle innervation. *Congenit Anom (Kyoto),* 53**,** 122-6.

MATSUDA, I., FUKAYA, M., NAKAO, H., NAKAO, K., MATSUMOTO, H., MORI, K., WATANABE, M. & AIBA, A. 2010. Development of the somatosensory cortex, the cerebellum, and the main olfactory system in Semaphorin 3F knockout mice. *Neurosci Res,* 66**,** 321-9.

MESSERSMITH, E. K., LEONARDO, E. D., SHATZ, C. J., TESSIER-LAVIGNE, M., GOODMAN, C. S. & KOLODKIN, A. L. 1995. Semaphorin III can function as a selective chemorepellent to pattern sensory projections in the spinal cord. *Neuron,* 14**,** 949-59.

MEUNIER, P. J., DELMAS, P. D., EASTELL, R., MCCLUNG, M. R., PAPAPOULOS, S., RIZZOLI, R., SEEMAN, E. & WASNICH, R. D. 1999. Diagnosis and management of osteoporosis in postmenopausal women: clinical guidelines. International Committee for Osteoporosis Clinical Guidelines. *Clin Ther,* 21**,** 1025-44.

MEYERS, P. A. & GORLICK, R. 1997. Osteosarcoma. *Pediatr Clin North Am,* 44**,** 973-89.

MIAO, H. Q., SOKER, S., FEINER, L., ALONSO, J. L., RAPER, J. A. & KLAGSBRUN, M. 1999. Neuropilin-1 mediates collapsin-1/semaphorin III inhibition of endothelial cell motility: functional competition of collapsin-1 and vascular endothelial growth factor-165. *J Cell Biol,* 146**,** 233-42.

MISHRA, R., KUMAR, D., TOMAR, D., CHAKRABORTY, G., KUMAR, S. & KUNDU, G. C. 2015a. The potential of class 3 semaphorins as both targets and therapeutics in cancer. *Expert Opin Ther Targets,* 19**,** 427-42.

MISHRA, R., THORAT, D., SOUNDARARAJAN, G., PRADHAN, S. J., CHAKRABORTY, G., LOHITE, K., KARNIK, S. & KUNDU, G. C. 2015b. Semaphorin 3A upregulates FOXO 3a-dependent MelCAM expression leading to attenuation of breast tumor growth and angiogenesis. *Oncogene,* 34**,** 1584-95.

MIYATO, H., TSUNO, N. H. & KITAYAMA, J. 2012. Semaphorin 3C is involved in the progression of gastric cancer. *Cancer Sci,* 103**,** 1961-6.

MOHSENY, A. B., SZUHAI, K., ROMEO, S., BUDDINGH, E. P., BRIAIRE-DE BRUIJN, I., DE JONG, D., VAN PEL, M., CLETON-JANSEN, A. M. & HOGENDOORN, P. C. 2009. Osteosarcoma originates from mesenchymal stem cells in consequence of aneuploidization and genomic loss of Cdkn2. *J Pathol,* 219**,** 294-305.

MORI, K., BERREUR, M., BLANCHARD, F., CHEVALIER, C., GUISLE-MARSOLLIER, I., MASSON, M., REDINI, F. & HEYMANN, D. 2007. Receptor activator of nuclear factor-kappaB ligand (RANKL) directly modulates the gene expression profile of RANK-positive Saos-2 human osteosarcoma cells. *Oncol Rep,* 18**,** 1365-71.

MORI, K., REDINI, F., GOUIN, F., CHERRIER, B. & HEYMANN, D. 2006. Osteosarcoma: current status of immunotherapy and future trends (Review). *Oncol Rep,* 15**,** 693-700.

MUKOUYAMA, Y. S., GERBER, H. P., FERRARA, N., GU, C. & ANDERSON, D. J. 2005. Peripheral nerve-derived VEGF promotes arterial differentiation via neuropilin 1-mediated positive feedback. *Development,* 132**,** 941-52.

MULLER, M. W., GIESE, N. A., SWIERCZ, J. M., CEYHAN, G. O., ESPOSITO, I., HINZ, U., BUCHLER, P., GIESE, T., BUCHLER, M. W., OFFERMANNS, S. & FRIESS, H. 2007. Association of axon guidance factor semaphorin 3A with poor outcome in pancreatic cancer. *Int J Cancer,* 121**,** 2421-33.

MUNDY, G. R., RODAN, S. B., MAJESKA, R. J., DEMARTINO, S., TRIMMIER, C., MARTIN, T. J. & RODAN, G. A. 1982. Unidirectional migration of osteosarcoma cells with osteoblast characteristics in response to products of bone resorption. *Calcif Tissue Int,* 34**,** 542-6.

MUTSAERS, A. J. & WALKLEY, C. R. 2014. Cells of origin in osteosarcoma: mesenchymal stem cells or osteoblast committed cells? *Bone,* 62**,** 56-63.

NAKASHIMA, K., ZHOU, X., KUNKEL, G., ZHANG, Z., DENG, J. M., BEHRINGER, R. R. & DE CROMBRUGGHE, B. 2002. The novel zinc finger-containing transcription factor osterix is required for osteoblast differentiation and bone formation. *Cell,* 108**,** 17-29.

NARAZAKI, M. & TOSATO, G. 2006. Ligand-induced internalization selects use of common receptor neuropilin-1 by VEGF165 and semaphorin3A. *Blood,* 107**,** 3892-901.

NASARRE, C., KONCINA, E., LABOURDETTE, G., CREMEL, G., ROUSSEL, G., AUNIS, D. & BAGNARD, D. 2009. Neuropilin-2 acts as a modulator of Sema3A-dependent glioma cell migration. *Cell Adh Migr,* 3**,** 383-9.

NASARRE, P., CONSTANTIN, B., ROUHAUD, L., HARNOIS, T., RAYMOND, G., DRABKIN, H. A., BOURMEYSTER, N. & ROCHE, J. 2003. Semaphorin SEMA3F and VEGF have opposing effects on cell attachment and spreading. *Neoplasia,* 5**,** 83-92.

NEUFELD, G. & KESSLER, O. 2008. The semaphorins: versatile regulators of tumour progression and tumour angiogenesis. *Nat Rev Cancer,* 8**,** 632-45.

NEUFELD, G., SABAG, A. D., RABINOVICZ, N. & KESSLER, O. 2012. Semaphorins in angiogenesis and tumor progression. *Cold Spring Harb Perspect Med,* 2**,** a006718.

NEVE, A., CORRADO, A. & CANTATORE, F. P. 2011. Osteoblast physiology in normal and pathological conditions. *Cell Tissue Res,* 343**,** 289-302.

NG, T., RYU, J. R., SOHN, J. H., TAN, T., SONG, H., MING, G. L. & GOH, E. L. 2013. Class 3 semaphorin mediates dendrite growth in adult newborn neurons through Cdk5/FAK pathway. *PLoS One,* 8**,** e65572.

NOBLE, B. S. 2008. The osteocyte lineage. *Arch Biochem Biophys,* 473**,** 106-11.

OHBA, T., CATES, J. M., COLE, H. A., SLOSKY, D. A., HARO, H., ICHIKAWA, J., ANDO, T., SCHWARTZ, H. S. & SCHOENECKER, J. G. 2014. Pleiotropic effects of bisphosphonates on osteosarcoma. *Bone,* 63**,** 110-20.

OZAKI, T., FLEGE, S., KEVRIC, M., LINDNER, N., MAAS, R., DELLING, G., SCHWARZ, R., VON HOCHSTETTER, A. R., SALZER-KUNTSCHIK, M., BERDEL, W. E., JURGENS, H., EXNER, G. U., REICHARDT, P., MAYER-STEINACKER, R., EWERBECK, V., KOTZ, R., WINKELMANN, W. & BIELACK, S. S. 2003. Osteosarcoma of the pelvis: experience of the Cooperative Osteosarcoma Study Group. *J Clin Oncol,* 21**,** 334-41.

OZAKI, T., FLEGE, S., LILJENQVIST, U., HILLMANN, A., DELLING, G., SALZER-KUNTSCHIK, M., JURGENS, H., KOTZ, R., WINKELMANN, W. & BIELACK, S. S. 2002. Osteosarcoma of the spine: experience of the Cooperative Osteosarcoma Study Group. *Cancer,* 94**,** 1069-77.

PAN, H. & BACHELDER, R. E. 2010. Autocrine Semaphorin3A stimulates eukaryotic initiation factor 4E-dependent RhoA translation in breast tumor cells. *Exp Cell Res,* 316**,** 2825-32.

PARKER, M. W., GUO, H. F., LI, X., LINKUGEL, A. D. & VANDER KOOI, C. W. 2012. Function of members of the neuropilin family as essential pleiotropic cell surface receptors. *Biochemistry,* 51**,** 9437-46.

PASCOE, H. G., WANG, Y. & ZHANG, X. 2015. Structural mechanisms of plexin signaling. *Prog Biophys Mol Biol,* 118**,** 161-8.

PASTERKAMP, R. J. 2012. Getting neural circuits into shape with semaphorins. *Nat Rev Neurosci,* 13**,** 605-18.

PETERSE, E. F. P., VAN LEEUWEN, T. N. & CLETON-JANSEN, A. M. 2017. In vitro studies of osteosarcoma: A researcher's perspective of quantity and quality. *J Bone Oncol.*

PIPER, M., PLACHEZ, C., ZALUCKI, O., FOTHERGILL, T., GOUDREAU, G., ERZURUMLU, R., GU, C. & RICHARDS, L. J. 2009. Neuropilin 1-Sema signaling regulates crossing of cingulate pioneering axons during development of the corpus callosum. *Cereb Cortex,* 19 Suppl 1**,** i11-21.

PIPERNO-NEUMANN, S., LE DELEY, M. C., REDINI, F., PACQUEMENT, H., MAREC-BERARD, P., PETIT, P., BRISSE, H., LERVAT, C., GENTET, J. C., ENTZ-WERLE, N., ITALIANO, A., CORRADINI, N., BOMPAS, E., PENEL, N., TABONE, M. D., GOMEZ-BROUCHET, A., GUINEBRETIERE, J. M., MASCARD, E., GOUIN, F., CHEVANCE, A., BONNET, N., BLAY, J. Y. & BRUGIERES, L. 2016. Zoledronate in combination with chemotherapy and surgery to treat osteosarcoma (OS2006): a randomised, multicentre, open-label, phase 3 trial. *Lancet Oncol,* 17**,** 1070-1080.

POTTS, J. T. & GARDELLA, T. J. 2007. Progress, paradox, and potential: parathyroid hormone research over five decades. *Ann N Y Acad Sci,* 1117**,** 196-208.

QIANG, Y. W., BARLOGIE, B., RUDIKOFF, S. & SHAUGHNESSY, J. D., JR. 2008. Dkk1-induced inhibition of Wnt signaling in osteoblast differentiation is an underlying mechanism of bone loss in multiple myeloma. *Bone,* 42**,** 669-80.

RALSTON, S. H., LANGSTON, A. L. & REID, I. R. 2008. Pathogenesis and management of Paget's disease of bone. *Lancet,* 372**,** 155-63.

REIDY, K. J., VILLEGAS, G., TEICHMAN, J., VERON, D., SHEN, W., JIMENEZ, J., THOMAS, D. & TUFRO, A. 2009. Semaphorin3a regulates endothelial cell number and podocyte differentiation during glomerular development. *Development,* 136**,** 3979-89.

RENZI, M. J., FEINER, L., KOPPEL, A. M. & RAPER, J. A. 1999. A dominant negative receptor for specific secreted semaphorins is generated by deleting an extracellular domain from neuropilin-1. *J Neurosci,* 19**,** 7870-80.

REYA, T. & CLEVERS, H. 2005. Wnt signalling in stem cells and cancer. *Nature,* 434**,** 843-50.

RODAN, G. A. & MARTIN, T. J. 2000. Therapeutic approaches to bone diseases. *Science,* 289**,** 1508-14.

ROHM, B., OTTEMEYER, A., LOHRUM, M. & PUSCHEL, A. W. 2000a. Plexin/neuropilin complexes mediate repulsion by the axonal guidance signal semaphorin 3A. *Mech Dev,* 93**,** 95-104.

ROHM, B., RAHIM, B., KLEIBER, B., HOVATTA, I. & PUSCHEL, A. W. 2000b. The semaphorin 3A receptor may directly regulate the activity of small GTPases. *FEBS Lett,* 486**,** 68-72.

ROLNY, C., CAPPARUCCIA, L., CASAZZA, A., MAZZONE, M., VALLARIO, A., CIGNETTI, A., MEDICO, E., CARMELIET, P., COMOGLIO, P. M. & TAMAGNONE, L. 2008. The tumor suppressor semaphorin 3B triggers a

prometastatic program mediated by interleukin 8 and the tumor microenvironment. *J Exp Med,* 205**,** 1155-71.

ROSS, F. P. 2006. M-CSF, c-Fms, and signaling in osteoclasts and their precursors. *Ann N Y Acad Sci,* 1068**,** 110-6.

SABAG, A. D., BODE, J., FINK, D., KIGEL, B., KUGLER, W. & NEUFELD, G. 2012. Semaphorin-3D and semaphorin-3E inhibit the development of tumors from glioblastoma cells implanted in the cortex of the brain. *PLoS One,* 7**,** e42912.

SABAG, A. D., SMOLKIN, T., MUMBLAT, Y., UEFFING, M., KESSLER, O., GLOECKNER, C. J. & NEUFELD, G. 2014. The role of the plexin-A2 receptor in Sema3A and Sema3B signal transduction. *J Cell Sci,* 127**,** 5240-52.

SAHAY, A., MOLLIVER, M. E., GINTY, D. D. & KOLODKIN, A. L. 2003. Semaphorin 3F is critical for development of limbic system circuitry and is required in neurons for selective CNS axon guidance events. *J Neurosci,* 23**,** 6671-80.

SAKURAI, A., DOCI, C. L. & GUTKIND, J. S. 2012. Semaphorin signaling in angiogenesis, lymphangiogenesis and cancer. *Cell Res,* 22**,** 23-32.

SANTACRUZ. *How the Synergistic Activation Mediator (SAM) Transcription Activation System works* [Online]. Santa Cruz website. Available: https://www.scbt.com/scbt/product/sema3a-crispr-knockout-and-activation-products-h?requestFrom=search [Accessed 7-10-2018 2018].

SCHWARZ, Q., GU, C., FUJISAWA, H., SABELKO, K., GERTSENSTEIN, M., NAGY, A., TANIGUCHI, M., KOLODKIN, A. L., GINTY, D. D., SHIMA, D. T. & RUHRBERG, C. 2004. Vascular endothelial growth factor controls neuronal migration and cooperates with Sema3A to pattern distinct compartments of the facial nerve. *Genes Dev,* 18**,** 2822-34.

SCHWARZ, Q., WAIMEY, K. E., GOLDING, M., TAKAMATSU, H., KUMANOGOH, A., FUJISAWA, H., CHENG, H. J. & RUHRBERG, C. 2008. Plexin A3 and plexin A4 convey semaphorin signals during facial nerve development. *Dev Biol,* 324**,** 1-9.

SHARMA, A., VERHAAGEN, J. & HARVEY, A. R. 2012. Receptor complexes for each of the Class 3 Semaphorins. *Front Cell Neurosci,* 6**,** 28.

SHEN, W. W., CHEN, W. G., LIU, F. Z., HU, X., WANG, H. K., ZHANG, Y. & CHU, T. W. 2015. Breast cancer cells promote osteoblastic differentiation via Sema 3A signaling pathway in vitro. *Int J Clin Exp Pathol,* 8**,** 1584-93.

SHIFLETT, M. W., GAVIN, M. & TRAN, T. S. 2015. Altered hippocampal-dependent memory and motor function in neuropilin 2-deficient mice. *Transl Psychiatry,* 5**,** e521.

SINGER, F. R. 2015. Paget's disease of bone-genetic and environmental factors. *Nat Rev Endocrinol,* 11**,** 662-71.

SMOLEN, J. S., ALETAHA, D., BARTON, A., BURMESTER, G. R., EMERY, P., FIRESTEIN, G. S., KAVANAUGH, A., MCINNES, I. B., SOLOMON, D. H., STRAND, V. & YAMAMOTO, K. 2018. Rheumatoid arthritis. *Nat Rev Dis Primers,* 4**,** 18001.

SOCIETY, A. C. 2018. *Key Statistics for Osteosarcoma* [Online]. [Accessed 6-9-2018 2018].

SOKER, S., TAKASHIMA, S., MIAO, H. Q., NEUFELD, G. & KLAGSBRUN, M. 1998. Neuropilin-1 is expressed by endothelial and tumor cells as an isoform-specific receptor for vascular endothelial growth factor. *Cell,* 92**,** 735-45.

STILLER, C. A. 2007. International patterns of cancer incidence in adolescents. *Cancer Treat Rev,* 33**,** 631-45.

STILLER, C. A., BIELACK, S. S., JUNDT, G. & STELIAROVA-FOUCHER, E. 2006. Bone tumours in European children and adolescents, 1978-1997. Report from the Automated Childhood Cancer Information System project. *Eur J Cancer,* 42**,** 2124-35.

SUN, J., WEI, X., WANG, Z., LIU, Y., LU, J., LU, Y., CUI, M., ZHANG, X. & LI, F. 2018. Inflammatory milieu cultivated Sema3A signaling promotes chondrocyte apoptosis in knee osteoarthritis. *J Cell Biochem,* 119**,** 2891-2899.

SUTTON, A. L., ZHANG, X., DOWD, D. R., KHARODE, Y. P., KOMM, B. S. & MACDONALD, P. N. 2008. Semaphorin 3B is a 1,25-Dihydroxyvitamin D3-induced gene in osteoblasts that promotes osteoclastogenesis and induces osteopenia in mice. *Mol Endocrinol,* 22**,** 1370-81.

SWEENEY, S. E. & FIRESTEIN, G. S. 2004. Rheumatoid arthritis: regulation of synovial inflammation. *Int J Biochem Cell Biol,* 36**,** 372-8.

TAKAHASHI, K., ISHIDA, M., HIROKAWA, K. & TAKAHASHI, H. 2008. Expression of the semaphorins Sema 3D and Sema 3F in the developing parathyroid and thymus. *Dev Dyn,* 237**,** 1699-708.

TAKAHASHI, T., FOURNIER, A., NAKAMURA, F., WANG, L. H., MURAKAMI, Y., KALB, R. G., FUJISAWA, H. & STRITTMATTER, S. M. 1999. Plexin-neuropilin-1 complexes form functional semaphorin-3A receptors. *Cell,* 99**,** 59-69.

TAKAHASHI, T., NAKAMURA, F., JIN, Z., KALB, R. G. & STRITTMATTER, S. M. 1998. Semaphorins A and E act as antagonists of neuropilin-1 and agonists of neuropilin-2 receptors. *Nat Neurosci,* 1**,** 487-93.

TAKAHASHI, T. & STRITTMATTER, S. M. 2001. Plexina1 autoinhibition by the plexin sema domain. *Neuron,* 29**,** 429-39.

TAKAMATSU, H. & KUMANOGOH, A. 2012. Diverse roles for semaphorin-plexin signaling in the immune system. *Trends Immunol,* 33**,** 127-35.

TAKEGAHARA, N., KANG, S., NOJIMA, S., TAKAMATSU, H., OKUNO, T., KIKUTANI, H., TOYOFUKU, T. & KUMANOGOH, A. 2010. Integral roles of a guanine nucleotide exchange factor, FARP2, in osteoclast podosome rearrangements. *Faseb j,* 24**,** 4782-92.

TAKEGAHARA, N., TAKAMATSU, H., TOYOFUKU, T., TSUJIMURA, T., OKUNO, T., YUKAWA, K., MIZUI, M., YAMAMOTO, M., PRASAD, D. V., SUZUKI, K., ISHII, M., TERAI, K., MORIYA, M., NAKATSUJI, Y., SAKODA, S., SATO, S., AKIRA, S., TAKEDA, K., INUI, M., TAKAI, T., IKAWA, M., OKABE, M., KUMANOGOH, A. & KIKUTANI, H. 2006. Plexin-A1 and its interaction with DAP12 in immune responses and bone homeostasis. *Nat Cell Biol,* 8**,** 615-22.

TAMAGNONE, L. 2012. Emerging role of semaphorins as major regulatory signals and potential therapeutic targets in cancer. *Cancer Cell,* 22**,** 145-52.

TAMAGNONE, L., ARTIGIANI, S., CHEN, H., HE, Z., MING, G. I., SONG, H., CHEDOTAL, A., WINBERG, M. L., GOODMAN, C. S., POO, M., TESSIER-LAVIGNE, M. & COMOGLIO, P. M. 1999. Plexins are a large family of receptors for transmembrane, secreted, and GPI-anchored semaphorins in vertebrates. *Cell,* 99**,** 71-80.

TANELIAN, D. L., BARRY, M. A., JOHNSTON, S. A., LE, T. & SMITH, G. M. 1997. Semaphorin III can repulse and inhibit adult sensory afferents in vivo. *Nat Med,* 3**,** 1398-401.

TANG, C., GAO, X., LIU, H., JIANG, T. & ZHAI, X. 2014. Decreased expression of SEMA3A is associated with poor prognosis in gastric carcinoma. *Int J Clin Exp Pathol,* 7**,** 4782-94.

TANG, H., WU, Y., LIU, M., QIN, Y., WANG, H., WANG, L., LI, S., ZHU, H., HE, Z., LUO, J., WANG, Q. & LUO, S. 2016. SEMA3B improves the survival of patients with esophageal squamous cell carcinoma by upregulating p53 and p21. *Oncol Rep,* 36**,** 900-8.

TANG, X. Q., TANELIAN, D. L. & SMITH, G. M. 2004. Semaphorin3A inhibits nerve growth factor-induced sprouting of nociceptive afferents in adult rat spinal cord. *J Neurosci,* 24**,** 819-27.

TANIGUCHI, M., MASUDA, T., FUKAYA, M., KATAOKA, H., MISHINA, M., YAGINUMA, H., WATANABE, M. & SHIMIZU, T. 2005. Identification and characterization of a novel member of murine semaphorin family. *Genes Cells,* 10**,** 785-92.

TANIGUCHI, M., NAGAO, H., TAKAHASHI, Y. K., YAMAGUCHI, M., MITSUI, S., YAGI, T., MORI, K. & SHIMIZU, T. 2003. Distorted odor maps in the olfactory bulb of semaphorin 3A-deficient mice. *J Neurosci,* 23**,** 1390-7.

TANIGUCHI, M., YUASA, S., FUJISAWA, H., NARUSE, I., SAGA, S., MISHINA, M. & YAGI, T. 1997. Disruption of semaphorin III/D gene causes severe abnormality in peripheral nerve projection. *Neuron,* 19**,** 519-30.

TAYLOR, D., HAZENBERG, J. G. & LEE, T. C. 2007. Living with cracks: damage and repair in human bone. *Nat Mater,* 6**,** 263-8.

TEITELBAUM, S. L. 2000. Bone resorption by osteoclasts. *Science,* 289**,** 1504-8.

TENG, Y., YIN, Z., LI, J., LI, K., LI, X. & ZHANG, Y. 2017. Adenovirus-mediated delivery of Sema3A alleviates rheumatoid arthritis in a serum-transfer induced mouse model. *Oncotarget,* 8**,** 66270-66280.

TETI, A. 2011. Bone development: overview of bone cells and signaling. *Curr Osteoporos Rep,* 9**,** 264-73.

THOMMESEN, L., STUNES, A. K., MONJO, M., GROSVIK, K., TAMBURSTUEN, M. V., KJOBLI, E., LYNGSTADAAS, S. P., RESELAND, J. E. & SYVERSEN, U. 2006. Expression and regulation of resistin in osteoblasts and osteoclasts indicate a role in bone metabolism. *J Cell Biochem,* 99**,** 824-34.

TONG, Y., HOTA, P. K., PENACHIONI, J. Y., HAMANEH, M. B., KIM, S., ALVIANI, R. S., SHEN, L., HE, H., TEMPEL, W., TAMAGNONE, L., PARK, H. W. & BUCK, M. 2009. Structure and function of the intracellular region of the plexin-b1 transmembrane receptor. *J Biol Chem,* 284**,** 35962-72.

TOYOFUKU, T., YOSHIDA, J., SUGIMOTO, T., ZHANG, H., KUMANOGOH, A., HORI, M. & KIKUTANI, H. 2005. FARP2 triggers signals for Sema3A-mediated axonal repulsion. *Nat Neurosci,* 8**,** 1712-9.

TROEN, B. R. 2003. Molecular mechanisms underlying osteoclast formation and activation. *Exp Gerontol,* 38**,** 605-14.

TSE, C., XIANG, R. H., BRACHT, T. & NAYLOR, S. L. 2002. Human Semaphorin 3B (SEMA3B) located at chromosome 3p21.3 suppresses tumor formation in an adenocarcinoma cell line. *Cancer Res,* 62**,** 542-6.

UCHIDA, Y., OHSHIMA, T., SASAKI, Y., SUZUKI, H., YANAI, S., YAMASHITA, N., NAKAMURA, F., TAKEI, K., IHARA, Y., MIKOSHIBA, K., KOLATTUKUDY, P., HONNORAT, J. & GOSHIMA, Y. 2005. Semaphorin3A signalling is mediated via sequential Cdk5 and GSK3beta phosphorylation of CRMP2: implication of common phosphorylating

mechanism underlying axon guidance and Alzheimer's disease. *Genes Cells,* 10**,** 165-79.

UDA, Y., AZAB, E., SUN, N., SHI, C. & PAJEVIC, P. D. 2017. Osteocyte Mechanobiology. *Curr Osteoporos Rep,* 15**,** 318-325.

VAITKIENE, P., SKIRIUTE, D., STEPONAITIS, G., SKAUMINAS, K., TAMASAUSKAS, A. & KAZLAUSKAS, A. 2015. High level of Sema3C is associated with glioma malignancy. *Diagn Pathol,* 10**,** 58.

VAN 'T HOF, R. J. 2012. Analysis of bone architecture in rodents using microcomputed tomography. *Methods Mol Biol,* 816**,** 461-76.

VAN DER WEYDEN, L., ADAMS, D. J., HARRIS, L. W., TANNAHILL, D., ARENDS, M. J. & BRADLEY, A. 2005. Null and conditional semaphorin 3B alleles using a flexible puroDeltatk loxP/FRT vector. *Genesis,* 41**,** 171-8.

VARSHAVSKY, A., KESSLER, O., ABRAMOVITCH, S., KIGEL, B., ZAFFRYAR, S., AKIRI, G. & NEUFELD, G. 2008. Semaphorin-3B is an angiogenesis inhibitor that is inactivated by furin-like pro-protein convertases. *Cancer Res,* 68**,** 6922-31.

VERLINDEN, L., KRIEBITZSCH, C., BEULLENS, I., TAN, B. K., CARMELIET, G. & VERSTUYF, A. 2013. Nrp2 deficiency leads to trabecular bone loss and is accompanied by enhanced osteoclast and reduced osteoblast numbers. *Bone,* 55**,** 465-75.

WAIMEY, K. E., HUANG, P. H., CHEN, M. & CHENG, H. J. 2008. Plexin-A3 and plexin-A4 restrict the migration of sympathetic neurons but not their neural crest precursors. *Dev Biol,* 315**,** 448-58.

WALKLEY, C. R., QUDSI, R., SANKARAN, V. G., PERRY, J. A., GOSTISSA, M., ROTH, S. I., RODDA, S. J., SNAY, E., DUNNING, P., FAHEY, F. H., ALT, F. W., MCMAHON, A. P. & ORKIN, S. H. 2008. Conditional mouse osteosarcoma, dependent on p53 loss and potentiated by loss of Rb, mimics the human disease. *Genes Dev,* 22**,** 1662-76.

WALLERIUS, M., WALLMANN, T., BARTISH, M., OSTLING, J., MEZHEYEUSKI, A., TOBIN, N. P., NYGREN, E., PANGIGADDE, P., PELLEGRINI, P., SQUADRITO, M. L., PONTEN, F., HARTMAN, J., BERGH, J., DE MILITO, A., DE PALMA, M., OSTMAN, A., ANDERSSON, J. & ROLNY, C. 2016. Guidance Molecule SEMA3A Restricts Tumor Growth by Differentially Regulating the Proliferation of Tumor-Associated Macrophages. *Cancer Res,* 76**,** 3166-78.

WANG, C., ZHOU, X., LI, W., LI, M., TU, T., BA, X., WU, Y., HUANG, Z., FAN, G., ZHOU, G., WU, S., ZHAO, J., ZHANG, J. & CHEN, J. 2017a. Macrophage migration inhibitory factor promotes osteosarcoma growth and lung metastasis through activating the RAS/MAPK pathway. *Cancer Lett,* 403**,** 271-279.

WANG, L. L. 2005. Biology of osteogenic sarcoma. *Cancer J,* 11**,** 294-305.

WANG, L. L., LEVY, M. L., LEWIS, R. A., CHINTAGUMPALA, M. M., LEV, D., ROGERS, M. & PLON, S. E. 2001. Clinical manifestations in a cohort of 41 Rothmund-Thomson syndrome patients. *Am J Med Genet,* 102**,** 11-7.

WANG, M., WANG, L., REN, T., XU, L. & WEN, Z. 2013. IL-17A/IL-17RA interaction promoted metastasis of osteosarcoma cells. *Cancer Biol Ther,* 14**,** 155-63.

WANG, Z., DING, M., QIAN, N., SONG, B., YU, J., TANG, J. & WANG, J. 2017b. Decreased expression of semaphorin 3D is associated with genesis and development in colorectal cancer. *World J Surg Oncol,* 15**,** 67.

WANG, Z., JIA, Y., DU, F., CHEN, M., DONG, X., CHEN, Y. & HUANG, W. 2017c. IL-17A Inhibits Osteogenic Differentiation of Bone Mesenchymal Stem Cells via Wnt Signaling Pathway. *Med Sci Monit,* 23**,** 4095-4101.

WHELAN, J., MCTIERNAN, A., COOPER, N., WONG, Y. K., FRANCIS, M., VERNON, S. & STRAUSS, S. J. 2012. Incidence and survival of malignant bone sarcomas in England 1979-2007. *Int J Cancer,* 131**,** E508-17.

WHITE, F. A. & BEHAR, O. 2000. The development and subsequent elimination of aberrant peripheral axon projections in Semaphorin3A null mutant mice. *Dev Biol,* 225**,** 79-86.

WOLMAN, M. A., LIU, Y., TAWARAYAMA, H., SHOJI, W. & HALLORAN, M. C. 2004. Repulsion and attraction of axons by semaphorin3D are mediated by different neuropilins in vivo. *J Neurosci,* 24**,** 8428-35.

WONG, O. G., NITKUNAN, T., OINUMA, I., ZHOU, C., BLANC, V., BROWN, R. S., BOTT, S. R., NARICULAM, J., BOX, G., MUNSON, P., CONSTANTINOU, J., FENELEY, M. R., KLOCKER, H., ECCLES, S. A., NEGISHI, M., FREEMAN, A., MASTERS, J. R. & WILLIAMSON, M. 2007. Plexin-B1 mutations in prostate cancer. *Proc Natl Acad Sci U S A,* 104**,** 19040-5.

WORZFELD, T. & OFFERMANNS, S. 2014. Semaphorins and plexins as therapeutic targets. *Nat Rev Drug Discov,* 13**,** 603-21.

WU, F., ZHOU, Q., YANG, J., DUAN, G. J., OU, J. J., ZHANG, R., PAN, F., PENG, Q. P., TAN, H., PING, Y. F., CUI, Y. H., QIAN, C., YAN, X. C. & BIAN, X. W. 2011. Endogenous axon guiding chemorepulsant semaphorin-3F inhibits the growth and metastasis of colorectal carcinoma. *Clin Cancer Res,* 17**,** 2702-11.

XIANG, R., DAVALOS, A. R., HENSEL, C. H., ZHOU, X. J., TSE, C. & NAYLOR, S. L. 2002. Semaphorin 3F gene from human 3p21.3 suppresses tumor formation in nude mice. *Cancer Res,* 62**,** 2637-43.

XIAO, W., MOHSENY, A. B., HOGENDOORN, P. C. & CLETON-JANSEN, A. M. 2013. Mesenchymal stem cell transformation and sarcoma genesis. *Clin Sarcoma Res,* 3**,** 10.

XU, R. 2014. Semaphorin 3A: A new player in bone remodeling. *Cell Adh Migr,* 8**,** 5-10.

YANCOPOULOS, G. D., DAVIS, S., GALE, N. W., RUDGE, J. S., WIEGAND, S. J. & HOLASH, J. 2000. Vascular-specific growth factors and blood vessel formation. *Nature,* 407**,** 242-8.

YAZDANI, U. & TERMAN, J. R. 2006. The semaphorins. *Genome Biol,* 7**,** 211.

YONG, L. K., LAI, S., LIANG, Z., POTEET, E., CHEN, F., VAN BUREN, G., FISHER, W., MO, Q., CHEN, C. & YAO, Q. 2016. Overexpression of Semaphorin-3E enhances pancreatic cancer cell growth and associates with poor patient survival. *Oncotarget,* 7**,** 87431-87448.

YUAN, L., MOYON, D., PARDANAUD, L., BREANT, C., KARKKAINEN, M. J., ALITALO, K. & EICHMANN, A. 2002. Abnormal lymphatic vessel development in neuropilin 2 mutant mice. *Development,* 129**,** 4797-806.

YUE, B., MA, J. F., YAO, G., YANG, M. D., CHENG, H. & LIU, G. Y. 2014. Knockdown of neuropilin-1 suppresses invasion, angiogenesis, and increases the chemosensitivity to doxorubicin in osteosarcoma cells - an in vitro study. *Eur Rev Med Pharmacol Sci,* 18**,** 1735-41.

ZHOU, H., WU, A., FU, W., LV, Z. & ZHANG, Z. 2014. Significance of semaphorin-3A and MMP-14 protein expression in non-small cell lung cancer. *Oncol Lett,* 7**,** 1395-1400.

ZHOU, X., MA, L., LI, J., GU, J., SHI, Q. & YU, R. 2012. Effects of SEMA3G on migration and invasion of glioma cells. *Oncol Rep,* 28**,** 269-75.

ZHU, H., CAI, H., TANG, M. & TANG, J. 2014. Neuropilin-1 is overexpressed in osteosarcoma and contributes to tumor progression and poor prognosis. *Clin Transl Oncol,* 16**,** 732-8.

ZHU, M., LIANG, R., PAN, L. H., HUANG, B., QIAN, W., ZHONG, J. H., ZHENG, W. W. & LI, C. L. 2013. Zoledronate for metastatic bone disease and pain: a meta-analysis of randomized clinical trials. *Pain Med,* 14**,** 257-64.

ZHU, X., ZHANG, X., YE, Z., CHEN, Y., LV, L. & HU, H. 2017. Silencing of semaphorin 3C suppresses cell proliferation and migration in MCF-7 breast cancer cells. *Oncol Lett,* 14**,** 5913-5917.

Appendix

10 Appendices

10.1 Materials and Reagents

Materials and reagents	Supplier
1.5ml Eppendorf tubes with cap	Starlab, Milton Keynes, UK
12% Criterion™ TGX™ Precast Midi Protein Gel, 12+2 well	Bio-Rad Laboratories, Hertfordshire, UK
Acetic Acid Glacial	Sigma Aldrich, Dorset, UK
AlamarBlue™ reagent	Invitrogen, Paisley, UK
Alizarin Red S	Sigma Aldrich, Dorset, UK
BD microlance needles (19, 21 and 25G)	Fisher Scientific, Leicestershire, UK
Bicinchoninic acid (BCA) solution	Sigma Aldrich, Dorset, UK
Bovine serum albumin	Sigma Aldrich, Dorset, UK
Calcium carbonate	Sigma Aldrich, Dorset, UK
CD14 microbeads human	Miltenyi Biotech, Gladbach, Germany
Centrifuge tubes 15ml	Scientific laboratory supplies (SLS), Nottingham UK
Centrifuge tubes 50ml	Fisher Scientific, Leicestershire, UK
Cetyl pyridinium chloride monohydrate	Sigma Aldrich, Dorset, UK
Clarity Western ECL Substrate	Bio-Rad Laboratories, Hertfordshire, UK
Collagenase (type 1A)	Sigma Aldrich, Dorset, UK
Copper (II)-sulfate	Sigma Aldrich, Dorset, UK
Corning™ Transwell™ Multiple Well Plate with Permeable Polycarbonate Membrane Inserts	Corning, Flintshire, UK
Cover slips	Fisher Scientific, Leicestershire, UK
CTX ELISA	IDS, Boldon, UK
DAKO	Agilent, CA, US
Dehydrate trisodium citrate	Sigma Aldrich, Dorset, UK

Diethanolamin	Sigma Aldrich, Dorset, UK
DL-Dithiothreitol (DTT)	Sigma Aldrich, Dorset, UK
DMSO	Sigma Aldrich, Dorset, UK
DPX mounting medium	VWR International, Leicestershire, UK
EDTA	Sigma Aldrich, Dorset, UK
Electrophoresis power supply	Bio-Rad Laboratories, Hertfordshire, UK
Eosin powder	VWR International LTD, Leicestershire, UK
Ethanol Absolute	Sigma Aldrich, Dorset, UK
Fetal calf serum (FCS)	Fisher Scientific, Leicestershire, UK
Filter Tips any size	Starlab, Milton Keynes, UK
Forceps watchmaker's	Fisher Scientific, Leicestershire, UK
Glycine	Acros organics, Geel, Belgium
Gill's II haematoxylin	VWR International LTD, Leicestershire, UK
Goat serum	Vector laboratories, Peterborough, UK
Histopaque	Sigma Aldrich, Dorset, UK
ImmPACT™ DAB	Vector laboratories, Peterborough, UK
Immunedge pen (PAP pen)	Vector laboratories, Peterborough, UK
Isopropanol	Fisher Scientific, Leicestershire, UK
Jackson ImmunoResearch Anti-rabbit secondary ab	Stratech Scientific Unit, Newmarket Suffolk, UK
Jackson ImmunoResearch Anti-goat secondary ab	Stratech Scientific Unit, Newmarket Suffolk, UK
Kaleidoscope Pre-stained standards	Bio-Rad Laboratories, Hertfordshire, UK
Magic Marker	Invitrogen, Paisley, UK
Magnesium chloride	Sigma Aldrich, Dorset, UK
Maxima H Minus First Strand cDNA Synthesis kit	Fisher Scientific, Leicestershire, UK
M-CSF mouse recombinant	R & D Systems, Abingdon, UK

Methanol	VWR International LTD, Leicestershire, UK
Microtubes (0.5, 1.5, 2ml)	Sarstedt Ltd, Leicester, UK
Minimum Essential Medium (αMEM)	Fisher Scientific, Leicestershire, UK
Minimum Essential Medium (DMEM)	Fisher Scientific, Leicestershire, UK
MS Columns	Miltenyi Biotech, Gladbach, Germany
N,N-Dimethylformamide	Sigma Aldrich, Dorset, UK
Napthol-AS-BI-phosphate	Sigma Aldrich, Dorset, UK
Neubauer Haemocytometer	Hawksley, Lancing, UK
Nucleospin RNA isolation kit	Machery-Nagel, Düren, Germany
PINP ELISA	IDS, Boldon, UK
Paraformaldehyde	Taab Lab, Berkshire, UK
Pararosanilin	Sigma Aldrich, Dorset, UK
Penicillin/Streptomycin	Fisher Scientific, Leicestershire, UK
Pierce™ Bovine Serum Albumin Standard Pre-Diluted Set	Fisher Scientific, Leicestershire, UK
Pierce Protein Concentrators, 9K MWCO	Fisher Scientific, Leicestershire, UK
Phosphatase inhibitor cocktail	Sigma Aldrich, Dorset, UK
Phosphate buffered saline	Sigma Aldrich, Dorset, UK
Phosphate buffered saline tablets	Sigma Aldrich, Dorset, UK
Pipette tips (all sizes)	Starlab, Milton Keynes, UK
Protease inhibitor cocktail	Sigma Aldrich, Dorset, UK
Proteome Profiler Human XL Cytokine Array Kit	R & D Systems, Abingdon, UK
4-Nitrophenyl phosphate disodium salt hexahydrate powder	Scientific laboratory supplies (SLS), Nottingham UK
Recombinant Human Semaphorin 3A Fc Chimera Protein, CF	R & D Systems, Abingdon, UK
Scalpel, disposable	VWR International LTD, Leicestershire, UK
Scissors (fine points and spring bow handles)	S Murray & Co Ltd, Surrey, UK

SignalStain® Antibody Diluent	Cell signaling technology, Leiden, the Netherlands
SignalStain® Boost IHC Detection Reagent (HRP, Rabbit)	Cell signaling technology, Leiden, the Netherlands
Sodium acetate trihydrate	VWR International LTD, Leicestershire, UK
Sodium barbiturate	Sigma Aldrich, Dorset, UK
Sodium chloride	Sigma Aldrich, Dorset, UK
Sodium dodecyl sulphate (SDS)	Bio-Rad Laboratories, Hertfordshire, UK
Sodium hydroxide	VWR International LTD, Leicestershire, UK
Sodium phosphate	Sigma Aldrich, Dorset, UK
Sodium tartrate dibasic dihydrate	Sigma Aldrich, Dorset, UK
Starguard® laboratory gloves	Starlab, Milton Keynes, UK
Sterile filter (0.2 and 0.45μm)	Pall lifesciences, Portsmouth, UK
Streptavidin/Biotin Blocking Kit	Vector laboratories, Peterborough, UK
Stripettes (5, 10, 25 and 50ml)	Fisher Scientific, Leicestershire, UK
Superfrost Plus™ Adhesion Microscope Slides	Fisher Scientific, Leicestershire, UK
Syringes (all sizes)	Fisher Scientific, Leicestershire, UK
Tissue culture 25, 75, 175cm^2 flasks	Fisher Scientific, Leicestershire, UK
Tissue culture microplates (6, 12, 24, 48 and 96-well plates)	Corning, Flintshire, UK
Transblot Turbo midi Size PVDF membrane	Bio-Rad Laboratories, Hertfordshire, UK
Transblot Turbo midi Size Transfer stacks	Bio-Rad Laboratories, Hertfordshire, UK
Tris	Bio-Rad Laboratories, Hertfordshire, UK
Tris-EDTA buffer	Sigma Aldrich, Dorset, UK
Tris-Glycine buffer 10x	Bio-Rad Laboratories, Hertfordshire, UK
Triton X-100™	Sigma Aldrich, Dorset, UK

Trizma® hydrochloride	Sigma Aldrich, Dorset, UK
Trizma® base	Sigma Aldrich, Dorset, UK
Trypsin/EDTA	Sigma Aldrich, Dorset, UK
Tween-20	Acros organics, Geel, Belgium
Ultraclear Xylene	Taab Lab, Berkshire, UK
L-Ascorbic acid	Sigma Aldrich, Dorset, UK
Western blot tips	Starlab, Milton Keynes, UK
XT-MOPS	Bio-Rad Laboratories, Hertfordshire, UK
Xylene	Sigma Aldrich, Dorset, UK
β-glycerophosphate disodium	Sigma Aldrich, Dorset, UK

10.2 Antibodies

Materials and reagents	Supplier
Rabbit anti-β-Actin	Cell signaling technology, Leiden, the Netherlands
Rabbit anti-β-catenin	Cell signaling technology, Leiden, the Netherlands
Rabbit anti-GAPDH	Cell signaling technology, Leiden, the Netherlands
Rabbit anti-GSK3β	Cell signaling technology, Leiden, the Netherlands
Rabbit anti-Lamin	Cell signaling technology, Leiden, the Netherlands
Rabbit anti-pGSK3β	Cell signaling technology, Leiden, the Netherlands
Rabbit anti-pIκB	Cell signaling technology, Leiden, the Netherlands
Rabbit anti-Sema3A	Abcam Abingdon, UK
Sheep anti-Nrp1 block	R & D Systems, Abingdon, UK

10.3 Apparatus

Apparatus	Supplier
Bench-top centrifuge	Fisher Scientific, Leicestershire, UK
Bench-top Eppendorf centrifuge	Fisher Scientific, Leicestershire, UK
ChemiDoc XRS+	Bio-Rad Laboratories, Hertfordshire, UK
Digital heatblok	VWR International LTD, Leicestershire, UK
NoAir Class II Biological safety cabinet	Walker, Glossop, UK
histoSTATION (milestone)	Milestone, Milan, Italy
Ika Vortex	Thistle Scientific, Glasgow, UK
Lab Vision™ PT Module	Fisher Scientific, Leicestershire, UK
Leica manual microtome	Leica microsystems, Wetzlar, Germany
Leica inverted phase contrast microscope	Leica microsystems, Wetzlar, Germany
Leica AF6000 Time lapse	Leica microsystems, Wetzlar, Germany
LeicaDMI4000B	Leica microsystems, Wetzlar, Germany
Nanodrop	Fisher Scientific, Leicestershire, UK
Ohaus Explorer® Analytical balance	Camlab, Cambridge, UK
Ohaus Portable Balance Scout Pro	Camlab, Cambridge, UK
Osteomeasure histomorphometry system	OsteoMetrics Inc, Atlanta, USA
Pannoramic 250 Flash III	3DHistech, Budapest, HUNGARY
Skyscan 1076 *in-vivo* Micro-CT	Brucker, Kontich, Belgium
SpectraMax® M5 microplate reader	Molecular devices, San Jose, USA
Stuart scientific shaker	Stuart, Staffordshire, UK
Stuart scientific see saw rocker	Stuart, Staffordshire, UK
Tissue processor	Microm Microtech, Brignais, France
Trans-Blot® Turbo™ Rapid Transfer System	Bio-Rad Laboratories, Hertfordshire, UK
Vertical Criterion™ gel tanks	Bio-Rad Laboratories, Hertfordshire, UK
Precision™ Circulating Water Baths	Fisher Scientific, Leicestershire, UK

10.4 Software

Software	Supplier
Chemotaxis and Migration Tool	Ibidi, USA
Endnote	Thomson Reuters, Toronto Canada
GraphPad Prism (version 7)	GraphPad Software Inc., CA-US
ImageJ	U. S. National Institutes of Health Bethesda
Image Lab™ Software	Bio-Rad Laboratories, Hertfordshire, UK
Leica Microscope Imaging Software	Leica microsystems, Wetzlar, Germany
Molecular devices, San Jose, USA	Molecular devices, San Jose, USA
Osteomeasure Software	OsteoMetrics Inc, Atlanta, USA
Qupath, Quantitative pathology software	Queen's University Belfast, Ireland
Skyscan CTAn analysis software	Cell signaling technology, the Netherlands
Skyscan CTVol software	Cell signaling technology, the Netherlands
Skyscan NRecon reconstruction system	Cell signaling technology, the Netherlands
Tscratch	ETH Zürich, Switzerland

10.5 Solutions and chemicals

TRacP solutions in vitro staining

Naphthol-AS-BI-phosphate

10 mg/ml Naphthol-AS-BI-phosphate in Dimethylformamide

Veronal buffer

1.17 g sodium acetate anhydrous and 2.94g sodium barbiturate both dissolved in 100 ml of dH_2O

Acetate buffer

0.82 g sodium acetate anhydrous dissolved in 100 ml of dH_2O and pH adjusted to 5.2 with 0.6 ml glacial acetic acid made up to 100 ml with dH_2O

Pararosanilin

1 g Pararosanilin dissolved in 20 ml of dH_2O and 5 ml of 5M HCl added to it

The solution was heated carefully whilst stirring and filtered after cooling.

TRAcP Staining Solution

The TRAcP staining solution was freshly prepared by mixing solution A and B as outlined below.

Solution A

150 ml of Napthol-AS-BI-phosphate

750 ml of Veronal buffer

900 ml Acetate buffer

900 ml Acetate buffer with 100 mM Sodium Tartate

Solution B

120 ml of Pararosanilin

120 ml of Sodium Nitrate (4% w/v)

TRacP solutions histomorphometry

Pararosanilin:

1 g Pararosanilin dissolved in 20 ml of dH_2O and 5 ml of 5M HCl added to it
The solution was heated carefully whilst stirring and filtered after cooling.

Acetate buffer 0.2M (pH 5.2):

5.44g sodium acetate trihydrate in 200ml distilled water.
pH to 5.2 with 50-60mls 1.2% acetic acid.

Acetate-tartrate buffer:

4.6g sodium tartrate in 200ml acetate buffer

Naphthol AS-BI phosphate:

20mg naphthol AS-BI phosphate in1ml dimethylformamide

4% sodium nitrite:

80mg sodium nitrite in 2ml distilled water.

Solution A

1ml naphthol/dimethylformamide per 50ml acetate-tartrate buffer

Solution B

mix 2ml pararosaniline stock with 2ml of 4% sodium nitrite solution.

Just before use, add 2.5ml of this hexazotised solution to 50ml acetate-tartrate buffer

Cell lysis solutions

RIPA Lysis buffer

1% Triton 100X, 0.5% (w/v) Sodium Deoxycholate, 0.1% (w/v) Sodium Dodecyl Sulphate (SDS), 50 mM Tris-HCl (pH 7.4) and 150 mM Sodium Chloride were dissolved in dH_2O.

Cytoplasmic fraction Lysis buffer

10 mM Tris [pH 7.5], 0.05% NP-40, 3 mM $MgCl_2$, 100 mM NaCl, 1 mM EGTA were dissolved in dH_2O

Western blot solutions

RIPA Lysis buffer

1% Triton 100X, 0.5% (w/v) Sodium Deoxycholate, 0.1% (w/v) Sodium Dodecyl Sulphate (SDS), 50 mM Tris-HCl (pH 7.4) and 150 mM Sodium Chloride were dissolved in dH_2O.

Cytoplasmic fraction Lysis buffer

10 mM Tris [pH 7.5], 0.05% NP-40, 3 mM $MgCl_2$, 100 mM NaCl, 1 mM EGTA were dissolved in dH_2O

Electrophoresis running buffer

100 ml of TGS (10X) in 900 ml of dH2O

Samples loading protein buffer (5X stock)

5.2 ml of 1M Tris-HCl pH adjusted to 6.8, 1 g of DL-Dithiothreitol (DTT), 3 g SDS, 6.5 ml glycerol and 130 µl of 10% (w/v) Bromophenol Blue.

Transfer buffer

200ml Biorad transfer buffer (5X), 600ml Nanopure water, 200 ml 100% Ethanol.

TBS

Dissolve 6.05 g Tris and 8.76 g NaCl in 800 mL of H2O. Adjust pH to 7.5 with 1 M HCl and make volume up to 1 L with H2O

TBST

0.1% (v/v) Tween-20 in TBS. Stored at room temperature.

Stripping buffer

1 mM DTT, 2% (w/v) SDS and 62.5 mM Tris-HCl (pH 6.7).

10.6 Copyright Clearance

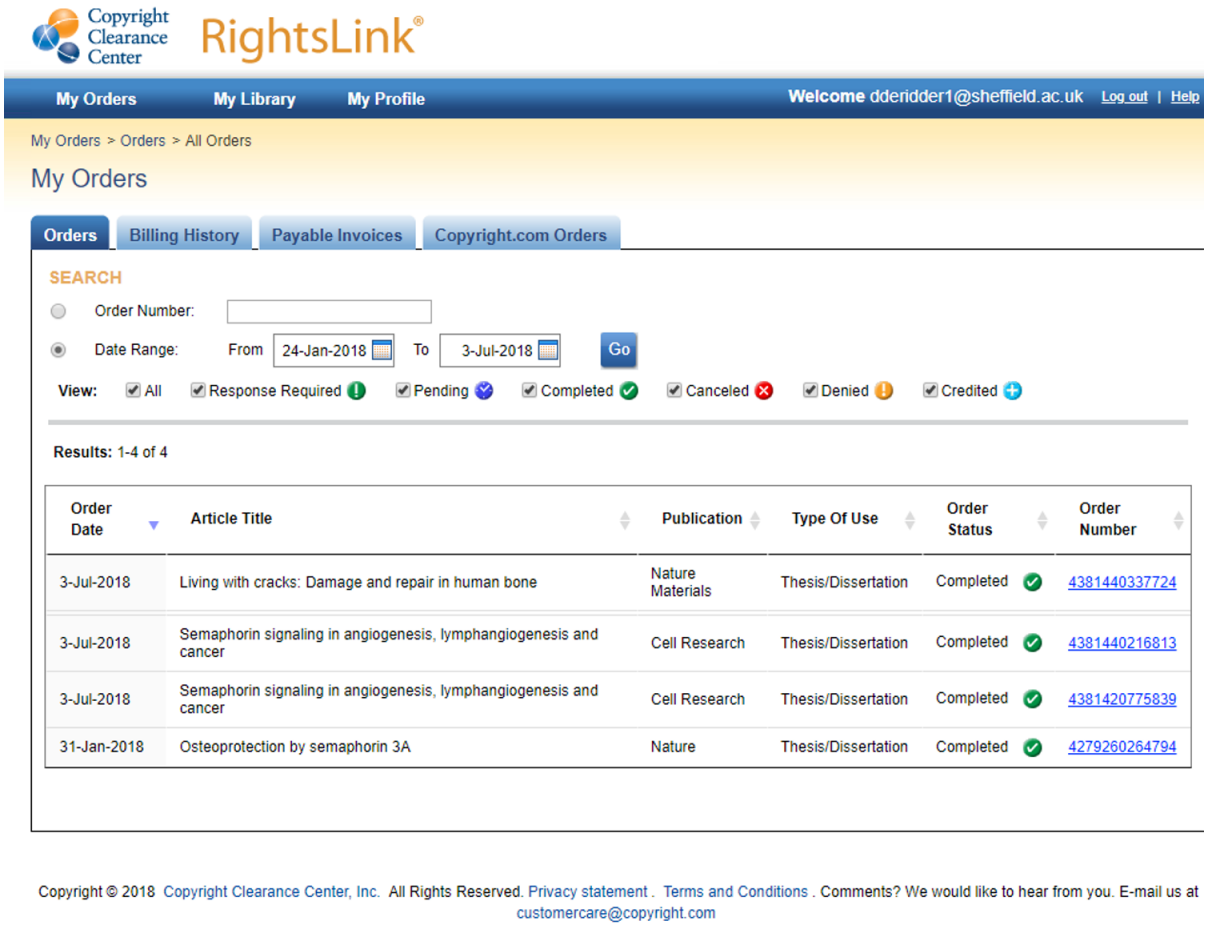

Figure 10.1 Copyright clearance
Related to Figure 1.1, Figure 1.3, Figure 1.4 and Figure 1.5 in chapter 1.